CHEMICAL REVIEWS

pubs.acs.org/CR

Review

Opportunities and Challenges for Organic Electrodes in Electrochemical Energy Storage

Philippe Poizot,* Joël Gaubicher, Stéven Renault, Lionel Dubois, Yanliang Liang, and Yan Yao

Cite This: *Chem. Rev.* 2020, 120, 6490−6557

Read Online

ACCESS | Metrics & More | Article Recommendations | Supporting Information

ABSTRACT: As the world moves toward electromobility and a concomitant decarbonization of its electrical supply, modern society is also entering a so-called fourth industrial revolution marked by a boom of electronic devices and digital technologies. Consequently, battery demand has exploded along with the need for ores and metals to fabricate them. Starting from such a critical analysis and integrating robust structural data, this review aims at pointing out there is room to promote organic-based electrochemical energy storage. Combined with recycling solutions, redox-active organic species could decrease the pressure on inorganic compounds and offer valid options in terms of environmental footprint and possible disruptive chemistries to meet the energy storage needs of both today and tomorrow. We review state-of-the-art developments in organic batteries, current challenges, and prospects, and we discuss the fundamental principles that govern the reversible chemistry of organic structures. We provide a comprehensive overview of all reported cell configurations that involve electroactive organic compounds working either in the solid state or in solution for aqueous or nonaqueous electrolytes. These configurations include alkali (Li/Na/K) and multivalent (Mg, Zn)-based electrolytes for conventional "sealed" batteries and redox-flow systems. We also highlight the most promising systems based on such various chemistries relying on appropriate metrics such as operation voltage, specific capacity, specific energy, or cycle life to assess the performances of electrodes.

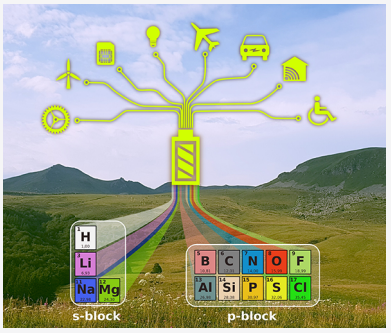

CONTENTS

Special Issue: Beyond Li-Ion Battery Chemistry

Received: July 30, 2019
Published: March 24, 2020

https://dx.doi.org/10.1021/acs.chemrev.9b00482
Chem. Rev. 2020, 120, 6490−6557

1. INTRODUCTION

1.1. Current Status in Electrochemical Energy Storage in Short

The need to build innovative electrochemical energy storage (EES) technologies and conversion solutions is now recognized to be particularly critical not only by specialists in the field but also by ordinary consumers eager to use different nomadic electronic devices which make their life easier, safer, and more enjoyable. Representative devices of EES are rechargeable (or secondary) batteries and (super)capacitors. Chemists, electrochemists, and materials science researchers helped by theoreticians (see for example the Materials Genome Project launched by G. Ceder[1]) have already thoroughly screened the periodic table of the elements in the quest to find the best electrode associations essentially focused on increased gravimetric and volumetric energy densities while improving the safety, power, lifetime, and cost. Thus, decades of intensive and innovative research have enabled us to develop and to place on the market different kinds of primary and secondary batteries able to power an increasingly diverse kind of applications from microchips to the emerging large-scale application markets.[2] Without describing them one by one, it must be underlined that the pioneered lead-acid (PbA) battery devised by G. Planté in 1859 is still in growing demand because it is unrivalled for microhybrid and internal combustion vehicles or large-scale power storage units (load-leveling applications, uninterrupted power supply (UPS) for entire cities) at this time; this technology is also robust, safe, and affordable associated with efficient recycling and disposal management programs notably to prevent lead emission.[3] Regarding Li-ion batteries (LIBs)—the current flagship technology to get high energy densities—thanks to substantial improvements and notably the discovery of new insertion positive electrode materials (e.g., $LiFePO_4$, LFP; $Li(Ni_{1/2-x}Mn_{1/2-x}Co_{2x})O_2$, NMC; Li-rich layered oxides $Li(Li_xM_{1-x})O_2$), they have become essential to power the vast world of electronic equipment, robots, ongoing electric transportation technologies, and some stationary applications too. Consequently, nickel/metal hydride (Ni/MH) rechargeable batteries, which have fully replaced nickel/cadmium (Ni/Cd) cells, are struggling to compete with LIBs in the light of recent achieved progress including at the price level. For the moment, Ni-MH batteries still power more than 10 million hybrid electric vehicles, and companies like BASF-Ovonic maintain their R&D activities.[4] Redox flow batteries (RFBs) represent another promising choice for stationary energy storage because this particular cell configuration operating basically with redox-active solutions is more durable and scalable than conventional "sealed" battery systems working with solid state electrode materials. The major plants ever built to date are essentially based on the vanadium/vanadium redox flow battery technology (VRFB)[5] first patented and developed by Skyllas-Kazacos in Australia in the mid 80s.[6−8] This rapid survey shows that all commercially available electrochemical storage solutions deal with redox-active inorganic systems, which poses now more than ever certain problems in terms of metal resource constraints, production cost, and environmental footprint in view of the ever growing demand.

1.2. Rise of Organics for Electrochemical Energy Storage

For several reasons, which will be thoroughly explained later, it is now recognized that searching for organic matter-based electrodes could bring new chemical opportunities to further improve existing EES technologies while opening new playgrounds to create innovative cell configurations. Thus, over the last ten years, tremendous progress has been made to promote electroactive organic systems attracting much interest from the broad electrochemical storage community. This occurs to such an extent that today we are witnessing a considerable increase in the literature on the subject, ranging from

https://dx.doi.org/10.1021/acs.chemrev.9b00482
Chem. Rev. 2020, 120, 6490−6557

nonaqueous/aqueous RFBs to nonaqueous/aqueous "sealed" batteries including both organic polymers and crystallized organic compounds as will be developed in this article. In only ten years, more than 45 review papers have been published for which the scope was initially broad but in view of the booming of primary research papers due to the versatility of the organic synthesis and molecular engineering. The most recent reviews are now focused on thematic research areas although it should be recognized that some of them overlap. In the following list sorted by year, the reader can find the series of review papers on organic-based EES published since 2012 including notably several remarkable contributions of both Chen's group at Nankai University and Schubert's group at Friedrich Schiller University: 2012,[9,10] 2013,[11,12] 2015,[13−15] 2016,[16−27] 2017,[28−35] 2018,[36−46] 2019.[47−58]

Basically, before 2011 the literature on the topic was clearly limited. The reference review article dealing with organic electrodes in this period was published by Novák et al. in 1997[59] on the basis of the existing literature focused at that time only on conducting polymers following the discovery of polyacetylene (PAc) by Shirakawa in 1974[60] and its subsequent chemical "p- or n-doping" (see section 4.3) to give a series of semiconductors and ultimately "organic metals" thanks to overlap of adjacent π-orbitals.[61−64] A few years later, the possible use of PAc as electrode material to store electricity was readily demonstrated by MacDiarmid taking advantage of both p- or n-doping.[65,66] Channels were opened to develop other conjugated polymers such as polyaniline (PAni), polypyrrole (PPy), or polythiophene (PT), which were particularly explored in the 80s as positive electrode materials in "dual-ion cell configurations" (see section 4.3) using metals or alloys as the negative electrode (e.g., lithium (Li), sodium (Na), or the stoichiometric lithium−aluminum alloy (LiAl)), which led to the first practical polymer batteries with the commercialization of two types of metal−organic dual-ion cells by Varta Corp. (with PPy) and Bridgestone Corp. (with PAni).[67−69] Note that for the discovery and the development of conductive polymers, Alan G. MacDiarmid, Alan J. Heeger, and Hideki Shirakawa were awarded the 2000 Nobel Prize in Chemistry.

However, shorter cycle life (~500 cycles), higher self-discharge values, and limited volumetric energy densities compared to the newcomer LIB commercialized by Sony Corp. in 1991 were some of the reasons for the abandonment at the end of the 20th century of efforts to make organic batteries from conjugated polymers. Note that in the 1990s organosulfur polymers were also investigated in Li batteries but as "n-type" electrode materials for which reversible Li^+ uptake/release reactions take place. Indeed, among the myriad of possible molecular organic arrangements, sulfur atoms can also be linked onto a carbon backbone (−C−S−S−C−) allowing the use of the redox-active disulfide bond; the charge transfer reaction involves 2 electrons together with the cleavage of the S−S bond. Pioneering research was performed by Visco and co-workers[70−72] with a survey of diverse groups of organodisulfide as positive electrode materials essentially main-chain type organosulfur polymers. For example, 2,5-dimercapto-1,3,4-thiadiazole (DMcT) with a theoretical specific capacity as high as 362 mAh g^{-1} is one of the best well-known organosulfur compounds. However, such electrode materials are generally impeded by sluggish kinetics along with a large polarization as well as solubility issues stemming from the repeated scission/reconstruction of disulfide bonds. Better results were obtained with side-chain type organodisulfide polymer such as poly(2,2′-dithiodianiline) (PDTDA) and other related derivatives, but long-lasting cyclings were never attempted.[73] Note that in the quest to develop lithium−sulfur (Li−S) batteries while limiting the polysulfide shuttle, high sulfur content organic materials have been recently investigated such as a new cross-linked disulfide material $C_6(SLi)_6$ developed by Wudl's group but the restored specific capacity is still limited with 1/4 of the theoretical value.[74]

A new class of polymers (nonconjugated) able to store electric energy and consisting of a stable organic polymeric chain bearing stabilized nitroxyl radicals such as 2,2,6,6-tetramethylpiperidinyl-*N*-oxy (TEMPO) radicals emerged in the early 2000s thanks to joint efforts of NEC Corp. and Nishide's group in Japan.[75−77] These studies have led to the development of the so-called organic radical batteries (ORBs) which are characterized by excellent rate performance, a flexible design, but moderate energy density values due to the adding of high amounts of conductive carbon in electrodes. The achievement of robust 0.3 mm-thick ORB prototypes compatible with functional smart card and wearable devices was, however, announced by NEC Corp. as early as 2012.[78] This innovative chemistry coupled with the emergence of promising high-capacity organic compounds characterized by multiple electroactive carbonyl (C═O) functional groups[79−83] (a redox-active moiety encountered in the chemistry of life and numerous natural substances) enabled the publication of a broader review in 2011 focused this time on the perspectives of organic batteries in addressing some eco-development issues through the possibility of integrating the concept of "renewability" in electrode material design and the prospect of realizing greener and sustainable batteries.[84] The use of organics emerges also in RFBs with a first organic/inorganic flow battery reported in 2009 by Xu et al.[85] based on the Cd−chloranil system operating in sulfuric acid aqueous medium. Two years later, an all-organic redox flow battery (ORFB) working in nonaqueous medium ($NaClO_4$/acetonitrile) was reported by Li et al.[86] employing 2,2,6,6-tetramethyl-1-piperidinyloxy as the posolyte and *N*-methylphthalimide as the negolyte, respectively. Many other examples were then reported in the literature as developed later (section 9). The interest taken over time by organics in the field of electrochemical storage can simply be assessed thanks to common data analysis tools like Scopus with suitable query string (Figure S1). The histogram shows that the number of publications (including articles, conference papers, reviews, book chapters, conference reviews) focused on organic-based electrochemical storage devices and published by year from 1972 onward follows a clear increase over the past 10 years. One can also observe two successive bumps ranging from 1980 to 2000 due to the investigations of conducting polymers then organodisulfide positive electrode materials followed by a larger increase thanks to the impetus given by ORBs.

Although beyond the scope herein, it seems instructive to briefly recall in this Introduction that the addition of electroactive molecules has also been shown to benefit carbon-based electrostatic double-layer capacitors (EDLCs) as well as the merging field of Li-ion capacitors.[87−102] As early as 1983, Saga Sanyo was the first company to integrate highly conducting organic material (tetracyanoquinodimethane, TCNQ) in electrolytic capacitors.[69] Electroactive molecules are used to significantly improve storage performance by adding a reversible faradaic contribution (pseudocapacitance) to the double-layer capacitance at the carbon electrode surface; these devices, referred to as supercapacitors or ultracapacitors, can work both

https://dx.doi.org/10.1021/acs.chemrev.9b00482
Chem. Rev. 2020, 120, 6490−6557

in aqueous and nonaqueous electrolyte media. Different chemistries such as the functionalization of the carbon surface by self-assembly or grafting of the redox-active organic molecule can be used.[87−97] Although covalent anchoring of the carbon substrate via the diazonium chemistry[94] appears as the main approach, some authors have also reported the direct incorporation of the redox-active organic molecules into the electrolyte formulation referred to as "redox electrolyte" to improve the specific capacitance of carbon-based electrochemical capacitors.[93,95,96] A relevant example of "organic" electrochemical pseudocapacitor consisting of activated carbon powder electrodes modified with naphthalimide and 2,2,6,6-tetramethylpiperidine-*N*-oxyl (TEMPO) was reported by Lebègue et al.[97] It shows an increase in specific capacitance up to 51%, an extended operating voltage of 2.9 V in propylene carbonate, compared to 1.9 V for the unmodified system, and a power 2.5 times higher. Alternatively, redox-active polymer electrodes can be employed including, for instance, PPy, PAni, and PT derivatives which offer advantages for making lightweight and flexible (micro)supercapacitors while being compatible with aqueous electrolytes.[98−100] Note that electroactive organic molecules have also recently been introduced as key materials to improve the sought-after "prelithiation" step of Li-ion capacitors as well as the sustainability while reducing the cost and complexity.[101,102]

It should be underlined that the boundary between faradaic organic-adding for supercapacitors and capacitive carbon-adding for organic batteries is sometimes not so clear. For instance, Wang's group[103] have reported a home-made hierarchical porous carbon nanotubes (HPCNTs) decorated with anthraquinone (AQ) molecules exhibiting ultrahigh specific capacitance of 710 F g^{-1} (measured at 1 A g^{-1}) when tested in 1 M H_2SO_4 aqueous solution with the optimized mass ratio 7:5 indicating a larger specific organic loading. Otherwise, recent years have seen the emergence of so-called carbon-supported organic electrode materials for LIBs/SIBs, that actually mirrors a strategy to counteract common physical limitations of most low-weight (neutral) organic molecules: their high solubility in organic electrolytes and poor electrical conductivity. By mixing these small organic molecules with large amounts of carbon (generally by impregnation), a better stability can be expected on cycling especially at high rate thanks to the establishment of $\pi-\pi$ stacking bonds with the surface of carbon particles (typical carbon loading: >55 wt %); this phenomenon being reinforced with extended aromatic cores. Note that biomolecules such as flavine[104] or dopamine[105] were reported. Chen and co-workers have reviewed this peculiar topic in 2015[13] by questioning some relevant points for practical applications such as the uniformity/reproducibility at large scale production of carbon-supported organic electrodes or the poor as-obtained energy density values (especially in volumetric metrics).

1.3. Goal, Scope, and Organization of This Review

Following these introductory elements, it is obvious that a consequent and growing amount of literature is now easily available on organic batteries after years of silence. However, it must be noted that because a certain disciplinary boundary naturally exists between inorganic and organic compounds and because the redox chemistry of organics is sometimes subtle (involving often reactive delocalized charges), reading research articles dealing with organic batteries (whatever the considered technology) could be somewhat challenging for nonspecialist readers. Therefore, the authors have thought it would be timely to bridge the gap by providing a kind of "tutorial"-oriented review for a broader audience to take smoothly in hands the most relevant points and achievements dealing with this peculiar field without being redundant with the multiple review articles already published today. Based on the latest selected and reliable input data from both general and specialized scientific literature (typically reported after 2015), this contribution aims also at providing the readers with a better critical view of the current evolution trends in our technology-oriented modern societies and the consecutive global demand for electrical energy sources, materials, and batteries before reviewing the main achievements obtained with organic-based electrode materials.

In practice, the layout of the article is structured in such a way as the reader will be able to select the parts that interest him most. From a chemical point of view, the following approach will be stepwise addressed in this review:

- *basic working principles and fundamental properties of key redox-active organic moieties and comparison with the formalism commonly used for inorganic materials together with corresponding cell configurations* (section 4),
- *a selection (with description) of original/promising organic-based batteries to date working either in the solid state ("sealed" batteries) or in solubilized state (ORFBs) for designing better realistic organic batteries in the future* (sections 5−9). *Note that the reader can find specific reviews on polymer-based organic batteries including radical polymers in refs* 10 and 18.

But as a preliminary step of this overview, it is thought particularly relevant for some readers to provide a snapshot of the global context that justifies there is room for reversible electroactive organic systems in the future electrochemical storage landscape in view of the particular conjunction of several critical factors facing mankind at the turn of the 21st century. Such a tricky exercise, which is seldom considered in other review articles, will constitute the background of sections 2 and 3 of this paper.

2. FOURTH INDUSTRIAL REVOLUTION: BATTERIES AT THE CROSSROADS

2.1. Background

Since the appearance on the market of LIBs 30 years ago the world has drastically changed. We have now entered the so-called Fourth Industrial Revolution![106] In short, the First Industrial Revolution used water and steam power to mechanize production, the Second used electric power to create mass production, and the Third, emerging in the 60s with the birth of computers, used electronics and information technologies to automate production. Starting at the end of the 20th century, the Fourth Industrial Revolution is built on the Third and is characterized by (*i*) a fusion of technologies that is blurring the lines between the physical, digital, and biological spheres, (*ii*) an exponential rather than a linear pace, and (*iii*) probably no control over either technology or the disruption that will come. Basically, the driving forces of this revolution are nestled in the digital and information technologies with more active roles for the artificial intelligence (AI) that enables innovations in "physical assets" such as autonomous vehicles, Internet of things (IoT), robotics, electric unmanned aerial vehicles (UAVs) or drones, 3-D printing, ... as well as "digital" innovations (e.g., blockchain[107]). It is worth noting that a rapid analysis of these innovative steps relies on a common

https://dx.doi.org/10.1021/acs.chemrev.9b00482
Chem. Rev. 2020, 120, 6490−6557

denominator which is the finer and finer control of the electron.

If we ignore herein that such innovations are also raising major ethical and spiritual questions,[106] the corollary of all this technology-oriented and more recently "connected" society is the ever-growing demand for energy especially for electrical power sources and related storage devices ranging from mWh to MWh: an era sometimes named "the Power Revolution". Unambiguously, it is well established that access to electricity improves life in a tangible way.[108] However, as previously pointed out in a former Perspective article a few years ago,[84] two related crucial threats cannot be ignored:

1. "Global warming" with its numerous and dangerous induced impacts (e.g., extreme and destructive climate events, rise in sea level with its aftermath, relocating industrial and farming areas, biodiversity alteration, new distribution of populations with conflicts over water and food, and so on). This major threat which seems to correlate to anthropogenic greenhouse gas (GHG) emissions represents not only ecological but also socio-ecological and economic issues. At the COP21/CMP11 (Conference of the Parties) meeting in Paris in 2015, 195 countries signed a legally binding agreement to keep global warming "well below 2°C above pre-industrial levels, and to pursue efforts to limit the temperature increase even further to 1.5°C" within this century. In practice, this means an 81% reduction of GHG intensity by 2050, which is equivalent to 4.4% annual improvement.[109] In 2018 almost all countries in the world have committed themselves to reduce their GHG emissions in their pledges to the *Paris Agreement*. Note that global warming is likely to reach 1.5 °C between 2030 and 2052 if it continues to increase at the current rate as reported by the Intergovernmental Panel on Climate Change (IPCC) special report on January 2019.[110]
2. The constant increase in the world population which results in more and more energy consumers and therefore more GHG emissions as nicely shown in Figure 1.

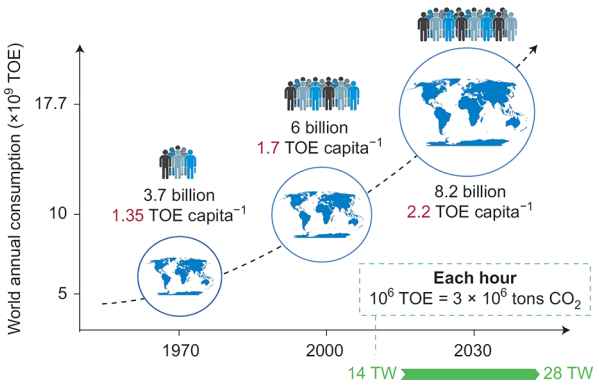

Figure 1. Forecast of the world's energy needs up to 2050. With the changing lifestyles of an increasing number of inhabitants, our energy rate demand will double from 14 TW (2010) to 28 TW (2050). TOE = ton of oil equivalent. Reproduced with permission from ref 112. Copyright 2015 Nature Publishing Group.

Predictions estimate around 9−10 billion the human load by the year 2050 (2.5 billion in Africa against 1.3 billion today) 66% of which will reside in urban areas in developing economies.[111] For comparison, the population was 700 million at the beginning of the first Industrial Revolution.

Although not yet fully accepted all over the world, such a mankind development still falls short in terms of sustainability and calls for a rapid and radical change in our current energy engineering together with a responsible behavior in our consuming fashion (pro-environmental behavior, "Nudge" theory, ...[113,114]). It is interesting for example to read the study of Dong et al.[115] on the nexus among carbon dioxide emissions, economic and population growth, and renewable energy across regions. Their data allow us to underline that economic growth is highly emission intensive, and economic growth often means rising energy consumption and increasing CO_2 emissions with a proportional effect of the population size. Hence our entering this Fourth Industrial Revolution can be perceived as a threat but also as an opportunity to rethink the development of mankind as a whole. Positive initiatives are now under way, and some policy makers and important energy stakeholders are making things happen probably also pushed by the ostensibly large number of recent extreme weather events[116] such as Category 5 Katerina hurricane in 2005. Basically, new political goals and innovative/disruptive economy models (like the "green growth" models, the circular economy governed by 3Rs, namely Reduce, Reuse, and Recycle) must also be formulated, notably in reference with CO_2 emission limits, in the quest for a long-term sustainability conjugating Ecology/Economy/Society. [The reader who would be interested in this exciting field could find relevant and very informative economic analyses in the specialized literature.[109,117−119]]

For a more technological point of view, *generation of decarbonized electricity* and *low-carbon transportation solutions* are the two main levers (in association with better *energy efficiency and conservation* and the *carbon capture utilization and storage*[120]) put traditionally forward to move toward a deep decarbonization of the energy system.[121] To better forecast the future in this regard, we recap below the main observed trends with supporting figures highlighting that rechargeable batteries are expected at the crossroads of several paths in the global demand pattern for electrical functionalities of today and tomorrow, some applications being to mitigate GHG emissions while others are probably less virtuous.

2.2. Decarbonizing the Power Supply and Its Related Storage Challenges

Regarding the future of electric grids, thanks to the efforts of worldwide researchers, engineers, and policy makers, remarkable progress has been made to connect renewable energy sources (RESs) for electricity generation.[122] For instance, the European Directive 2009/28/EC[123] aims at promoting the use of RESs in the European Union (EU) with a targeted value of 20% by 2020 with specific values regarding each member state. The most exploited RESs are hydroelectric, photovoltaic (PV), and wind. Other emerging renewable technologies include wave and tidal energy conversion and biomass energy conversion. Therefore, some predictions seem to indicate that GHG emissions in the power sector could be drastically reduced thus becoming a major contributor to decarbonization (Figure 2). Although the total electricity production is expected to more than double between 2010 and 2050 giving rise to the incredible value of more than 40 000 TWh of generated energy per year (notably to power the electromobility, see below), total emissions for the power sector could be divided by more than four according the Deep

https://dx.doi.org/10.1021/acs.chemrev.9b00482
Chem. Rev. 2020, 120, 6490−6557

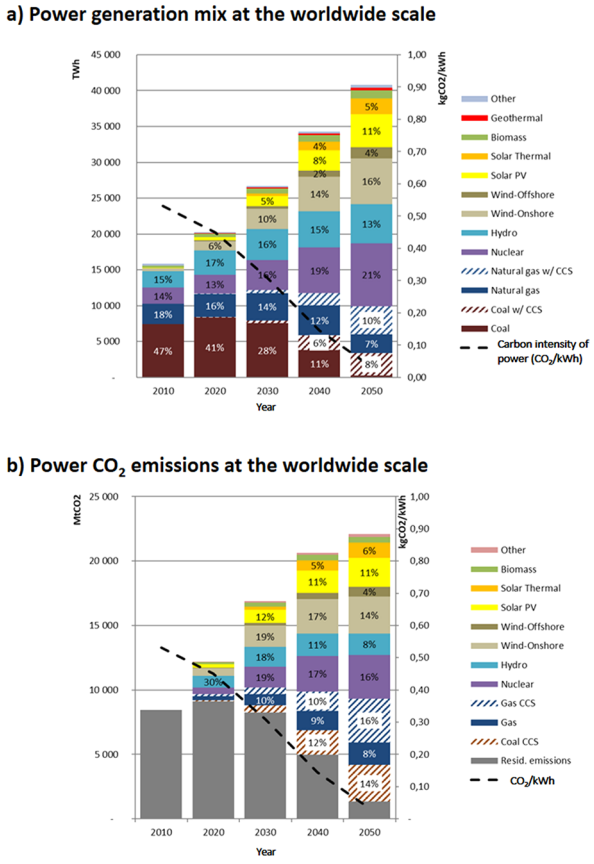

Figure 2. (a, b) Decarbonization Wedges in the power sector extracted from the ANCRE's report[124] (with permission) elaborated in the DDPP and by considering the most ambitious scenario in each country; "worldwide scale" refers to only the 16 most emitting countries. These histograms show the emission trajectories for the electricity sector in the absence of any technological evolution and (in gray) the evolutions of the emissions within the framework of decarbonization scenarios; the difference between the two corresponds to reductions that allow different technologies (e.g., solar in yellow and orange, hydro in blue); CCS meaning carbon capture and sequestration. Further descriptions of the "Decarbonization Wedges" methodology can be found in ref 126.

Decarbonization Pathway Project (DDPP)[124,125] by considering the most ambitious scenario in the 16 largest GHG-emitting countries representing 75% of current GHG emissions. According to these scenarios, the electricity mix could be completely modified with almost 90% of power generation from non-CO_2 emitting technologies, among which 54% is from renewable sources (together with 21% from nuclear power plants); coal is today responsible for 42% of CO_2 emissions worldwide. The electricity sector could be widely decarbonized by 2050 with a reduction from the current 530 gCO_2 kWh^{-1} to about 33 gCO_2 kWh^{-1} [the complete description of the "Decarbonization Wedges" methodology as well as additional subscenarios have been recently published by Mathy et al.[126]].

However, huge infrastructure investments will obviously be needed to satisfy such perspectives in electricity generation. For instance, some of these newly developed technologies (e.g., PV, wind power) cannot serve as stable energy sources alone because of their natural sensitivity to weather, landform, or other environmental conditions (i.e., variability and high ramping characteristics) requiring sophisticated planning and operation scheduling to ensure the necessary and subtle balance between electricity production and consumption. New technologies are currently being developed to upgrade existing electricity grid infrastructures that will enable so-called "smart grids", which are characterized by improved grid reliability and utilization, the synergies between the power electronics, control, and communication fields as well as the change from radial networks to mesh networks with the possibility to reconfigure and self-heal.[127,128] Thus, the role of IoT will be eminent with a significant reduction of costs associated with sensors, bandwidth, processing, and memory/storage.[129]

Consequently, energy storage is increasingly seen as a valuable asset for electricity grids and one of the important tools of mitigation not only as a technical solution for network management, ensuring real-time load leveling, but it is also a means of better utilizing RESs by avoiding load shedding in times of overproduction. For the moment, the worldwide stationary electrical storage remains by far dominated by pumped storage hydropower (98% of the installed power) but the use of rechargeable batteries is emerging fast as underlined in 2011 by Dunn et al.[130] in a visionary paper; the wide use of batteries is now clearly included in the roadmap storage technologies.[131,132] Already widely used for load-leveling applications and UPS for entire cities (especially the PbA technology), the reduction of costs in the electrochemical storage technologies is attracting considerable interest for short-term storage (for a period of seconds to a few days) using "sealed" batteries and redox-flow batteries (RFBs) as shown in Figure 3. Thus, LIBs in various chemistries are even

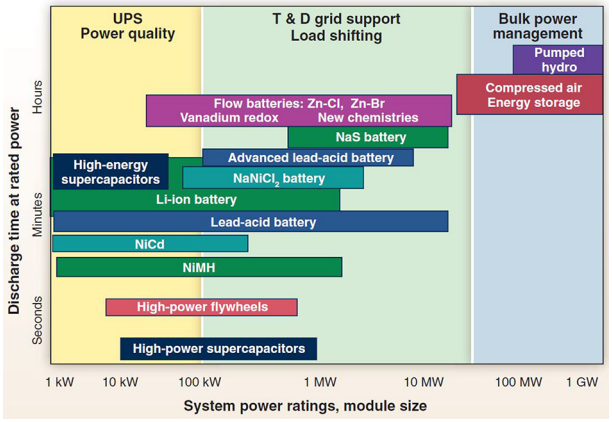

Figure 3. Comparison of discharge time and power rating for various electrical energy storage technologies highlighting the broad contribution of batteries with various chemistries; the latter being only based on inorganic electroactive materials, essentially metals. Reproduced with permission from ref 130. Copyright 2011 Science Publishing Group.

more seriously envisaged[132] because the cost of battery storage has declined fast in a few years with a drop of 73% between 2010 to 2016 to reach \$273 kWh^{-1} as market value while a value of \$73 kWh^{-1} is forecast in 2030.[133] Competing with gas-fired peaking plants is made possible. For example, more than 18 000 LIB packs (400-MW peak hour battery) would replace a gas-fired power in California.[134] Interestingly, the analysis of 3 years of real usage of LIBs (1 MW/250 kWh using 384 modules connected in series) installed and in operation in Hawaii has been recently reported by Dubarry et al.[135]

For such stationary applications, the capital invested and operational costs (maintenance, energy lost during cycling,

https://dx.doi.org/10.1021/acs.chemrev.9b00482
Chem. Rev. 2020, 120, 6490−6557

aging) are very important factors to consider for the entire life of the system. The reader could find compared cost factors in the literature including PbA, RFBs, LIBs, and so on.[5,130,136] The cost of storage can be calculated through the so-called levelized cost of stored energy (LCOE) defined as the total lifetime cost of the investment divided by the cumulated generated energy by this investment. The LCOE values at 25 years for an installed storage power of 1 MW are estimated at 0.338 and €1.978/kWh for RFBs and LIBs, respectively (against 3.072 for the PbA technology).[137]

2.3. Decarbonizing the Transportation Sector Through the Electrification Scheme

Beyond the electric grid, the pressure on batteries is also particularly intensive due to the deployment of decarbonized transportation systems through the massive use of electric motors (the so-called "electromobility" or "e-mobility") although the use of biofuels, oil-based fuels, and liquefied natural gas (LNG) has recently gained more attention.[121,138] [LNG consists mostly of CH_4 and has the potential to reduce SO_2-emissions over 90%, NOx-emissions with 80%, and CO_2-emissions 20%, which seems a competitive alternative in this sector provided there is less than 2% leakage.] Indeed, the transport sector's dependence on fossil fuels is another big part of the necessary transition toward a climate-neutral and sustainable society. Transport is a major source of total GHG emissions (22%), with road transport being the biggest contributor and responsible for about 72% of CO_2 emissions worldwide according to IPCC analyses.[139] Note that over 1.2 billion vehicles were in service in 2015 according to the International Organization of Motor Vehicle Manufacturers (OICA).[140] Moreover commercial air transportation still represents about 11% of global fuel consumption across all sectors, 2% of global CO_2 emissions, and 13% of emissions in the transport sector alone.[141] Beyond the dangerous GHG emissions when using Internal combustion engines (ICEs), the electric motor intrinsically possesses several advantages that have always been known such as better energy efficiencies (>90% because not subject to the Carnot cycle limitations of heat engines). They are also quieter, easy to miniaturize, and more importantly simpler in their design making the direct motor and wheel coupling possible. Conversely, a conventional ICE powered car typically has 10 000 moving parts (essentially within the drive train) against only 150 in battery electric vehicles (BEVs) today and only one of which is in the drive train as underlined by Parker.[142] The gains in maintenance as well as in energy efficiency are obvious.

Historically, the invention of ICE occurred in the middle of the 19th century just like that of the electric motor but at a time when oil and its derivatives were becoming cheap and widely available whereas high energy batteries did not exist yet. Gaston Planté had just invented the first rechargeable battery with its PbA technology (then improved by Camille Faure in 1881), which enabled however the first automobile speed record in 1899 (100 km h^{-1} but only on 2 km range) thanks to the first BEV named *"La jamais contente"* powered by 750 kg of Fulmen PbA batteries. In the early 1900s, 38% of the US automobile market was captured by electric vehicles. Even after this feat, ICEs would increasingly supplant the electric car for the next century especially thanks to Ford's innovations with the consequences that we are now witnessing. Now vehicle emission regulations have been forcing the automotive industry worldwide to reduce its carbon footprint especially in the EU, China, and India while governments around the world (like the Electric Vehicles Initiative (EVI))[143] are providing incentives to the citizens for buying electrified vehicles (EVs). The French government is to take the initiative to propose an ambitious Euro 7 emission standard at European level and set the goal of ending the sale of cars emitting greenhouse gases in 2040! The Swedish automaker Volvo has announced that from 2019 all its new models would be either hybrid or 100% electric. Note that EVs include battery electric vehicles (BEVs), plug-in hybrid electric vehicles (PHEVs), and fuel-cell electric vehicles (FCEVs). As a reminder, the key difference between BEVs and PHEVs is that FCEVs use a primary electrochemical cell (*i.e.*, fuel cell) to power the electric motor; the recharging step of FCEVs needing hydrogen as a fuel instead of electricity.

Based on the current roadmap reported by the International Energy Agency (IEA) in the BLUE Map scenario[144] (Figure 4a), rechargeable batteries are likely to remain the better choice to power light duty vehicles (LDV) in the next 2 decades whereas FCEVs are considered as the future vision for the global automotive industry beyond 2040−2050 because this technology and related hydrogen supply infrastructures are still not at the desirable level,[121,145] with the production of low-carbon H_2 being required too. For the present time progress made in recent years to improve battery performance and reduce costs[133] has already enabled the use of LIBs in numerous e-mobility applications such as two-wheelers, buses, taxis, shared cars, ride-hailing services, and the upcoming self-driving (or driverless) cars.

Thus, sales of new electric cars worldwide surpassed 1 million units in 2017 (for 3 million EVs in circulation), a record volume which represents a growth in new electric car sales of 54% compared with 2016 (more than half of global sales of electric cars were in the People's Republic of China) whereas the EV30@30 scenario makes as projection 228 million EVs (excluding two- and three-wheelers) on the road by 2030 as shown in Figure 4b;[143] the EV30@30 campaign redefining the EVI ambition originally set at 20 million EVs on the road by 2020. More recently, Hache et al.[146] have reported a bottom-up analysis using the Times Integrated Assessment Model (TIAM-IFPEN version) to forecast the diffusion of electrified road transportation modes by integrating two climate scenarios (4 and 2 °C) and two shapes of mobility (high/low mobility). The electric vehicles fleet could reach up to 1/3 of global fleet by 2050 in the 4 °C scenarios, while it could be up to 3/4 in the 2 °C scenarios both with high mobility, mostly located in Asian countries (China, India, and other developing countries in Asia) due to the large presence of 2- and 3-wheelers (Figure S2). Consequently, electric transportation is integrated into the smart grid/smart cities master plans[147] first because the electricity needs will boom but also as a means of flexibility since integrating BEVs/PHEVs into the electric utility grid facilitates both vehicle-to-grid (V2G) and grid-to-vehicle applications owing to the bidirectional nature of the power flows between the BEVs/PHEVs and the grid.

Last but not least, developing electric/hybrid aircraft is in progress too because electric propulsion has the potential to revolutionize aviation opening real opportunities for cleaner, quieter travel to completely new types of transportation models. In November 2017 Airbus announced the launching of E-Fan X with its partners Siemens and Rolls-Royce which is an ambitious technology demonstrator project: a hybrid civil aircraft, another emerging sector calling for high-performance batteries. Other equivalent projects exist such as the ZUNUM

https://dx.doi.org/10.1021/acs.chemrev.9b00482
Chem. Rev. 2020, 120, 6490−6557

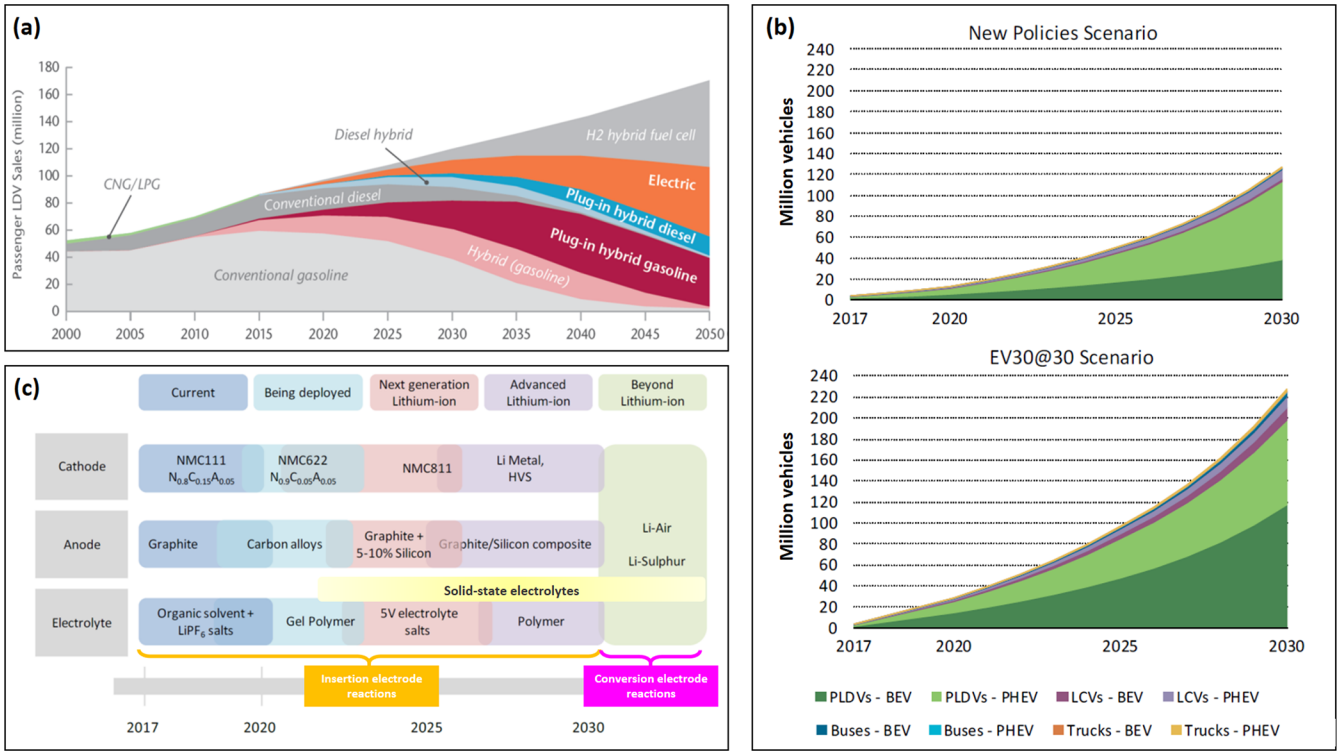

Figure 4. (a) Annual light-duty vehicle (LDV) sales according to the BLUE Map scenario,[144] 2000−2050 reported by IEA; combined EV/PHEV sales should share at least 50% of LDV sales worldwide by 2050. (b) Global EV stock for 2017−2030 excluding two- and three-wheelers by considering both New Policies Scenario and the EV30@30 Scenario reported by IEA[143] (PLDVs = passenger light duty vehicles; LCVs = light commercial vehicles; BEVs = battery electric vehicles; PHEV = plug-in hybrid electric vehicles). (c) Battery technology roadmap adapted from IEA[143] (HVS = high voltage spinel). Adapted with permission, copyrights of IEA.

Aero airliner project supported by Boeing. Interesting innovations can therefore be expected in the next decade even if there is a long way to go for large-scale practical applications.

2.4. Digitalization and Growing Consumption of Electronic Devices

The boom in electronic devices and digital technologies has been going on for almost 30 years, and batteries are generally needed to power them. The worldwide development of mobile phones is probably the most vivid example. As underlined by Galetovic et al.[148] in a very interesting world mobile phone industry study, the number of mobile phones sold rose 62-fold between 1994 and 2013 whereas in June 2015 there were around 7.5 billion subscriber connections, one for every person on the planet. But all this has an energy cost but also an environmental one. As an example, the entire mobile phone system in a small country like Italy consumes approximately 2200 GWh per year (0.7% of the national electricity consumption) while producing potential e-waste from end-of-life devices totaling over 11 thousand tons for the period from 2007 to 2012.

Today, consumer electronics (CE) mainly encompasses the whole range of home electronic equipment, from audio systems, home automation, home computing, and low-power electronics to multimedia systems. In addition, IoT has nowadays gained an incredible attraction[149,150] imparting networked connectivity to everyday objects in the physical world with numerous implications in logistics, manufacturing, retailing, environmental monitoring, healthcare monitoring, industrial monitoring, traffic monitoring, ... (as well as important monitoring in the smart grid and EVs to relate to the previous paragraph). In 2015, IBM predicted that 1 trillion devices would be connected to the Internet and the IoT. In 2017, a Cisco-revised forecast called for 50 billion devices to be connected by 2020 and, most recently, the GSMA Association predicted 25 billion IoT devices by 2025! Interesting data are reported by "The Shift Project" in several reports.[151] For example, the energy consumption of Information and Communication Technologies (ICT) is increasing by 9% every year while the share of ICT in GHG emissions has increased by half since 2013, rising from 2.5% to 3.7% in a few years.

Remarkable progress has also been made in many aspects of robotics for which 10 grand challenges have recently been pointed out in a Perspective article published in *Science Robotics*[152] including one related to power and energy sources to make the deployment of mobile robotics possible. In particular, "service robots" which smartly mix IoT and AI to assist human beings—typically by performing a job that is dirty, dull, distant, dangerous or repetitive, including household chores—are on the verge of equipping our homes and some public places. Impressive statistics and forecast have been announced by The International Federation of Robotics in the Executive Summary World Robotics 2018 Service Robots reports.[153] For instance, it was estimated in 2017 that nearly 6.1 million robots for domestic tasks, including vacuum cleaning, lawn-mowing, window cleaning and other types, were sold which corresponds to a 31% increase compared to 2016. The market for elderly and handicap assistance is also expected to increase substantially within the next 20 years.

In the same vein of recent developments, benefiting of electric propulsion R&D, the market of drones (UAVs) is also expected to rise at unprecedented rates due to growing interest

https://dx.doi.org/10.1021/acs.chemrev.9b00482
Chem. Rev. 2020, 120, 6490−6557

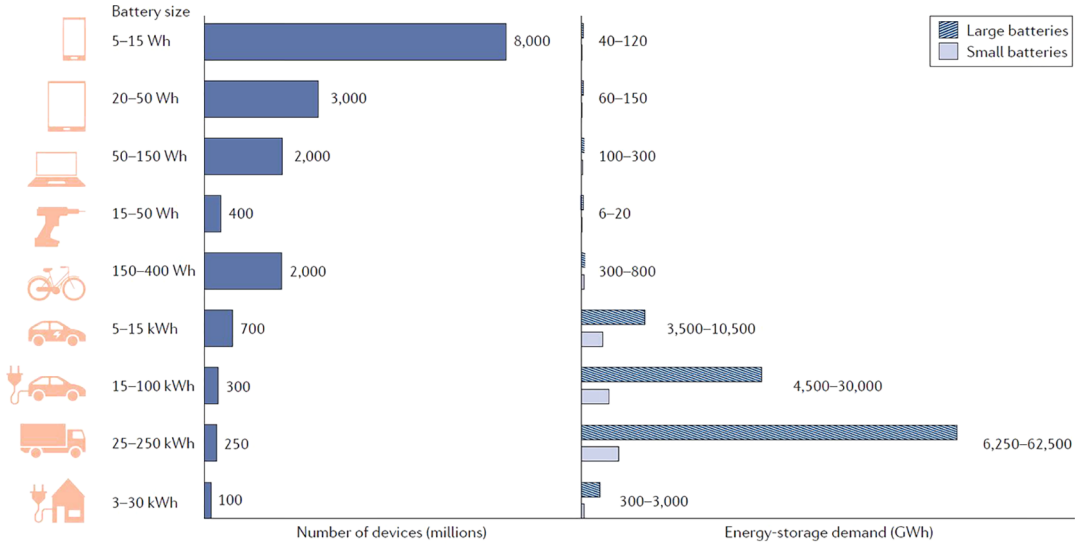

Figure 5. Estimated number of devices and related energy demand for 2016−2050. Note that all possible needs are not considered like the electric grid. Reproduced with permission from ref 154. Copyright 2019 Nature Publishing Group.

in monitoring applications by the military, researchers, farmers, hobbyists, and investors in e-business since drones offer superior abilities over their ground alternatives. It should be pointed out that using drones for commercial deliveries was something improbable ten years ago. Interestingly, Vaalma et al.[154] have very recently established a scenario-based supply and demand analysis concerning LIBs for 2016−2050 considering some selected applications including portable electronic devices and tools as well as several electrified road transportation modes and small stationary energy-storage devices (Figure 5). Clearly, if portable electronics dominates in terms of number of devices, they account for much less in terms of the total energy-storage demand if electric vehicles and residential energy-storage devices reach the high production numbers estimated in their scenarios.[154] However, several key applications such as the powering of domestic robots, drones, or IoT are not included in the scenario.

2.5. Summary

To sum up this overview, we are unambiguously facing a tremendous need for EES for a double reason, first as a key ingredient of the future energy engineering to fight global warming and, second, as a central hub for the emergence of disruptive technologies consecutive to the continuous modernization and development of mankind. The scale-up of industrial facilities for the production of rechargeable batteries, especially LIBs due to their high energy density values, is consequently an opened and sensitive question. The production is currently dominated by East-Asian competitors; with Panasonic (Japan) and LG Chem (South Korea), these leading manufacturers on the automotive market are closely followed by Samsung SDI (South Korea), CATL (China), and SK Innovation (South Korea). With its Gigafactory built in Nevada, Tesla (with Panasonic as a partner) is now on the road too on US soil whereas in the EU, things are moving forward to reduce its dependence on the Asia and US suppliers. Sweden's Northvolt has raised in June 2019 $1 billion in equity capital to complete funding for its future Gigafactory while France and Germany launched an Airbus-style €6 billion foray into the battery-building business. Considering a typical battery capacity range of 20−75 kWh, these factory capacities translate into a yearly production volume ranging between 6 000 to 400 000 packs.[143] To better visualize the world LIB manufacturing capacity and related international trade flows, Figures S3−4 report the thorough mapping analysis performed by Mayyas et al.[155] based on reliable collected data in 2016; the total LIB manufacturing capacity for this year was 189 762 MWh including 114 484 MWh for automobile LIBs. Finally, Bloomberg NEF announced in November 2018 a need for 1800 GWh by 2030 of LIBs including annual passenger EVs and E-buses, consumer electronics, and stationary storage; roughly eight out of every 10 batteries sold annually will find their way into a passenger electric vehicle;[156] however, details regarding the modeling and technical assumptions are not available. Anyway, the bottom line is battery production will have to be strongly scaled up in any scenario because a significant difference between supply and demand could occur.

But departing from these capability considerations, it is particularly important to avoid any pitfalls in this frenetic endeavor and make sure that proposed technical solutions are themselves sufficiently eco-friendly and sustainable. In other words, such large-scale perspectives force us to consider the environmental impact of rechargeable batteries (notably LIBs) as well as dependencies on raw materials. This critical point will be specifically discussed in the next section on the base of a selection of relevant data again ranging from chemical element abundance to potential environmental concerns related to their production and disposal.

3. MATERIAL SUPPLY FOR ELECTROCHEMICAL STORAGE: RESOURCE CONSTRAINTS ISSUES, ENVIRONMENTAL BURDEN, AND OPPORTUNITIES PROVIDED BY ORGANIC ELECTRODE MATERIALS

Even if some currents of thought advocate a negative or zero growth as a solution, it is believed that technology and its progressive developments should constitute the most important pillars of energy saving and GHG reducing. Nevertheless, it seems also established that with all decarbonization innovations notably in the broad field of energy, new environmental and resource issues are introduced with the growing need for ores and refined metals;[126,157] which partly offset the gains of

https://dx.doi.org/10.1021/acs.chemrev.9b00482
Chem. Rev. 2020, 120, 6490−6557

innovative solutions; a phenomenon known in the economic field as the "Jevons' paradox" or the Rebond effect.[158,159] In a very interesting paper published in 2011, Graedel wrote:[160] *Assessors of technology no longer tend to ask, "What is being used?" but rather, "What is not being used?" The answer to the last question is, increasingly, "Almost nothing."* In the last 20 years (1994−2014), world mining production of indium, rare earth elements (REEs), lithium, and cobalt increased from 149 to 819 tons, 64.5 to 133 ktons, 6.0 to 36.0 ktons, and 18.5 to 112.0 ktons, respectively, together with e-waste which is at the world scale unfortunately poorly collected and recycled.[161] Hence the large quantities of waste electrical and electronic equipment (WEEE) generated have raised a serious alarm on their potential adverse health and environmental consequences when incorrectly disposed of.

In 2012, Vesborg and Jaramillo[162] very nicely studied the tricky question about the scalability in the supply of chemical elements (and the related cost in energy) to promote technologies for energy harvesting, conversion or storage at the required TW-level for a sustainable future. Numerous relevant data are provided in this article such as correlations between crustal abundance and production of dozens of chemical elements while underlining the significant energy costs associated with providing the current flow of raw materials for energy technologies. Today's turbine blade alloys and coatings for wind energy converter make use of as many as a dozen metals while Electrical and Electronic Equipment (EEEs) incorporate some 60 metals most of which are classified as "critical metals" (CMs).[160,163,164] In short, CM refers roughly to imbalances between metal supply and demand (real or anticipated) at national, regional, or very local level, which induces variable appreciations, several definitions, and assessment methodologies. An extension to "critical raw materials" (CRMs) and the "criticality" term have appeared in the literature too.[146,164] For instance, through the Raw Materials Initiative (RMI) adopted in 2008,[146,165] the European Commission[166] has defined CRM when it faces high supply risks (e.g., geological, geopolitical, or production risk) or high environmental risks and is of high economic importance; 14 CRMs were identified in 2011, 20 in 2014, and 27 in 2017 as shown in Figure S5. Interestingly, Li is not considered as CM for the European Commission while the US has included it in its own list as reported by the Department Of the Interior in 2018.[167]

Respective to the scope of this article, the relevant question is therefore to establish if the current available and future battery technologies depend on high material resource constraints and at what cost in terms of environmental burden. A few elements of an answer will be provided below.

3.1. Resource Constraints Forecast in Conventional Material Supply

Based on the present state-of-the-art and whatever the considered technologies, electrode reactions involve redox-active inorganic compounds especially metal-based electroactive components, which is an historic heritage of the pioneered redox chemistry (the voltaic pile followed by the PbA secondary cell) as well as the material engineering that resulted (Figure 3). For instance, if we consider the battery technology roadmap for electrified vehicles (Figure 4c) it is expected that at least until 2030 matured and advanced insertion inorganic positive electrode materials will be essentially based on the 3d-metal redox chemistry. However, it is also widely acknowledged that traditional Li-ion batteries are starting to approach their limits especially for long-range EVs. Beyond 2030 other battery chemistries are envisaged namely post-LIB systems. First, it is commonly forecast that conversion-based cathode reactions could be used (with O_2 and S) in Li-metal battery configuration (Figure 4c), which supposes however the achievement of consequent improvements.[168] Recent R&D trends also indicate an expected switch from liquid (organic) electrolytes to ceramic electrolytes (or solid state electrolytes, SEEs) notably following the recent discovery of lithium superionic conductors at room temperature by Kanno and co-workers (σ_{Li^+} = 25 mS cm^{-1} for $Li_{9.54}Si_{1.74}P_{1.44}S_{11.7}Cl_{0.3}$).[169,170] All-solid-state batteries operating at moderate temperatures offer an attractive option for non-flammable batteries while achieving both high power and high energy densities because it is also a relevant option to reopen the safe use of pure alkali metals especially Li as anode material when paired with high-potential insertion materials (5 V spinel materials, Figure 4c) or with conversion S/O_2-based cathodes.[171] Nevertheless, this ceramic electrolyte option could require again the consumption of more inorganic materials such as metal-based sulfides, oxides, or phosphates.[169,172] It is worth noting that the emerging field of Na and Na-ion batteries which are also considered in the post-LIB field logically follows the same trajectory in terms of materials choice and design as a sister material chemistry of Li-based batteries.[173,174] In addition, it should be remembered that major built RFBs also draw their chemical power from 3d-metals as well as already underlined above.

While the number of publications and other reports has greatly increased in recent years on the potential bottlenecks in material supplies due to the ramping up of LIBs,[146,155,154,175−177] the resource issue questionings in the field of energy storage are not new especially for EV fleets since interesting estimates were already reported by Andersson and Råde[178] as early as 2001 by taking into account almost all cell chemistries at that time: Li-metal polymer (LMP), LIBs, sodium nickel chloride (NaNiCl or ZEBRA batteries), Ni-metal hydrides (Ni-MH), and PbA. Generally speaking, batteries that contain two or more scarce metals may suffer from being limited by the availability of any of them. With the pressure on LIBs and future Li-based technologies, the main current concern is about the potential risks surrounding the supply (and related price volatility) of lithium and 3d-metals with battery-grade quality (Co and Ni, essentially), which also raises the tricky question of the mining interdependencies of elements;[155] note that natural graphite is commonly reported as CRM. Indeed, the supply of cobalt is complicated by the fact that this element is not typically the primary product of mining operations; it is a coproduct of nickel (50%) mining.[179] Figure S6 shows a mapping and quantified data regarding the world mining industry production for materials used in LIBs.[155] Taking 2016 as the year of reference, the battery industry's demand for lithium and cobalt is 46% and 50% of the world production, respectively.[154] It should also be underlined that 54% of the mining production of Co comes from the Democratic Republic of Congo, a country characterized by socio-political instability, a persistent economic stagnation, and no environmental policies; the country could lose 40% of its forests by 2050 notably due to mining activities.[180]

To ensure continuous flows of raw materials, new agreements are set up between critical material suppliers and different customers; for example, Apple Inc. seems interested in buying long-term supplies of cobalt directly from miners.[181] As previously stated by Andersson and Råde,[178] closed loop recycling

https://dx.doi.org/10.1021/acs.chemrev.9b00482
Chem. Rev. 2020, 120, 6490−6557

solutions and a high level of collection of spent batteries are required to ensure that the stock of available metals for batteries is not drained. The case of PbA batteries constitutes a textbook example with a collection of spent batteries above 99.9% thanks to environmental rules due to the lead toxicity together with existing efficient recycling processes of this simpler battery chemistry based essentially on Pb(Bi). In 2016, almost all end-of-life LIB were batteries from consumer electronics and 95% of spent LIB were unfortunately landfilled.[182] Unlike recycling of PbA batteries, recycling of LIBs seems for the moment not economically profitable albeit recycling LIBs could save up to 51.3% of the natural resource required to produce virgin materials (concept of Urban Mines).[182] Today, most recyclers focus on recovering expensive materials mainly from positive electrode powders, but lithium is rarely recovered (less than 1% of lithium is recycled). Stronger political incentives seem required to promote recycling. In the EU, the 2006/66/EC European directive[183] imposes a minimum recycling efficiency of Li-batteries at 50% by average weight into materials for their original purpose or for other purposes and second, encourages technological developments that improve the environmental performance of batteries throughout their entire life. The reader can get precise and recent data regarding recycling end-of-life batteries, processing, and collections reported in refs 146, 155, 182, and 184−187. Another hot point is that predictions underlined that all the material demand just for EV batteries will have to be supplied by resource extraction at least up to 2030 whatever the collection and recycling of spent battery electrode materials due to the eight-to-ten-year lifetime of EV batteries.[143] Note that reuse of EV batteries can offset the production burden of new batteries by extending battery service life.

3.2. Sustainability and Environmental Aspects

Beyond battery resource considerations which are getting all the attention today, let us also remember that mining operations are destructive for the environment and energy-greedy and fall short of both the sustainability and CO_2 footprint criteria.[84,112] Moreover, the scarcity of most of these elements in the earth crust (Figure 6) could make their excavation more and more energy intensive and costly depending on the nature of the deposit because it must be kept in mind that elemental availability cannot be judged by crustal abundance alone (see ref 162 for more details). Moreover, after the extraction of ores, several refining steps are necessary to obtain the final reagents which will be engaged thereafter in high temperature synthesis reactions ($T \approx 600$ °C) to produce the desired electrode material.

At this stage, relevant data to evaluate potential environment concerns as well as the related energy cost for the production of batteries can be found in life cycle assessment (LCA) studies. Although LCA can be considered as a standardized methodology, it depends on the inventory database used and system boundaries. Consequently, LCA results in the literature differ significantly due to these uncertainties. Peters et al.[192] have reported in 2017 an interesting review of LCA studies on LIBs. After a thorough review of 113 available publications on the topic, a total of 36 LCA studies were identified as very reliable because they provide detailed results for LIB production and sufficient information to recalculate the reported results. The conclusion is, on average, a cumulative energy demand (denoted "embodied energy") of 328 kWh is needed across all chemistries to produce 1 kWh of stored electrochemical energy producing GHG emissions of 110 gCO_2eq.

Beyond LIBs, other similar values concerning PbA, Ni-MH, or VRFBs can be found in the literature too.[193,194] Note that the majority of existing studies are focused on GHG emissions or energy demand; however, other Eco indicators such as human toxicity (HTP) might be even more important.[192,195] More importantly, such LCA studies are restricted at the manufacturing outlet ("cradle-to-gate analyses" and not "cradle-to-grave analyses"), so they do not take into account both collection and recycling steps. Yet the results obtained show that battery manufacturing is energy-intensive because of the involvement of quite high flows of exergy mainly due to the chemical nature of the commonly used materials (inorganic compounds).[112,162]

As a result, one common recommendation of current LCA analyses is the deployment of batteries with higher round-trip efficiency to extend the cycle life in operation but also the need for low-carbon innovations in future technologies while favoring the use of naturally abundant chemical elements of low toxicity. Within this background, one current trend in the post-LIB field is to reinvestigate Na-ion batteries as candidates for medium and large-scale stationary energy storage in light of possible concerns in terms of cost and abundancy of lithium.[174,196,197]

3.3. Positioning Redox-Active Organic Species in the Battery Landscape

Within this background, which is particularly tense in many ways, the idea of taking advantage of organic chemistry for the electrochemical storage of energy can make sense. As stated in the Introduction, the idea to use organic electrode materials (OEMs) for rechargeable batteries is not new and goes back to the discovery of reversible redox-activity of conducting polymers in the late 70s following the discovery of PAc by Shirakawa[61−64] and its subsequent electrochemical activity (doping) both in oxidation and in reduction.[65,66] These findings led to the development of various conducting polymers as well as a first attempt to emerge in the marketplace before the boom of high-energy LIBs.[59,69] Today the motivations are different and authors agree that organics can be notably seen as a pathway to stabilize the pressure on the CRM for energy storage while seeking to improve the environmental footprint as well as finding innovative storage solutions.[42,84] Of course, OEMs have limitations especially when talking about volumetric energy density that can be achieved due to their intrinsic low volumetric mass densities (<2 g cm^{-3}). Excluding ORFBs, this issue can be exacerbated by the need for large carbon addition when preparing composite electrodes. Moreover, their greater propensity to solubilize in liquids compared to inorganic compounds is an issue for solid electrodes but an asset for ORFBs. The development of organic batteries is clearly in its early stages compared to 150 years of intensive research and innovations dedicated to conventional inorganic-based electrochemical storage devices explaining why some room is expected to be given to redox-active organic species in the battery landscape. To be convinced, Figure 7 reports an interesting assessment for the electrochemical storage of OEMs classified by families.[31] In fact, organics exhibit several interesting assets as recapped below.

First, organics make potential access to low cost and greener chemistry possible because they are mainly composed of C, H, O, N, and S, which are naturally abundant elements as well as the main constituents of biomass (Figure 6).[191] This situation

https://dx.doi.org/10.1021/acs.chemrev.9b00482
Chem. Rev. 2020, 120, 6490−6557

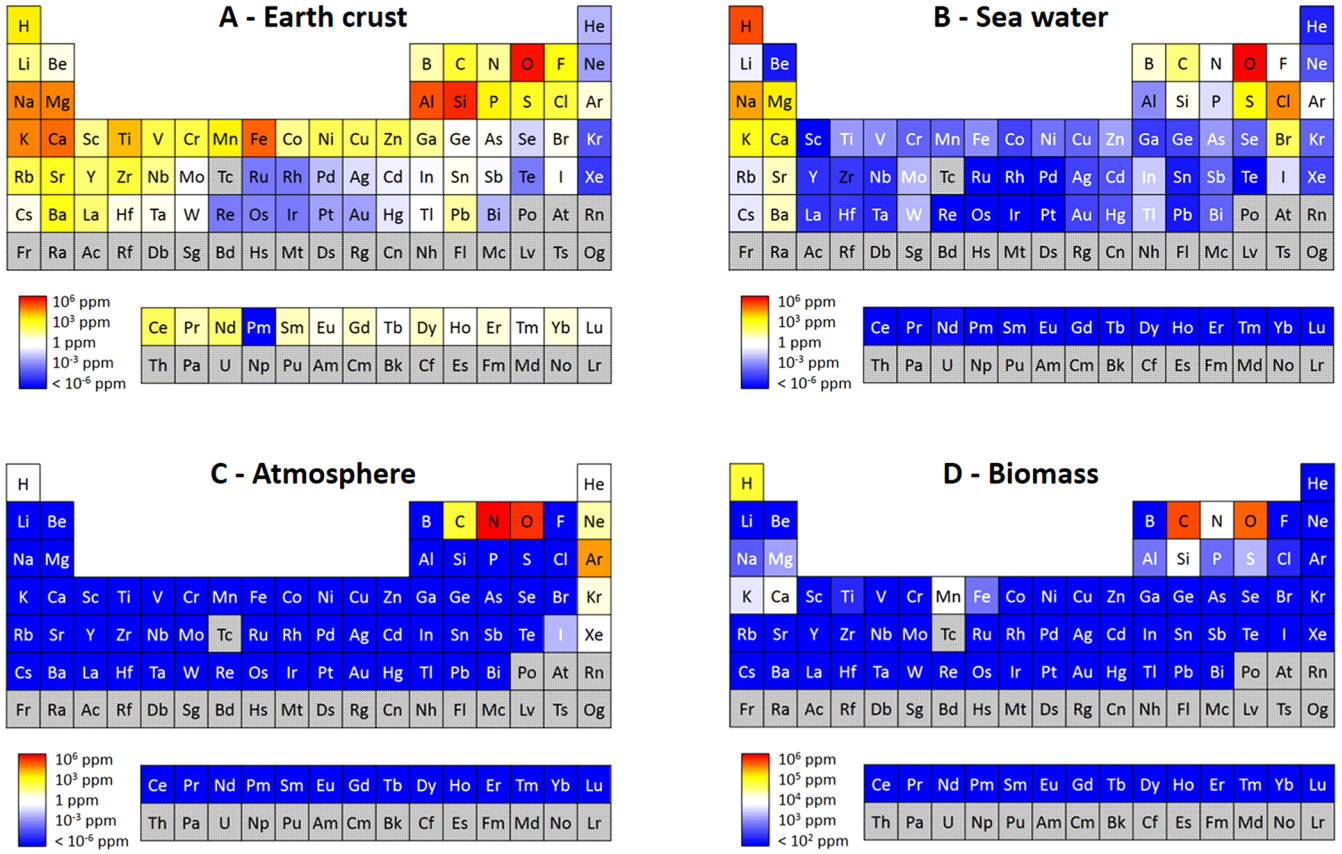

Figure 6. Periodic tables showing the abundance of elements in the Earth's crust (A), in the seawater (B), in the atmosphere (C), and in biomass (D); elements in gray indicate natural and/or radioactive elements. Courtesy of L. Simonin, CEA-Liten, adapted from ref 188 taking into account data from refs 189−191. This analysis highlights that among the naturally occurring elements only a few of them are abundant in each of these four compartments, which demonstrates the importance of developing recycling solutions too.

offers opportunities to prepare electrodes (and other components in a cell like binders)[198] from renewable resources benefiting from ongoing progress in the vast field of biorefineries too.[199−201] Hydrolysis lignin features were even assessed in primary Li-cell[202] or more interestingly in combination with PPy in an interpenetrating lignosulfonate/PPy thin-film composite electrode tested in 0.1 M aqueous $HClO_4$ as electrolyte, with the catechol moiety in lignin being used for reversible electron and proton storage/uptake.[203] Several naturally occurring polyphenols (e.g., ellagic acid,[204] purpurin,[205] lawsone[206]) were electrochemically assessed in Li/Na half cells; however, the proof of concept of making a "renewable" all-organic Li-ion battery was first demonstrated with oxocarbon derivatives as active electrode materials ten years ago.[82−84] Esquivel and co-workers[207] have also demonstrated opportunities for portable and disposable single-use applications to power small devices with the concept of PowerPAD (Power: Portable And Disposable), a fully organic and completely biodegradable battery designed to operate for relatively short periods of time (from minutes to 1−2 h). The promising field of ORFBs (see section 9) has also demonstrated interest in the use of redox-active naturally occurring polyphenols/quinones for abundancy and cost reasons.[20,34] At this stage, it must be underlined that common routes to synthesize OEMs in this emerging field deal with petrochemicals. However, even if large scale production were used for high-performance OEMs in the future, petrochemicals are higher-value products than petroleum products for combustion (only a small fraction (≈4%) of oil worldwide is used to make chemicals[42]). In terms of cost, it is difficult to make predictions for petrochemical reagents notably if in the future the demand for petroleum products used for combustion decreases; the access to new markets and applications can change the game. However, it is generally accepted that fluorinated derivatives are among the most expensive compounds.

Second, simplified recycling managements of organic spent batteries (Figure S7) can be expected notably with solid electrodes since organic structures are typical fuels that can be consumed by combustion at medium temperatures producing heat (energy recovery). Interestingly, if spent organic batteries were inadvertently not collected (spread out in the wild), the loss of scarce and costly metallic chemical is notably reduced compared to the current battery technologies. Moreover, the use of biodegradable materials can be envisaged too.

Last but not least, organic chemistry offers high structural designability providing great opportunities to find novel and innovative electrode materials with specific properties including the elaboration of multimodal systems such as electrochemical/chemical or electrochemical/photochemical rechargeability.[208−210] More importantly, physicochemical properties can be rationally tuned using well-established principles of organic chemistry and molecular engineering giving access to redox-active species able to work:

- from dissolved to solid state (including polymers) in aqueous or nonaqueous electrolytes making them versatile in terms of electrochemical storage devices including access to flexible devices;

https://dx.doi.org/10.1021/acs.chemrev.9b00482
Chem. Rev. 2020, 120, 6490−6557

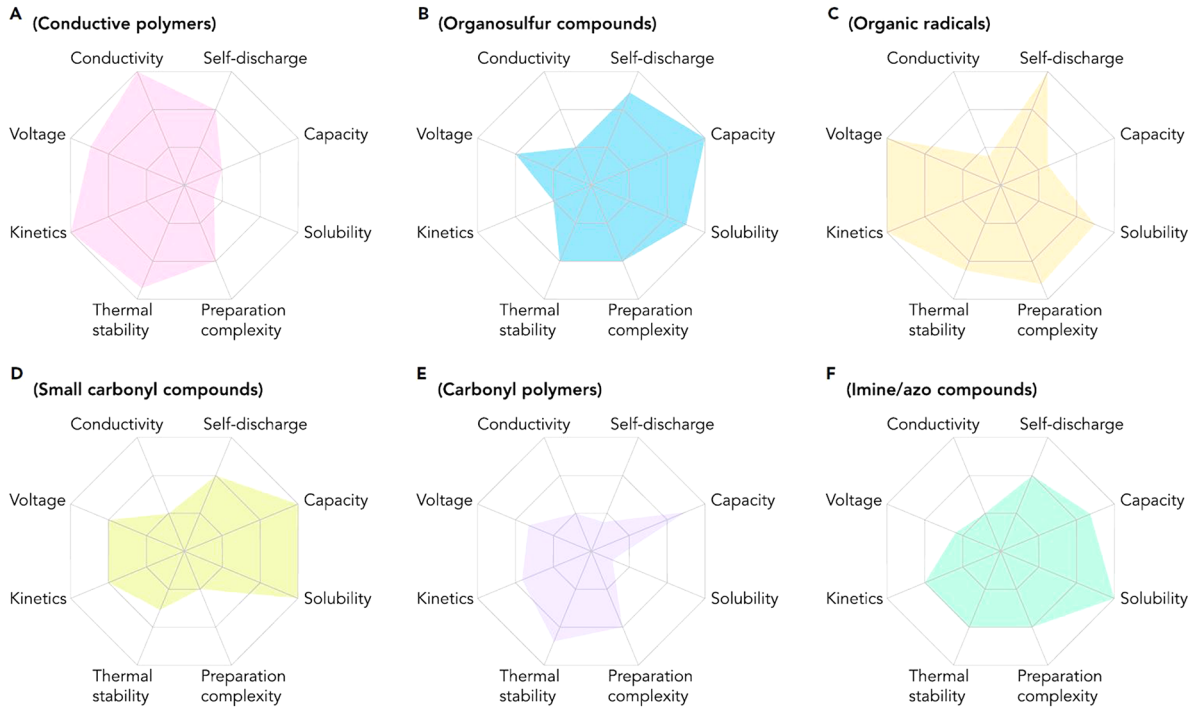

Figure 7. Overview of fundamental properties of different types of organic electrode materials. Reproduced with permission from ref 38. Copyright 2018 Elsevier Ltd.

- through two electrochemical storage mechanisms (n- or p-type electrode reaction with cation or anion charge compensation) making various electrode configurations possible (see the next section);
- at adjusted redox potential because the electron density at the molecular level can be easily tuned by mesomerism in conjugated systems and more importantly by inductive effects using either electron-withdrawing (−I) groups or electron-donating (+I) groups. For example, computational modeling concerning the one-electron reduction potential of various substituted quinones shows a possible potential tuning (ΔE°) of about 1.5 V;[211]
- with potentially reversible multielectron reactions which could counterbalance a slightly too important molecular weight;
- with multivalent cation and bulky ions (e.g., Mg^{2+}, K^{+}, PF_6^{-}) because organics (polymers and crystallized host structures) can better accommodate structural changes thanks to weak-bond networking;
- potentially without any metal following the concept of "molecular organic-ion battery".[212−214]

Whether organic chemistry offers high structural designability through this multiplicity of chemical combinations at the molecular level, it could be somewhat challenging to grasp the electrochemical working principle of the reported OEMs in the literature for researchers more familiar with inorganic electrode materials. In the next section we will try to make understandable all the redox functioning of organic molecular assemblies with the basics of electrochemical cells as a starting point.

4. FUNDAMENTALS OF ORGANIC ELECTRODE COMPOUNDS FOR ELECTROCHEMICAL STORAGE

4.1. Basics of Electrochemical Cells

As reported in all undergraduate chemistry books, primary and secondary (rechargeable) cells (or batteries) produce discharge DC current for an output voltage of a few volts by direct conversion of chemical energy by virtue of two opposite oxidation−reduction processes occurring at two separated electrodes (current collectors) maintained in ionic contact through an electrolytic medium (Figure 8).[84] In such a situation, the two half redox reactions taking place at electrodes are called "electrochemical reactions". During discharge (spontaneous cell reaction or galvanic cell reaction), the electrochemical reduction reaction occurs at the positive electrode whereas the electrochemical oxidation reaction occurs at the negative electrode. For rechargeable cells, the terminology should be obviously reversed during charge (electrolysis cell reaction). Therefore, to avoid confusions, the terms "positive" electrode or "negative" electrode are preferred whatever the considered cell reaction (i.e., charging or discharging), with the positive electrode always displaying the highest potential value. Note that a cell is the basic electrochemical unit. A battery is composed, strictly speaking, of two or more such cells connected in series or parallel. However, the term battery has evolved, especially in the language of the end user; therefore, the term "battery" will be used herein without this distinction for the sake of simplicity.

The use of two antagonist redox couples is then required with (e.g., Ox_1/Red_1 and Ox_2/Red_2 characterized by standard potentials $E^{\circ}(Ox_1/Red_1) > E^{\circ}(Ox_2/Red_2)$) to reach high electromotive force ($emf = E_{I=0}$, in V) at the cell level under zero current since *emf* depends on the difference $E^{\circ}(Ox_1/Red_1) - E^{\circ}(Ox_2/Red_2) > 0$ or more generally on the difference $E(+) - E(-) > 0$. In short, it depends on the thermodynamics of the chosen electrode chemistries because $E_{I=0}$ is related to the Gibbs free energy change of the galvanic cell reaction, $\Delta_r G$, as follows: $\Delta_r G = -n \cdot E_{I=0} \cdot F$ (n being the number of electrons involved in the cell reaction and F is the Faraday constant, equal to 96,485 C mol^{-1}). Under discharge current (I, in mA), for example, the operating voltage, $E_{I\neq 0}$, is lower than the $E_{I=0}$

https://dx.doi.org/10.1021/acs.chemrev.9b00482
Chem. Rev. 2020, 120, 6490−6557

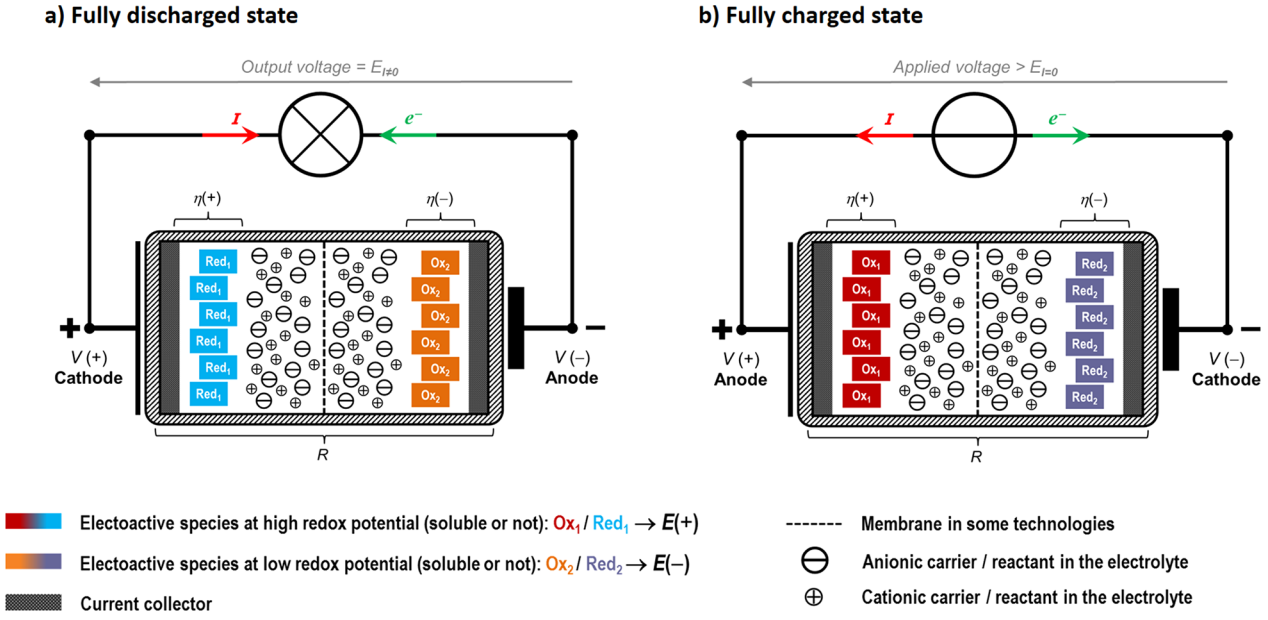

Figure 8. General architecture of an electrochemical cell for energy storage whatever the considered technology is. Note that additional electrolyte can be stored externally and then pumped through the cell in the particular case of a flow battery (see Section 9). (a) Cell under discharge (namely galvanic cell) at 100% depth-of-discharge (DOD). (b) Cell under charge (namely electrolysis cell) at 100% state-of-charge (SOC); the electromotive force value ($emf = E_{I=0}$) is, in principle, at the maximum value. The measured capacity, Q (in mAh), is experimentally obtained by integrating the operating time with current: $Q = \int_0^t I(t)\cdot dt = I\cdot\Delta t$ which gives rise to $Q = I\cdot\Delta t$ whereas the energy, ε (in mWh), is obtained by multiplying Q with the voltage $E_{I\neq0}$.

value because of (i) kinetic limitations at the electrodes (overpotentials or polarization losses, η) and (ii) ohmic drop ("$R\cdot I$" term) due to the overall ohmic resistance (R, in Ω) of electrodes and electrolytes as shown below:

$$E_{I\neq0} = [E(+) - E(-)] - [\eta(+) + \eta(-)] - [R\cdot I]$$

Obviously, high $E_{I=0}$ values with minimum losses in operation are sought after together with high capacity values, Q, in C (or Ah a unit more generally used in the field of electrochemical generators). By virtue of Faraday's law, the theoretical expected Q value of a cell is proportional to n and the amounts of the redox (electroactive) chemical species. Normalizations of Q are often reported to make performance comparison easier giving rise for example to specific capacity (Q_m) per gram of electroactive compound and volumetric capacity (Q_v) per cm^3 of electroactive compound (M being the molar mass and ρ the specific density of the electroactive species, respectively):

$$Q_m\ (\mathrm{C\ g^{-1}}) = n\cdot F/M \text{ or } Q_m\ (\mathrm{mAh\ g^{-1}}) = n\cdot 26805/M$$

$$Q_v\ (\mathrm{C\ cm^{-3}}) = n\cdot F\cdot\rho/M \text{ or } Q_v\ (\mathrm{mAh\ cm^{-3}}) = n\cdot 26805\cdot\rho/M$$

Multiplying Q with $E_{I\neq0}$ at any time during the discharge makes the calculation of the as-obtained energy, ε (in mWh). Of course, high reversibility of the cell reaction (good cyclability), high Coulombic efficiency, and low self-discharge are notably required for long-lasting cycling of rechargeable batteries. More details can be found in specialized books (see for example, ref 2).

4.2. Bridging the Gap between Inorganic and Organic Redox Chemistry

As previously recapped, oxidation−reduction reactions make electricity production possible when properly used in a two-electrode cell design. Hence, redox-active chemical systems (especially reversible ones) constitute the workhorse of the electrochemist in the design of electrochemical generators. Beyond exploiting the potential values of redox couples (thermodynamics) to decide if the interest for a given system is related to positive or negative electrode application, the electrochemist follows with a great deal of interest variations of oxidation states (*OS*; or oxidation number, *ON*) of chemical elements constituting the considered redox couples because it allows us to readily understand and rationalize the formal involved redox center as well as subsequently determine the number of electrons involved in the half-reaction. Latimer appears to be the first to introduce this concept within the context of redox half-reactions.[215]

According to the IUPAC definition,[216] the *OS* of an atom is the charge of that atom after an ionic approximation of its heteroatomic bonds. The bonds between atoms of the same element are not replaced by ionic bonds; they are divided equally. In other words, to determine the *OS* of a given atom, it is therefore considered that all heteroatomic bonds in which it participates are 100% ionic and the electrons of each of these bonds are assigned to the most electronegative atom (Allen's scale). Moreover, IUPAC recommends two closely related general algorithms for *OS* calculation in molecules, ions, and extended solids:[216]

- **Algorithm of assigning bonds.** This algorithm works on structural Lewis formulas of molecules and ions which show all valence electrons.
- **Algorithm of summing bond orders.** This algorithm works on structural Lewis formulas and bond graphs for an extended solid, especially iono-covalent structures.

However, as thoroughly explained above, because the used redox chemistry in battery applications is related to the *OS* change of the 3d-metallic redox centers (e.g., Ti, V, Mn, Fe, Co, Ni) or elemental/diatomic substances (e.g., Li, Na, Mg, C, O_2, Si, P, S, Sn),[11] a set of more general rules for determining *OS* is more readily used (e.g., *"the sum of OS for all atoms in the*

https://dx.doi.org/10.1021/acs.chemrev.9b00482
Chem. Rev. 2020, 120, 6490−6557

species is zero to ensure electroneutrality", "Fluorine: − 1", "Oxygen: − 2 unless combined with fluorine", and so on) as nicely recalled by Walsh et al.[217] Although not recommended by IUPAC, this simplest method is quite sufficient to assign *OS* of most (inorganic) ions and extended solids. Complications occur when two identical atoms have different *OS* in the same compound like observed with several inorganic compounds based on chemical elements prone to catenation (*e.g.*, C, N, S, Si, I). This is precisely the situation encountered with organic compounds, which justifies the use of the algorithm of assigning bonds recommended by IUPAC based on Lewis formulas of molecules and ions to determine *OS* or organics. In practice, after assignment of electrons of each bond to the most electronegative element, the *OS* of element "*i*" is calculated as follows:

$$OS(i) = \text{valence electrons of the element } "i" - \sum \text{assigned electrons}$$

Two selected examples are shown below including the case of the inorganic thiosulfate anion ($S_2O_3^{2-}$) considering that the sulfur−sulfur bond is practically a single bond together with *p*-benzoquinone as representative redox-active organic molecule. Note that only half of *OS* are reported due to the molecule symmetry whereas the green lines indicate the electrons assigned per atom. To briefly comment on the redox activity of *p*-benzoquinone, each carbon atom bearing the oxygen (in bold) exhibits an *OS* value of +2 that is decreased at +1 after the two-electron reduction to produce *p*-hydroquinone.

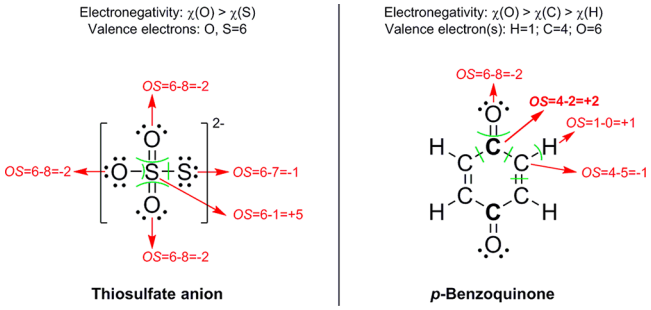

4.3. Reversible Organic Redox Chemistry and Cell Configurations

Oxidation−reduction processes in organic chemistry, which commonly involve both *s* and *p* orbitals, can be classified in two different groups. In the first group, the electronic process is accompanied by atom transfer reaction (e.g., gain of oxygen for oxidation or hydrogen for reduction) including possible fragmentation or condensation subsequent reactions.[218] However, such organic redox reactions are basically used for organic synthesis purpose as shown below in the case of the hydrogenation reaction of the most accessible double bond of limonene (reduction process of the C═C double bond with decreasing of the *OS* of the two carbon atoms whereas the two incorporated H atoms exhibiting an *OS* of +1).

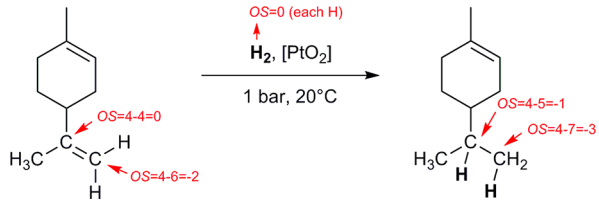

More interestingly for us are the redox processes for which no formation or rupture of electron-pair single bonds occurs after simple charge transfer reaction. In this latter case, stepwise transfer of single electrons must in principle be taken into account[219] giving potentially access to reversible organic redox couples like conventional third-kind electrode reactions (e.g., $Ce^{4+} + e^- \rightleftharpoons Ce^{3+}$). However, caution should be exercised because one-electron oxidation or reduction of a neutral or ionic organic scaffold produces generally reactive ion radicals or radicals with possible subsequent reaction such as radical coupling. Consequently, some chemical tricks have to be used to ensure the production of stable (persistent) radical structures after charge transfer.[220,221] Thus, simple π-extension and substituents of resonance electron donating or withdrawing groups (mesomerism) make delocalization of spin and charge density possible which deeply reduces the reactivity of the odd electron (e.g., galvinoxyl or tris(pentachlorophenyl)-methyl radicals). Aromatization after electron transfer and appropriate steric protection play also important role to protect a reactive radical center. Robust functional groups bearing an unpaired electron also exist such as nitroxide radicals (>N−O$^\bullet$). In this family, 2,2,6,6-tetramethylpiperidinyl-*N*-oxy (TEMPO) constitutes the most representative example. Beyond the realization of magnetic organic materials,[221] the nitroxide redox chemistry is at the origin of the rise of ORBs,[10,75−77] a field particularly studied by Nishide, Oyaizu, and co-workers as previously underlined in the Introduction. Finally, the general structure principles that lead to multistage organic redox systems (expected reversible from a redox point of view) are owed to Deuchert and Hünig[219] reported in a comprehensive article published in 1978.

Figure 9a recalls the three general key organic structures and their related charge transfer steps deriving from Hünig's classification together with representative examples of chemical compounds. Basically, two electrochemical storage mechanisms are accessible with organics characterized either by anion charge compensation (p-type system or System A) or by cation charge compensation (n-type system or System B); System C being a mixed assembly also named "bipolar" system. At otherwise constant conditions it is worth noting that redox-active p-type moiety exhibits as a rule higher formal potential values compared to n-type systems.[219] Figure 9b shows the corresponding cell configurations. For instance, developing Li-ion organic batteries requires two n-type compounds (Figure 9b-1). The p-type redox reactivity is rarely encountered with inorganic electrode materials. Except carbonaceous materials which intercalate ions at relatively high potential (use as positive electrode),[222−225] only a few conversion-type electrode materials have been reported to date (for F-ion batteries) exhibiting however poor electrochemical performances.[226] On the other hand, p-type organic compounds enable, in principle, the development of anionic rocking-chair cells[227,228] and potentially full "molecular" organic-ion batteries if the shuttling anion is metal free (Figure 9b-2). Nevertheless, the cell assembly most often encountered in the literature remains the dual-ion battery (Figure 9b-3) as recently review by Zhou et al.[229] The use at the electrode level of advanced mixed p/n-type organic scaffolds that exchange simultaneously cations and anions can also be envisaged as recently shown in aqueous batteries with naphthalene diimide repeating units coupled to bipyridinium.[230−232] The molecular engineering can even allow cation shuttling in the electrolyte while using p-type electrodes as reported by Nishide, Oyaizu, and co-workers

https://dx.doi.org/10.1021/acs.chemrev.9b00482
Chem. Rev. 2020, 120, 6490−6557

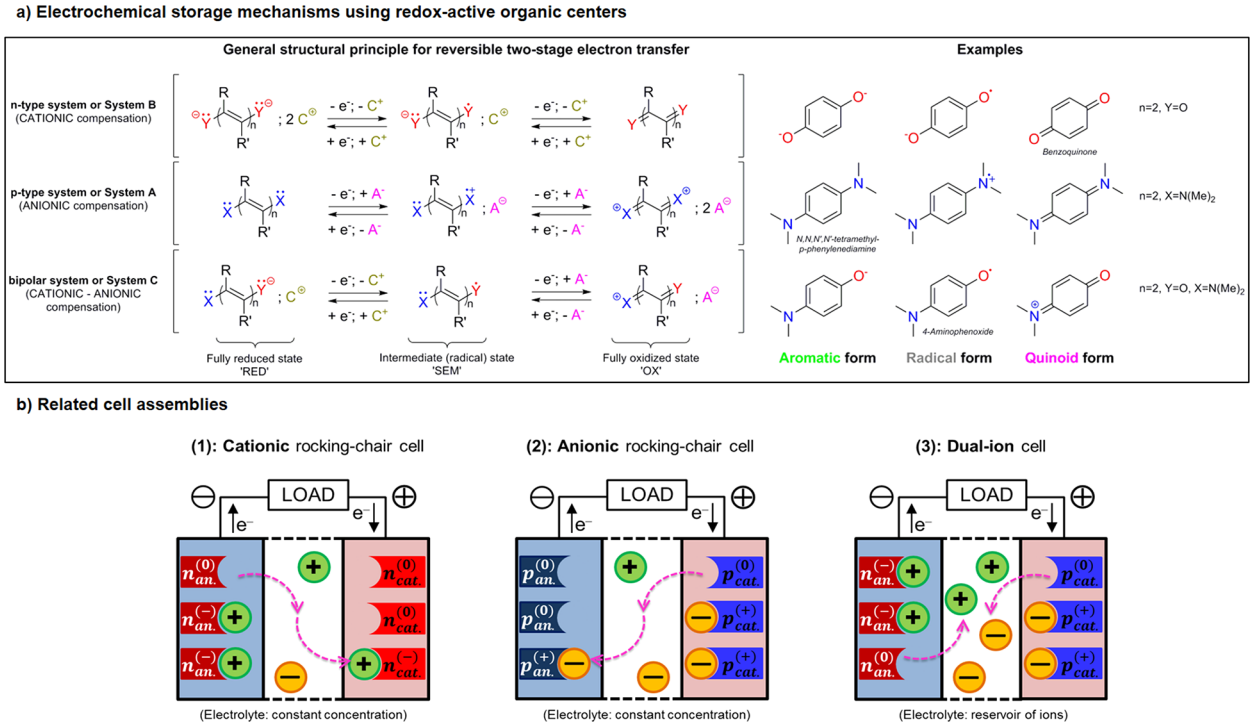

Figure 9. (a) Key reversible redox-active organic systems at the molecular level and their related charge transfer steps (adapted from refs 219 and 234) together with representative examples exhibiting the redox rocking from aromatic to quinoid form. X/Y could be N, O, S, P, π-systems but also carboxylate, anhydride, or amide functional groups; R, R′ being potentiality integrated within the same cyclic structure. Note that that p- and n-type structures correspond to system A and B, respectively, according to Hünig's classification.[219] (b) Corresponding cell configurations obtained by playing with both n- and p-type systems shown during the discharge process. Again, additional electrolyte can be stored externally and then pumped through the cell in the particular case of a flow battery (see Section 9). Adapted with permission from ref 36. Copyright 2018 Elsevier Ltd.

with copolymer compositions of TEMPO−sulfonate anionic group.[233]

Finally, before reporting our selection (with description) of the best organic-based batteries to date, a summary of the organic families of interest for electrochemical storage is shown in Table 1 demonstrating the richness in terms of formal redox center as well as the relevance of conjugated structures in general.

5. PERFORMANCES OF NONAQUEOUS LITHIUM−ORGANIC BATTERIES

This section constitutes the first in a series of five (from section 5 to 9) in which a personal selection of organic-based rechargeable cells will be described and commented on. Nonaqueous Li−organic batteries have by far the longest history among all branches of battery OEMs applications. The results from these pieces of research have also directly fueled or inspired the design of OEMs for other emerging organic batteries. Several comprehensive review articles have covered virtually every category of OEMs used in Li−organic batteries;[9,39,43,47] hence, another comprehensive write-up on the topic is not intended herein. Instead, we will focus on the best performance ever achieved by OEMs in these batteries as well as the design rationale behind these successes. In particular, three key performance parameters will be reviewed: operating potential, specific capacity, and cycling stability. The properties and cell performance of these materials are summarized for comprehensive comparison (Table 2).

5.1. Positioning the Operation Voltage

A large variety of redox active functional groups have been explored for designing OEMs for Li-based batteries, and the voltages of cells based on these OEMs vary by a wide extent as a result. Depending on their operating potentials, OEMs may be used either as positive electrode (>2.2 V vs Li^+/Li) or negative electrode (<1.5 V vs Li^+/Li) active materials. Again, OEMs intrinsically showing the highest potentials, e.g. >3.5 V vs Li^+/Li, are p-type compounds which, upon charge, lose electrons and accept anions from the electrolytes (Figure 9). As previously mentioned, conductive polymers, which had been intensively studied as positive electrode materials to enable Li batteries (dual-ion cell configuration, Figure 9b-3), fall into this category too. Prime examples include the PAc[292] (Table 2, entry 1), PAni, PPy, PT, and poly(*p*-phenylene) families.[59] Their operating potentials vary according to the type of polymer backbones and can approach 4 V vs Li^+/Li due to the p-type redox activity. The charge storage mechanism of conductive polymers is based on multiple π-conjugated repeating units stabilizing one positive charge via charge delocalization. Unfortunately, as more charges are stored, fewer repeating units are available to stabilize the charges, and the polymers become less stable.

More recent designs of high-potential p-type OEMs relied on dedicated redox centers for positive charge stabilization. These redox centers usually involve either carbon, oxygen, or nitrogen centers stabilized by aromatic structures and electron-donating functional groups. The polycyclic aromatic hydrocarbon coronene mimics mini graphene sheets and reversibly gives out 0.68 electrons per molecule upon charging (Table 2, entry 2).[235] It delivers one of the highest average discharge potentials of 4.0 V vs Li^+/Li among OEMs. 2,3,6,7,10,11-Hexamethoxytriphenylene (HMTP) undergoes a full one-electron redox reaction despite the smaller polycyclic aromatic

https://dx.doi.org/10.1021/acs.chemrev.9b00482
Chem. Rev. 2020, 120, 6490−6557

Table 1. A Few Electrochemical Storage Mechanisms in Redox-Active Organics Together with Examples[a]

Reversible redox-active moiety	Classification	General redox mechanism	Example of electrode reaction
Conjugated carbonyl	n-type	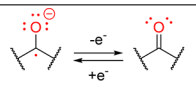	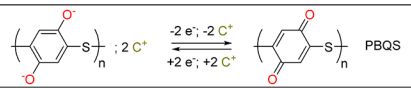
Organodisulfide	n-type	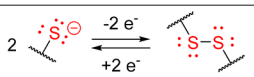	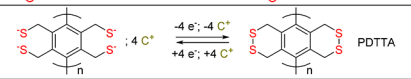
Conjugated azo group	n-type	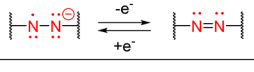	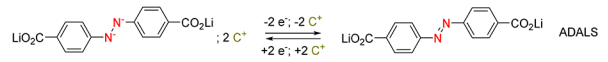
Conjugated nitrile	n-type	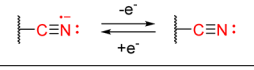	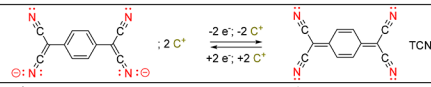
Conjugated amine	p-type	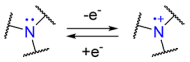	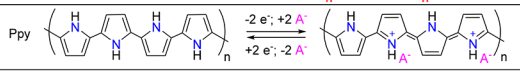
Conjugated etheroxide	p-type	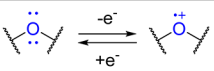	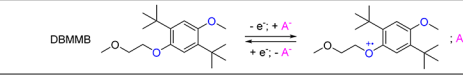
Conjugated thioether	p-type	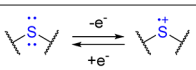	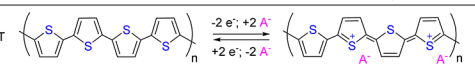
Nitroxide radical	n/p-type (bipolar)	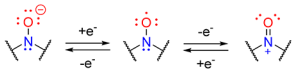	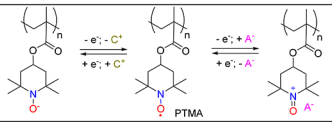

[a]PBQS: poly(benzoquinonyl sulfide); PDTTA: poly(5,8-dihydro-1*H*,4*H*-2,3,6,7-tetrathia-anthracene; ADALS: azobenzene-4,4′-dicarboxylic acid lithium salt; TCNQ: tetracyanoquinodimethane; PPy: polypyrrole; DBMMB: 2,5-di-*tert*-butyl-1-methoxy-4-[2′-methoxyethoxy]benzene; PT: polythiophene; PTMA: poly(2,2,6,6-tetramethylpiperidinyloxy-4-yl methacrylate). Note the redox-active nitroxide radical is bipolar, in practice, good kinetics are only attempted with the p-type activity.

hydrocarbon core than that found in coronene (Table 2, entry 3).[236] The auxiliary electron-donating methoxy groups seem to have contributed to the higher p-doping level albeit with a lower discharge potential of 3.5 V vs Li^+/Li. Tetrathiafulvalene (TTF) is a π-conjugated molecule famous for its distinctive electronic properties in the highly stabilized oxidized form. OEMs incorporating the TTF structure, such as 2,2′-bis[5-(1,3-dithiol-2-ylidene)-1,3,4,6-tetrathiapentanylidene] (TTPY, Table 2, entry 4) and pentakis-fused TTF (Table 2, entry 5), show almost full utilization of two electrons per TTF unit in the molecules thanks to the strong stabilizing power of the sulfur atoms.[237] Pentakis-fused TTF shows a higher voltage than that of TTPY (3.56 against 3.4 V vs Li^+/Li) due to the higher number of electrons involved in the reaction (Figure 10A).[238]

Beyond conjugated hydrocarbon and thioether families, the one-electron oxidation reaction of nitroxide radical[10,75−77] has spawned a large body of literature on radical polymer electrodes (Table 1). The poster-child building block of radical polymers is 2,2,6,6-tetramethyl-1-piperidinyloxy (TEMPO), where the nitroxide radical is sterically stabilized by the neighboring methyl groups. Polymers incorporating the TEMPO block, most notably poly(2,2,6,6-tetramethyl-1-piperidinyloxy-4-yl methacrylate) (PTMA) (Table 2, entry 6), deliver discharge potential of ∼3.55 V vs Li^+/Li (Figure 10B).[75,239] The potential can be tuned by using different nitroxide-containing cores. For example, poly(2,2,5,5-tetramethyl-3-oxiranyl-3-pyrrolin-1-oxyl ethylene oxide) (PTEO, Table 2, entry 7), which contains the 2,2,5,5-tetramethyl-1-pyrrolidineoxy (PROXYL) core, shows a higher potential of 3.7 V vs Li^+/Li.[240] Recently, a nonradical oxygen center was reported in the form of dibenzo-1,4-dioxin (DD) (Figure 10C, Table 2, entry 8).[241] A remarkably high discharge potential of 4.1 V vs Li^+/Li was observed, though only one out of the two oxygen atoms in the molecule contributed to charge storage. Nitrogen centers in aromatic amines may be easier to incorporate into a molecule from the organic synthesis point of view. Triphenylamine (TPA) is among the most studied building blocks in organic electronics. TPA-based OEMs, such as triphenylamine-based polymers (PTPA, Table 2, entry 9) show competitive discharge potentials of ∼3.6 V vs Li^+/Li.[242] Many other aromatic amines have been studied as OEMs as well including small molecules[243,244] and organic salt forms such as dilithium 2,5-(dianilino)terephthalate (Li_2DAnT), which are quite less soluble than non-salt molecules as further explained below (Table 2, entry 10).[245]

Compared with p-type OEMs, the n-type counterparts have attracted greater research interest because of giving access to the reversible storage of Li^+ and potentially to cationic "rocking-chair"-type batteries when n-type electrode materials are properly designed (Figure 9). *p*-Benzoquinone (*p*-BQ) is one of the most studied n-type building blocks for OEMs (Table 1). The basic *p*-BQ molecule shows two discharge plateaus at 2.9 and 2.5 V vs Li^+/Li with equal capacities, averaging to a discharge potential of 2.7 V vs Li^+/Li (Figure 10D, Table 2, entry 12).[246] OEMs resembling the *p*-BQ structure show similar potentials as *p*-BQ. BBQ, a dimer of *p*-BQ, and 1,4,5,8-phenanthrenediquinone (PADQ), a three-ring molecule incorporating two *p*-BQ units show discharge potentials at 2.9 and 2.77 V vs Li^+/Li, respectively (Table 2, entry 18, 19).[247,248] The slightly higher potential than that of *p*-BQ may be related to the limited specific capacity (i.e., relatively small depth of discharge) rather than performance improvement by design, however. Polymers that incorporate the *p*-BQ structure without much modification to the building block preserve the discharge potential. PBQS and poly(2,5-dihydro-*p*-benzoquinonyl sulfide) (PDBS)

https://dx.doi.org/10.1021/acs.chemrev.9b00482
Chem. Rev. 2020, 120, 6490−6557

Table 2. Performances of Selected Nonaqueous Li−Organic Batteries

#	Cell configuration (ionic carriers)	Positive electrode (or "cathode") active material	Negative electrode (or "anode")	Electrolyte	Output voltage (V)	Cycling stability: retention, cycles, rate or current density	Specific capacity (mAh g^{-1}) and Specific energy (Wh kg^{-1})[a]	Ref.
1	ClO_4^-	 Polyacetylene	Li	1 M $LiClO_4$ in PC	4.0	N/A	200, 471	[292]
2	PF_6^-	 Coronene	Li	1 M $LiPF_6$ in EC/DEC	4.0	92%, 960, 20 mA g^{-1}	40, 140	[235]
3	PF_6^-	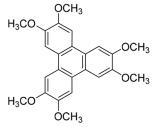 HMTP	Li	1 M $LiPF_6$ in EC/DEC	3.5	92%, 80, 1 C	67, 190	[236]
4	BF_4^-	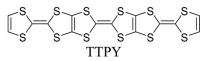 TTPY	Li	1 M $LiBF_4$ in EC/DEC	3.3	84%, 100, 0.2 C	168, 349	[237]
5	PF_6^-	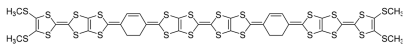 Pentakis-fused TTF	Li	1 M $LiPF_6$ in EC/DEC	3.56	72%, 30, 0.2 C	196, 414	[238]
6	PF_6^-	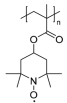 PTMA	Li	1 M $LiPF_6$ in EC/DEC	3.55	95%, 200, 2 C	103, 269	[239]
	Li^+, PF_6^-		Li	1 M $LiPF_6$ in EC /DMC/DEC (w/w/w 1:1:1)	3.0	55%, 20 000, 100 mA g^{-1}	100, 269	[279]
7	PF_6^-	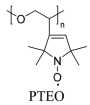 PTEO	Li	1 M $LiPF_6$ in EC/DEC	3.7	80%, 1 000, 10 C	85, 242	[240]
8	ClO_4^-	 DD	Li	5 M $LiClO_4$ in EC/DMC	4.1	N/A	80, 256	[241]
9	PF_6^-	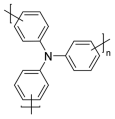 PTPA	Li	1 M $LiPF_6$ in EC/DMC (v/v 1:1)	3.6	95%, 500, 2 000 mA g^{-1}	98, 263	[242]
10	ClO_4^-	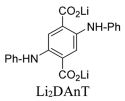 Li_2DAnT	Li	1 M $LiClO_4$ in PC	3.2	87%, 100, 3.7 mA g^{-1} (carbon free)	180, 376	[245]
11	PF_6^-	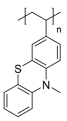 PVMPT	Li	1 M $LiPF_6$ in EC:DMC (1: 1 v/v)	3.5	93%, 10000, 10 C	50, 149	[280]
12	Li^+	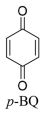 *p*-BQ	Li	1 M LiTFSI in DOL/DME	2.7	32%, 20, 50 mA g^{-1}	429, 1004	[246]
13	Li^+	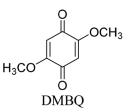 DMBQ	Li	1 M $LiClO_4$ in γ-butyl lactone	2.7	82%, 10, 20 mA g^{-1}	320, 798	[270]

https://dx.doi.org/10.1021/acs.chemrev.9b00482
Chem. Rev. 2020, 120, 6490−6557

Table 2. continued

#	Cell configuration (ionic carriers)	Positive electrode (or "cathode") active material	Negative electrode (or "anode")	Electrolyte	Output voltage (V)	Cycling stability: retention, cycles, rate or current density	Specific capacity (mAh g^{-1}) and Specific energy (Wh kg^{-1})[a]	Ref.
14	Li^+	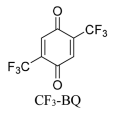 CF_3-BQ	Li	1 M $LiPF_6$ in EC/DEC (v/v 3:7)	3.0	37%, 20, 0.1 mA	162, 466	[250]
15	Li^+	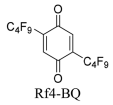 Rf4-BQ	Li	1 M $LiPF_6$ in EC/DEC (v/v 3:7)	3.0	50%, 20, 0.1 mA	115, 335	[250]
16	Li^+	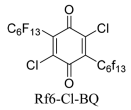 Rf6-Cl-BQ	Li	1 M $LiPF_6$ in EC/DEC (v/v 3:7)	3.1	55%, 20, 0.1 mA	177, 525	[250]
17	Li^+	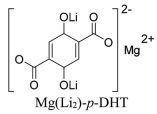 $Mg(Li_2)$-*p*-DHT	Li	1 M $LiPF_6$ in EC/DMC (w/w 1:1)	3.4	92%, 80, 23 mA g^{-1}	100, 340	[252]
18	Li^+	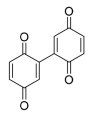 BBQ	Li	2.75 M LiTFSI in G4	2.8	67%, 20, 40 mA g^{-1}	358, 917	[247]
19	Li^+	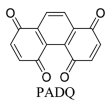 PADQ	Li	1 M $LiPF_6$ in DMC/EMC/EC (v/v/v 1:1:1)	2.77	N/A	370, 935	[248]
20	Li^+	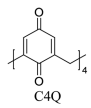 C4Q	Li	PMA/PEG-based gel polymer electrolyte with $LiClO_4$/DMSO loading	2.6	90%, 100, 0.2 C	422, 989	[272]
21	Li^+	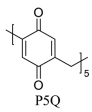 P5Q	Li	PMA/PEG-$LiClO_4$-SiO_2 composite	2.6	89%, 50, 0.2 C	409, 964	[273]
22	Li^+	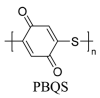 PBQS	Li	1 M LiTFSI in DOL/DME (v/v 1:1)	2.7	86%, 1 000, 5000 mA g^{-1}	275, 691	[246]
23	Li^+	 PDBS	Li	1 M $LiPF_6$/EC/DMC (v/v 1/1)	2.0	53%, 100, 15 mA g^{-1}	250, 470	[274]
24	Li^+		Li	1 M LiTFSI in DOL/DME (v/v 1:1)	2.5	50%, 20, 50 mA g^{-1}	200, 475	[249]
25	Li^+	 Li_2PDBS	Li	1 M LiTFSI in DOL/DME (v/v 1:1)	2.0	87%, 1 500, 500 mA g^{-1}	247, 464	[249]

https://dx.doi.org/10.1021/acs.chemrev.9b00482
Chem. Rev. 2020, 120, 6490−6557

Table 2. continued

#	Cell configuration (ionic carriers)	Positive electrode (or "cathode") active material	Negative electrode (or "anode")	Electrolyte	Output voltage (V)	Cycling stability: retention, cycles, rate or current density	Specific capacity (mAh g^{-1}) and Specific energy (Wh kg^{-1})[a]	Ref.
26	Li^+	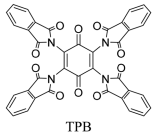 TPB	Li	1 M LiTFSI in DME:DOL (v/v 1:2)	2.5	91%, 100, 0.2 C	223, 527	[287]
27	Li^+	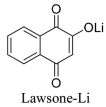 Lawsone-Li	Li	1 M LiTFSI in DME:DOL (v/v 1:2)	2.4	98%, 1 000, 0.5 C	280, 627	[271]
28	Li^+	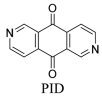 PID	Li	1 M $LiPF_6$ in EC/DMC (w/w 1:1)	2.71	80%, 20, 0.1 C	207, 532	[258]
29	Li^+	 P14AQ	Li	1 M LiTFSI in DOL + DME (v/v 2:1)	2.1	98%, 100, 0.2 C	263, 517	[275]
30	Li^+	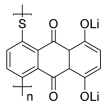 Poly-LiDHAQS	Li	1 M LiTFSI in DOL/DME (v:v 2:1)	2.5	60%, 1 200, 2 C	330, 760	[276]
31	Li^+	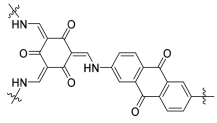 DAAQ-TFP	Li	1 M LiTFSI in TEGDME	2.4	98%, 1 800, 500 mA g^{-1}	107, 250	[283]
32	Li^+	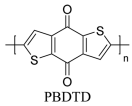 PBDTD	Li	1 M $LiClO_4$ in DOL/DME (v/v 1:1)	2.5	96%, 250, 0.1 C	200, 475	[288]
33	Li^+	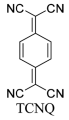 TCNQ	Li	1 M $Li[Tf_2N]$ in $[EMIm][Tf_2N]$ and 1 M $LiClO_4$ EC/DEC	2.8	78%, 100, 0.2 C	260, 682	[254]
34	Li^+	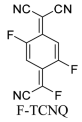 F-TCNQ	Li	1 M $LiPF_6$ in EC/DEC	3.1	N/A	183, 542	[255]
35	Li^+	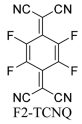 F2-TCNQ	Li	1 M $LiPF_6$ in EC/DEC	3.15	N/A	110, 342	[255]
36	Li^+	 1,8-PhenQ	Li	1 M $LiPF_6$ EC/EMC (v/v 1:3)	2.94	NA	230, 638	[256]

https://dx.doi.org/10.1021/acs.chemrev.9b00482
Chem. Rev. 2020, 120, 6490−6557

Table 2. continued

#	Cell configuration (ionic carriers)	Positive electrode (or "cathode") active material	Negative electrode (or "anode")	Electrolyte	Output voltage (V)	Cycling stability: retention, cycles, rate or current density	Specific capacity (mAh g^{-1}) and Specific energy (Wh kg^{-1})[a]	Ref.
37	Li^+	 4,5-PhenQ	Li	1 M $LiPF_6$ in EC/DMC (w/w 1:1)	2.74	N/A	231, 597	[257]
38	Li^+	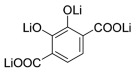 Li_4-*o*-DHT	Li	1 M $LiPF_6$ in EC/DMC (v/v 1:1)	2.85	95%, 30, 0.2–5 C	105, 299	[234]
39	Li^+	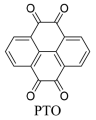 PTO	Li	1 M $LiPF_6$ in EC–DMC	2.59	27%, 50, N/A	360, 853	[257]
40	Li^+	 Polydopamine	Li	1 M $LiPF_6$ in EC:DMC (v/v 3:7)	2.5	106%, 10 000, 0.1 A g^{-1}	108, 263	[105]
41	Li^+	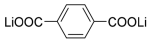 Li terephthalate	Li	1 M $LiPF_6$ in EC/DMC (w/w 1:1)	0.8	78%, 50, 0.1 C	300, N/A	[261]
42	Li^+	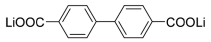 Li_2BPDC	Li	1 M $LiPF_6$ in EC/DMC (v/v 1:1)	0.7	60%, 25, 1 C	250, N/A	[264]
43	Li^+	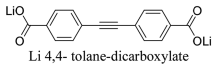 Li 4,4- tolane-dicarboxylate	Li	1 M $LiPF_6$ in EC/DMC (v/v 1:1)	0.65	90%, 50, 0.025 C	130, N/A	[265]
44	Li^+	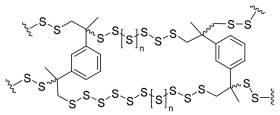 poly(S-*r*-DIB)	Li	0.38 M LiTFSI, 0.31 M $LiNO_3$ in DOL/DME	2.1	82%, 100, 167 mA g^{-1}, 0.1 C	1000, 1668	[266]
45	Li^+	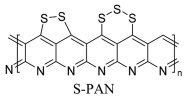 S-PAN	Li	1 M $LiPF_6$ in EC/DEC	1.8	73%, 1 000, 0.4 C	1200, 1648	[268]
46	Li^+	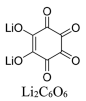 $Li_2C_6O_6$	Li	1 M $LiPF_6$ in EC/DEC	2.1	N/A	580, 1059	[82]
47	Li^+	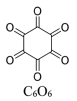 C_6O_6	Li	0.3 M LiTFSI-[PY13][TFSI] at 70°C	1.7	82%, 100, 50 mA g^{-1}	902, 1243	[269]
48	Li^+	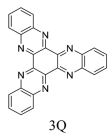 3Q	Li	1.0 M LiTFSI in DOL/DME	2.0	70%, 10 000, 20 C	395, 717	[277]
49	Li^+	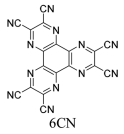 6CN	Li	1 M $LiClO_4$ in EC/DEC (v/v 1:1)	2.4	83%, 30, 0.2 C	300, 668	[278]

https://dx.doi.org/10.1021/acs.chemrev.9b00482
Chem. Rev. 2020, 120, 6490–6557

Table 2. continued

#	Cell configuration (ionic carriers)	Positive electrode (or "cathode") active material	Negative electrode (or "anode")	Electrolyte	Output voltage (V)	Cycling stability: retention, cycles, rate or current density	Specific capacity (mAh g^{-1}) and Specific energy (Wh kg^{-1})[a]	Ref.
50	Li^+	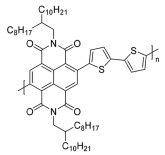 P(NDI2OD-T2)	Li	1 M $LiClO_4$ in DOL/DME (v/v 1:1)	2.4	96%, 3 000, 10 C	54, 128	[281]
51	Li^+	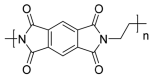 PPDIE	Li	4 M LiFSI-DME	2.0	82%, 10 000, 10 C	180, 344	[282]
52	Li^+	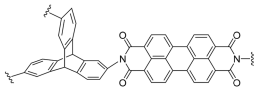 PDI-Tc	Li	1 M $LiPF_6$ in EC/DME (v/v 1:1)	2.4	80%, 500, 2 C	76, 179	[284]
53	Li^+	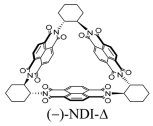 (−)-NDI-Δ	Li	1 M LiTFSI and 0.2 M $LiNO_3$ in DOL/DME (v/v 1:1)	2.5	60%, 300, 10 C	146, 352	[285]
54	Li^+	 Benzoic-PDI	Li	1 M $LiPF_6$ in EC:DEC (v/v 1:1)	2.4	88%, 200, 5 C	90, 211	[286]
55	Li^+	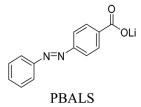 PBALS	Li	7 M LiTFSI in DME:DOL (v/v 1:1)	1.4	85%, 500, 10 C	95, N/A	[289]

[a]Specific energy considers the weight of both the cathode and anode materials. For p-type OEMs, $LiBF_4$ is considered as the Li salt due to its relatively light weight.

show some of the highest discharge potentials for n-type polymer OEMs (Figure 10D, Table 2, entry 22, 23).[246,249]

Since the discharge potentials of *p*-BQ-containing OEMs are noticeably lower than those of *p*-type OEMs as well as common intercalation compounds (>3.5 V vs Li^+/Li), efforts have been made to obtain higher potentials. Installation of perfluoroalkyl groups and chlorine atoms at the carbon ring of *p*-BQ gives rise to CF_3-BQ (Table 2, entry 14), Rf4-BQ (Table 2, entry 15), and Rf6-Cl-BQ (Table 2, entry 16), which show increased potentials of 3.0−3.1 V vs Li^+/Li.[250] The introduction of these auxiliary groups, however, inevitably decreases the specific capacity and could be counterproductive when high specific energy is the goal. Dilithium (2,5-dilithium-oxy)-terephthalate ($Li_2(Li_2)$-*p*-DHT or Li_4-*p*-DHT) may be seen as a carboxylate-substituted *p*-BQ (crystallized "host" electrode material) synthesized at its discharged (lithiated) state;[208,251] with its polyanionic structure making this material highly insoluble.[84] Since its life as an OEM starts from charging, like commercial positive electrode materials in LIBs do, it is one of the few n-type OEMs that can be paired with a Li-free anode, a great benefit for industrial cell production. However, this very interesting organic was hampered by a relatively low operating potential (2.55 V vs Li^+/Li). Replacing the Li^+ in the carboxylate groups with high-electronegativity cations such as Mg^{2+} and Ca^{2+} amazingly increases the redox potential several hundreds of millivolts (Figure 10E).[252] Thus the resulting magnesium (2,5-dilithium-oxy)-terephthalate ($Mg(Li_2)$-*p*-DHT) shows the highest working potential (3.45 V vs Li^+/Li) among n-type OEMs approaching the well-known $LiFePO_4$ electrode material (Table 2, entry 17). Note that an attempt to switch from the carboxylate functional groups present in Li_4-*p*-DHT to the sulfonate substituent giving rise to the tetralithium salt of 2,5-dihydroxy-1,4-benzenedisulfonate (Li_4-*p*-DHBDS)[253] enables also a voltage gain (+650 mV) but with inferior electrochemical performance upon cycling.

A closely related structure to *p*-BQ is tetracyanoquinodimethane (TCNQ), where the oxygen atoms in *p*-BQ are replaced by the even more electron-withdrawing dicyanomethylene groups (Table 2, entry 33). TCNQ itself is known as an electron acceptor for preparation of charge transfer salts, such as TTF-TCNQ. In a Li-battery, TCNQ discharges at 2.9 V vs Li^+/Li, a noticeable improvement over *p*-BQ.[254] Further increase in potential was achieved by installing electron-withdrawing groups to the carbon ring. As the number of fluorine atoms installed to TCNQ increased from two (F-TCNQ) to four (F2-TCNQ), the average discharge potential increased from 3.1 to 3.15 V vs Li^+/Li (Figure 10F, Table 2, entry 34, 35).[255]

The *ortho*-regioisomer of *p*-BQ gives rise to higher discharge potentials in general. The simplest molecule, *ortho*-benzoquinone (*o*-BQ), has not been directly studied probably due to chemical stability issues, but *o*-BQ as a building block for OEMs is well documented. The pyridine rings-fused 1,8-diaza-

https://dx.doi.org/10.1021/acs.chemrev.9b00482
Chem. Rev. 2020, 120, 6490−6557

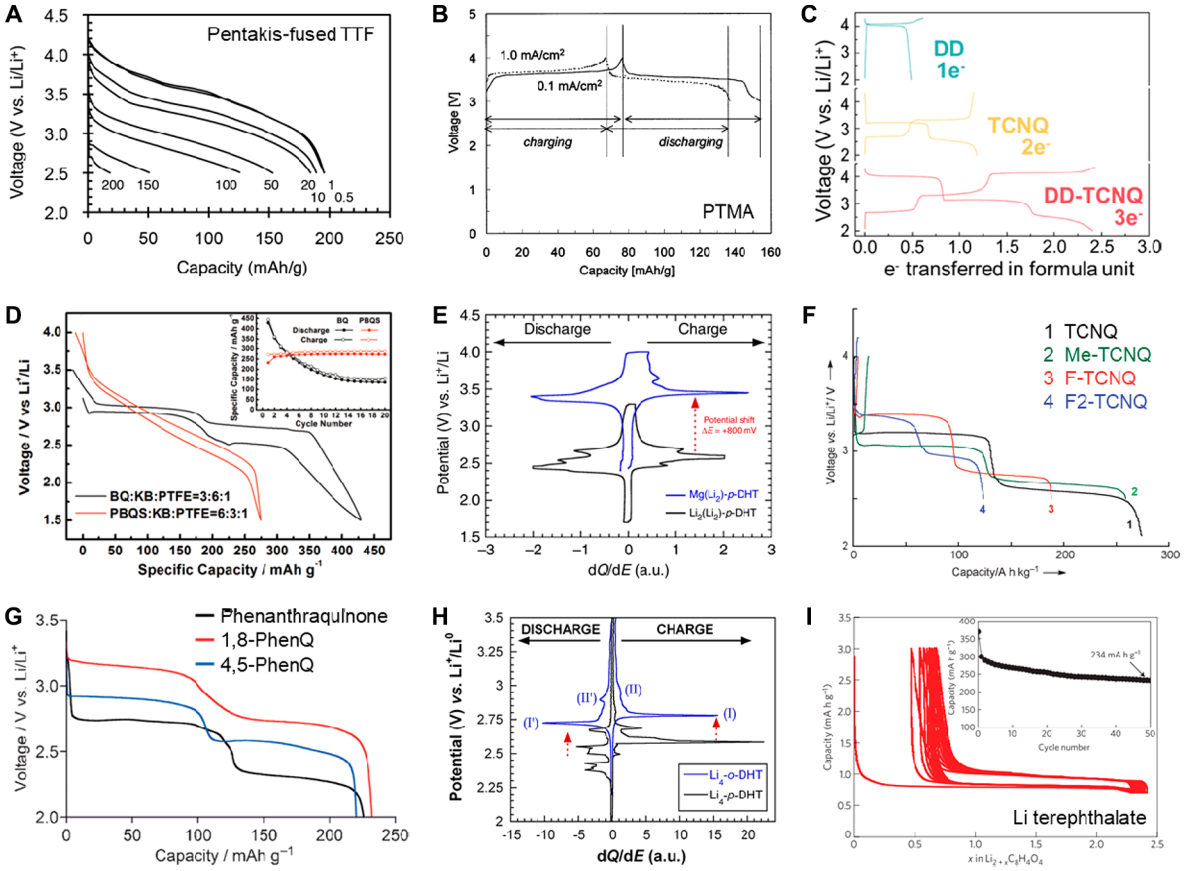

Figure 10. Voltage profiles of selected high-potential positive OEMs and low-potential negative OEMs measured vs Li including (A) pentakis-fused TTF (reproduced with permission from ref 238. Copyright 2014 The Royal Society of Chemistry), (B) PTMA (reproduced with permission from ref 75. Copyright 2002 Elsevier Ltd.), (C) DD (reproduced with permission from ref 241. Copyright 2019 Elsevier Ltd.), (D) BQ and PBQS (reproduced with permission from ref 246. Copyright 2015 John Wiley & Sons, Inc.), (E) $Li_2(Li_2)$-*p*-DHT and $Mg(Li_2)$-*p*-DHT (reproduced from ref 252), (F) TCNQ, F-TCNQ, and F2-TCNQ (reproduced with permission from ref 255. Copyright 2013 John Wiley & Sons, Inc.), (G) 1,8-PhenQ and 4,5-PhenQ (reproduced with permission from ref 257. Copyright 2013 The Royal Society of Chemistry, (H) Li_4-*o*-DHT (reproduced with permission from ref 234. Copyright 2014 American Chemical Society), and (I) Li terephthalate (reproduced with permission from ref 261. Copyright 2009 Nature Publishing group).

9,10-phenanthrenequinone (1,8-PhenQ, Table 2, entry 36) and 4,5-diaza-9,10-phenanthrenequinone (4,5-PhenQ, Table 2, entry 37) discharge at 2.94 and 2.74 V vs Li^+/Li (Figure 10G), respectively, both higher than the 2.71 V for their *p*-BQ-containing isomer pyrido[3,4-g]isoquinoline-5,10-dione (PID).[256−258] Interestingly, the position of nitrogen atoms in the fusing pyridine rings has a considerable impact on discharge potential: the pyridine nitrogen and the carbonyl oxygen being adjacent (as in the case of 1,8-PhenQ) promote favorable coordination of Li^+, which leads to extra gain in potential. This explains the noticeably higher potential of 1,8-PhenQ than that of 4,5-PhenQ (+200 mV as gain). As previously attempted with *p*-DHT redox-active ligand, attaching carboxylate functional groups to the carbon ring of the reduced form of *o*-BQ gives rise to another highly insoluble and lithiated electrode material namely (2,3-dilithium-oxy)-terephthalate (Li_4-*o*-DHT, Table 2, entry 38), which can be prepared from biomass too.[234] Alike Li_4-*p*-DHT, this regioisomer is able to release/uptake Li ions over dozens of cycles but at higher operating potential (2.85 V vs Li^+/Li) due to specific electronic effects[211] occurring in orthoquinones (Figure 10H). Since only one out of the two lithoxy groups in the carbon ring appears redox active, it may be reasonable to assume that upon possible full utilization, an even higher average potential could be achieved.

N-type OEMs with sufficiently low operating potential can be used as negative electrode materials as well. Many conductive polymers can be n-doped at <1 V vs Li^+/Li, but the doped states usually lack stability, and the doping level is typically half of that for the p-doping of the same polymer.[259] Two other mechanisms are currently being actively researched: lithiation of π-conjugated carboxylate and "superlithiation" (see section 7.3) of π-conjugated systems.[260] A pioneering report on carboxylate negative electrodes concerned dilithium terephthalate[261] which discharged at 0.8 V vs Li^+/Li (Figure 10I, Table 2, entry 41). [Note: For a negative electrode material tested in a Li cell, the charging potential is more relevant, however, discharging potential is used here for consistency.] Since this work, the family of π-conjugated carboxylates has been widely extended, and it has been shown that the working potential can be slightly adjusted by playing with the electronic effects on the organic skeleton notably by Lakraychi et al.[262,263] Replacing the phenyl group in dilithium terephthalate with biphenyl gives the dilithium 4,4′-biphenyl dicarboxylate (Li_2BPDC, Table 2, entry 42) with a discharge potential of 0.7 V vs Li^+/Li.[264] The lower potential compared with Li terephthalate was ascribed to the π-conjugation enhancement destabilizing the LUMO orbitals of the molecule. Further expansion of the π-conjugated system to diphenylacetylene

https://dx.doi.org/10.1021/acs.chemrev.9b00482
Chem. Rev. 2020, 120, 6490−6557

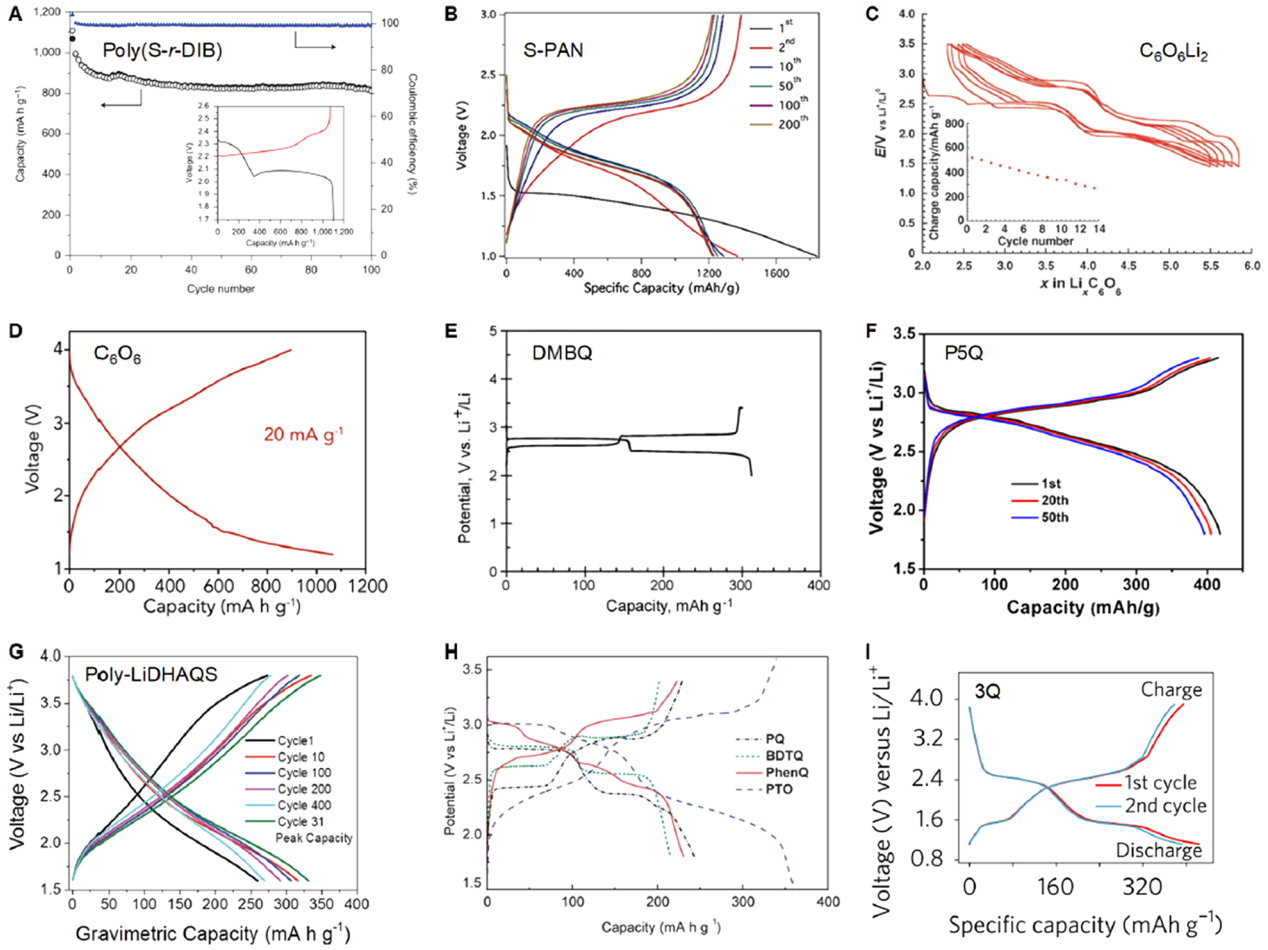

Figure 11. Voltage profiles of selected high-capacity OEMs measured vs Li including (A) poly(S-*r*-DIB) (reproduced with permission from ref 266. Copyright 2013 Nature Publishing group), (B) S-PAN (reproduced with permission from ref 268. Copyright 2015 American Chemical Society), (C) $Li_2C_6O_6$ (reproduced with permission from ref 82. Copyright 2008 John Wiley & Sons, Inc.), (D) C_6O_6 (reproduced with permission from ref 269. Copyright 2019 John Wiley & Sons, Inc.), (E) DMBQ (reproduced with permission from ref 270. Copyright 2010 Elsevier Ltd.), (F) P5Q (reproduced with permission from ref 273. Copyright 2014 American Chemical Society), (G) poly-LiDHAQS (reproduced with permission from ref 276. Copyright 2017 John Wiley & Sons, Inc.), (H) PTO (reproduced from ref 257. Copyright 2013 The Royal Society of Chemistry), and (I) 3Q (reproduced with permission from ref 277. Copyright 2013 Nature Publishing group).

results in dilithium 4,4′-tolane-dicarboxylate, which discharges at an even lower potential of 0.65 V vs Li^+/Li (Table 2, entry 43).[265] OEMs that undergo the peculiar "superlithiation" process (see section 7.3) exhibit sloping discharge profiles that start from >1.5 V and eventually approach 0 V vs Li^+/Li and then charge at ≥1 V vs Li^+/Li on average. Due to the uniqueness of the reaction, these OEMs are to be separately covered in section 7.

5.2. Organic Electrode Materials with High Specific Capacity

To gain high specific capacity, both formula weight and number of transferrable electrons are key considerations. Among the major classes of organic electrodes, organosulfur compounds offer the largest capacities. In particular, organosulfur polymers bearing polysulfide bonds not only exhibit high capacities but also stable cycling. Poly(sulfur-*random*-1,3-diisopropenylbenzene) (poly(S-*r*-DIB)) is one such example, which was copolymerized between molten S_8 and 1,3-diisopropenylbenzene (DIB) through inverse vulcanization.[266] The DIB feed ratios can be varied between 10−50 wt % during the synthesis. Galvanostatic voltage profiles of poly(S-*r*-DIB) with 10 wt % DIB show distinct discharge plateaus at 2.3 and 2.1 V vs Li^+/Li (Figure 11A, Table 2, entry 44). The initial discharge capacity is 1100 mAh g^{-1}. Sulfur-polyacrylonitrile (S-PAN) is another organosulfur polymer attracting significant attention due to the ease of synthesis and high performance.[267] S-PAN was formed by mixing and heating sulfur and polyacrylonitrile (PAN). It is interesting to note that S-PAN exhibits good capacity retention in a carbonate-based electrolyte, a behavior in sharp contrast with sulfur, which works well only in ethereal electrolytes.[268] S-PAN shows a single plateau at 2.1 V with a high specific capacity of 1200 mAh g^{-1} (Figure 11B, Table 2, entry 45).

Carbonyl group undergoes reversible one-electron reduction to form a radical anion. When multiple carbonyls are conjugatedly connected as in quinones, the uncoupled electrons generated during reduction could combine intramolecularly to form multivalent anions. The theoretical capacity of carbonyl-based electrodes is typically lower than that of organosulfur polymers. Dilithium rhodizonate ($Li_2C_6O_6$) undergoes reversible four-electron reaction per C_6O_6 ring (Table 2, entry 46). The observed initial discharge capacity of 580 mAh g^{-1} set the record capacity among carbonyl-based OEMs since its discovery in 2008 (Figure 11C).[82] The fact that $Li_6C_6O_6$ can be prepared from a renewable natural precursor opens up new

https://dx.doi.org/10.1021/acs.chemrev.9b00482
Chem. Rev. 2020, 120, 6490−6557

pathways toward sustainable batteries for future clean energy economy. Recently, cyclohexanehexone (C_6O_6) was claimed to be successively synthesized and surpass $Li_2C_6O_6$ in terms of specific capacity (Table 2, entry 47).[269] C_6O_6, a cyclic ketone composed of carbonyls without redundant mass, exhibits a higher capacity of 902 mAh g^{-1} (i.e., six-electron reaction per formula) (Figure 11D). Note that such an ultrahigh capacity was observed in an ionic liquid-based electrolyte measured at 70 °C. The compound exhibits sloping and polarized cycling curves, in contrast to the multiple plateaus observed for $Li_2C_6O_6$.[82]

After the C_6O_6 motif, *p*-BQ offers the highest theoretical specific capacity among common n-type OEM building blocks. *p*-BQ itself can deliver a specific capacity of 429 mAh g^{-1} during the initial discharge, but the capacity retention was only 32% after 20 cycles due to its high solubility in organic solvents.[246] Due to the ready dissolution of *p*-BQ into nonaqueous electrolyte solutions, many OEMs containing the *p*-BQ unit have been developed to reduce dissolution while maintaining high capacity. They may be categorized into three types according to their molecular sizes. The first type includes molecules with one single *p*-BQ core modified with electron donating or withdrawing groups. Installation of methoxy functional groups on *p*-BQ results as DMBQ, which improves the stability compared to *p*-BQ albeit the discharge capacity is reduced to 320 mAh g^{-1} (Figure 11E, Table 2, entry 13).[270] Lawsone-Li is another example showing modification of naphthoquinone (NQ) with lithoxy results in lawsone-Li salt. Lawsone (2-hydroxy-1,4-naphthoquinone) is a nature-derived red-orange dye. Lithium cells based on lawsone-Li as positive electrode material displayed a capacity of 280 mAh g^{-1} and a cycle life of 1000 cycles (Table 2, entry 27).[271]

The second type includes molecules with multiple *p*-BQ units. 2,2′-Bis-*p*-benzoquinone (BBQ), calix[4]quinone (C4Q), and pillar[5]quinone (P5Q) contain two, four, and five *p*-BQ units, respectively (Table 2, entries 18, 20, and 21). It seems that dissolution of oligomers could still be observed in liquid electrolytes; therefore, polymer electrolytes containing poly(methacrylate) (PMA) and poly(ethylene glycol) (PEG) were used to increase capacity retention. Compared to BBQ (358 mAh g^{-1}), P5Q and C4Q show higher specific capacity of 409 and 422 mAh g^{-1} (Figure 11F).[247,272,273]

The third type includes polymers with (modified) *p*-BQ units. PBQS, PDBS, and Li_2PDBS present three examples of *p*-BQ-based polymers when using sulfur as the linker (Table 2, entry 22−25).[246,249,274] Among the three polymers, PBQS shows the highest specific capacity of 275 mAh g^{-1} for 1000 cycles. Due to the addition of lithoxy and hydroxy groups on PBQS, Li_2PDHBQS and PDBS exhibit slightly lower specific capacity of ∼250 mAh g^{-1}. Anthraquinone (AQ) can be considered as *p*-BQ with extended conjugation, which also has the solubility issue. Polymerization approach has been equally successful for AQ. P14AQ and poly-LiDHAQS are two polymers based on AQ. The specific capacities are 263 and 330 mAh g^{-1}, respectively (Figure 11G, Table 2, entries 29 and 30).[275,276]

A closely related structure to *p*-BQ is pyrene-4,5,9,10-tetraone (PTO) where two *o*-BQ units are connected with extended π-conjugated structure (Table 2, entry 39). PTO undergoes a four-electron reduction with a specific capacity of 360 mAh g^{-1} in EC/DMC and an average discharge voltage of 2.59 V vs Li^+/Li (Figure 11H).[257] TCNQ can also be formed by replacing the oxygen atoms in *p*-BQ with more electron-withdrawing dicyanomethylene groups (Table 2, entry 33). The discharge capacity of TCNQ is lowered to 260 mAh g^{-1} albeit voltage is increased to 3.2 V.[254]

π-Conjugated heteroaromatic molecules represent another class of OEMs with high specific capacity. Fused quinoxaline building blocks afford multiple redox-active sites centered on N atoms. Hexaazatrinaphthylene (3Q) enables six-electron reduction with a specific capacity of 395 mAh g^{-1} (Figure 11I, Table 2, entry 48).[277] When hybridized with graphene, 3Q shows 70% capacity retention after 10 000 cycles. Hexaazatriphenylenehexacarbonitrile (6CN, Table 2, entry 49) shows higher redox voltage at 2.4 V vs Li^+/Li by replacing the benzene groups in 3Q with electron-withdrawing cyanide groups.[278] When the discharge potential cutoff is set at 1.5 V vs Li^+/Li, 6CN shows a specific capacity of 300 mAh g^{-1}.

5.3. Organic Electrode Materials with Long Cycle Life

Researchers have almost always attributed the capacity decay of OEMs to either chemical degradation or dissolution. In typical nonaqueous Li electrolytes, chemical degradation of OEMs is rarely observed; hence, material dissolution from the solid electrode into the electrolyte is the main degradation mechanism. For the most part, increasing the cycling stability of OEMs in nonaqueous Li batteries equals minimizing the solubility of OEMs in electrolytes. As long as material dissolution is effectively suppressed, apparently most OEMs can deliver stable cycling performance. Even small-molecule OEMs that readily decay due to dissolution can be made stable when a sufficiently large amount of high-surface-area carbon adsorbent is included in the positive composite electrode as previously underlined in section 1.2.[13] Due to practical considerations, cycling performances enabled by intricate adsorbents are not a priority for this review.

The most stable OEMs for nonaqueous Li batteries have been polymers. Polymer OEMs containing varying types of redox centers, from p-type to n-type, from nitroxides (e.g., PTMA)[279] to aromatic amines (e.g., poly(3-vinyl-*N*-methylphenothiazine) or PVMPT)[280] to quinones (e.g., polydopamine)[105] to imides (e.g., poly{[*N*,*N*′-bis(2-octyldodecyl)-1,4,5,8-naphthalenedicarboximide-2,6-diyl]-alt-5,5′-(2,2′-bithiophene)} or P(NDI2OD-T2), Table 2, entry 50 and poly(ethylene-pyromellitic diimide) or PPDIE, Table 2, entry 51),[281,282] have all been reported to cycle for thousands to tens of thousands of cycles. It may be reasonable to extrapolate that, with proper polymerization, OEMs of all types can be made stable, even though synthetic difficulty may vary from type to type. With judicious selection of polymerization strategies, two- and three-dimensional polymer OEMs have been synthesized based on aromatic amines (e.g., polytriphenylamine or PTPA),[242] quinones (e.g., 2,6-diaminoanthraquinone-1,3,5-triformylphluroglucinol or DAAQ−TFP),[283] and imides (e.g., perylene diimide−triptycene or PDI−Tc, Table 2, entry 52).[284] These additional architectures are proposed to further improve cycling stability.

The advantage of polymer OEMs in cyclability does not preclude molecular OEMs from being important. Molecular materials can still be preferred for their well-defined structures, high specific capacity, flexibility in processing, and so on. Therefore, approaches to improve the cyclability of small molecules are still being developed. Considering the success of polymer OEMs, a widely practiced strategy is to increase the molecular weight of molecules or simply oligomerization. Both 3Q and coronene are big planar molecules which benefit from relatively strong van de Waals interaction and effective π−π

https://dx.doi.org/10.1021/acs.chemrev.9b00482
Chem. Rev. 2020, 120, 6490−6557

stacking.[235,277] Even when the active cores are not as big, it is still convenient to connect multiple building blocks together to artificially increase the molecular weight. Some examples include a triangle molecule (−)-NDI-Δ[285] (Table 2, entry 53) which incorporates three naphthalenediimide (NDI) units plus linkers, benzoic-PDI[286] (Table 2, entry 54) which attaches more aryls to the already large molecule perylenediimide (PDI), and 2,3,5,6-tetraphthalimido-1,4-benzoquinone (TPB)[287] which incorporates two seemingly unrelated redox centers (tetraphthalimide and *p*-BQ) into one molecule. These molecules exhibit cycling stabilities that clearly set them apart from simple molecules without sacrificing most advantages of molecular OEMs. The large size of these molecules is blurring the boundary between molecules and polymers. In fact, some "polymer" OEMs such as poly(benzo[1,2-b:4,5-b′]-dithiophene-4,8-dione-2,6-diyl) (PBDTD)[288] contain few repeating units (e.g., ≤5) per polymer chain. They may as well be considered as molecular OEMs.

Other strategies for stabilizing molecular OEMs include salt formation and grafting as previously mentioned.[84] Salt formation has long been an established strategy to stabilize molecular OEMs: ionic groups introduced to OEMs increase their intermolecular interactions and decrease the similarity in polarity with nonaqueous electrolytes, thus decreasing solubility.[82] Some recent excellent examples include $Mg(Li_2)$-*p*-DHT,[252] lawsone-Li,[271] and 4-(phenylazo) benzoic acid lithium salt (PBALS, Table 2, entry 55)[289]; all show barely any capacity decay after hundreds of cycles. Grafting is also a known, if still exotic, method for enabling small-molecule OEMs. The key to successful grafting is rational functionalization of high-capacity OEM building blocks for covalent linking to high-surface-area substrates. Grafted naphthoquinone (n-type) and pyrene (p-type) derivatives can show no obvious capacity decay over a long cycling period.[290−292]

We would like to note that although the cycle numbers for the examples discussed above vary from hundreds to tens of thousands, these numbers, in a lot of cases, seem to be limited by how fast the researchers felt comfortable to cycle their cells instead of the actual stability of the OEMs. Figure 12 summarizes the discharge potentials and active material-level specific capacities of Li−organic batteries discussed in this section and compares them with those of state-of-the-art inorganic electrode materials. Note that the specific capacities of batteries with p-type OEMs are impacted by the weight of the Li salt in the electrolyte (dual-ion cell configuration, Figure 9b-3).

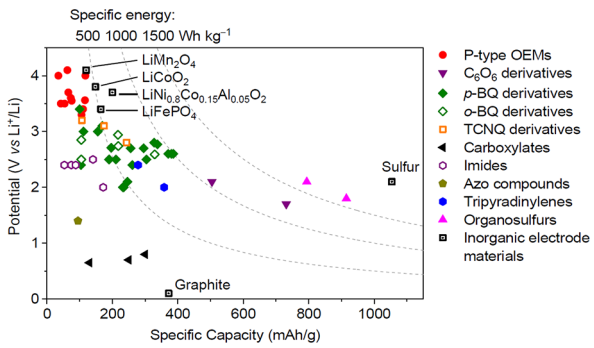

Figure 12. Comparison of the discharge potentials and specific capacities of state-of-the-art OEMs and inorganic electrode materials for Li batteries. Specific capacity calculation considers the weight of the lithiated form of positive electrode materials and delithiated form of negative electrode materials (e.g., azo compounds, carboxylates, and graphite). The highest observed reversible capacities are used instead of theoretical values.

For comparison convenience, the calculation of all batteries with p-type OEMs considers $LiBF_4$ as the Li salt. Although p-type OEMs have comparable discharge potentials and specific capacities as those of inorganic electrode materials, batteries based on them fall short in specific energy where the weight of the electrolyte is included. Therefore, p-type OEMs are not yet contenders as high-energy battery cathode materials but may find applications in, for example, fast charging devices and wearables. Many quinone-based OEMs have surpassed inorganic electrode materials in terms of specific energy at the active material level (i.e., only the weight of active materials is included in calculation). In practice, however, most high-energy OEMs still require too much conductive agents in their electrode composites for decent performance, which decreases specific energies at the cell level. Another challenge for OEMs is to simultaneously achieve high specific energy and high cycling stability. Future development of OEMs for nonaqueous Li batteries demands deeper understandings of their electron and ion conduction mechanics as well as performance degradation mechanisms and strategies to address them.

6. PERFORMANCES OF NONAQUEOUS SODIUM−ORGANIC BATTERIES

For decades, nonaqueous organic sodium-ion batteries have been overshadowed by other electrochemical energy systems (such as inorganic lithium-ion batteries, inorganic sodium-ion batteries, and later organic lithium-ion batteries) and have only been sporadically investigated.[293] However, in 2012, three different groups published their works on disodium terephthalate within a time frame of four months, marking then the beginning of the recent boom in this field.[294−296] Since then, disodium terephthalate has been regularly investigated as a model compound for composite electrode formulation.[297−301] In parallel, many other new materials were reported in the literature as already exhaustively covered in recent reviews.[16,40,41,302] Considering that strategies known to affect the potential with inductive effects (electron-withdrawing/donating groups) or appropriate aromatic ring design will have similar effects in organic LIBs and SIBs, the only distinctions to keep in mind are the differences in electrochemical potential for the reference metal (−3.04 V vs SHE for the Li^+/Li redox couple against −2.71 V vs SHE for the Na^+/Na redox couple) and atomic differences. For instance, a sodium carboxylate is expected to insert a sodium ion at an average potential slightly lower than the potential of lithium ion insertion for the corresponding lithium carboxylate with the same aromatic system −0.33 V (e.g., 0.9 V vs Li^+/Li average redox potential for dilithium terephthalate and 0.4 V vs Na^+/Na for disodium terephthalate: 0.5 V difference instead of 0.33 V). Similarly, the strategies for improving the specific capacity or reducing the dissolution phenomenon of active species within the electrolyte system such as polymerization work usually as well for organic SIBs as they do for organic LIBs and hence will not be repeated in this section. As a reminder, the use of sodium instead of lithium is also motivated by higher abundance and lower cost of the resource, with Na being widely distributed in the earth's crust and oceans (Figure 6) and nontoxic.

As previously stated, only the materials delivering the best performances in specific capacity, operating potential, and

https://dx.doi.org/10.1021/acs.chemrev.9b00482
Chem. Rev. 2020, 120, 6490−6557

Table 3. Performances of Selected Nonaqueous Na−Organic Batteries

#	Positive electrode (or "cathode") active material	Negative electrode (or "anode") active material	Electrolyte	Output voltage (V)	Cycling stability: retention, cycles, rate or current density	Specific capacity (mAh g^{-1}) and Specific energy (Wh kg^{-1}) per mass of positive active material if not specified otherwise, Final coulombic efficiency, Loading (mg cm^{-2})	Ref.
	Organic electrode materials with high/low voltage						
1	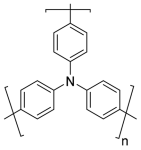	Na	Saturated $NaPF_6$ in DOL/DME (v/v 1:1)	3.6	82%, 200, 5 C (500 mA g^{-1})	95, 342, 99, n.d.	[307]
2	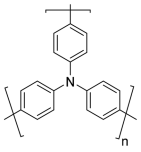	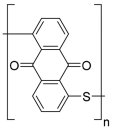	Saturated $NaPF_6$ in DOL/DME (v/v 1:1)	~1.8	85%, 500, 8 C	180-155,[a] 324,[a] 99, n.d.	[307]
3	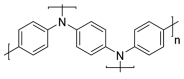	Na	0.5 M $NaPF_6$ in EC/PC (v/v 1:1)	3.38	68%, 1 000, 1 C	94-64, 318, n.d., 1.0-2.0	[308]
4	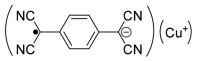	Na	1 M $NaClO_4$ in EC/PC (v/v 1:1)	~3.6	78%, 1 200, 1 C (300 mA g^{-1})	98, 353,~100, n.d.	[309]
5	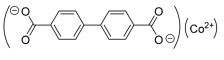	Na	1 M $NaClO_4$ in PC	~0.5	79%,[b] 1 000, (100 mA g^{-1})	209, 105, ~100, n.d.	[317]
	Na-ion organic batteries						
6	$Na_{0.75}Mn_{0.70}Ni_{0.23}O_2$	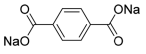	1 M $NaPF_6$ in EC/EMC (v/v 3:7)	~3.6	93%,[b] 50, C/13 (20 mA g^{-1})	111,[c] 400,[c] 99, 1.3-2.5	[296]
7	$Na_3V_2O_2(PO_4)_2F$	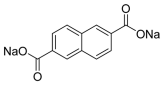	1 M $NaClO_4$ in PC	3.3	50%, 20, C/10 (13 mA g^{-1})	270-135,[a] 891,[a] 73, 2	[324]
8	$Na_4Fe(CN)_6$	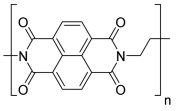	1 M $NaClO_4$ in EC/DEC (v/v 1:1)	1.2	73%, 100, 1 C (140 mA g^{-1})	158-102,[d] 190,[d] 95, n.d.	[325]
9	$Na_3V(PO_4)_3$	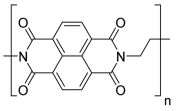	1 M $NaClO_4$ in EC/DEC (v/v 1:1)	1.2	70%, 100, 1 C (140 mA g^{-1})	150,[d] 180,[d] 95, n.d.	[325]
10	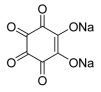	Na-predoped hard carbon	1 M $NaClO_4$ in PC	~2.2	85%,[b] 40, C/10 (18 mA g^{-1})	178-152,[c] 356,[c] n.d., 3.1	[326]
11	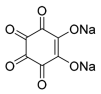	Na P@C 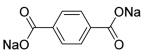 Disodium terephthalate	0.6 $NaPF_6$ in DEGDME	1.5 1.3 1.25	91%, 50, 500 mA g^{-1} 83%, 50, 500 mA g^{-1} 85%, 30, 50 mA g^{-1}	390, 585, ~100, 3-20 264,[a] 281,[a] ~100, 3-20 137,[a] 141,[a] ~100, 3-20	[327] [327] [327]

https://dx.doi.org/10.1021/acs.chemrev.9b00482
Chem. Rev. 2020, 120, 6490−6557

Table 3. continued

#	Positive electrode (or "cathode") active material	Negative electrode (or "anode") active material	Electrolyte	Output voltage (V)	Cycling stability: retention, cycles, rate or current density	Specific capacity (mAh g^{-1}) and Specific energy (Wh kg^{-1}) per mass of positive active material if not specified otherwise, Final coulombic efficiency, Loading (mg cm^{-2})	Ref.
12	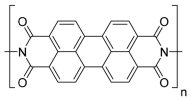	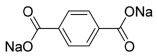	1 M $NaPF_6$ in PC	~1.6	70%, 20, 50 mA g^{-1}	73-51,[d] 117,[d] n.d., 1.4	[328]
13	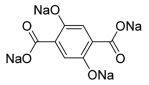	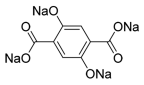	1 M $NaClO_4$ in EC/DMC (v/v 1:1)	~2.0	76%, 100, C/10 (19 mA g^{-1})	204-155,[c] 65,[c] 99, 1.0-1.8	[329]
			Organic electrode materials with high specific capacity				
14	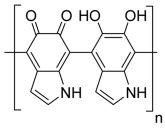	Na	1 M $NaPF_6$ in EC/PC (v/v 1:1)	1.0	100%,[b] 1024, 50 mA g^{-1}	500, 500 ,~100, 1.0	[330]
15	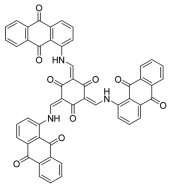	Na	1 M $NaClO_4$ in EC/DMC (v/v 1:1)	~1	95%, 500, 100 mA g^{-1} 97%, 2600, 1 A g^{-1}	320, 320, ~100, 0.7 218-258, 250, ~100, 0.7	[331]
16	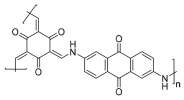	Na	1 M $NaClO_4$ in EC/DMC (v/v 1:1)	~0.9	82%, 100, 100 mA g^{-1} 99%, 10 000, 5 A g^{-1}	420, 378, ~100, n.d. 198, 178, ~100, n.d.	[332]
17	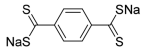	Na	1 M $NaClO_4$ in EC/DMC/FEC	1.3	66%, 250, 500 mA g^{-1}	567, 737, ~100, 1.0	[333]
			Organic electrode materials with high stability				
18	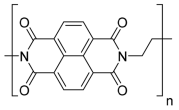	Na	1 M $NaClO_4$ in EC/PC/FEC	2.1	90%, 1 000, 10 C	90-80, 189, ~100, 0.7	[338]
19	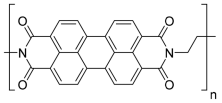	Na	1 M $NaPF_6$ in EC/DMC (v/v 1:1) 1 M $NaPF_6$ in EC/DMC (v/v 1:1)	~2.2	87.5%, 5 000, 0.8 C (200 mA g^{-1}) 100%, 1000, 1 A g^{-1}	111, 285, ~100, n.d. 100, 220, ~100, 0.8	[339] [340]
20	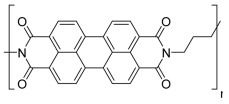	Na	1 M $NaPF_6$ in EC/DMC (v/v 1:1)	~2.1	97%, 1 000, 1 A g^{-1}	95, 200, ~100, 0.8	[340]
21	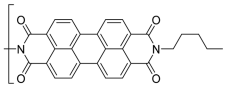	Na	1 M $NaPF_6$ in EC/DMC (v/v 1:1)	~2.1	93%, 1 000, 1 A g^{-1}	82, 172, ~100, 0.8	[340]

https://dx.doi.org/10.1021/acs.chemrev.9b00482
Chem. Rev. 2020, 120, 6490−6557

Table 3. continued

#	Positive electrode (or "cathode") active material	Negative electrode (or "anode") active material	Electrolyte	Output voltage (V)	Cycling stability: retention, cycles, rate or current density	Specific capacity (mAh g^{-1}) and Specific energy (Wh kg^{-1}) per mass of positive active material if not specified otherwise, Final coulombic efficiency, Loading (mg cm^{-2})	Ref.
22	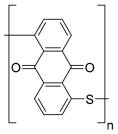	Na	0.1 M $NaPF_6$ in DME/DOL (v/v 1:1)	1.6	84%, 1 000, 0.5 C	157-132, 251,~100, 2.0	[341]
23	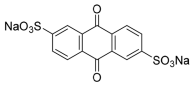	Na	1 M $NaPF_6$ in DME	1.8	90%, 1 000, 1 A g^{-1}	104-94, 187, ~100, 1.8-2	[342]
24	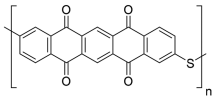	Na	1 M $NaPF_6$ in DME	1.6	88%, 10 000, 514 C (50 A g^{-1})	110, 176, ~100, 1.0	[334]
25	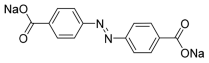	Na	1 M $NaPF_6$ in DEGDME	1.25	81%, 1 000, 10 C 85%, 2 000, 20 C	140-113, 175, ~100, 1.5 115-98, 144, ~100, 1.5	[335]
26	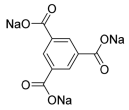	Na	1 M $NaBF_4$ in TEG/DME	~0.5	75%, 1 500, 10 C	100, 50, ~100, 2.0-2.5	[336]
27	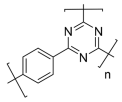	Na	1 M $NaClO_4$ in PC	~2.6	80%, 7 000, 1 A g^{-1}	~90, 234, ~100, ~1.5	[337]
28	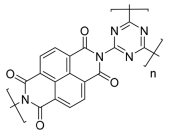	Na	1 M $NaClO_4$ in EC/DEC (v/v 1:1)	~1.25	~100%,[c] 1 000, 5 A g^{-1}	107, 134, ~100, n.d.	[343]
29	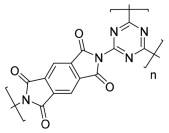	Na	1 M $NaClO_4$ in EC/DEC (v/v 1:1)	~1	83%,[b] 1 000, 5 A g^{-1}	89, 89,~100, n.d.	[343]
30	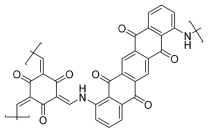	Na	1 M $NaPF_6$ in DME	1.65	86%,[f] 1 000, 0.56 C (100 mA g^{-1}) 95%,[f] 1 400, 5.6 C (1 A g^{-1})	177-145, 292, ~100, n.d. 128-121, 211, ~100, n.d.	[344]

[a]Based on cathode material weight. [b]The first cycle is not taken into account. [c]Based on anode material weight. [d]Based on cathode and anode.

cycling stability will be presented in the subsequent section (Table 3).

6.1. High/Low Voltage Organic Electrode Materials and Hybrid/All-Organic High Output Voltage Na-Ion Batteries

The design of high and low voltage OEMs for SIBs has clearly taken inspiration from the lithium equivalents. "p-type" materials (*i.e.*, anion insertion materials) are hence the most common compounds able to react at potential >3.0 V vs Na^+/Na, while materials reacting at low potential <1.5 V vs Na^+/Na belong to "n-type" (*i.e.*, cation insertion materials). Conductive polymers are an example of a type of material which could belong to any or both of these categories. Early research on conductive polymers for SIBs has been carried out by Yang's group, who used polyaniline derivatives (p-type),[303] doped PPy[304,305] (p-type), or PT[306] (n-type) in some of the first articles in this field. Soon after, they reported the activity of polytriphenylamine (PTPAn, Table 3, entry 1) as p-type material with PF_6^- ingress.[307] Each triphenylamine unit can lose one electron and intercalate one anion upon oxidation at an average redox potential of 3.6 V vs Na^+/Na forming then quinoneimine units (Figure 13A). PTPAn displays stable reversible capacity even at high C-rate with 88 mAh g^{-1} at a

https://dx.doi.org/10.1021/acs.chemrev.9b00482
Chem. Rev. 2020, 120, 6490−6557

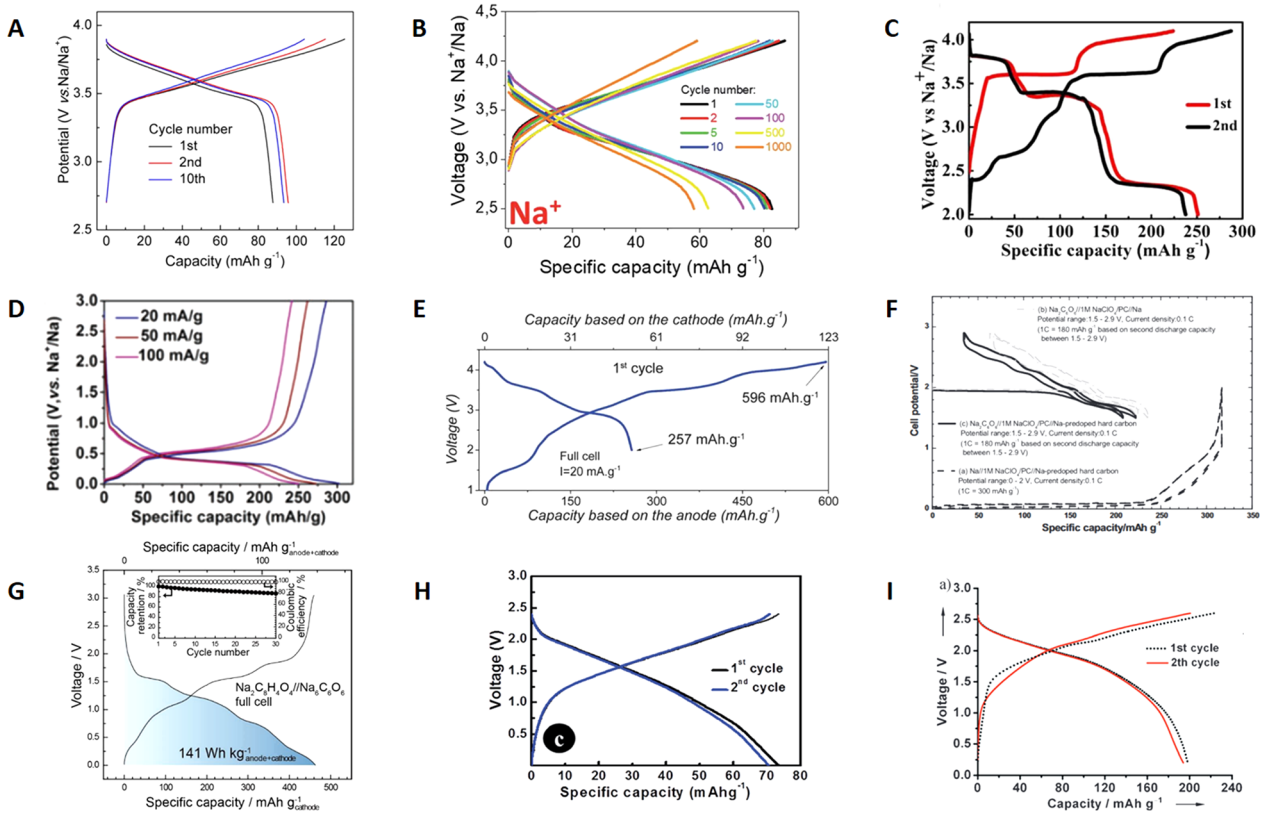

Figure 13. Voltage profiles of selected OEMs measured vs Na and all-organic Na-ion full cells including (A) PTPAn (reproduced from ref 307), (B) PDPPD (reproduced with permission from ref 308. Copyright 2019 The Royal Society of Chemistry), (C) CuTCNQ (reproduced with permission from ref 309. Copyright 2017 John Wiley & Sons, Inc.), (D) Co-bpdc (reproduced with permission from ref 317. Copyright 2018 The Royal Society of Chemistry), (E) $Na_{0.75}Mn_{0.70}Ni_{0.23}O_2$//$Na_2C_8H_4O_4$ (from ref 296. Copyright 2012 Royal Society of Chemistry), (F) $Na_2C_6O_6$// Na predoped carbon (reproduced with permission from ref 326. Copyright 2013 Elsevier Ltd.), (G) $Na_2C_6O_6$//$Na_2C_8H_4O_4$ (reproduced with permission from ref 327. Copyright 2017 Nature Publishing Group), (H) PI//$Na_2C_8H_4O_4$ (reproduced with permission from ref 328. Copyright 2015 The Royal Society of Chemistry), and (I) $Na_4C_8H_2O_6$//$Na_4C_8H_2O_6$ (reproduced with permission from ref 329. Copyright 2014 John Wiley & Sons, Inc.).

current of 20 C and 97% capacity retention over 200 cycles when cycled at a current of 5 C. This material has also been cycled in dual-ion cell configuration paired with poly(anthraquinoyl sulfide) (PAQS, Table 3, entry 2), an n-type material. This cell has an average voltage of 1.8 V and exhibits surprisingly high rate capability with 118 mAh g^{-1} reversible capacity (anode limitation design) at 32 C rate. At a rate of 8 C, the cell displays 85% capacity retention over 500 cycles. Poly(*N*,*N*′-diphenyl-*p*-phenylenediamine) (PDPPD, Table 3, entry 3) can be seen as another p-type derivative of polyaniline and can be used in lithium, sodium, or potassium batteries.[308] At an average redox potential of 3.38 V vs Na^+/Na, its initial capacity is 94 mAh g^{-1} and sustains 76% of this value after 500 cycles at a 1 C rate (Figure 13B). But the most striking performance of this polymer is certainly its ability to deliver capacity at current as high as 1000 C. At a current rate of 1, 10, 50, or 100 C, the capacity losses are reasonable after 1000 cycles.[308]

Metal organic compounds can also be used as positive electrode materials for SIBs. One such example is CuTCNQ (Table 3, entry 4).[309,310] In its original redox state, CuTCNQ is a salt formed of cuprous ions (Cu^+) and $TNCQ^-$ anion. Three redox stages could be obtained from this material at ca. 2.5, 3.4, and 3.9 V vs Na^+/Na, corresponding to $TNCQ^{2-}$/$TNCQ^-$, $TNCQ^-$/$TNCQ^0$, and Cu^+/Cu, respectively (Figure 13C). When nanostructured as flower-like nanorods anchored on 1-D carbon nanofibers (CNFs), CuTNCQ/CNFs composite displays reversible capacity of 137 mAh g^{-1} with 85% capacity retention after 300 cycles at a rate of 300 mA g^{-1} using the 3 redox couples. If restricted to a cutoff voltage of 2.5−4.1 V vs Na^+/Na which corresponds to $TNCQ^-$/$TNCQ^0$ and Cu^+/Cu^0 redox couples, the cell exhibits a capacity retention of 78% after 1200 cycles for an average redox potential of 3.6 V vs Na^+/Na. But in this case, the high redox potential is shifted up due to the contribution of a metal center, unlike p-type OEMs.

For low potential OEMs for SIBs, carboxylates (e.g., disodium terephthalate, disodium naphthalene dicarboxylate,[311] disodium pyridine-2,5-dicarboxylate,[312] disodium 4,4′-biphenyldicarboxylate,[313] and so on) or Schiff bases[314−316] have already been covered in recent reviews.[16,40,41,302] The only recent example that will be covered here is the case of a metal organic framework (MOF) made of cobalt and 4,4′-biphenyldicarboxylate ligands (Co-bpdc, Table 3, entry 5).[317] According to the authors, the cobalt ions do not undergo reduction during the electrochemical process, leaving the redox activity to the sole organic moiety. The reversible sodium insertion/deinsertion occurs at an average potential of 0.5 V vs Na^+/Na and exhibits stable capacity of ca. 300 mAh g^{-1} with 90% capacity retention for 50 cycles at 20 mA g^{-1} or 264 mAh g^{-1} and 79% capacity retention for 1000 cycles at 100 mA g^{-1} (Figure 13D).

https://dx.doi.org/10.1021/acs.chemrev.9b00482
Chem. Rev. 2020, 120, 6490−6557

The interest for low potential OEMs for SIBs started to rise when poor long-term stability or safety issues were reported with classical inorganic materials or soft/hard carbons, while positive inorganic electrodes gave promising results.[173,318−322] The larger ion diffusion pathways in OEMs are believed to be appropriate for the large sodium ions (as compared to lithium ions) while more constrained ion diffusion pathways in inorganic materials might be too restricted for sodium intercalation at low potentials.[323] Ideally, a good compromise could be found with hybrid organic/inorganic sodium-ion batteries using inorganic materials as the positive electrode and OEMs as the negative electrode. One early example is the full sodium-ion cell made of disodium terephthalate as negative electrode and $Na_{0.75}Mn_{0.70}Ni_{0.23}O_2$ as positive electrode (Table 3, entry 6).[296] With 3.6 V as output voltage, this cell delivers 257 mAh g^{-1} initial capacity (anode limitation design) with limited capacity loss after 50 cycles (93% capacity retention, (Figure 13E). Interestingly, its stability is better for this full cell rather than the two half-cells using both electrodes and metallic sodium as counter electrode. However, this better stability for a hybrid organic/inorganic sodium-ion full cell is not systematic. In the case of a $Na_3V_2O_2(PO_4)_2F$/rGO// disodium naphthalene-2,6-dicarboxylate cell with an average redox potential of 3.3 V vs Na^+/Na, a severe capacity decay is noticeable after merely 20 cycles (Table 3, entry 7), while the half-cells display a better capacity retention.[324] Other examples with acceptable stability include $Na_4Fe(CN)_6$//poly 1,4,5,8-naphthalenetetracarboxylic dianhydride (PNTCD) and $Na_3V(PO_4)_3$//PNTCD.[325] However, like most diimide compounds, the average redox potential of PNTCD is 2.1 V vs Na^+/Na, which considerably restricts the average output voltage of the full cells to 1.2 V (Table 3, entry 8, 9).

Examples of a hybrid organic/inorganic sodium-ion full cell using an OEM as the positive electrode are scarcer. One of the few cases is disodium rhodizonate which was cycled vs Na-predoped hard carbon with improved cyclability as compared to cycling vs metallic sodium (Table 3, entry 10 and Figure 13F).[326] Comparably to its lithium counterpart, disodium rhodizonate is able to reversibly intercalate four sodium ions (Table 3, entry 11).[327] When nanosized, it delivers up to 484 mAh g^{-1} with several electrochemical features corresponding to the different sodium ion insertions. Disodium rhodizonate can also be cycled in a hybrid organic/inorganic full cell vs phosphorus encapsulated in a carbon scaffold (P@C) or in an all-organic configuration vs disodium terephthalate (Figure 13G).

All-organic Na-ion batteries is an attractive concept without sensitive metals (price, rarity, geopolitics) such as cobalt, nickel, or lithium. But merely some examples have been reported in the literature. In addition to previously mentioned cases (Table 3, entries 2 and 11), a cell using *N,N′*-diamino-3,4,9,10-perylenetetracarboxylic polyimide (PI) as the positive electrode and disodium terephthalate as the negative electrode has been described (Table 3, entry 12, Figure 13H).[328] The limited output voltage of 1.6 V is here also connected to the choice of a polyimide whose average redox potential is 2.2 V vs Na^+/Na.

There is still to date only one example of an all-organic rocking chair sodium-ion battery published by Chen's group (Table 3, entry 13 and Figure 13I).[329] The tetrasodium salt of 2,5-dihydroxyterephthalic acid (Na_4DHTPA or Na_4-*p*-DHT) is used in the same time as both positive and negative electrodes in a symmetrical cell as previously demonstrated in the case of the lithium chemistry.[251] With 2 V as output voltage, this cell is hampered by the irreversible capacity of the negative electrode and displays reversible capacity of 198 mAh g^{-1} with 76% capacity retention after 100 cycles at a rate of C/10.

6.2. Organic Electrode Materials with High Specific Capacity

All materials selected in this section are able to deliver more than 300 mAh g^{-1} over tens of cycles without conductive additive contribution. Interestingly, besides the previously mentioned disodium rhodizonate, many other high-capacity materials for SIBs involve the intercalation of sodium ions onto unsaturated carbons, as a sodium equivalent of the mechanism coined as "superlithiation" (see section 7.3), which will be thoroughly covered in the section 7.3.[21,260] Consequently, their electrochemical features display similarities such as the requirement for large polarization values, sloping curves, and poor round trip efficiency. A first example is polydopamine (PDA, Table 3, entry 14) employed as both electrode and redox-active binder material, obtained as a mixture of *ortho*-catechol and *ortho*-quinone.[330] After a first cycle with low Coulombic efficiency which could be explained by the solid electrolyte interface (SEI) formation and proton/sodium exchange in the catechol moieties, it shows an impressive stable capacity of 500 mAh g^{-1} with no obvious capacity loss over 1024 cycles.

The group of Zhouguang Lu has investigated several derivatives of tri-*β*-ketoenamine linked compounds, either as a single molecule or as covalent organic frameworks (COF).[331,332] If cycled at low potential vs Na^+/Na, after the expected reduction of carbonyls from the anthraquinone moieties, the enolization of carbonyls of the tri-*β*-ketoenamine generates a triradical. The storage of three additional sodium ions is allowed by the reduction of the carbon backbone. Surprisingly, neither the triradical intermediate nor the organosodium species display major stability issues. In the case of TSAQ (Table 3, entry 15), the electrodes show a highly reversible capacity of 320 mAh g^{-1} with capacity retention higher than 95% after 50 cycles at a current density of 100 mA g^{-1}.[331] When cycled at a current 10 times higher, a capacity above 220 mAh g^{-1} is sustained for 2600 cycles (Figure 14A). For DAAQ-COF (Table 3, entry 16), which can be seen as a COF derivative of TSAQ, the specific capacities are highly dependent on the particle size, even if this parameter does not seem to hamper the stability. The best performances are obtained with 4−12 nm particles that can sustain specific capacity above 400 mAh g^{-1} for 100 cycles. More impressively, when cycled at a current as high as 5 A g^{-1}, ca. 200 mAh g^{-1} are maintained for 10 000 cycles (Figure 14B).

As an alternative to carboxylates such as disodium terephthalate, their sulfur derivatives thiocarboxylates have been investigated, where either one or two of the oxygen atoms of the carboxylate function are replaced by sulfur atom in this series of analogues.[333] The best performances are obtained with the compound Table 3, entry 17 with capacity as high as 567 mAh g^{-1} at a current density of 50 mAh g^{-1} and limited capacity loss after 250 cycles. Considering this compound has a larger molecular weight as compared to disodium terephthalate, its theoretical capacity per exchanged electron is lower (97.7 mAh g^{-1} against 127.5 mAh g^{-1}). However, while disodium terephthalate is limited to two electrons exchanged, compound 17 can accommodate up to 6 electrons with partial reversible reduction of its benzene ring through the "supersodiation" process (similar to "superlithiation", see section 7.3).

https://dx.doi.org/10.1021/acs.chemrev.9b00482
Chem. Rev. 2020, 120, 6490−6557

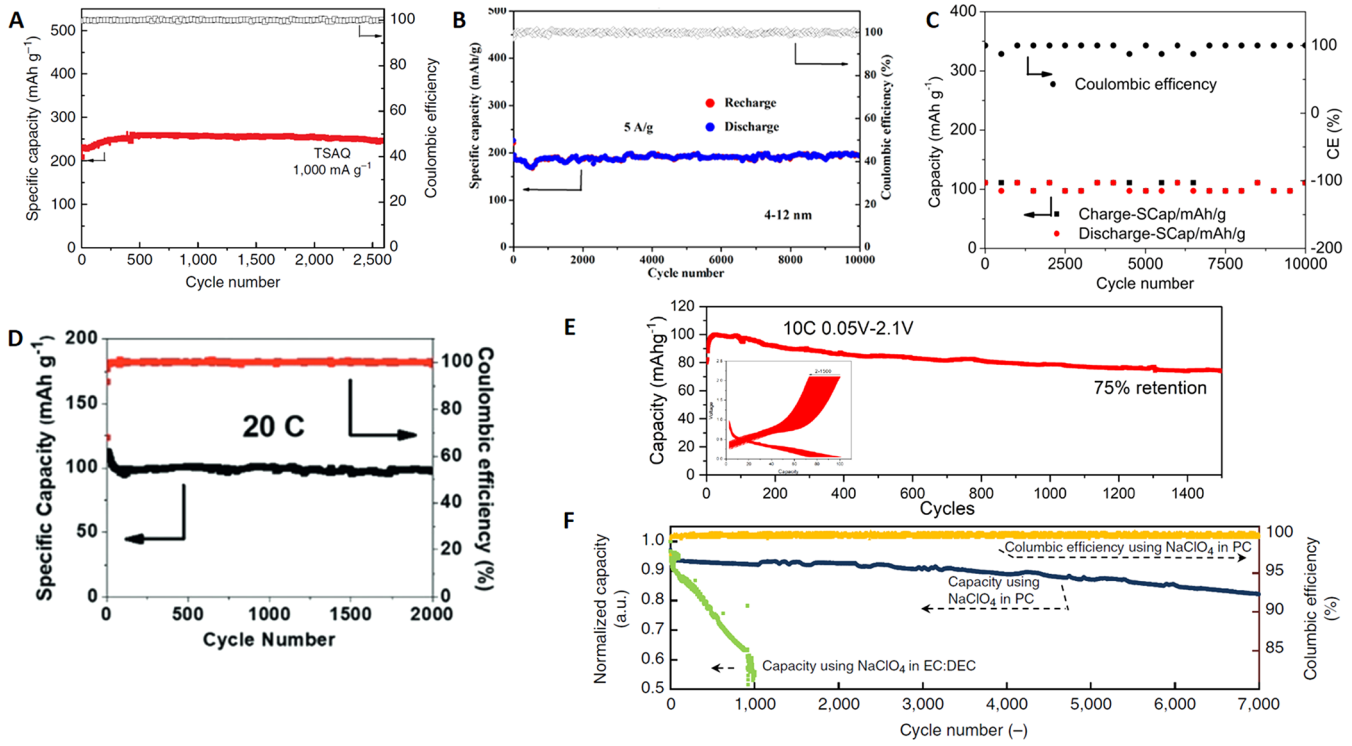

Figure 14. Capacity retention of selected OEMs measured vs Na including (A) TSAQ (reproduced from ref 331), (B) DAAQ-COF (reproduced with permission from ref 332. Copyright 2019 American Chemical Society), (C) PPTS (reproduced with permission from ref 334. Copyright 2018 Elsevier Ltd.), (D) ADASS (reproduced with permission from ref 335. Copyright 2018 John Wiley & Sons, Inc.), (E) $Na_3C_9H_3O_6$ (reproduced with permission from ref 336. Copyright 2018 John Wiley & Sons, Inc.), and (F) BPOE (reproduced from ref 337).

6.3. Organic Electrode Materials with Long Cycle Life

In general, poorer stabilities are observed for SIBs as compared to LIBs due to SEI layer compounds dissolution in the electrolyte system, to the very unstable metallic sodium for the half-cell configurations (dendrites formation), or to Na_xC formed from sodium intercalation into the conductive additive at low potential. Achieving 1000 cycles or more for SIBs without severe capacity loss is hence a challenge. However, some OEMs are able to sustain high capacities for such long cycling. Some examples were previously commented (Table 3, entries 3, 4, 5, 14, 15, and 16).

As already seen, the average redox potential of polyimides is usually in the 2.1−2.2 V vs Na^+/Na potential range. Consequently, they suffer less long-term instability due to extreme potential windows. Polyethylenediamine 1,4,5,8-naphthalenetetracarboxylic dianhydride (PEDA-NTCDA, Table 3, entry 18),[338] polyethylenediamine 3,4,9,10-perylene-tetracarboxylic dianhydride (PEDA−PTCDA, Table 3, entry 19),[339,340] polypropylenediamine 3,4,9,10-perylenetetracarboxylic dianhydride (PPDA−PTCDA, Table 3, entry 20),[340] and polyhexylenediamine 3,4,9,10-perylenetetracarboxylic dianhydride (PHDA−PTCDA, Table 3, entry 21)[340] have all been cycled for at least 1000 cycles with negligible capacity loss. Especially, PEDA−PTCDA retained 87.5% of its initial capacity after 5000 cycles (Figure 14C).[339]

Anthraquinones reversibly insert sodium at average redox potential slightly lower as compared to polyimides (*i.e.*, 1.6–1.8 V vs Na^+/Na), limiting also the risk of side reactions. Anthraquinones as polymers (PAQS, Table 3, entry 22)[341] or as salts (disodium 9,10-anthraquinone-2,6-disulfonate, $Na_2AQ26DS$, Table 3, entry 23)[342] have been successfully cycled for 1000 cycles. An anthraquinone derivative, poly(pentacenetetrone sulfide) (PPTS, Table 3, entry 24) exhibits a remarkable stability at a very high rate of 50 A g^{-1} corresponding to a full charge in 7 s. After 10 000 cycles, it still maintains 97 mAh g^{-1} (Figure 14C).

Azobenzene-4,4′-dicarboxylic acid sodium salt (ADASS, Table 3, entry 25) is a material that can reversibly insert two sodium ions on its azo (−N═N−) function at an average redox potential of 1.25 V vs Na^+/Na.[335] It can be cycled at a high current of 10 or 20 C for 1000 and 2000 cycles, respectively, with moderate capacity losses (Figure 14D). The average redox potential of sodium carboxylates is rather low (usually in the 0.3−0.8 V range vs Na^+/Na) which makes side reaction likely to occur during long time cycling. Still, the group of Palani Balaya succeeded to cycle trisodium-1,3,5-benzene tricarboxylate (Table 3, entry 26) for 1500 cycles at a rate of 10 C with 75% capacity retention with a lower cutoff potential of 50 mV (Figure 14E).[336]

Several covalent organic frameworks (COFs) have shown excellent cyclability. An early example from the literature is a p-type material (Table 3, entry 27) that reversibly inserts anion (ClO_4^-) at an average potential of 2.6 V vs Na^+/Na and sustains 80% of its capacity after 7000 cycles at a rate of 1 A g^{-1} (Figure 14F).[337] Other triazine-based COFs have been used as n-type materials with the integration of carbonyl-containing moieties (Table 3, entry 28, 29).[343] After a stabilization period corresponding to 30 cycles, they sustain most of their capacities over 1000 cycles at a high rate of 5 A g^{-1}. In addition to the previously mentioned tri-β-ketoenamine derivatives, which have already shown excellent stability (Table 3, entry 15, 16), the pentacenetetrone derivative 30 is able to maintain 95% of its capacity after 1400 cycles at a rate of 1 A g^{-1}.[344]

https://dx.doi.org/10.1021/acs.chemrev.9b00482
Chem. Rev. 2020, 120, 6490−6557

Table 4. Performances of Selected Nonaqueous K−Organic Batteries

#	Positive electrode (or "cathode") active material	Negative electrode (or "anode") active material	Electrolyte	Output voltage (V)	Cycling stability: retention, cycles, rate or current density	Specific capacity (mAh g^{-1}) and Specific energy (Wh kg^{-1}) per mass of positive active material if not specified otherwise, Final coulombic efficiency, Loading (mg cm^{-2})	Ref.
1	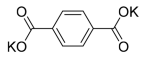	K	1 M KPF_6 in DME	0.6	95%,[a] 500, 1 A g^{-1}	194, 116, ~100, 1.2-1.6	[346]
2	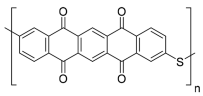	K	1 M KPF_6 in DME	1.7	74%, 3 000, 24 C (5 A g^{-1})	258, 439, 99, 1.0-2.0	[347]
3	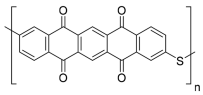	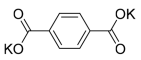	1 M KPF_6 in DME	~1.1	66%, 100, 100 mA g^{-1}	254,[b] 122,[b] 99, 1.0-2.0	[347]
4		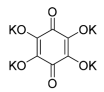	1.25 M KPF_6 in DME	~1.25	n.d., 10, 25 mA g^{-1}	~28,[b] 35[b] n.d., 1.5-2.0	[348]
5		K	1 M KPF_6 in PC/FEC (v/v 98:2)	4.05	86%, 100, 50 mA g^{-1} 55%, 500, 2 A g^{-1}	125, 487, 88, 2.0 85, 351, 88, 2.0	[349]
6	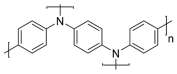	K	0.5 M KPF_6 in EC/DEC (v/v 1:1)	3.52	63%, 1 000, 10 C	62-39, 218, n.d., 1.0-2.0	[308]
7	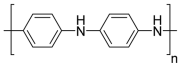	K	PMMA / 0.8 M KPF_6 in EC/DEC/FEC (v/v/v 45:45:10)	3.15	98%, 100, 50 mA g^{-1}	125, 394,n.d., 3.0	[350]

[a]The first cycle is not taken into account. [b]Based on cathode material weight.

To sum up, the development of organic SIBs has gained remarkably increased attention since 2012 and is considered as an interesting alternative to organic LIBs making the development of cationic rocking-chair batteries made of abundant elements possible. Although great achievements have been made, many challenges still remain to tackle problems such as capacity fading or low energy density. Polymerization, metal/covalent organic frameworks, or insoluble salts are successful strategies to suppress the former, and very long cycling batteries have been reported without structural instability. As compared to their inorganic counterparts, promising results have been obtained for negative electrodes as an alternative to metallic sodium, graphite, or even hard/soft carbons. Improving the energy density is more complex and requires advanced electrode design in order to suppress as much conductive additive as possible. Nevertheless, the combination of renewable organic materials together with the high abundance of sodium raw materials provides an appealing concept, which is enough for encouraging continuous progress, and research in this field should certainly be esteemed.

7. PERFORMANCES OF OTHER NONAQUEOUS ORGANIC BATTERIES

7.1. Performances of Nonaqueous Potassium−Organic Batteries

Surprisingly, despite the natural abundance of potassium, its relative low-cost, and the low electrochemical potential of K^+/K (−2.94 V vs SHE), K−ion batteries (KIBs) have not been thoroughly investigated until recently,[345] with the motivation being related to its abundancy like Na compared to Li. One scientific reason is the large 1.38 Å ionic radius of K^+ (0.76 Å for Li^+, 1.02 Å for Na^+), which makes a challenge the design of inorganic materials able to reversibly insert such large ions into a rigid and constrained framework. Considering their larger interlayer spacing and flexible framework, OEMs for KIBs have then attracted the attention of researchers in parallel with the early development of their inorganic counterparts and not years or decades later unlike LIBs or SIBs. The research on OEMs for KIBs has clearly taken advantage of the years of development of OEMs for LIBs and SIBs and organic templates, which have been proven successful in these devices, have been adapted for KIBs, swapping from lithium or sodium salt to potassium salts when necessary.

One such example is the dipotassium terephthalate (Table 4, entry 1) which intercalates/deintercalates potassium ion at an average potential of 0.6 V vs K^+/K with a well-defined plateau after the first cycle.[346] It exhibits reversible capacity up to 249 mAh g^{-1}, and good capacity retention of 95% over 500 cycles is obtained when cycled at a rate of 1000 mA g^{-1} (Figure 15A). Quinone derivatives have already displayed their robustness in other EES devices. Poly(pentacenetetrone sulfide) (PPTS, Table 4, entry 2) can be cycled for 3000 cycles at a rate of 5 A g^{-1} with limited capacity decay (Figure 15B).[347] Interestingly, at such a high rate, the Coulombic efficiency is much higher as compared to cycling at a rate of 0.1 A/g (~99% against ~90%), which is due to the highly reactive metallic potassium counter electrode and dendrite formation according to the authors.

These two materials have been cycled in an all-organic full cell (thereby without metallic potassium) which delivers 254 mAh g^{-1}

https://dx.doi.org/10.1021/acs.chemrev.9b00482
Chem. Rev. 2020, 120, 6490−6557

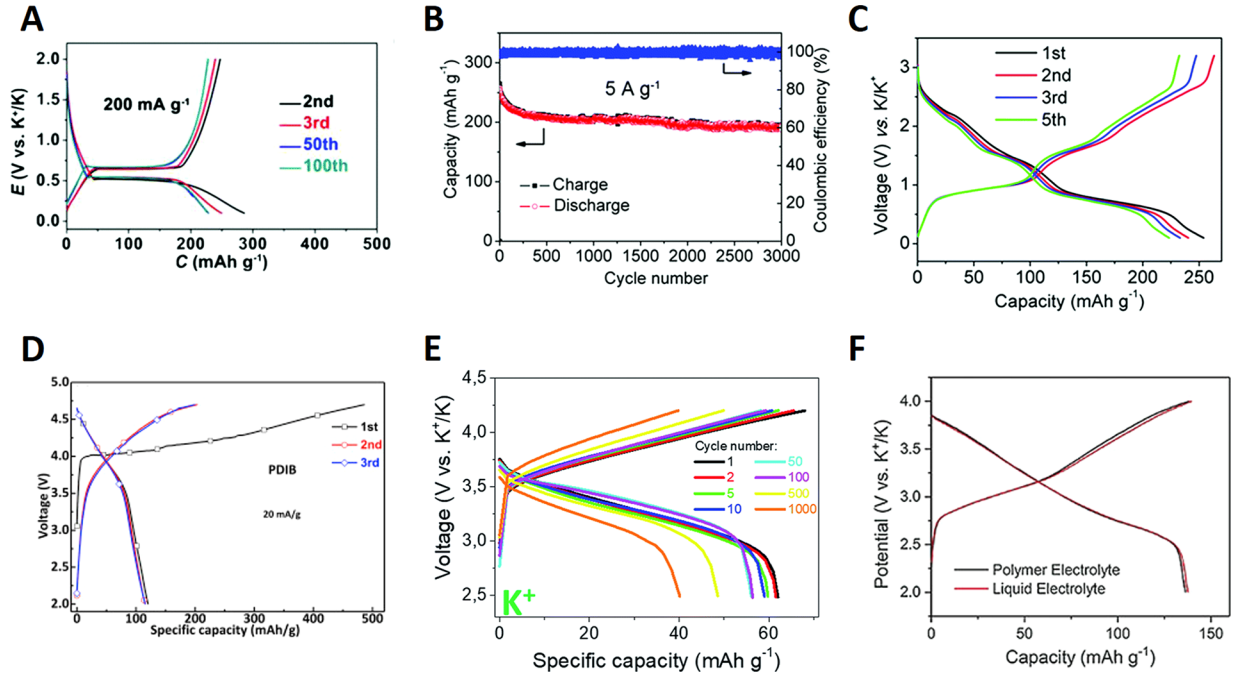

Figure 15. Voltage profiles or capacity retention of selected OEMs measured vs K including (A) $K_2C_8H_4O_4$ (reproduced with permission from ref 346. Copyright 2017 The Royal Society of Chemistry), (B) PPTS (reproduced with permission from ref 347. Copyright 2019 The Royal Society of Chemistry), (C) PPTS//$K_2C_8H_4O_4$ (reproduced with permission from ref 347. Copyright 2019 The Royal Society of Chemistry), (D) PVK (reproduced with permission from ref 349. Copyright 2019 Elsevier Ltd.), (E) PDPPD (reproduced with permission from ref 308. Copyright 2019 The Royal Society of Chemistry), and (F) PAni (reproduced with permission from ref 350. Copyright 2018 John Wiley and Sons).

initial capacity and 66% capacity retention after 100 cycles with an average Coulombic efficiency of 99% (Table 4, entry 3, Figure 15 C). Another example of an all-organic full cell has been realized by Chen's group using dipotassium rhodizonate as the positive electrode of tetrapotassium salt of tetrahydroxyquinone as the negative electrode (Table 4, entry 4).[348] Unfortunately, this cell displays very limited stability.

Materials with an average redox potential above 3.0 V vs K^+/K all belong to the p-type class and hence insert anions instead of potassium ions (dual-ion cell configuration, Figure 9b-3). The highest redox voltage for an organic KIB to date has been obtained using poly(*N*-vinylcabazole) (PVK) which can insert PF_6^- at an average redox potential of 4.05 V vs K^+/K but with poor Coulombic efficiency (Figure 15D).[349] Other remarkable performances have been obtained with PDPPD (3.52 V vs K^+/K, Figure 15E)[308] and polyaniline (PAni, 3.15 V vs K^+/K, Figure 15F).[350]

In short, the research on KIBs is still in its infancy after starting to bloom in 2015 for inorganic electrode materials and 2016 for OEMs. One major challenge is the replacement of metallic potassium with a more stable negative electrode. But this has not prevented the development of long-term cycling batteries with more than 1000 cycles (Table 4, entries 2 and 6; see also refs 351−356).

7.2. Nonaqueous Multivalent Metal−Organic Batteries (Mg, Al, Zn)

Among the investigated post-LIB systems, rechargeable batteries based on multivalent metal-ion shuttling (including Mg^{2+}, Ca^{2+}, Al^{3+}, Zn^{2+}) are expected to offer significant improvement in volumetric energy density simply by using the corresponding metal as the negative electrode material (e.g., ≈3833 mAh cm^{-3} theoretical volumetric energy density for Mg compared to ∼2046 mAh cm^{-3} for Li metal). In addition, the abundancy of such elements is not critical (2.5% of the earth's crust for Mg against 0.0017% for Li).[357,358] The current status is that few regular host inorganic electrode compounds, based on which Li-ion batteries are established, are able to deliver reasonable electrode performance for storing multivalent metal-ions. For Mg batteries, the flagship multivalent-metal batteries, Chevrel phase Mo_6X_8 (X = S, Se), continue to be the only reliable positive electrode materials despite the limited specific energy of the Mo_6X_8−Mg systems (up to 140 Wh kg^{-1}).[359,360] Recent discoveries of spinel Ti_2S_4 and sulfur as Mg positive electrode materials in conjunction with the continuous development of non-nucleophilic chloride-free electrolytes greatly expanded the technology, but sluggish kinetics remain and stability issues are real.[361,362] This is where OEMs start to look interesting: some OEMs have been reported to show adequate kinetics even at room temperature and deliver higher specific energies than those achieved by inorganic intercalation compounds at elevated temperatures. Due to these early successes, OEMs are now regarded by some as a wild card to enable multivalent-metal batteries.[48,358,363] The properties and cell performance of these materials are summarized for comprehensive comparison (Table 5).

The promises aside, it is necessary to emphasize that multivalent chemistries are more complicated than monovalent ones, and the ion storage mechanism has not received enough scrutinization for many OEMs. For example, Mg^{2+} is notoriously difficult to be dissociated from electrolyte solution species such as Cl^- and ethereal solvent molecules.[364,365] While most studies on Mg−organic batteries employed Cl^--containing electrolytes, a very recent study showed that probably all n-type OEMs store $MgCl^+$ instead of the presumed Mg^{2+} in these electrolytes.[366] This unintended storage mechanism would effectively make most Mg−organic batteries hybrid batteries, that is, the charge carrier ions at the positive and negative electrodes are different, and the electrolyte solution

https://dx.doi.org/10.1021/acs.chemrev.9b00482
Chem. Rev. 2020, 120, 6490−6557

Table 5. Performances of Selected Nonaqueous Multivalent Metal−Organic[e]

#	Cell configuration (ionic carriers)	Positive electrode (or "cathode") active material	Negative electrode (or "anode") active material	Electrolyte	Output voltage (V)	Cycling stability: retention, cycles, rate or current density	Specific capacity (mAh g^{-1}) per mass of positive active material if not specified otherwise and Specific energy (Wh kg^{-1}) per mass of the two active materials plus anions involved in the electrode reactions, Final coulombic efficiency, Loading (mg cm^{-2})	Ref.
1	N/A[a]	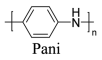 Pani	(Pt)	0.025 M $MgSO_4$ in EMIES	2.09	53%, 60, 667 mAh g^{-1}	116, N/A	[367]
2	Mg^{2+}, ClO_4^-	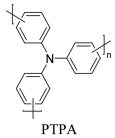 PTPA	AC	1 M $Mg(ClO_4)_2$ in AN	3.2	N/A	N/A	[368]
3	Mg^{2+}, $TFSI^-$	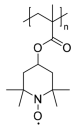 PTMA	Mg	0.3 M $Mg(TFSI)_2$ in G1/G2	~2.3	N/A	38, 62	[369]
4	N/A[b]	carbyne polysulfide	Mg	0.25 M $Mg(AlCl_2EtBu)_2$ in THF	1.25	71%, 23, 5.4 mA g^{-1}	328, N/A	[373]
5	N/A[b]	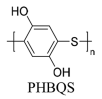 PHBQS	Mg	0.16 M $3MgCl_2$–$2Mg(TFSI)_2$ in G4/DOL	1.8	c	158, N/A	[371]
6	N/A[b]	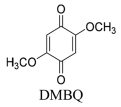 DMBQ	Mg	0.5 M $Mg(ClO_4)_2$ in GBL	0.95	85%, 5, 260 mA g^{-1}	260, N/A	[374]
				0.5 M $Mg(TFSI)_2$–2 $MgCl_2$ in DME	1.63	38%, 30, 0.2C	226, N/A	[370]
7	Mg^{2+}	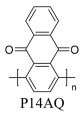 P14AQ	Mg	0.2 M $Mg(TFSI)_2$ in G2	1.36	72%, 100, 130 mA g^{-1}	180, 227	[366]
8	Mg^{2+}	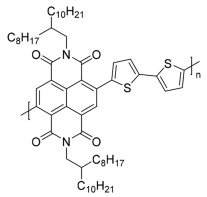 P(NDI2OD-T2)	Mg	0.2 M $Mg(TFSI)_2$ in G2	1.45	87%, 2 500, 300 mA g^{-1}	54, 76	[366]
9	N/A[b]	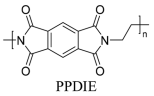 PPDIE	Mg	$PhMgCl–AlCl_3$ in THF	1.2	89%, 200, 150 mA g^{-1}	140, N/A	[282]
10	$AlCl_4^-$, Al^{3+}	 polythiophene	Al	2EMImCl–3Al Cl_3	1.35	80%, 100, 16 mA g^{-1}	88, 76	[375]
11	$AlCl_4^-$, Al^{3+}	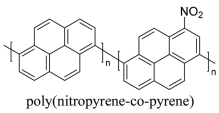 poly(nitropyrene-co-pyrene)	Al	EMImCl–1.3Al Cl_3	1.75	76%, 1 000, 200 mA g^{-1}	70, 85	[377]

https://dx.doi.org/10.1021/acs.chemrev.9b00482
Chem. Rev. 2020, 120, 6490−6557

Table 5. continued

#	Cell configuration (ionic carriers)	Positive electrode (or "cathode") active material	Negative electrode (or "anode") active material	Electrolyte	Output voltage (V)	Cycling stability: retention, cycles, rate or current density	Specific capacity (mAh g^{-1}) per mass of positive active material if not specified otherwise and Specific energy (Wh kg^{-1}) per mass of the two active materials plus anions involved in the electrode reactions, Final coulombic efficiency, Loading (mg cm^{-2})	Ref.
12	N/A[d]	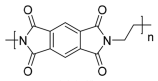 PPDIE	Al	2EMImCl–3Al Cl_3	0.5	75%, 100, 150 mA g^{-1}	140, N/A	[282]
13	$AlCl_2^+$, Al^{3+}	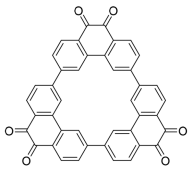 PQ-Δ	Al	3EMImCl–4Al Cl_3	1.39	59%, 5 000, 2 A g^{-1}	94, 97	[380]
14	Zn^{2+}, $TFSI^-$	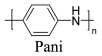 Pani	Zn	0.3 M $Zn(TFSI)_2$ in PC	0.8	85%, 2 000, 1 C	154, 44	[376]

[a]Could be either SO_4^{2-} or $CH_3CH_2SO_3^-$. [b]Could be either Mg^{2+} or $MgCl^+$. [c]Only showed the initial "activation" cycles where capacity was increasing. [d]Could be either Al^{3+} or $AlCl^{2+}$ or $AlCl_2^+$. [e]Abbreviations: EMIES = 1-ethyl-3-methylimidazolium ethyl sulfate; AN = acetonitrile; G1 = monoglyme; G2 = diglyme; G4 = tetraglyme; TFSI = bis(trifluoromethane)sulfonimide; DOL = dioxolane; THF = tetrahydrofuran; GBL = γ-lactone; EMIm = 1-ethyl-3-methylimidazolium; PC = propylene carbonate; DME = dimethoxyethane.

must contain enough of the necessary ions to maintain charge balance. Cell specific capacity will be heavily limited by the weight of the electrolyte solution as a result. Since unambiguous determination of the stored species in most previously reported Mg–organic batteries has been overlooked, it would be difficult to estimate the actual specific capacity of those systems. In fact, such negligence is not specific to Mg–organic batteries studies but Mg-ion storing positive electrode material research in general. In the future, this situation can be reverted by dedicated characterizations and rational selection of electrolyte solutions. This section mainly concerns the apparent specific capacity of OEMs and only discusses storage mechanism where sufficient experimental evidence of stored species is available.

Similar to nonaqueous Li–organic batteries, the highest discharge potentials for Mg–organic batteries have been reported for p-type OEMs. Conductive polymer polyaniline (PAni), nitrogen-centered PTPA, and oxygen radical-centered PTMA all discharge at >2 V vs Mg^{2+}/Mg, with PTPA showing the highest discharge potential at 3.2 V vs Mg^{2+}/Mg.[367−369] Note that none of these materials were tested in electrolyte solutions where reversible Mg plating/stripping is possible. Among n-type OEMs, *p*-BQ-based molecule DMBQ and polymer poly(hydrobenzoquinonyl-benzoquinonyl sulfide) (PHBQS) show the highest discharge potentials of 1.63 and 1.8 V vs Mg^{2+}/Mg, respectively (Figure 16B, C).[370,371] Other carbonyl compounds based on anthraquinone and imides discharge at lower potentials, as they also do in Li batteries.[372] As far as specific capacity is concerned, the organosulfur compound carbyne polysulfide shows the highest 328 mAh g^{-1} (Figure 16A), with carbonyl compounds DMBQ (up to 260 mAh g^{-1}) and P14AQ (180 mAh g^{-1}) following (Figure 16C, D).[366,373,374] The change of charge carrier ion from Li^+ to Mg^{2+} does not seem to alter the cycling stability generally observed for Li^+-storing polymer OEMs. P(NDI2OD-T2) and PPDIE lose 13% and 11% of their initial capacities after 2500 and 200 deep cycles, respectively, which stability is rarely seen from inorganic positive electrode materials (Figure 16E).[282,366] While these are quite some attractive numbers, there is no OEM that simultaneously shows high discharge potential, specific capacity, and cycling stability. There are also few OEMs that have been confirmed to store Mg^{2+} instead of complex ions. Therefore, there is a lot of opportunity lying ahead for developing better OEMs for Mg-organic batteries.

OEMs for other nonaqueous multivalent metal-ions storage are quite rare. Most OEMs reported for multivalent-metal–organic batteries have been p-type materials where storage of anions rather than cations takes place (dual-ion cell configuration). Conductive polymers PT and PAni have been studied in Al and Zn batteries, respectively, showing decent to great cycling stability.[375,376] Poly(nitropyrene-co-pyrene) shows the highest discharge potential for an Al–organic battery at 1.75 V with great 75% capacity retention after 1000 cycles.[377] Note that for Al batteries, only graphite, also a p-type material in this case, shows viable performances despite limited specific capacity.[378,379] OEMs are thus welcomed additions to the technology. More interestingly, very recent studies show that efficient storage of Al in n-type OEMs is also possible. Phenanthraquinone triangle PQ-Δ uniquely stores $AlCl_2^+$ instead of $AlCl_4^-$ which basically every other decent cathode stores, hence opening up a brand new design space for Al positive electrode materials (Figure 16F).[380] PPDIE also seems to store cationic Al species considering it being an n-type material at the corresponding potential (0.5 V vs Al^{3+}/Al), though more characterization would be needed to reveal the nature of the stored ions.[282]

Overall, OEMs indeed look promising as unique enablers for the otherwise quite problematic multivalent-metal batteries, even though detailed studies regarding the ion storage mechanism and performance improvement have only just begun.

7.3. Comments on The Peculiar Multiple Cation Insertion Phenomenon in Organics

The electrochemical process coined as "superlithiation" corresponds to a two-electron reduction of a carbon–carbon

https://dx.doi.org/10.1021/acs.chemrev.9b00482
Chem. Rev. 2020, 120, 6490−6557

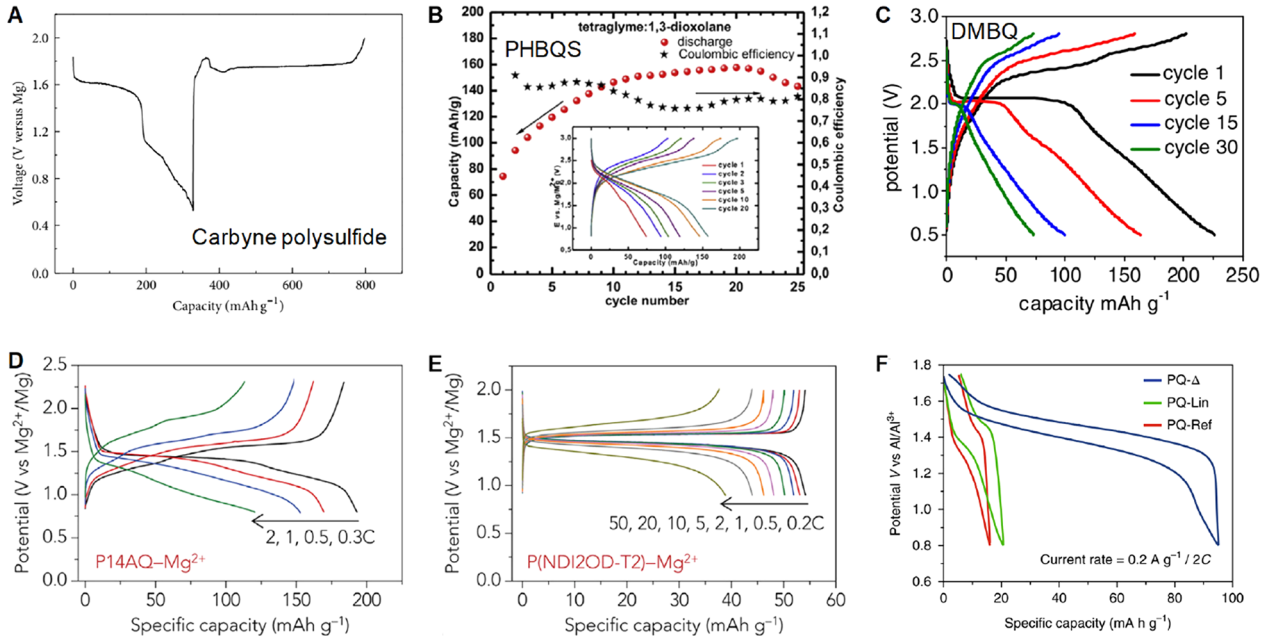

Figure 16. Voltage profiles of selected OEMs studied measured vs Mg (A–E) and Al (F). (A) Carbyne polysulfide (reproduced from ref 373), (B) PHBQS (reproduced with permission from ref 371. Copyright 2016 Elsevier Ltd.), (C) DMBQ (reproduced with permission from ref 370. Copyright 2016 The Electrochemical Society), (D) P14AQ (reproduced with permission from ref 366. Copyright 2018 Elsevier Ltd.), (E) P(NDI2OD-T2) P14AQ (reproduced with permission from ref 366. Copyright 2018 Elsevier Ltd.), and (F) PQ-Δ (reproduced with permission from ref 380. Copyright 2016 Nature Publishing Group).

double bond with a concomitant uptake of two lithium ions for charge compensation (Scheme 1A). Consequently, a material with solely sp^2 hybridized carbons could in theory reach a 1/1 Li/C ratio when fully reduced, allowing us to reach extremely high specific capacities. It was first established in 2012 in an article from Taolei Sun where 1,4,5,8-naphthalenetetracarboxylic dianhydride (NTCDA), a material with 4 carbonyls and 14 sp^2 hybridized carbons, could insert 18 lithium ions.[381] This work was accompanied by an NMR study which displayed particularly shielded ^1H peaks for the "superlithiated" NTCDA, matching their proposed mechanism.

Remarkably, some template molecules seem to be subjected to diverse multiple alkali metal ions insertions; the process is hence not limited to lithium ion uptake. For instance, 3,4,9,10-perylene-tetracarboxylicacid-dianhydride (PTCDA) is able to uptake up to 28 lithium ions,[381] 15 sodium ions[382] or 11 potassium ions (Scheme 1B).[383] It is interesting to note that the larger the radius of the concerned cation, the fewer could be inserted onto PTCDA, possibly due to steric hindrance. However, in the case of PTCDA, the mere reduction of the first two carbonyls is a reversible process, while the reduction of the last two and the "superlithiation/sodation/potation" is not. Nonetheless, over the course of the last years, many materials have been described reacting according to reversible "superlithiation" and are able to deliver specific capacities sometimes exceeding 1000 mAh g^{-1} for hundreds of cycles.

The typical electrochemical feature of the "superlithiation" process is a sloping curve without obvious plateau requiring a large potential window to achieve high Coulombic efficiency (typically 0.05–3 V) and exhibiting a large hysteresis (polarization) sometimes exceeding 1 V (Figure 17A). Despite the attractive specific capacities obtained with these materials and the intriguing science (but still poorly understood) behind it, these electrochemical features make them of no practical use. Nevertheless, while initially believed to be connected with fused aromatic rings or to be kinetically limited, numerous examples have been described with a single[260] or no aromatic ring[384] and with excellent capacity at a high current rate, and there is still hope for further developments of this redox process. By nature, "superlithiated" materials are typically investigated as negative electrode (starting with a cation uptake). The only case of a "superlithiated" positive electrode (starting with a cation release) is lithium carbide Li_2C_2, where up to one lithium ion can be released from the structure.[385,386] As previously mentioned, this review does not try to be exhaustive, and just a few examples will be presented here. The total amount of articles on materials which could be related to a "superlithiation" process has exceeded 100. For the sake of clarification, OEMs containing a transition metal such as metal–organic frameworks, coordination polymers, or organometallic compounds have been excluded, considering that their specific capacity has a contribution from the transition metal in addition to the "superlithiation" corresponding to the organic moiety.

Polyanthraquinone-triazine (PAT) is a COF using repeating units similar to COFs previously mentioned. However, unlike the other triazine-based and anthraquinone-based COFs, PAT undergoes a 17-electron reduction per repeating unit, corresponding to the reduction of 2 carbonyls (2 electrons), the triazine unit (3 electrons) and the 2 benzene rings of the anthraquinone moiety (12 electrons), leading to a maximum reversible capacity of 770 mAh g^{-1} (Table 6, entry 1, and Figure 17B).[387] Interestingly, the capacity decreases in the first 30 cycles before slowly increasing with time over 400 cycles, which has been assigned to a slow activation process. This behavior has been observed for several "superlithiated" materials, such as F-PDI-3-TC (Table 6, entry 2).[388] Its initial capacity is merely 95.7 mAh g^{-1} but reaches 783 mAh g^{-1} after 1000 cycles (Figure 17C). Other examples include poly(benzobisimidazobenzophenanthroline) (BBL) and poly(1,6-

https://dx.doi.org/10.1021/acs.chemrev.9b00482
Chem. Rev. 2020, 120, 6490–6557

Scheme 1. (A) Electrochemical Storage Mechanism of the "Superlithiation"; (B) Multiple Cation Insertion for PTCDA

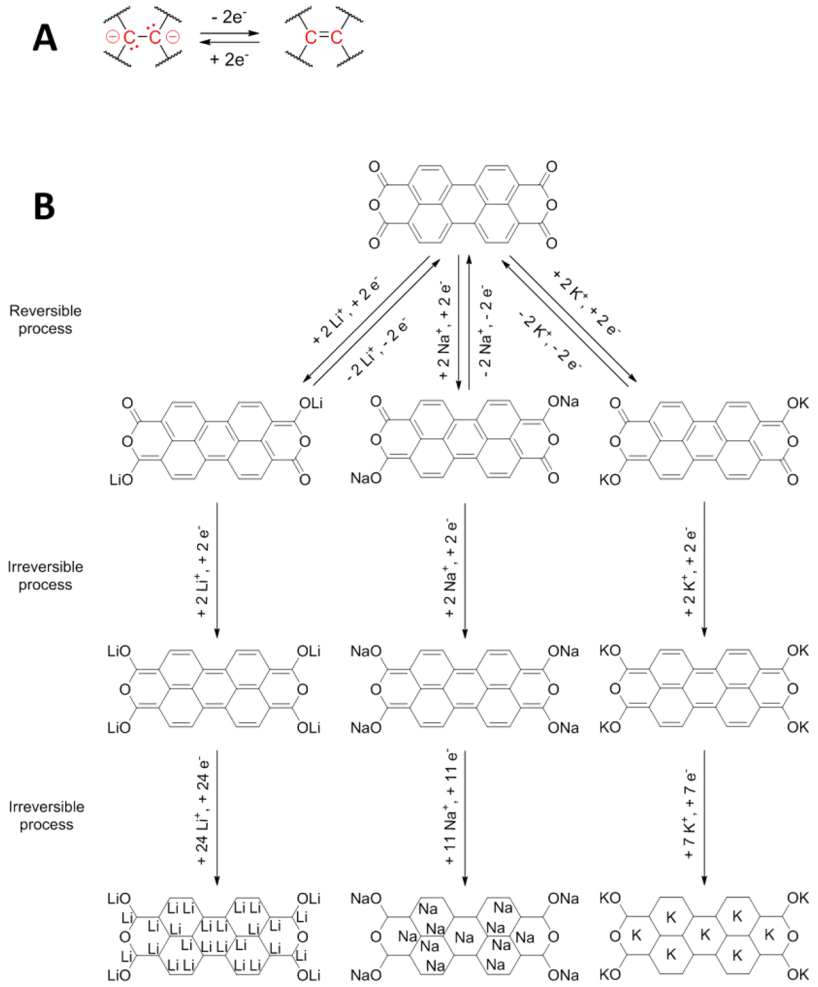

dihydropyrazino[2,3g]quinoxaline-2,3,8-triyl-7-(2*H*)-ylidene-7,8-dimethylidene) (PQL) that can reach up to 1 285 mAh g^{-1} and 1 550 mAh g^{-1} of reversible capacity, respectively (Figure 17D, E).[389,390] For these last two materials, the capacity and kinetics are improved when cycled at 50 °C instead of room temperature. BBL and PQL display discharge capacities of 496 mAh g^{-1} and ca. 500 mAh g^{-1} at the 1000th cycle at a rate of 3 and 2.5 C, respectively.

Briefly, "superlithiation" is a peculiar but fascinating electrochemical process giving access to extremely high reversible capacities. However, very little is understood about it such as why some specific structures are subjected to "superlithiation" and others structurally closely related are not. But the main limitation is clearly the poor round trip energy efficiency of devices using "superlithiated" materials which, if not solved, will restrain this process to a scientific curiosity with no practical applications for the moment.

8. SOLID ORGANIC ELECTRODES FOR AQUEOUS BATTERIES

8.1. Introductory Statement

Although there are fewer examples in the literature concerning the use of OEMs in aqueous electrolyte, this application is of interest for developing low cost and environmentally friendly electrochemical storage solutions. Aqueous rechargeable batteries featuring low-cost and nonflammable water-based electrolytes are intrinsically safe and do not rely heavily on battery management systems, thereby providing robustness and cost advantages over competing lithium-ion batteries that use volatile and toxic organic electrolytes. However, the state-of-the-art aqueous rechargeable batteries show short cycle life and fall short of meeting large-scale applications where frequent replacement of batteries is undesirable. This is typical of PbA batteries (200 cycles for deep cycling) where the lead electrode undergoes irreversible passivation of $PbSO_4$. Similarly, the capacity retention of nickel-based alkaline batteries is altered by the volume variations of the electrodes on cycling. On the contrary, neutral aqueous ion rocking-chair batteries such as introduced by J. Dahn in 1994[391] appear more attractive in terms of cycle life due to smoother ion intercalation mechanisms, but again, the commonly investigated chemistry was based on inorganic electrode materials; albeit, Alt et al.[392] reported as soon as 1972 an organic based aqueous cell using the tetrachloro-1,4-benzoquinone (TCQB) in 4 M sulfuric acid. Such a cell exhibited a redox potential of 0.67 V vs saturated calomel electrode (SCE) associated with the protonation of the quinone structure.

One of the intentions of the authors is to provide in this section a critical view on the latest advances and challenges in the exploration of organic based aqueous cell chemistries, including a quantified comparison of their properties against those of inorganic materials including the tricky question of the volumetric energy density. As part of this review, we feel

https://dx.doi.org/10.1021/acs.chemrev.9b00482
Chem. Rev. 2020, 120, 6490−6557

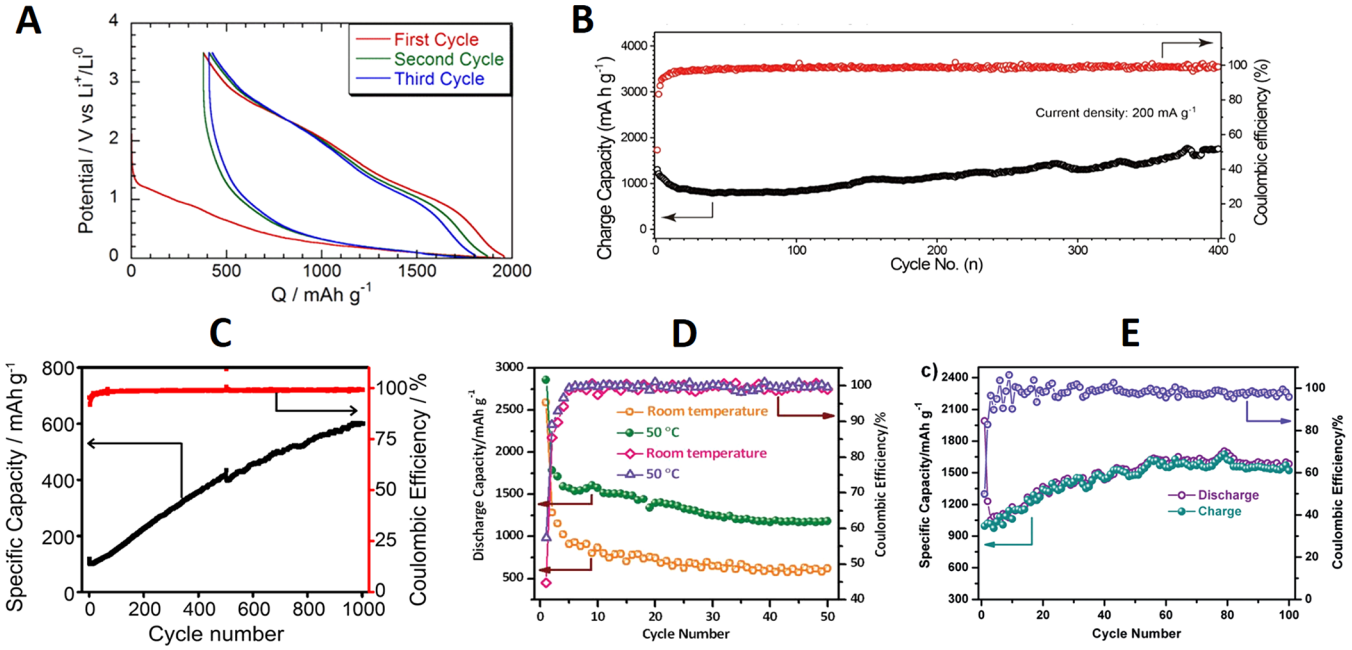

Figure 17. (A) Typical voltage profile of a "superlithiated" material: Li_2BDP (reproduced with permission from ref 260. Copyright 2016 American Chemical Society). (B–E) Capacity retention of selected OEMs: (B) PAT (reproduced with permission from from ref 387. Copyright 2018 American Chemical Society), (C) F-PDI-3-TC (reproduced with permission from ref 388. Copyright 2019 American Chemical Society), (D) BBL (reproduced with permission from ref 389. Copyright 2015 John Wiley and Sons), and (E) PQL (reproduced with permission from ref 390. Copyright 2015 John Wiley and Sons).

Table 6. Performances of Selected OEMs Exhibiting the "Superlithiation" Phenomenon

#	Positive electrode (or "cathode") active material	Negative electrode (or "anode")	Electrolyte	Output voltage (V)	Cycling stability: retention, cycles, rate or current density	Specific capacity ($mAh\ g^{-1}$) and Specific energy ($Wh\ kg^{-1}$) per mass of positive active material, Final coulombic efficiency, Loading ($mg\ cm^{-2}$)	Ref.
1	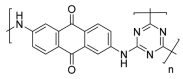	Li	1 M $LiPF_6$ in EC/DMC	~0.9	n.d.,[a] 400, 200 mAh g^{-1}	1 770, 1 593, ~99, 1.1	[387]
2	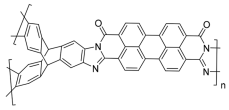	Li	1 M $LiPF_6$ in EC/DEC	~0.9	n.d.,[a] 1 000, 200 mAh g^{-1}	783, 705, ~99, n.d.	[388]
3	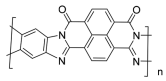	Li	1 M $LiPF_6$ in EC/DEC	~0.9	48%, 50, 100 mAh g^{-1}	1 285, 1 156, ~99, n.d.	[389]
4	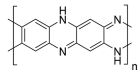	Li	1 M $LiPF_6$ in EC/DEC	~0.9	n.d.,[a] 100, 100 mAh g^{-1}	1 550, 1 395, ~99, n.d.	[390]

[a]Due to an activation process, the capacity increases with time.

it is therefore interesting to evaluate the effective chances of organics to realize user/market-acceptable aqueous batteries. In addition, we believe that such a comparison would not be complete if another bottleneck of this technology that is the price of active materials is not compared. To address these points, the latest literature data associated with the most advanced and industry relevant inorganic material for molar range aqueous battery (as opposed to water-in-salt type ones that will be briefly discussed, *vide infra*) which is the carbon coated $Na(Li)Ti_2(PO_4)_3$ (referred to as C@NTP or C@LTP) is considered below.

Volumetric Capacity Aspect

On paper, this is not one of the most important factors for stationary energy storage although in practice, low energy density could also mean more layers in the stack (for a given electrode thickness) and therefore a higher price due to a larger amount of passive elements. The volumetric capacity of the $C@Na(Li)Ti_2(PO_4)_3$ ($2.6\ g/cm^3$) can reach up to 231[393]–300[394] mAh cm^{-3} (93–118 mAh g^{-1}, respectively) taking into account the carbon coating ($2.0\ g{\cdot}cm^{-3}$). Interestingly, such volumetric capacities are actually lower than that obtained for a

https://dx.doi.org/10.1021/acs.chemrev.9b00482
Chem. Rev. 2020, 120, 6490–6557

quinone derivative also used on the negative side, the poly pyrene-4,5,9,10-tetraone (PPTO): 1.68 g cm^{-3}, 338 mAh cm^{-3}, 201 mAh g^{-1} cycled in Na^+-based aqueous electrolyte.[395] Although the PPTO electrode contained 30 wt.% of carbon additive its electrode volumetric capacity (144 mAh cm^{-3}) remains in the vicinity of that derived for the titanium phosphate ones: 121 mAh cm^{-3}, ref 393 and 152 mAh cm^{-3}, ref 394. It is also important to point out that the previous results were obtained from relatively thin electrodes with areal capacity in the vicinity or below 1 mAh cm^{-2}.

For thicker ones (close to 2 mAh cm^{-2}), Y. M. Chiang's group[396] obtained 310 mAh cm^{-3} by volume of C@NTP at 0.6 C, which turns into 161 mAh cm^{-3} by volume of composite electrode. Industrially relevant aqueous batteries were demonstrated by Whitacre with impressive electrode loadings (between 20 and 450 mg·cm^{-2}) using NTP derived from very cheap synthesis protocols.[397] These good results pair, however, with a lower volumetric capacity of the C@NTP material (182 mAh cm^{-3} in approximately 20 mAh cm^{-2} pouch cells and 159 mAh cm^{-3} in approximately 1 mAh cm^{-2} coin cells[397]) which falls down to 83 and 77 mAh cm^{-3} in terms of electrode volume for pouch and coin cells, respectively, using the corresponding electrode chemistry. In comparison, the highest areal capacity demonstrated with organic materials lies in the vicinity of 4.5 mAh cm^{-2}.[232,398] Indeed, Perticarari et al.[232] achieved nearly 100 mAh cm^{-3} of material and 66 mAh cm^{-3} of electrode using a diblock oligomer and 25 wt.% of carbon additive for 4.5 mAh cm^{-2} while Nishide's group obtained 3 mAh cm^{-2} using on a carbon nanotube hybridized poly (2,2,6,6-tetramethylpiperidin-4-yl) acrylamide (PTAm) polymer.[398]

To sum up, this short literature analysis of both inorganic and organic active materials for aqueous batteries near neutral pH highlights that some of the proposed organic electroactive materials have already surpassed inorganic ones in term of volumetric capacity in the case of thin electrodes and are not too far behind in the case of thick ones.

Cost Aspect

According to Whitacre,[397] NTP can be produced with precursor materials cost of $4 per kg upon two synthesis steps, ball milling and calcination. Taking $5/kg/step, which is an average in the pigment industry, an estimate of the NTP price should be roughly 14$/kg. In comparison, competitive organic materials (in terms of volumetric capacity) in neutral molar aqueous media such as PNDI and PPTO are approximately $4−6/kg and $10−15/kg, respectively, highlighting similar or even lower prices can indeed be achieved for organics.

Lastly, it is noted that **water-in-salt (WiSE)**[399] or **hydrate-melt**[400] **electrolytes** have emerged as interesting opportunities to significantly improve the energy density and the Coulombic efficiency and mitigate corrosion issues (materials, current collectors, ...) of these new classes of "water containing" batteries. A comprehensive and critical review of the scientific understanding as well as the electrochemical and physical properties of these new electrolytes has been recently published by Yamada et al.[401] It is noted that the ability of WiSE electrolytes to extend the electrochemical window can be significantly improved by using an immiscible electrolyte additive, the 1,1,2,2-tetrafluoroethyl-2′,2′,2′-trifluoroethyl ether (HFE). The latter electrochemically decomposes at the surface of the materials and by virtue of its hydrophobicity expels water molecules from the inner-Helmholtz interface of the electrode thereby mitigating hydrogen formation at the expense of a more efficient SEI.[402] Because, some articles commented in this review refer to these types of electrolytes, we feel that a few general comments should be recalled regarding this type of battery chemistry. First, such highly concentrated electrolytes have a volumetric density in the range of 1.6−1.9 g cm^{-3}, which partially offsets the gain in energy density. For instance the mass of a 700 cm^2 stack cell such as presented in ref 232 (taking 5 mAh cm^{-2} electrodes of 580 μm-thick and 40% porosity) increases by 14% considering a WiSE electrolyte of 1.7 g cm^{-3} compared to a "salt in water" 1 M one. Second, the viscosity of these electrolytes is approximately ten times higher than molar range ones which considerably increases the wetting time of the electrodes and especially thick ones.[401] Last but not least, the price of these electrolytes is obviously the most challenging issue to be overcome before commercialization can be considered. Indeed, recent results point to the fact that expensive imide based anions (as opposed for instance to acetate ones) would have a significant role in the widening of the electrochemical window on the negative electrode side.[403]

Based on the previous comments, this section aims at providing the reader with a selection of relevant organic materials, that is to say those that allow performances approaching or higher than lead acid battery ones but with much extended cyclability. Accordingly, the lower limits were set to roughly 30 Wh kg^{-1} per mass of the two materials and a capacity retention >80% after 500 cycles at 1 C rate or equivalent. The intention of the authors is to give a critical view of the selected papers and also to highlight advantages and drawbacks vs those associated with inorganic materials. Key performances are reported in (Table 7) along with materials structures, aqueous electrolyte formulations, cycling conditions and electrode loading. Note that this critical review is focused on neutral pH batteries because they inherently offer reduced production costs and mitigated corrosion issues. Results are subcategorized into hybrid cells, where only one of the electrodes contains an organic electroactive material and all organic cells.

8.2. Hybrid Organic−Inorganic Batteries

8.2.1. Aqueous Lithium-Ion Batteries (ALIBs). Some of the most attractive organic materials for aqueous battery to date are among the polyimide derivatives. These materials indeed combine both a high capacity (typically 130−160 mAh g^{-1}, 208−256 mAh cm^{-3}) and a low price ($4−6/kg[395]). To our knowledge such a dual advantage has not been reached by any inorganic materials used in the aqueous battery field. The electrochemical reduction/oxidation of a polyimide core is highly reversible in water at neutral pH. The redox centers have been identified as involving the aromatic-carbonyl system of the imide functional moiety following two redox steps. The first one corresponds to the formation of a radical-anion upon enolization of a carbonyl group by one electron, followed by a second electron reduction into the dianion quinoid form.[404] Further reduction cannot be reached in molar range electrolyte at neutral pH before water hydrolysis is triggered. The delocalization of excess electron density in the reduced states has been studied by FTIR and UV−vis spectroscopy.[405] Dong et al.[406] introduce a mixed liquid/solid cationic rocking chair aqueous battery using a I_3^-/I^- based posolyte and a polyimide derivative negative electrode (poly(1,4,5,8-naphthalenetetracarboxylic)dianhydride-derived polyimide, PNTCDA) separated by a Nafion membrane allowing the Li^+ (or Na^+) diffusion. This system delivers roughly 35 000 deep cycles at a high current of

https://dx.doi.org/10.1021/acs.chemrev.9b00482
Chem. Rev. 2020, 120, 6490−6557

Table 7. Performances of Selected Aqueous Organic Batteries

#	Cell configuration (ionic carriers)	Positive electrode (or "cathode") active material	Negative electrode (or "anode") active material	Electrolyte	Output voltage (V)	Cycling stability: retention, cycles, rate or current density	Specific capacity (mAh g^{-1}), Specific energy (Wh kg^{-1}) Final coulombic efficiency, Loading (mg cm^{-2})	Ref.
Hybrid organic/inorganic aqueous systems								
1	Li^+ (or Na^+)	I_3^-/I^-	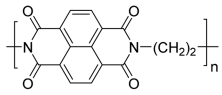	$LiNO_3$ 1 M (pH 7)	~0.7-0.8	80%, 35 000, 10 A g^{-1},	~110,[a] ~88,[a] ~100, 1	[406]
2	Li^+ - ion	$LiMn_2O_4$	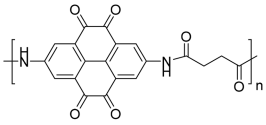	Li_2SO_4 2.5 M (pH 7)	1.13	80%, 3 000 (3 500 h), 280 mA g^{-1}	81,[b] 92,[b] 92%, -, 2	[395]
3	K^+	$K_xFe_yMn_{1-y}[Fe(CN)_6]_w \cdot zH_2O$	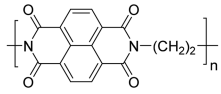	KCF_3SO_3, 22 M	1.27	73%, 2 000, 4 C	63,[b] 80,[b] ~100, 5-6 all these values are at 0.5 C	[411]
4	Zn^{2+}	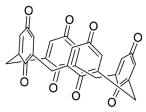	Zn	$Zn(CF_3SO_3)_2$ 3 M	1	87%, 1 000, 500 mA g^{-1}	197,[c] 80,[d] ~100, 2.5-10	[412]
5	Mg^{2+}	$Na_{1.4}Ni_{1.3}Fe(CN)_6 \cdot 5H_2O$	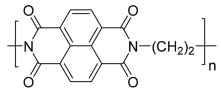	$MgSO_4$ 1 M	1.3	57, 5 000, 2 A g^{-1}	35,[b] 45,[b] ~100, 2-3, all these values are at 0.5 A g^{-1}	[413]
6	Mg^{2+}	$Li_3V_2(PO_4)_3$@C	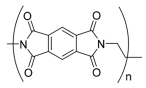 @MCNT	$Mg(TFSI)_2$ 4 m	1.9	87%, 1 000, 2 C	52,[b] 62.4,[b] ~100, 2-3, all these values are at 1C (0.1 A g^{-1})	[414]
7	Ca^{2+}	$K_{0.02}Cu[Fe(Cu)_6]_{0.66} \cdot 3.7H_2O$	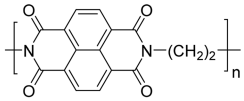	$Ca(NO_3)_2$ 2.5 M (pH 5.1)	1.2	88, 1 000, 10 C	45,[b] 54,[b] ~100, 5, all these values are at 1 C	[415]
8	NH_4^+ - ion	$(NH_4)_{1.47}Ni[Fe(CN)_6]_{0.88}$	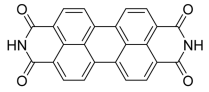	$(NH_4)_2SO_4$ 1 M (pH 6)	1	67%, 1 000, 0.120 mA g^{-1}	35,[b] 43,[b] 97.6%, 2-5	[416]
All-organic aqueous systems								
9	Cl^- - ion	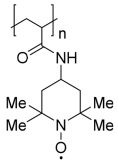	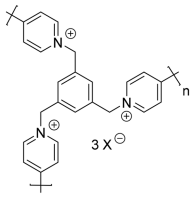	NaCl 0.1 M (pH 7)	1.3	80%, 2 000, 10.5 A g^{-1}	165,[a] 214,[a] - (100 nm to 1 μm thin films)	[418]
10	BF_4^- - ion	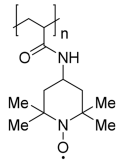	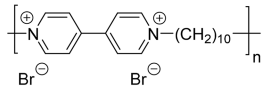	$NaBF_4$ 0.1 M (pH 7)	1.2	75-80%, >2 000, 60 C (67 μA·cm^{-2})	104,[c] 108,[c] 95 (100 nm thin films)	[419]
11	Dual-ion ($TFSI^-/Li^+$)	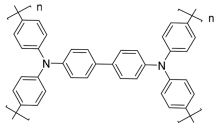	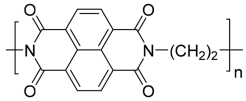	LiTFSI 21 m (pH 7)	1	85%, 700, 0.5 A g^{-1}	105,[c] 53,[c] ~100, 1	[420]

https://dx.doi.org/10.1021/acs.chemrev.9b00482
Chem. Rev. 2020, 120, 6490−6557

Table 7. continued

#	Cell configuration (ionic carriers)	Positive electrode (or "cathode") active material	Negative electrode (or "anode") active material	Electrolyte	Output voltage (V)	Cycling stability: retention, cycles, rate or current density	Specific capacity (mAh g^{-1}), Specific energy (Wh kg^{-1}) Final coulombic efficiency, Loading (mg cm^{-2})	Ref.
12	Mixed dual and anionic rocking-chair (ClO_4^-/Na^+)	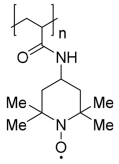	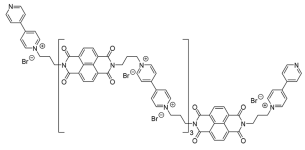	$NaClO_4$ 2.5 M (pH 7)	1.1	70%, 1680 (1100 h), 0.075 to 0.6 A g^{-1}	33[b], 36[b], >99.6, all these values are at 0.075 A g^{-1}, 10	[231]
13	Mixed dual and anionic rocking-chair (ClO_4^-/Na^+)	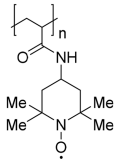	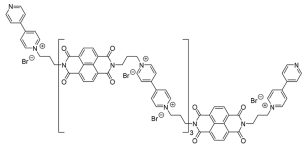	$NaClO_4$ 2.5 M (pH 7)	0.8	97%, 500 h, 0.075 A g^{-1}	35,[b] 28,[b] ~100, 85 (4.5 mAh cm^{-2})	[232]

[a]Based on anode material weight. [b]Based on cathode and anode materials weight. [c]Based on cathode material weight. [d]Based on the whole cell weight.

10 A g^{-1} (55 C nominal, that leads to a nominal ratio (number of cycles/C-rate) = 636) before reaching 80% of the initial capacity (Q_0 = 105 mAh g^{-1}) (Table 7, entry 1).

More recently, another negative electrode organic material was shown to stand out of the crowd, the quinone derivative PPTO.[395] The latter exhibits storage properties rivaling those of any inorganic materials from mildly acidic to strongly basic media. In neutral 2.5 M Li_2SO_4 aqueous electrolyte, this material enables 92 Wh $kg^{-1}_{materials}$ (208 Wh L^{-1}) when paired with $LiMn_2O_4$ at an average voltage of 1.13 V (Table 7, entry 2). This performance is in the same range as the competing system $LiTi_2(PO_4)_3$-$LiMn_2O_4$ (90 Wh $kg^{-1}_{materials}$ (243 Wh L^{-1}, 1.5 V) thanks to the extremely high capacity of the PPTO electrode material (229 mAh g^{-1}, 366 mAh cm^{-3} at 1 C rate). In addition, this PPTO-based cell shows quite a promising capacity retention of more than 3500 h (3000 cycles) (Figure 18). Among all aqueous systems that have been reviewed herein, PPTO/$LiMn_2O_4$ is by far the most promising one in the authors' opinion. In addition, as a quinone derivative, the fully reduced form of PPTO (PPTO-Li_4) can support reversible oxidation by dissolved oxygen without impacting its charge−discharge properties.[395] This is an important advantage over $LiTi_2(PO_4)_3$ for instance, which was shown to undergo rapid capacity fading in nondeaerated electrolyte. Indeed, PPTO based cell can therefore support the "oxygen cycle" (Figure 18), which is a built-in safety mechanism for aqueous battery at high charge states. Importantly, in such events the local pH at the negative electrode can be fairly alkaline (pH 13). However, thanks to the combination of the chemical inertness of the quinone core, as well as the poor solubility, and robust amide linkage of the PPTO derivative, a capacity retention of 83% was demonstrated after 1200 h cycling in these pH conditions.[395] Accordingly, this oxygen consumption capability of quinones enables in principle, to increase the state of charge of the positive electrode material (such as $LiMn_2O_4$ for instance) without significantly altering the mass balancing of the cell therefore paving the way toward the use of materials working at even higher potentials.

8.2.2. Aqueous Sodium-Ion Batteries (ASIBs). As for Li-ion batteries, Na-based aqueous batteries must be investigated to counteract possible upcoming issues associated with geo-localized Li resources. One of the first instances of hybrid ASIBs bearing an organic electroactive material uses a polyimide derivative PNDI at the negative electrode and a $NaVPO_4F$ based positive electrode in a 5 M $NaNO_3$ aqueous electrolyte.[404] This system shows, however, a very poor capacity retention (−25% in 20 cycles) that was mainly ascribed to $NaVPO_4F$ (−30% loss of capacity in 20 cycles) compared to −17% for PNDIE.[404] Yao's group[395] slightly improved these cyclability results to nearly 80% of capacity retention after 80 cycles (150 h) by substituting $Na_3V_2(PO_4)_3$ for $NaVPO_4F$ and PPTO (208 mAh g^{-1}) for PNDIE (160 mAh g^{-1}). To date, ASIB hybrid aqueous batteries are therefore not competitive with corresponding ALIB as reported above especially in terms of capacity retention. For this reason, ASIB related research has mainly focused on the use of inorganic compounds[173] such as $NaFePO_4$[407] as well as fully inorganic systems based on Prussian (white)blue,[408] carbon coated phosphates (NTP[397] and $Na_3MnTi(PO_4)_3$,[409]) and manganese oxides $Na_{0.44}MnO_2$[396] and $Na_{0.44}[Mn_{1-x}Ti_x]O_2$.[410] We note however, that all these materials enable capacity values in the range of 40 to 60 mAh g^{-1} and energy density values in the range of 30−40 Wh kg^{-1} per mass of materials in molar range electrolyte which is the average value generally observed for most organic based aqueous cells.

8.2.3. Aqueous Potassium-Ion Batteries (AKIBs). Full organic−inorganic hybrid AKIBs have not been reported until very recently owing to the scarcity of suitable electroactive materials and electrolytes. Hu's group[411] demonstrated an AKIB cell based on an Fe-substituted Mn-rich Prussian blue $K_xFe_yMn_{1-y}[Fe(CN)_6]_w \cdot zH_2O$ (KFeMnHCF) as the positive electrode and the 3,4,9,10-perylenetetracarboxylic diimide derivative as the negative one in a 22 M KCF_3SO_3 water-in-salt electrolyte (Table 7, entry 3). The low water activity of the latter allowed not only to mitigate dissolution of both electrode materials but also to charge the positive electrode up to 1.2 V vs Ag/AgCl electrode, which allowed KFeMnHCF to reversibly reach 135 mAh g^{-1} at 0.5 C above 0 V vs SCE. In addition, thanks to the mitigation of phase transitions by Fe substitution, KFeMnHCF achieves 70% capacity retention at 100 C over 10 000 cycles. This pioneering AKIB system shows a high energy density of 80 Wh kg^{-1} by mass of the two electrodes at a power density of 41 W kg^{-1} (0.5 C) and 73% capacity retention over 2000 cycles at 4 C (Figure 19A−C) which makes it one of the most attractive systems to date. Interestingly, authors have evaluated their system in pouch cell

https://dx.doi.org/10.1021/acs.chemrev.9b00482
Chem. Rev. 2020, 120, 6490−6557

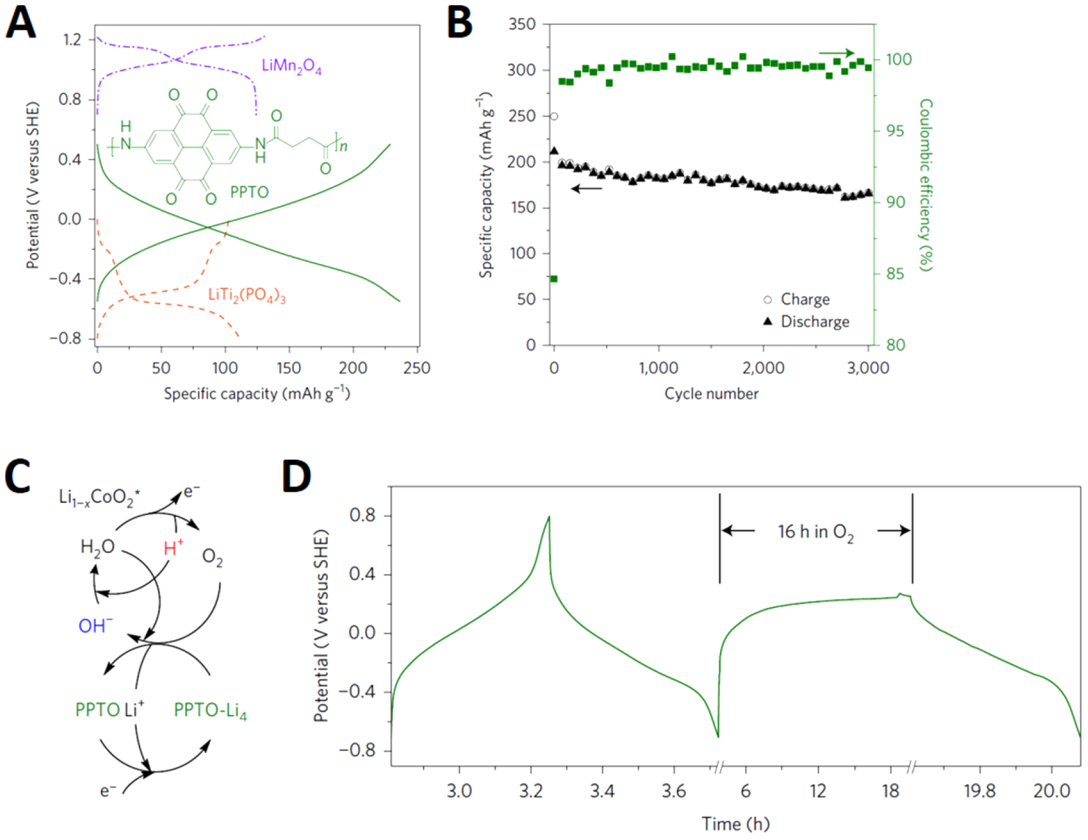

Figure 18. Characteristics of PPTO as an anode material for ALIBs. (A) Galvanostatic charge−discharge profiles for PPTO (280 mA g^{-1}), $LiTi_2(PO_4)_3$ (120 mA g^{-1}), and $LiMn_2O_4$ (140 mA g^{-1}) in 2.5 M Li_2SO_4 (pH 7). (B) Capacity retention of a $LiMn_2O_4$−PPTO cell during galvanostatic cycling at 1 C in 2.5 M Li_2SO_4 (pH 7). (C) Schematic explaining the oxygen cycle in ALIBs: H_2O is oxidized at the catalytic sites (*) on the cathode (for example, $LiCoO_2$) to generate O_2 and HC; the latter is then reduced by the charged anode (for example, PPTO-Li_4) to afford OH^-. (D) Oxygen consumption by charged PPTO: a PPTO electrode is first electrochemically discharged (oxidized) and charged (reduced) under Ar for one cycle, then left to rest under O_2, and finally put under Ar and charged again. Reproduced from ref 395. Copyright 2017 Nature Publishing Group.

configuration and at several temperatures to better grasp the prospect of large-scale applications: an 11 mAh pouch cell was shown to exert superior performance at low rates (i.e., 0.5 C/0.1 C) and low/high temperatures (*i.e.*, −20 °C/−10 and 25 °C/60 °C) and was able to operate from −20 to 60 °C (Figure 19 D,E).

8.2.4. Aqueous Multivalent Metal-Ion Batteries (Mg, Ca, Zn). *Zn^{2+}*. Chen's group demonstrated that high energy values could be obtained at the cell level (pouch cell) by pairing quinones (calix[4]quinone, referred to as C4Q) to a zinc negative electrode in a 3 M $(ZnCF_3SO_3)_2$ aqueous electrolyte (Table 7, entry 4).[412] This system develops 1 V as output voltage and up to 337 mAh g^{-1} by mass of materials at low current density (5 mA g^{-1}). The pouch cell achieved 220 Wh kg^{-1} at 500 mA g^{-1} considering the electroactive mass fraction of the materials (which are 89% for the C4Q and 49% for Zn) and 80 Wh g^{-1} by mass of the whole cell with an energy efficiency close to 80%. However, due to the dissolution of the C4Q, a Nafion membrane was required to stabilize the capacity retention at 87% after 1000 cycles (−0.015%/cycle). It is instructive to note that although the development of mild electrolyte based Zn batteries is still in its infancy, this kind of system clearly brings energy densities in the same order as those associated with the use of "water-in-salt" electrolytes. This point should therefore motivate more research in the near future to enhance the depth of discharge and cyclability and prevent the use of membranes.

Mg^{2+}. Xia et al.[413] recently developed a 33 Wh kg^{-1} (1 V as output voltage) per mass of active materials considering $Na_{1.4}Ni_{1.3}Fe(CN)_{6.5}H_2O$ paired with poly[*N*,*N*′-(ethane-1,2-diyl)-1,4,5,8-naphthalene tetracarboximide (PNDIE) using 1 M $MgSO_4$ aqueous electrolyte (Table 7, entry 4). This assembly allowed to achieve 1000 cycles at 2 C rate while keeping approximately 88% of the initial capacity. Interestingly, Wang et al.[414] obtained nearly two times more energy density (62.4 Wh kg^{-1} per mass of materials) using $Li_3V_2(PO_4)_3$, as the positive electrode and lighter diimide derivatives (polypyromellitic dianhydride), as the negative electrode (Table 7, entry 6). Compared to the more often used naphthalene derivative, the smaller delocalization backbone of the polypyromellitic destabilizes the radical anion and dianions that form on reduction and push the potential to lower values. The cell shows indeed a high voltage of 1.9 V which can be realized by using a relatively concentrated electrolyte (4 M $Mg(TFSI)_2$).[414] This resulted in a promising capacity retention of nearly 87% after 1000 cycles at 2 C rate.

Ca^{2+}. Ca^{2+} is another interesting abundant ion to play with in aqueous media. Yao's group[415] recently showed that the diffusion of Ca^{2+} is higher than that of Mg^{2+} both in the solid state and in the aqueous electrolyte media. These results were ascribed to smaller size of the hydrated Ca^{2+} complex and its more facile dehydration during the charge transfer process. This group assembled a battery with a copper hexacyanoferrate

https://dx.doi.org/10.1021/acs.chemrev.9b00482
Chem. Rev. 2020, 120, 6490−6557

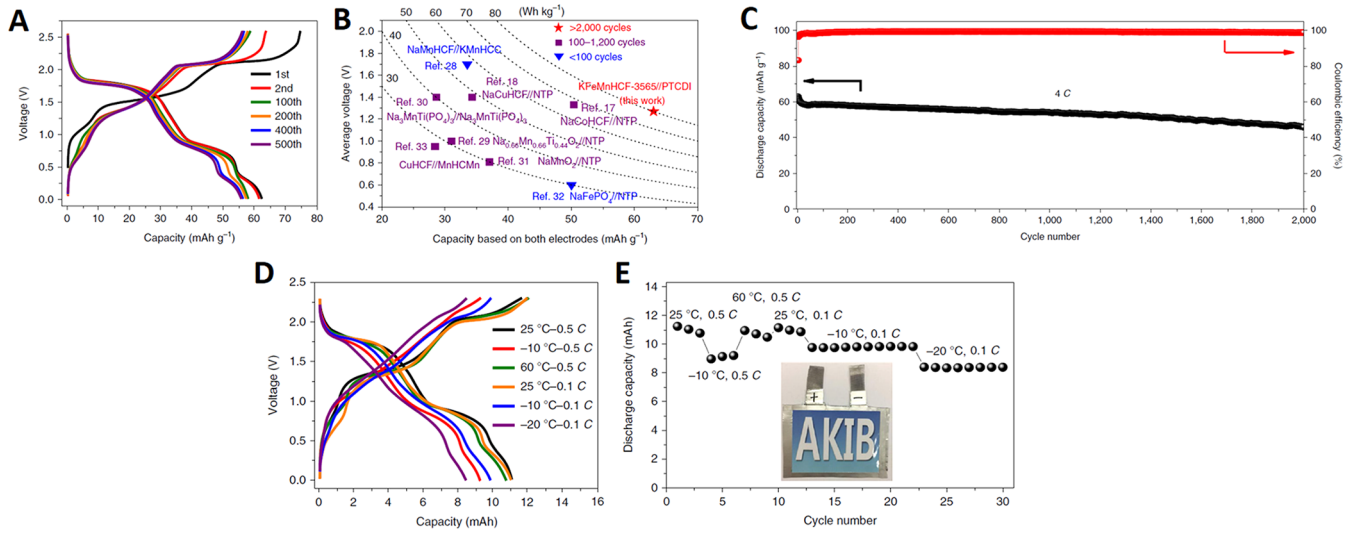

Figure 19. Performance of the $K_{1.85}Fe_{0.33}Mn_{0.67}[Fe(CN)_6]_{0.98}\cdot 0.77H_2O$|22 M KCF_3SO_3|PTCDI full battery. (A) Charge−discharge curves for coin cells at 4 C from 0 to 2.6 V (1 C = 0.13 A g^{-1}). (B) Comparison of average voltage, capacity based on total mass of both electrodes, lifespan, and energy density for the full battery with reported aqueous Na-ion full batteries. (C) Long-term cycling performance of the coin cell at 4 C. (D, E) Corresponding electrochemical performance measured in pouch cell at different rates (0.5/0.1 C) and temperatures (−20/−10/25/60 °C). Reproduced with permission from ref 411. Copyright 2019 Nature Publishing Group.

compound of composition $K_{0.02}Cu[Fe(Cu)_6]_{0.66}\cdot 3.7H_2O$ (CuHCF) coupled to the PNDIE polyimide derivative in a 2.5 M $Ca(NO_3)_2$ aqueous electrolyte (Table 7, entry 7). CuHCF was found to proceed to insertion/deinsertion of 0.3 Ca^{2+} ion at a 0.2 C through a single-phase solid solution reaction rate at a potential of 0.72 V vs Ag/AgCl electrode. This mechanism which is paired with the Fe^{3+}/Fe^{2+} electroactivity leads to a specific capacity of 58 mAh g^{-1} (theoretical capacity Q_{th} = 65 mAh g^{-1}) that retains 88% of its initial capacity after 2000 cycles at 5 C. On the other hand, PNDIE fully reacts with Ca^{2+} at −0.45 V vs Ag/AgCl electrode with a reversible capacity of 160 mAh g^{-1} (theoretical capacity $Q_{th.}$ = 183 mAh g^{-1}). At 1 C rate, the full cell delivered 54 Wh kg^{-1} of active materials for an output voltage of 1.2 V. In addition, the battery still provides 88% capacity retention after 1000 cycles at 10 C.

8.2.5. Aqueous Ammonium-Ion Battery. Little is reported with ammonium as shuttling ion. However, it must be mentioned that Ji and co-workers[416] reported such an aqueous battery using Ni-based Prussian white at the positive electrode paired with 3,4,9,10-perylenetetracarboxylic diimide using 1 M $(NH_4)_2SO_4$ as electrolyte (pH 6) (Table 7, entry 8). This cell enables up to 43 Wh kg^{-1} per mass of active materials with 1 V of voltage at 1.5 C and achieves a capacity retention of 67% upon 1000 cycles at 3 C rates (120 mA g^{-1}) with an average Coulombic efficiency of 97.6%.

8.3. All-Organic Aqueous Batteries

Due to the lack of high potential n-type organic materials,[417] cation-rocking chair cells have not been reported yet. Today, all-organic aqueous cell electrochemistry is indeed either related to counteranions or both countercation and anions (one at each electrode referred to as "dual mode" and the two at one electrode referred to as "intermixed mode"). First reports were released by Nishide, Oyaizu, and co-workers.[418] They used a redox polymer resulting from the attachment of a (2,2,6,6-tetramethylpiperidin-1-yl)oxy known as "TEMPO" side groups to a polyalkane chain backbone, with poly (2,2,6,6-tetramethylpiperidin-4-yl) acrylamide (referred to as PTAm) as the positive electrode material. This material was paired to two different polyviologen derivatives, either the highly cross-linked polyviologen hydrogel (poly tripyridiniomesitylene)[418] which enabled ∼1.3 V as output voltage (Table 7, entry 9) or the poly(*N*-4,4′-bipyridinium-*N*-decamethylene dibromide) (Table 7, entry 10) leading to a cell average voltage of 1.2 V.[419] Although both cells demonstrated more than 2000 cycles in 0.1 M Na-based aqueous electrolytes, electrodes were thin film deposits in the sub- to micron-thick range. Recently however, this group[398] has made decisive advances by demonstrating a thick composite electrode made of PTAm with a loading of 3 mAh cm^{-2}. The latter was obtained by hybridizing PTAm with a 3-D self-assembled mesh of single-walled carbon nanotubes (SWNT). This thick electrode could still reach nearly 80 mAh g^{-1} of material at 10 C rate. Although SWNT represents only 1% of the total electrode mass, it is noteworthy that authors demonstrated the importance of the contacts with the current collectors by showing such a high kinetics also stems from the optimization of the current collector/electrode contacts.[398]

Dong et al.[420] cycled a p-type conjugated tertiary poly triphenylamine obtained by oxidative polymerization of the triphenylamine (PTPAn). The latter shows a sloppy discharge profile resulting from the superimposition of two pairs of broad peaks centered at 0.2 and 0.8 V vs SCE associated with the *para* and *meta* conformational isomers. Overall the discharge of this compound enables approximately 105 mAh g^{-1}_{PTPAn} at 0.5 A g^{-1} (4.6 C-rate). However, the strong oxidative power of the N^+ species triggers the hydrolysis of water molecules that could be mitigated by the use of a "water-in-salt" electrolyte of 21 m LiTFSI. PTPAn was then coupled to 1,4,5,8-naphthalenetetracarboxylic dianhydride-derived polyimide (PNTCDA) as the negative electroactive material (Table 7, entry 11). During charge $TFSI^-$ and Li^+ react with the oxidized PTPAn and reduced PNTCDA, respectively (dual mode), enabling a maximum of 53 Wh kg^{-1} per mass of electroactive materials and a capacity retention of 85% after 700 cycles at 0.5 A g^{-1} (4.6 C-rate).[420]

Some of us reported a possible new avenue to design aqueous batteries materials based on diblock-oligomers bearing

https://dx.doi.org/10.1021/acs.chemrev.9b00482
Chem. Rev. 2020, 120, 6490−6557

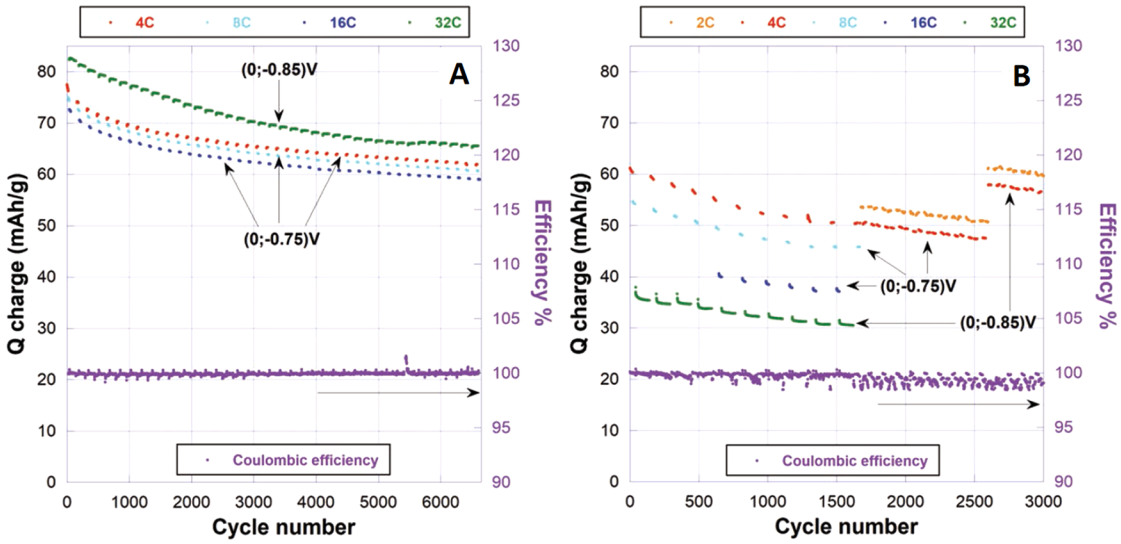

Figure 20. Capacity retention on charge (oxidation of the material) and corresponding Coulombic efficiency curves for diblock-oligomers bearing p-type viologen and n-type naphthalene diimide moieties composite electrodes in (A) 2.5 M $NaClO_4$ aqueous electrolyte and (B) ocean water. Reproduced with permission from ref 231. Copyright 2019 John Wiley and Sons.

p-type viologen and n-type naphthalene diimide moieties. These types of structures enable simultaneous release and uptake of anions (ClO_4^-, Cl^-) and cations (Na^+, Mg^{2+}) respectively by a single electrode (intermixed mode) with the promise of mitigated volume variations on cycling.[230] The best performances were obtained using an oligomer that can reach up to 105 mAh g^{-1} per mass of material and 80 mAh g^{-1} per mass of electrode.[231] The extremely fast kinetics of longer diblock oligomer also allowed to reach an unmatched specific capacity of 60 mAh $g^{-1}_{electrode}$ (0.7 mAh cm^{-2}) without any conducting additive while the optimum amount of carbon black additive was found to be 10 wt % at C-rate and below. Its capacity retention is remarkable for several thousand cycles (6500 cycles, ≈40 days) in 2.5 M $NaClO_4$ aqueous electrolyte as well as plain ocean water (≈3000 cycles, ≈75 days) (Figure 20).[231] A 40 Wh $kg^{-1}_{materials}$ full cell demonstration was shown with more than 1600 cycles using the commercial 4-hydroxy TEMPO benzoate as the positive material and 0.7 mAh cm^{-2} as electrode loading (Table 7, entry 12). It is noted that a concentrated (but cheap) electrolyte (8 M $NaClO_4$) was required to prevent dissolution of the TEMPO derivative.[231,232] The same system was also evaluated using millimeter thick electrodes of 8 mAh cm^{-2} (nominal) leading to a stable areal capacity of nearly 4.5 mAh cm^{-2} for 500 cycles at 1C rate. To further demonstrate the practicability of the system, the same electrodes were evaluated in pouch cells. The output voltages were 0.78 V (C-rate) and 1.1 V (C/8-rate) leading to 22 Wh kg^{-1} (C-rate) and 36 Wh kg^{-1} (C/8-rate) per mass of materials with a 97% capacity retention over 500 h cycling at both C and C/8 rates (Table 7, entry 13).[232]

8.4. Summary and Outlooks

Neutral aqueous batteries based on organic electroactive materials have been reviewed and discussed. New results point to the fact that some competitive organic materials have now surpassed inorganic ones even in terms of volumetric capacity while relatively large amounts of electrode carbon additive have been proved unnecessary for some derivatives. In addition, we feel that this review highlights a decisive advantage of organic materials since most of them offer a highly versatile ionic compensation chemistry characterized by possible reactions with many different cations (monovalent and divalent), anions, and even both simultaneously. This aspect, that is encountered for the Prussian blue family for cations, opens up a large panel of possibilities regarding the cell chemistry, with the additional advantage to be coupled to much larger storage capacity and, in some instance, with the possibility of supporting the oxygen cycle.

Although it still remains far from that achieved with some inorganics,[397] the technology readiness level (TRL) of organic based aqueous batteries has increased in the latest papers by the use of either highly loaded electrodes and/or pouch cell configurations. However, studies devoted to the impact of electrode formulation are scarce. As an example, the polytetrafluoroethylene (PTFE) binder that is predominantly used so far because of its readiness is presumably not the most appropriate for the wettability of composite electrodes, for the volume variations on cycling, as well as from an industrial production point of view.

Among the different cell chemistries that have been reviewed herein, three main topics attract research work: all organic systems, hybrid ones bearing an inorganic electroactive material, and water-in-salt electrolytes. Because of the prohibitive price incurred by the water-in-salt type electrolytes and although related energy densities can today approach that encountered for Li-ion batteries, we believe this strategy will remain confined to fundamental studies unless cheap salts are found to replace the capability of imide based ones to form stable SEI. On the other hand, both all organic and hybrid organic batteries using molar electrolytes now can show promising capacity retention at the cell level. However, this aspect still remains to be confirmed in large format batteries, at different temperatures and by including self-discharge tests. Regarding energy density and except for a few examples of hybrid cells, most results are in the range of 40−60 Wh kg^{-1} per mass of materials. However, as opposed to purely inorganic based aqueous batteries, the combination of attractive energy density, 80−90 Wh kg^{-1} per mass of materials, with promising cyclability (>3000 h) can be reached thanks to the large capacity of organics. In addition, owing to its large voltage and low price,

https://dx.doi.org/10.1021/acs.chemrev.9b00482
Chem. Rev. 2020, 120, 6490−6557

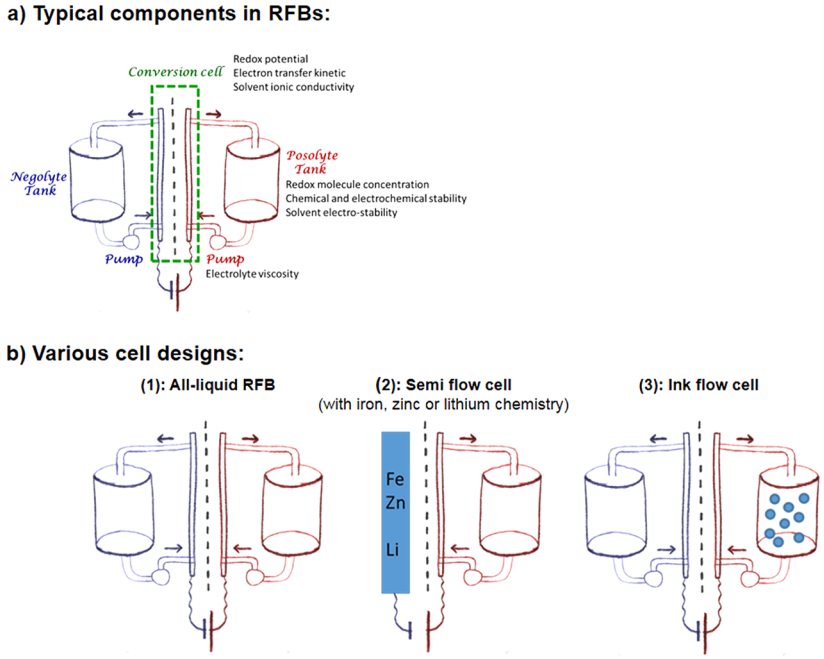

Figure 21. (a) Redox-flow battery schematic with main relevant parameters referred to redox-active compounds. (b) Possible cell configurations.

the Zn system based on mild electrolyte is certainly an option to be considered more deeply in the future.

Lastly, to close this section it appears interesting to recall that the ever decreasing price of Li batteries (and the increasing TRL of their novel high energy chemistries) turns them into a serious option for (off)in-grid application.[421] In this context, the authors believe that the effective chances of organics to realize user/market-acceptable aqueous batteries (at least for complementary applications) stem from their low toxicity, their abundancy, as well as their recyclability which could turn out to be efficient and profitable.

9. ORGANICS IN REDOX-FLOW BATTERIES

9.1. Specificities of Redox-Flow Batteries

Although we have already described the different cell assemblies using organics, some complementary details are required to better grasp the specificities of redox-flow cell for electrochemical storage (Figures 8,9). Basically, such a cell can be seen as a fuel cell where the fuel and oxidizer would be replaced by fluids with redox components in solution. As the associated electrochemical reactions are reversible, the device can be easily recharged. RFBs are energy storage devices with the advantage of dissociating power density (electrode surface area, number of cells in the conversion cell) and energy (tank volume). As currently energy densities remain low, these devices are more dedicated to stationary energy storage. The duration of storage (hour, day, week) depends mainly on the type of chemistry used.

Many recent reviews related to ORFBs have been conducted in the literature.[15,20,23,24,31,34,35,44,45,422] These reviews focus on describing the implemented redox molecules and the different strategies used to integrate them into a redox-flow device. This section will only focus on systems that are most advanced in terms of performance and that have been tested in systems as close to the application as possible and at least in a flow cell. In terms of concentration, there are many publications where tests are carried out in a very diluted medium, so we have decided to retain only studies on the most concentrated electrolytes. In solvent-based media, generally speaking, the performance is much weaker than in the case of aqueous electrolytes, so the selection we made was less drastic.

A RFB consists of three main components: an electrochemical conversion cell where electrochemical reactions take place, tanks to store redox-active fluids, and finally pumps to allow the circulation through the cell of the two electrolytes (posolyte/negolyte) containing the redox-actives species (Figure 21a). Behind this apparent simplicity lies a device that remains very difficult to optimize. Among the main parameters or components associated with the chemistry used, we can mention:

- the nature of the solvent that composes the electrolyte, on which depends the accessible potential window, as well as the power density (ionic conduction) of the conversion cell;
- the redox compounds solubility; it is important that the different redox states of each couple have the highest possible solubility. The number of electrons exchanged during the redox reaction must modulate this solubility; the important parameter is the quantity of electrons exchanged by the solution (mole electrons per liter);
- the electron transfer kinetics with the electrode surface; electron transfers must be fast and perfectly reversible to avoid losses due to overvoltage problems. In general, for a redox-flow conversion cell, faradic efficiencies are very good; main losses come from overvoltage problems at the electrodes (different potentials between charge and discharge);
- the chemistry itself which must obviously be stable enough without bringing corrosion problems that would shorten the battery life. RFBs must have a very long lifetime (>20 years) in order to make its components more cost-effective than in a regular "sealed" battery (membrane, pumps cost, etc, ...) since stationary storage applications are targeted as previously underlined;[130,136]

https://dx.doi.org/10.1021/acs.chemrev.9b00482
Chem. Rev. 2020, 120, 6490−6557

- the membrane, which allows the two compartments to be chemically and electrically separated, while allowing the diffusion of ions that ensure the system electroneutrality without crossover.

9.1.1. Short Overview on Inorganic-Based Redox-Flow Batteries. As already mentioned in the Introduction, the most advanced and commercialized flow systems are based on inorganic materials with acidic aqueous electrolyte: vanadium, zinc−bromine, hydrogen−bromine, and so on.[5,423−425] Each system has its own limitations: cost in the case of vanadium, formation of dendrites for zinc, need to use platinum in the case of H_2, toxicity (Br_2). Energy efficiencies are between 65 to 80% in the case of vanadium RFB for current densities of up to 100 mA cm^{-2} and an operating voltage of 1.25 to 1.4 V. Energy densities of 55 Wh L^{-1} have been achieved. These values should be strongly tempered because at high vanadium concentrations (2 M), electrolytes become very sensitive to temperature, they precipitate easily or become very viscous preventing their circulation, so the concentrations commonly used are rather in the order of 1.6 M. The shutdown system self-discharge would be in the order of 0.1% per week.

From a practical point of view, many problems of matter transfer (solvent, ...) related to electro-osmosis through ion exchange membranes appear during operations. As a result, the volume of electrolytes in each tank changes according to the number of cycles and it is necessary to "redistribute" them by transferring a volume of electrolyte from one compartment to another, this approximately every 200 cycles. With this periodic rebalancing, life times of more than 2000 cycles and 10 years can be achieved. This is independent of corrosion problems that require regular replacement of parts, involving high maintenance costs. In the case of chemistries other than vanadium, electrolyte "rebalancing" is not possible as each compartment has a different chemistry and the management of these solvent transfers becomes problematic. Despite these important limitations, at the moment no "alternative" chemistry can compete with inorganic flow batteries in terms of application.

9.1.2. Possible Cell Configurations for Redox-Flow Batteries. Different types of ORFB have been described in the literature, with the most common being those where both electrolytes are liquid (Figure 21b). In the case where the only purpose is to evaluate a specific molecule, it is possible to use a symmetrical cell (same compounds in each compartment); however, this implies to have access to the two redox states of the molecule. There are also intermediate devices between a flow battery and a solid battery known as semisolid flow battery as proposed by Chiang's group.[426] This latter approach, which generally has the disadvantage of using highly viscous dispersions that require oversized pumps, will not be discussed in this review.

9.1.3. Redox-Active Organic Species and Solvents. Redox-active organic moieties identified in the ORFB literature are the same as those found in solid batteries and also deduced from the general classification reported in Table 1 including the use of pure p- or n-type structures as well as mixed systems. They are however "functionalized" in order to increase solubility in the chosen solvent. These molecules can be combined in an undifferentiated way to form either a rocking chair cation ion or anion ion cell or a dual ion cell (Figure 9). It should be noted that in the latter case, unlike in the case of "sealed" batteries, since the volume of electrolyte is generally very large compared to the mass of active material, the dual-ion cell geometry does not create any problems (significant loss of conductivity of the electrolyte). The main redox-active moieties are nitroxide, viologen, perylene diimide, ferrocene, quinone, thio, amino, phenol, ... (Figure S8). In a general way, there is a strong lack of redox-active structures able to work at very low potential (as in the case of carboxylates in organic "sealed" batteries working with solid state compounds) in order to obtain higher voltage systems. The main problem to address with redox molecule is stability. Since redox-active compounds are solubilized in the electrolyte, they are more subject to decomposition than solid electrodes. Thus, upon cycling, molecules can react together with solvent or electrolyte giving rise to poor performances. This especially at high concentrations (>0.5 M) which enhance decomposition kinetics.

The main role of the solvent is to dissolve the redox molecule in order to make it transportable between the tanks and the conversion cell. It must also ensure the ionic conductivity necessary to achieve electroneutrality at all points of the solution and avoid polarization phenomena in the conversion cell. For this purpose, the best solvent is water; its high polarity combined with its ability to dissociate electrolytes results from the fact that aqueous solutions have very high ionic conductivities. Moreover, in terms of cost, water is the cheapest solvent and presents the fewest safety problems (nonflammable, nontoxic). However, aqueous electrolytes display low electrochemical stability window (1.23 V from thermodynamics up to 1.5 V for kinetics reason). Organic solvents have the advantage of having larger electrochemical stability windows (>4.5 V in the case of acetonitrile or carbonates), but electrolyte dissociation is less efficient, resulting in an ionic conductivity of about 100 times less than in aqueous solvent.

Organic solvents are chemically unreactive, so they prevent degradation phenomena in solution and increase the lifetime of redox molecules. This also makes possible the stabilization of certain highly reactive redox molecules (e.g., radicals) and makes them relevant for redox-flow applications. The main solvents used are acetonitrile, carbonates, ethers, esters, and, more anecdotally, DMSO. Generally speaking, the solubility of organic molecules is not so different between aqueous and organic electrolytes, for two reasons: in organic media high concentrations of salts are used to increase the conductivity of solutions, with the consequence that the solubility of molecules decreases. An adapted functionalization renders the redox molecules highly soluble in water. The maximum concentrations achievable in a complete electrolyte (salt + solvent) are in the order of 2−3 M. As the conversion cells have not yet been really optimized for organic solvents, at the moment the solvent strongly conditions the type of batteries: high power density (0.1−0.3 W cm^{-2}) in aqueous solution (low voltage, high conductivity) and high energy density (>100 Wh L^{-1}) in organic solvent (high voltage, low conductivity). It is of course possible to mix several solvents, even if this makes electrolyte development more complex.[427] This approach remains difficult to master because it is difficult to combine the advantages of solvents without also combining the disadvantages.

One way to get around this is to use hydrotropes. A hydrotrope is a concentrated aqueous solution (several molars) of a small organic molecule such as urea, *para*-toluene sulfonic acid, nicotinic acid, and so on. Organic molecules are generally much more soluble in a hydrotrope than in water and the electrochemical properties are preserved or improved. The use of urea, for example, increases the solubility of benzoquinone by a factor of 7.[428] Other strategies have been used to make redox

https://dx.doi.org/10.1021/acs.chemrev.9b00482
Chem. Rev. 2020, 120, 6490−6557

organic molecules "liquid". The use of ionic liquid was tested by following different paths: as a solvent, with an organic or aqueous cosolvent, and finally by making redox ionic liquids. The use of eutectics based on highly concentrated salts in a solvent has produced interesting results because they produce highly conductive solutions capable of dissolving highly polar redox organic molecules.[429] Finally, some redox molecules developed to be highly soluble have been found to be liquid due to their low solid-state cohesion. However, the addition of salt is necessary to make the liquid ionically conductive, resulting in a significant increase in viscosity. While these alternative strategies have proved to be relevant, they have not yet made possible the development of large-scale devices capable of competing with inorganic flow cells in terms of power density, energy density, or stability (cycling and calendar aging).

The use of ionized salt is necessary to enhance the solvent ionic conductivity and maintain electroneutrality during the electrochemical process. In aqueous media, acid (H_2SO_4) or base (KOH) could be used if the redox molecule does not react with them. Salts like sodium or lithium associated with nitrate, and chloride or sulfate could be used in neutral pH. In organic medium, salts need to be highly soluble and dissociated, so lithium or tetra-alkylammonium cation associated with noncoordinating anion such as PF_6^-, BF_4^-, or $TFSI^-$ is mainly used, even if these salts are much more expensive than the ones used in aqueous solvents. Independently of the solvent, the choice of the supporting salt is very important on the electrochemical behavior of the redox molecule.

One of the main problems remaining for RFB concerns the fact that the electrolyte in a highly concentrated solution tends to be very viscous (both in inorganic or organic RFB). In organic RFB, the problem is more important in the way that organic molecules possess a higher molecular weight compared to inorganic ones (M(V) = 50.9 g mol^{-1}). This means, for example, that an organic redox molecule with a molecular weight of 200 g mol^{-1}, typically nonfunctionalized anthraquinonoid derivative, at a concentration of 1 M corresponds to 200 g of molecule in 1 L of solution. In some cases, the solution became as viscous as honey, precluding their use in flowing cells, apart from using a lot of energy to power the pump. A high viscosity also lowers the molecule diffusion in solution, with a direct effect on the apparent electron transfer kinetic and ionic conductivity. As a result, highly concentrated electrolytes suffer from higher cell overvoltage either in charge or in discharge.

9.1.4. Favoring Highly Soluble Redox-Active Species. In order to make redox organic molecules highly soluble in the desired medium, it is necessary to functionalize them with appropriately selected groups. In aqueous media, ionic functions or functions with a large number of heteroelements (e.g., O or N) will be favored to increase the interactions between the redox compound and water molecules. The main ionic functions used are sulfonates,[430] phosphates,[431] carboxylates,[432] ammonium,[433] or hydroxo.[434] These ionic functions have also the advantage of increasing the ionic conductivity of the solution, allowing in some cases to eliminate the use of supporting salts. Neutral substituents such as PEGs are also used regularly. However, it is necessary to remain attentive to the positions chosen to graft these solubilizing groups, because the functionalization of redox molecules can completely change the electrochemical response and make it irreversible. The solubility of nonfunctionalized organic molecules is generally better in organic media. However, in most cases, functionalization is necessary to achieve the solubility necessary to develop an efficient flow battery. In organic media, neutral substituents are preferred, such as alkyl chains or PEGs. Alkyl chains are not necessarily the most efficient because of their low polarity, which is not optimal in polar solvents and which hinders the solubilization and dissociation of salts. PEG chains have the advantage of being more polar and their effect on solubility is more important. By choosing certain chain lengths, it is even possible to obtain liquid redox compounds. Finally, these PEG chains are capable of strongly complexing the alkaline cations contained in the supporting salt, thus improving its dissociation and increasing the conductivity of the solution.

For the redox-flow system, the membrane is an important element; it allows the two compartments to be physically separated to avoid the mixing of species but must permit the passage of ions to ensure the electroneutrality of each of the compartments. In most cases, an ion exchange membrane is used, cationic in the case of a cationic rocking chair battery, anionic in the case of an anionic rocking chair battery, and one or the other in the case of a dual ion configuration. In aqueous environments, the most efficient membranes are mainly made of perfluoro sulfonated polymer. These membranes are very stable and have a high ionic conductivity. They have the disadvantage of not being as stable in organic media or they tend to swell and become porous. Alternative organic membranes have been developed, but unfortunately for the moment they are not as stable as the perfluoro one. To counter this, ceramic membranes have been used, particularly in the case of mixed devices using a lithium electrode. As the cost of such membranes is important, different strategies have been deployed to try to replace them with simpler separators. Size based separators (dialysis membranes) combined with redox molecules in the form of poly/oligomer to block diffusion from one compartment to the other.

9.2. Aqueous Organic Redox-Flow Batteries

9.2.1. Generality. In aqueous media, the most studied organic molecules are undoubtedly quinones and both methyl-viologen and TEMPO derivatives. Such electrolytes have the advantage of being highly dissociating for the supporting salts, forming solutions of high ionic conductivity allowing high power densities cycling. The highest conductivities are obtained in acidic environments since proton is the cation with the highest mobility (the Grotthuss mechanism). Similarly, the hydroxide ion is the most mobile anion, so many studies in aqueous media are also carried out in basic media. However, these two electrolytes have the disadvantage of being very reactive toward organic molecules: protons are responsible for degradation by acid catalysis (polymerization etc..), and hydroxide ions are good nucleophiles (hydroxylation). For example, it should be remembered that cleaning glassware in organic chemistry is often carried out in potash baths.

In the case of quinones, these reactions are particularly troublesome (e.g., Michael reaction) and very effective in both acidic and basic media, so that after a few cycles, the initial molecule is completely transformed and in general the associated loss of capacity is significant.[435] Similarly, quinones tend to dimerize, decreasing the capacity that can be addressed.[436] As far as methyl viologen derivatives are concerned, they are stable only in a neutral or acidic medium; in a basic medium an elimination reaction takes place resulting in the loss of redox properties. These compounds also tend to dimerize, resulting in one electron reactions instead of two.[437] Similarly, in highly acidic environments, TEMPOs undergo degradation reactions.[438]

https://dx.doi.org/10.1021/acs.chemrev.9b00482
Chem. Rev. 2020, 120, 6490−6557

In all cases, it is necessary to develop sometimes complex strategies to avoid these adverse reactions for the battery operation and stability. In terms of solubility, by functionalization it is possible to achieve solubility values in about 2 M. In the case of quinones, the electrochemical and solubility properties are very strongly dependent on the number and substitution positions.[430] Thus 9,10-anthraquinone-2,7-disulfonic acid (AQDS) retains a high electrochemical reversibility while being highly soluble, which is not the case for other disulfonates.[439] Generally speaking, aqueous ORFBs have many advantages: nontoxic, low solvent and salt costs, highly conductive solution. However, they pose two important and very difficult problems: the small window of potential associated with this solvent and its reactivity with organic molecules.

9.2.2. Main Examples of Aqueous ORFB. Many works have been carried out over the last 5 years in the field of aqueous ORFBs, we have chosen a few didactic examples to show the diversity of approaches and the performances that can be obtained with this technology to date.

Aziz's group (Harvard University) has conducted numerous studies on the use of quinone for ORFBs, or combined organic/inorganic batteries (quinone -Br_2, quinone ferrocyanide).[434,440] Their studies focus mainly on the use of sulfonated (AQDS acid medium) or hydroxylated (DHAQ basic medium) quinones that can achieve electron concentrations >1 M (Figure 22a). The output cell voltage obtained with the full system 0.5 M DHAQ/0.4 M ferrocyanide is about 1.2 V. The battery was tested for 100 cycles at a current density of 100 mA cm^{-2} and showed an energy efficiency greater than 80% and a capacity retention of 90%. The maximum power density is 400 mW·cm^{-2}. No significant degradation of the electrolyte seems to occur. With ADQS in sulfuric acid medium (1 M) as negative electrolyte, associated with 3.5 M hydrobromic acid and dibromine (0.5 or 2 M) the cell voltage is 0.8 V. Different types of carbon felt and membranes have been tested to optimize battery performances. With a 212 Nafion membrane and 2 M Br_2, 3 M HBr, the battery reaches a power peak at 1 W cm^{-2} which is extremely high for a flow battery. It should be noted, however, that this was possible thanks to extremely high electrolyte flows (400 mL min^{-1}) for an electrode surface area of 2 cm^2, which is very demanding on the consumption of the pumps.

Schubert's group (University of Jena) has developed an approach combining methyl viologen derivatives (low potential) and nitroxide (high potential).[441,442] These organic compounds are reversible in electrochemistry and have very high electron transfer kinetics. The voltages of the cells reached are 1.4 V (Figure 22b). The TEMPTMA derivative has a solubility of 2.3 M in a solution of NaCl 1.5 M which corresponds to a theoretical capacity of 61 Ah. The flow battery combining MV and TEMPTMA (2 M each) addresses the maximum capacity of the electrolyte up to a current density of about 100 mA cm^{-2}. The energy efficiency is greater than 70%. At 80 mA cm^{-2} the battery is stable over 100 cycles without significant degradation of performance. To avoid using an ion exchange membrane, polymers have been developed from these molecular units. Due to the steric encumbrance of these polymers, a simple porous membrane is sufficient to prevent the two compartments from mixing. Ten Ah L^{-1} electrolytes are made by dissolving these polymers in 2 M NaCl solution. The battery thus formed is capable of cycling up to current densities of 50 mA cm^{-2} without significant loss of capacity. The properties are stable over 90 cycles with a loss of less than 10% in capacity. The energy density of redox fluids is in the order of 10 W L^{-1}.

Liu's group (Utah State University) has developed several types of chemistry based mainly on viologen derivatives (negative) and either ferrocene derivatives or dibromine in positive compartment (Figure 22c).[443,444] In particular, they used a sulfonate substituted viologen derivative to make a mixed organic/inorganic (Br_2) RFB. The output voltage of the cell is about 1.4 V. The synthesized molecule has been tested in a neutral medium (NH_4Br) at concentrations up to 1.5 M (3 N). The power densities obtained are as high as 227 mW cm^{-2} for a current density of 300 mA cm^{-2}. The stability in charge and discharge over 50 cycles shows a loss of capacity per cycle of 0.11%; the energy efficiency is 78% at 40 mA cm^{-2}. The energy density of these ORFBs is 30.3 Wh L^{-1}. Tests have shown that the use of carbon nanotubes on current collectors improves battery performance, significantly reducing overpotential issues. This group has also developed ammonium-substituted ferrocene derivatives to improve solubility in aqueous media (>2 M in 2 M NaCl). The batteries produced have a cell voltage of 1 V and energy efficiencies that are highly dependent on current density (72% at 40 mA cm^{-2} and 43% at 100 mA cm^{-2}). Aging studies carried out over 700 cycles have shown very high stability (about 0.00014% loss of capacity per cycle).

Narayanan et al.[445,446] from University of Southern California have developed an ORFB where posolyte and negolyte are quinone based: disulfonated anthraquinone (AQDS) or monosulfonated in negative compartment and disulfonated *ortho*-benzoquinone (BQDS or tiron) as positive electrolyte (Figure 22d). These two compounds have high solubility in acid electrolytes. The cell voltage is 0.8 V at a current density of 80 mA cm^{-2}. This voltage drops sharply as the current density increases. Several cell geometries and current collectors (carbon felts) have been tested to increase the performance of these batteries. The energy efficiency of a battery composed of BQDS and AQDS 1 M is 70% over 100 cycles. In any case, due to the reactivity of these redox molecules, these batteries have low cycling stability.

Finally, Jin et al.[432] from Nanjing University have modified a naphthoquinone by substituting it with a carboxylate group (HCNQ) to increase solubility in a neutral or basic medium (Figure 22e). The battery made with an alkaline electrolyte (KOH 1 M) and 0.5 M HCNQ combined with ferrocyanide exhibits an output voltage of 1 V. Power densities of 250 mW cm^{-2} were measured at a current density of about 400 mA cm^{-2}. The capacity loss measured over 50 cycles is 0.12% per cycle, probably resulting from the reactivity of the reduced form of HCNQ. To increase stability, it would be necessary to modify the structure of these quinones to block hydroxylation reactions.

Concerning ORFBs, the aqueous medium is undoubtedly the one with the best performance in terms of energy efficiency and current density. Contrary to what was anticipated, the solubility of redox molecules in aqueous medium is not much lower than what can be measured in organic medium. The power and energy densities are high and in some cases at the same level as those found in the case of inorganic BFRs (vanadium). Although different conversion cell geometries are being tested in some studies, it would now be useful to conduct systematic studies to try to minimize losses due to ohmic drops, or problems related to cross diffusion through the membrane. In general, many of these systems suffer from

https://dx.doi.org/10.1021/acs.chemrev.9b00482
Chem. Rev. 2020, 120, 6490−6557

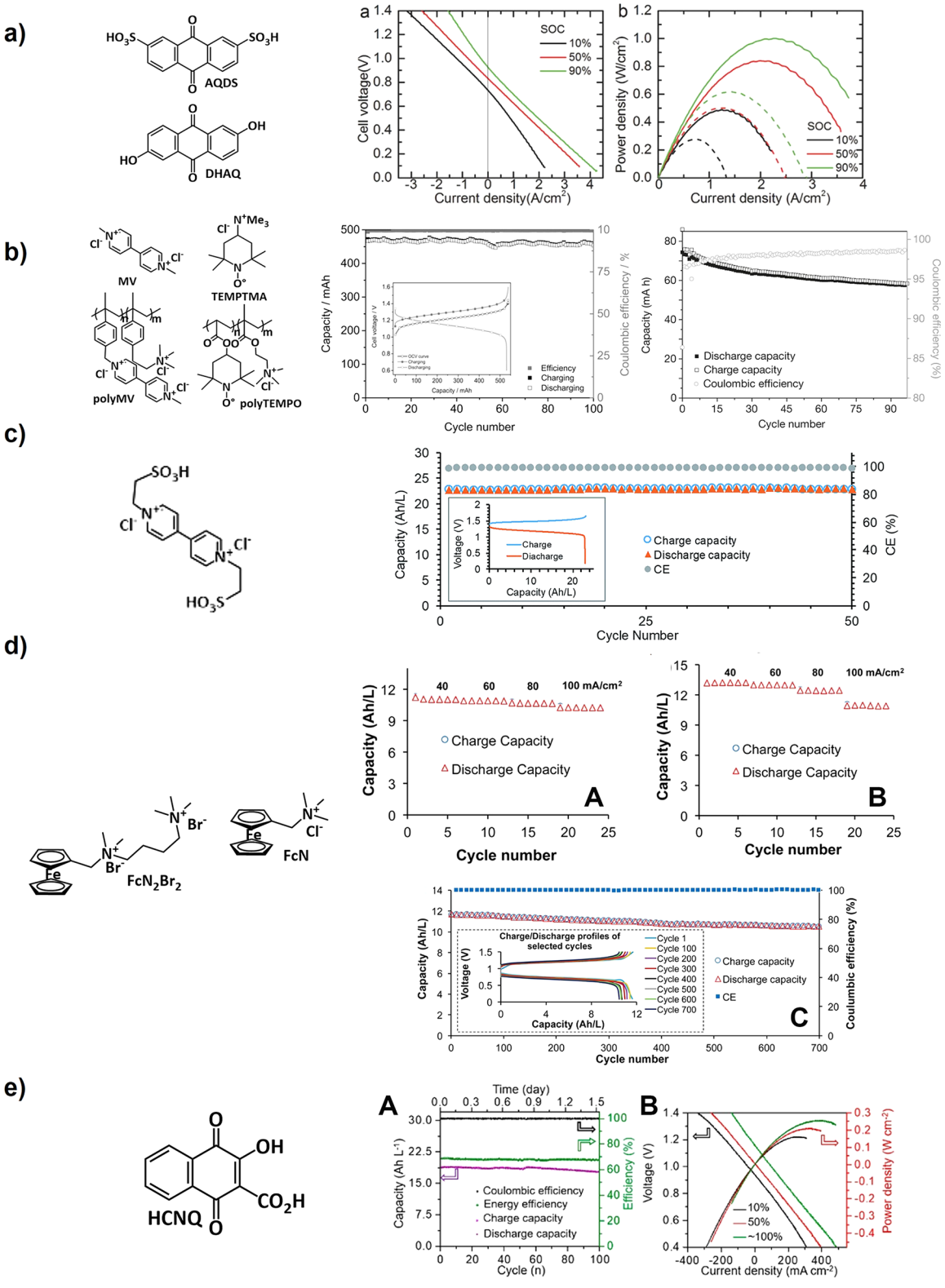

Figure 22. (a) Performance of ORFB composed of AQDS and Br_2 showing both the cell voltage vs current density and the power density vs current density (reproduced with permission from ref 440. Copyright 2016 The Electrochemical Society). (b) Cycling capacity and efficiency of ORFB made of: MV and PEMPTMA (center); polymerized MV and TEMPO (left) (reproduced with permission from refs 441 and 442. Copyright 2015 John Wiley and Sons and Nature Publishing Group). (c) Cycling curve and aging behavior of the ORFB developed by Liu et co-workers. Concentration of redox molecule 1 M in NH_4Br (reproduced with permission from ref 443. Copyright 2019 The Royal Society of Chemistry). (d) Capacity vs cycle number at different current densities for (A) FcNCl, (B) FcN_2Br_2 at 0.5 M, and (C) cycling stability of FcNCl/MV battery (0.5 M electrolyte) over 700 cycles (reproduced with permission from ref 444. Copyright 2017 American Chemical Society). (e) Capacity vs cycle number at different current densities for an HCNQ cell (0.5 M) in A. Corresponding voltage and power density vs current density in B (reproduced with permission from ref 432. Copyright 2018 American Chemical Society).

https://dx.doi.org/10.1021/acs.chemrev.9b00482
Chem. Rev. 2020, 120, 6490−6557

poor cyclability, particularly in concentrated conditions, due to the numerous possible decomposition reactions.

9.3. All-Organic Redox-Flow Batteries

Redox batteries using an organic solvent have been strongly developed in the literature during the years 2000−2010, mainly with compounds from coordination chemistry with several stable redox states; more recently, the use of organic molecules has strongly increased. The main advantage of working with organic solvents is to have larger potential windows and therefore to increase the energy density. The voltages obtained with devices where both fluids circulate are at most in the order of 2.5 V. This is mainly due to the fact that when the molecules are in solution no SEI can be formed. SEI layers are formed on the surface of particles inserting Li at very low potential and protect the solvents from decomposition. Due to main solvent stability window, it is necessary that the redox potential of the compound used in the negative electrolyte should be at the most in the order of 1 V vs Li^+/Li. Therefore, hybrid devices have been developed combining a Li-based negative and an organic positive flow cell. Another difficulty comes from organic electrolytes: low ionic conductivity, about 100 times lower than aqueous electrolytes. This results in important ohmic drop and decreases the voltage efficiency. Thus, a complete optimization of the cell core would be necessary to counter this phenomenon.

Various cells configurations are used to test new compounds by (*i*) associating two organic redox couples, (*ii*) carrying test in symmetric cells, or (*iii*) Li/RFB hybrid cells. The latter, due to the low potential of Li, have very high energy density, up to about 200 Wh L^{-1} but power density remains very low due to current limitation (less than 1 mA cm^{-2}). However, to date, no redox solvent-based electrolyte battery has been able to achieve a true industrial scale demonstrator. Many questions remain to be answered, such as the associated costs, safety, and solubility, electrolyte viscosity, which is generally very high in concentrated organic media, and calendar and cycling stability over very long periods. For example, there are few studies where highly concentrated electrolytes (0.5−1 M) are tested in flux configuration mainly due to the high solutions viscosity. The few systems we have selected to discuss are the most advanced and representative of these devices.

9.3.1. Main Results in Mix Configuration (Li/Organic RFB). The Pacific Northwest National Laboratory (PNNL) has particularly tested several types of strategies and redox molecules in mixed configuration.[447−449] First, anthraquinone derivatives modified to increase their solubility were used, then TEMPO, and finally ferrocene derivatives. As the latter does not provide better properties than other approaches, it will not be discussed in this review, only the first two strategies are described below.

Wang et al.[447] proposed to modify anthraquinones with PEG groups (15D3GAQ) to promote the solubility of the molecule as well as the complexing effect toward Li ions. The electrolyte is composed of a solution of $LiPF_6$ 1 M in PC. This solvent forms a stable SEI with respect to Li metal. The static cell is composed of a Li sheet and a simple Celgard separator that confines the redox molecule to the positive compartment; the concentration of 15G3GAQ being 0.25 M. An average voltage of 2.3 V is measured when the battery is cycled to 0.1 mA cm^{-2} (Figure 23a). The battery properties are stable up to a cycling current of 0.5 mA cm^{-2} but collapse beyond that. Two plateaus corresponding to the two consecutive transfers of 1 electron are observed respectively at 2.15 and 2.40 V (during charging), respectively. An energy efficiency of 82% is measured; the cycling stability evaluated over 40 cycles shows a loss of about 0.8% in capacity per cycle. The measured energy density is about 25 Wh L^{-1}, with the low concentration used to make the electrolyte (0.5 M in electron) being compensated by the output cell voltage (2.3 V).

Xu, Wang, and co-workers found that TEMPO was highly soluble in carbonate solvents.[448] Thus in an EC/PC/EMC mixture (4:1:5 w/w) 2.3 M $LiPF_6$, TEMPO is soluble up to 2 M. However, it should be noted that the solutions obtained are very viscous and difficult to circulate (67.1 cP at 2 M, 4.02 cP at 0.1 M). The flow cell consists of a Li/graphite mixed negative electrode, a porous physical separator, and a carbon felt through which the electrolyte circulates. The energy density was measured with the cell at 2 M TEMPO and 126 Wh L^{-1}, with an energy efficiency of 70%. Stability in concentrated condition does not seem very high, in dilute solution (0.1 M), capacity losses are about 0.2% per cycle. As there is no ceramic membrane, the cycling currents are higher, up to 5 mA cm^{-2}.

Finally, Lu et al.[450] reported the use of 10-methylphenothiazine (MPT) melted, then mixed with carbon black (Ketjenblack EC-600JD), and finally ground when solidified. The electrolyte consists of a saturated solution of MPT (0.3 M) in an EC/DEC 1 M $LiPF_6$ mixture to which the ground solid is added. The MPT in solution acts as a redox shuttle to electrochemically address the solid MPT. It should be noted that without carbon, solid MPT is not electroactive. Mixtures of 0%, 20%, and 40% (in vol.) solid and electrolyte were tested. The electrolytes were tested in static and flow cells. The flow cell is composed of a Li sheet, a ceramic separator (LAGP) and of the electrolyte circulating on a carbon paper. On the cycling curves (Figure 23b), the electrolyte alone (0%) has a plateau at 3.55 V vs Li^+/Li and a capacity of 7 Ah L^{-1}, which corresponds to 87% of the theoretical capacity. With 20% mixture, the cycling curves maintain the same behavior, but the capacity is increased to 27 Ah L^{-1}. The 50% mixture allows to reach a capacity of 55 Ah L^{-1}, which corresponds to an electron concentration of 2.23 M. The energy density of the 40% electrolyte is 190 Wh L^{-1}, one of the highest energy densities demonstrated to date. This is mainly due to the high cell voltage (3.55 V) even if the MPT/carbon Ketjenblack mixture significantly increases the capacity of the solution.

The main problem with these mixed Li/organic molecules flow cell approaches comes from the very low current densities (often less than 1 mA cm^{-2}) that can be passed through the device. This is particularly true if the separator between the two compartments is a ceramic membrane. When the separator is porous, it would appear that the SEI formed on the surface of the Li in the carbonates is beneficial. It would act as an ion exchange membrane while blocking electron transfers to the redox molecules. Thus, molecules in solution close to the negative electrode could not be reduced, which would explain the high Coulombic efficiency of these devices. On the other hand, at high concentration in redox molecules, the SEI is modified and/or no longer succeeds in blocking these electron transfers and the Coulombic efficiency falls strongly (Coulombic efficiency 99% at 0.1 M, 91% at 0.8 M, 85% at 1.5 M, and 84% at 2 M).[448] Finally, these devices do not allow the power and energy density to be separated; they are therefore more limited in terms of application.

9.3.2. Main Results in Liquid All-Organic Cell Configuration. Argonne laboratory and their collaborators have optimized the structure of phenolic ethers used as

https://dx.doi.org/10.1021/acs.chemrev.9b00482
Chem. Rev. 2020, 120, 6490−6557

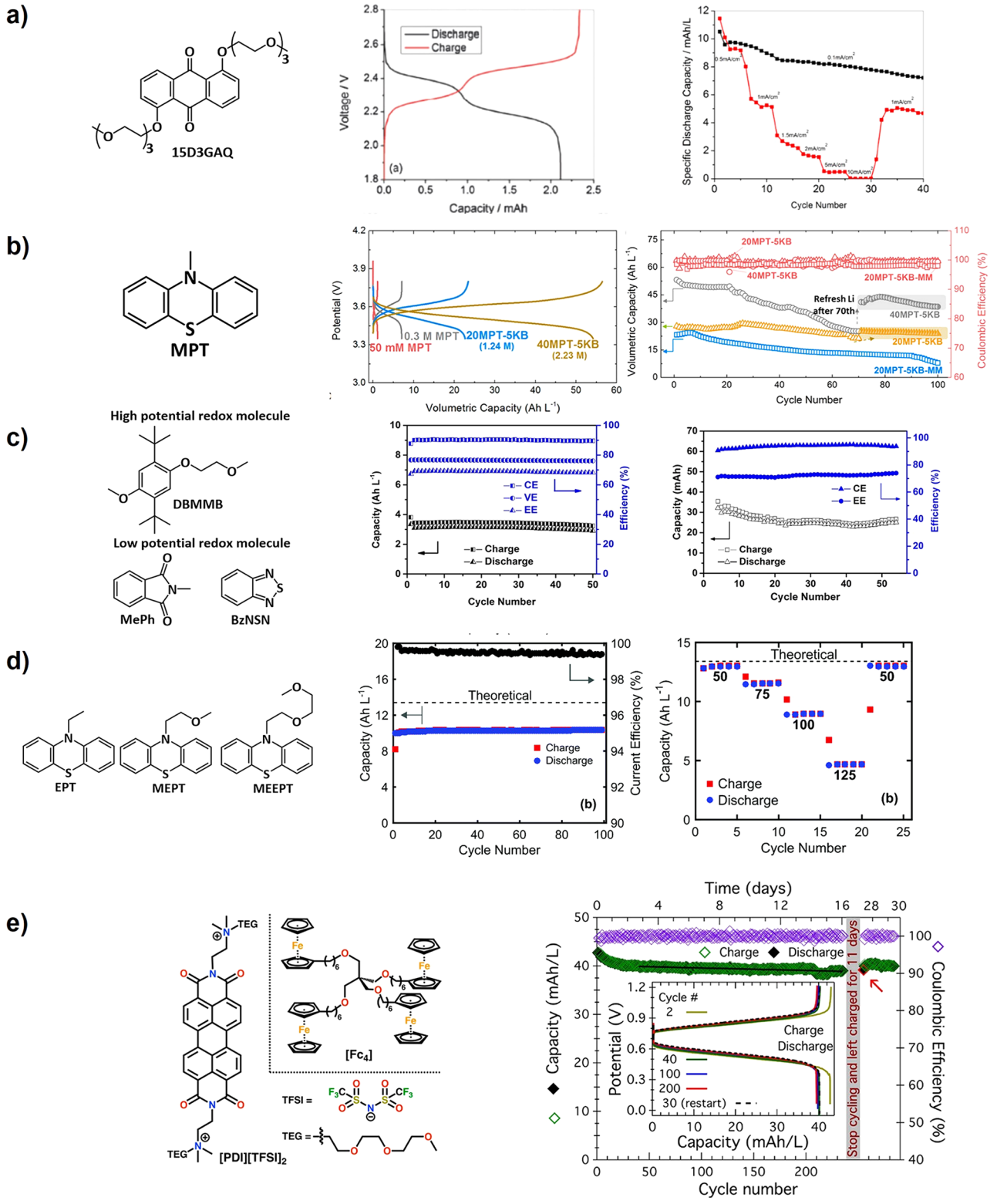

Figure 23. (a) Cycling performance and rate capability reported by Wang and co-workers of the cell with 0.25 M 15D3GAQ as posolyte and lithium foil as anode (reproduced with permission from ref 447. Copyright 2012 The Royal Society of Chemistry). (b) Cycling performance of the Li/MPT flow cell reported by Lu and co-workers (reproduced with permission from ref 450. Copyright 2018 American Chemical Society). (c) Cycling performances of ORFBs based on MePh/DBMMB 0.3 M in DME− M LiTFSI (left) or BzNSN/DBMMB 0.5 M in ACN 1 M LiTFSI (right) reported by Wei and co-workers (reproduced with permission from refs 452 and 453. Copyright 2016 and 2017 American Chemical Society). (d) Symmetric flow cell characterization of MEEPT 0.5 M in ACN 0.5 M $TEABF_4$ reported by Milshtein and co-workers (reproduced with permission from ref 454. Copyright 2016 The Royal Society of Chemistry). Constant current cycling at 100 mA cm^{-2} (left), capacity vs cycle number at different current densities (right). (e) Molecule used by Sisto and co-workers to develop dialysis membrane-based ORFBs (left) together with the cycling performance (right), reproduced from ref 455.

https://dx.doi.org/10.1021/acs.chemrev.9b00482
Chem. Rev. 2020, 120, 6490−6557

high-potential molecules in order to increase their solubility, and stability.[451] DBMMB offers the best compromise in terms of viscosity, stability and diffusion coefficient. Its redox potential is about 0.78 V vs Ag^+/Ag, so it has been retained and implemented against several low-potential and highly soluble molecules: BzNSN and *N*-methylphthalimide (MePh).[452,453] MePh has a reduction potential of about −1.79 V vs Ag^+/Ag in 1 M LiTFSI DME electrolyte. A major effort has been made to choose a porous membrane of the Celgard or Daramic-type that is effective in preventing species mixing and does not generate a too high ohmic drop. A Daramic 175 membrane was selected to make a complete redox-flow cell using an equimolar mixture of DBMMB and MePh at 0.3 M in 1 M LiTFSI DME electrolyte. Although tested only over about 50 cycles, the cell capacity is constant at about 3 Ah L^{-1} for an energy density of 9.3 Wh L^{-1}. This cell is able to work at current densities close to those used in aqueous ones: 50 mA·cm^{-2} with no significant degradation of its performance. At this current level, the energy efficiency remains above 60%. It is interesting to note that at low current the Coulombic efficiency is not very good due to the cross diffusion of species through the porous membrane while at high current density the voltage efficiency drops due to the ohmic drop. The redox potential of BzNSN is −1.58 V vs Ag^+/Ag in 1 M LiTFSI ACN electrolyte, with its solubility being 2.1 M when considering 2.1 M LiTFSI ACN as the electrolyte.

An electrolyte containing an equimolar mixture of BzNSN and DBMMB (0.5 M) in 1 M LiTFSI ACN as electrolyte was cycled in a redox-flow cell composed of two carbon felt electrodes and a Daramic type separator (800 μm). Due to the viscosity of the solution and the problems of cross diffusion through the membrane, the current density applied is 10 mA·cm^{-2}. The energy yield is 72%, mainly due to ohmic drops. The energy density is in the order of 6−8 Wh L^{-1}. The stability of the cell is not very good (50 cycles) probably due to the reactivity at high concentration of the species that compose the electrolyte. These studies have shown that DBMMB derivatives are potentially relevant for the design of a fully organic redox-flow battery. They are extremely soluble in organic electrolytes (2−3 M) and the radicals resulting from their oxidation are stable in DME solvents. The two low-potential molecules tested, particularly BzNSN, are soluble up to 5 M, but their solutions are highly viscous precluding their use in flowing cell.

Kentucky University has developed organically soluble phenothiazine derivatives.[454] MEEPT has been selected as the most efficient compound: it is liquid at room temperature, and its solubility in 0.5 M nBu_4NBF_4 ACN is greater than 2 M. It is electrochemically stable, and it is possible to prepare both forms, neutral and oxidized, easily by chemical methods. The core of the conversion cell has been optimized to reduce both ohmic drop and losses related to fluid flowing through the system (channel electrodes). The optimized cell has a resistance of about 3.3 Ω cm^{-2}. The assembly was tested in a symmetrical configuration with an electrolyte composed of 0.5 M MEEPT at 50% state of charge with a theoretical capacity of 13.4 Ah L^{-1}. In constant current cycling at 50 and 100 mA·cm^{-2}, the measured capacity is respectively 97.3% and 60% of the theoretical capacity. Over 100 cycles (80.6 h in total) at 100 mA cm^{-2}, the capacity is maintained, and no significant loss is observed.

Columbia University, NY, has developed a flux battery based on perylene diimide derivatives (negative) and ferrocene tetramere (positive), both of which can achieve electron concentrations > 1 M.[455] The interest of this work is to demonstrate that cellulose dialysis membranes, combined with redox compounds with a large hydrodynamic radius, are very efficient to avoid mixing the two electrolytes. The authors also carried out studies on aging both in cycling and calendars (even if carried out in diluted solution). They were able to demonstrate that in 11 days in the charged state, no significant loss of capacity was noted. The cell could be cycled 450 times with an average capacity loss of 0.00614% per cycle.

All organic redox-flow cell faces a lot of problems to develop a commercially viable system able to really compete with aqueous inorganic chemistries. This is mainly due to the fact that the molecular parameters are all interdependent. The fact of wanting high cell voltages implies the use of compounds where reduced (materials with very low potential) or oxidized (materials with very high potential) forms are poorly stabilized and therefore very reactive. From a solubility point of view, the use of highly concentrated solutions further increases decomposition phenomena. This often results in poor cycling stability and is in addition to the fact that calendar aging is almost never achieved or under very diluted conditions that are more favorable.[456] Organic solutions that are highly concentrated generally become highly viscous, causing problems for flowing (pumps power consumption) and voltage efficiencies as these solutions become less conductive. The diffusion coefficients of redox species and ions decrease when viscosity increases with the result of lower apparent electron transfer kinetics. This results in high overvoltage values and low energy yields, often well below 60%. This probably explains why there are no flow cell studies at concentrations above 2 M in the literature, while several molecules have higher solubility values. The main interest of the studies in organic media is that due to the swelling of conventional ion exchange membranes and a high cross over, combined with low electrolyte conduction (high overvoltage), the community has been forced to develop membrane-free approaches, some of which have proven to be relevant.

9.4. Summary

The use of organic molecules to make electrolytes for flow batteries is now well described in the literature. Dozens of different molecules have been tested in various cell configurations. From a properties and behavior point of view, electrolytes based on organic molecules face the same problems as inorganic compounds: solubility, high viscosity of concentrated solutions with the result of a decrease in apparent electron transfer kinetics (overvoltage between charge and discharge), and a high power consumption by the pumps. Since the intrinsic stability of organic molecules in solution is lower than the stability of inorganic compounds, cycling and calendar stability are generally less good.

This stability aspect remains the key point to go further. Many parameters must be taken into account to understand the degradation of ORFB performance: molecules in solutions are much more reactive than in the solid state, in addition they are in contact with different materials (plastic, stainless steel, and so on) which can act as catalysts. Most of these compounds are sensitive at least in one redox state to oxygen traces, which is difficult to prevent in the long term (leakage). Reactions are also possible, for example, with other components of the electrolyte, such as the solvent (substitution reactions, hydrolysis, ...), the supporting salts, or the molecule itself (dimerization or polymerization reaction). In addition, reactivity may change with molecules redox states, a reduced

https://dx.doi.org/10.1021/acs.chemrev.9b00482
Chem. Rev. 2020, 120, 6490−6557

one will be more sensitive to reactions with an electrophile, while oxidized molecules will be more sensitive to reactions with nucleophiles. Therefore, it is necessary that all other components of the electrolytes be as unreactive as possible. It can be expected thanks to functionalizations to stabilize a molecule by blocking some degradation reactions. For example, the reduced state of dihydroxyanthraquinone tends to degrade through oxidative coupling. To avoid this side reaction, the functionalization of hydroxyl groups by PEG, alkyl carboxylate, or alkyl phosphate chains has been successfully proposed. However, these new molecules become sensitive to hydrolysis reactions and degradation reactions can occur.[431,457] This observation is general; attempting to stabilize a molecule in a given electrolyte may result in a change of its reactivity or redox property that makes the molecule less or no more relevant for the application.

In most cases, crossover phenomena through the membranes are harmful. To compensate forthis, the development of stable molecules in at least three stable redox states, which can serve both as posolytes and as negolytes (such as vanadium), would greatly improve the stability of ORFBs. This would also allow the reservoirs to be rebalanced when the transfer of solvent by electro-osmosis becomes too high. All these constraints result in rather low overall energy yields (65%) compared to other battery-based storage systems (90%) but much better than the cycle associated with hydrogen: "electrolyzer, storage, fuel cell" whose total efficiency is around 25%. From the grid point of view, the real advantage of RFBs is that they decouple power and energy; they are the only storage systems that allow this.

For the development and credibility of ORFBs, it is now necessary to rationalize the tests and studies carried out in the literature. Indeed, few tests are carried out under the same conditions and these are generally not representative of the final application. For example, it is important that systems should be tested at the highest possible concentrations. Systematic studies of cycling and calendar aging must be carried out. During cycling studies, it is important that the time of each cycle be representative of the RFB application (*i.e.*, 4 to 12 h of energy storage). With regard to the flow rates used to carry out the measurements, very often they are disproportionately high to compensate for the high viscosity of the concentrated solutions. Moreover, depending on the cell geometry used, the flow rate does not have an important meaning. It would be more interesting to indicate the linear velocity of the fluid on the surface of the electrodes and to keep these values as low as possible to avoid that the pumps consume more energy than the energy stored in the battery.

10. CONCLUDING REMARKS

Almost 170 years after the invention of the first operational rechargeable battery by G. Planté thanks to metal-based electrode materials, this tutorial review was intended to highlight several opportunities offered at the turn of the 21st century by the reversible redox chemistry to promote innovative electrochemical devices based on naturally abundant chemical elements (including biomass) while improving the environmental footprint. Indeed, we have shown in this article that the world has drastically changed since Planté's invention through the ongoing modernization of our societies but at the price of continuous consumption of both energy and nonrenewable materials at the expense of the environment.[115] Changing the historic roadmap followed by our current energy engineering is nowadays mandatory in the general interest. In this context, global demand for batteries multiplies to store renewable energy, promote electromobility, and power the continued development of portable electronics and emerging technologies (mobile devices, IoT, AI, robotics, etc.). Seeking to develop innovative, efficient, and less polluting and energy consuming chemistries is therefore important today while jointly developing better recycling solutions (and second use).

Depicted as a parallel and relatively recent research field in the history of rechargeable electrochemical storage systems, we have sequentially summarized the present state-of-the-art and highlighted important works that have contributed to the recent progress in organic-based rechargeable systems by covering all possible technologies and cell configurations to date. The as-obtained performance figures have been described without avoiding limitations. Some of the key performance metrics of organic electrode compounds such as specific energy, working potential, and cycling stability already look promising, and material design strategies specific to these metrics have been preliminarily established. Challenges remain for developing efficient storage solutions that simultaneously excel in all these metrics. It seems probable that the practical use of organics for the electrochemical storage in a near future could be through the development of ORFBs due to their attractive features of high power density and low cost for large-scale energy storage.

In terms of solid electrode materials (for "sealed" batteries), electroactive molecules with simple structures such as simple quinones could offer the best balance between high discharge potential and high specific capacity, but stable cycling requires proper immobilization of these molecules which, until now, cannot be done without impacting potential and capacity. Two directions may directly counter this dilemma. The first is a chemical path revolving no-compromise immobilization. Rational connection of molecular building blocks complemented by suitable synthesis methods has been successful in preserving the full redox characteristics of active cores as seen in OEMs like PAQS and P(NDI2OD-T2). The second is to suit OEMs with solid electrolytes where dissolution is a nonissue. Solid-state batteries are emerging as an alternative to the traditional liquid electrolytes to enable safer and higher-energy batteries. The nondissolving nature of solid electrolytes is an additional perk specifically useful for organic batteries. In addition, p-type materials could offer access to molecular (metal-free) batteries as well as possible assemblies with n-type systems to promote dual-ion cells.

Continued evolution of organic batteries will inevitably involve a better understanding of involved electrochemical mechanisms (especially in the solid state) as well as the development of new OEMs, which is both a strong suit for organic compounds from the fundamental study point of view and a potential uncertainty for practical applications. Organic compounds are known to have good tuning knobs to manipulate the molecular structures and many subsequent properties, but complicated functionalization can drive up synthesis cost. Two currently practiced approaches could lead to a balance between performance and cost. One scours through structures that can be synthesized from cheap raw materials via simple, few-step, and high-yield reactions, the other prioritizes function and performance with no specific focus on minimizing cost. At an early stage of research and development, the former approach rarely affords high-performance candidates due to the limited options, while the latter could end up with prohibitive costs. Overtime, however, the building blocks found by the former and

https://dx.doi.org/10.1021/acs.chemrev.9b00482
Chem. Rev. 2020, 120, 6490−6557

the design strategies established by the latter will merge the two approaches and strike the balance.

Beyond the direct using of redox-active organics as the main active electrode compounds, other functionalities can be used in an electrochemical cell such as the hybridization of the conventional inorganic active materials with organic redox-active polymers giving rise to fast electrode kinetics. Thus let us recall that electrical properties of solid composite electrodes are critical to electrochemical performances, whatever the considered technology. This is especially the case for thick electrodes which are highly sought-after because they enable in principle simultaneous increase in volumetric and specific energy densities and decrease in price. It is estimated that 20 to 80% of power losses in the case of a thick electrode originate from insufficient electronic conduction.[458] The design of electronic conductivity at different scales is not easy, because it is currently based on the use of carbon-based conductive additives that are difficult to disperse homogeneously on the one hand, and on the other hand, that renders difficult the manufacturing of thick composite electrodes, because of the unstable nature of the electrode inks. In addition, the loss of intercluster and interparticle contacts due to volume variations of active materials is a major cause of the aging of battery electrodes.[459] It is therefore mandatory to add polymeric binders (insulators), with the downside of a difficult compromise between electronic conductivity and mechanical properties of the composite electrode.[460] The use of electron conducting binders or even redox binders ("smart binder") appears therefore quite attractive, since it would enable the design of electrodes with lower amount of carbon and binder additives. This objective was pursued in the particular case of $LiMPO_4$ (M = Fe, Mn). As early as 2006, Goodenough and co-workers showed that carbon-coated $LiFePO_4$ particles can be directly connected to the current collector using a matrix of p-doped PPy or PAni,[461−463] while Gräetzel was actually the first to connect non-carbon-coated $LiMPO_4$ (M = Fe, Mn) particles to the current collectors using molecular wires.[464] In the latter, the Fermi levels of the organic matter and the active material need to be adjusted while the adsorbed wires should be percolated to allow for cross-surface charge. This approach was also recently investigated by Nishide and Oyaizu using nonconjugated radical polymers (radicals are densely introduced as the pendant groups) that were specifically designed for fast charging of $LiFePO_4$ or $LiCoO_2$.[465] Schougaard and co-workers also showed a poly(3,4-ethylenedioxythiophene) coating at the surface of bare $LiFePO_4$ particles advantageously replaced the carbon coating.[466] Targeting the contemporary concerns of industry-relevant electrodes and especially thicker ones, Gaubicher and Blanchard[467] used a short thiophene-based π-conjugated system as a molecular junction between uncoated $LiFePO_4$ and multiwall carbon nanotubes within undensified 2 mAh cm^{-2} electrodes. Electrochemical and electrical properties of such electrodes demonstrate the key role of molecular junctions to reach power and cyclability performances comparable to those of carbon-coated $LiFePO_4$ electrodes.

To conclude, although this research activity is still in its infancy and much remains to be done to get attractive performances, redox-active organic compounds can be perceived today more than ever as an alternative chemical choice depending on the targeted application. We hope that this review will be a source of original and fresh ideas for our readers.

ASSOCIATED CONTENT

Supporting Information

The Supporting Information is available free of charge at https://pubs.acs.org/doi/10.1021/acs.chemrev.9b00482.

Evolution of the global EV stock by vehicle's category; estimated world LIB manufacturing capacity for automotive applications, International trade flows, and LIB cell manufacturing capacities in 2016; critical raw Materials in the EU, 2017; world mining industry production for materials used in LIBs in 2016; the concept of renewable organic battery; selection of redox-active units used in ORFBs. (PDF)

AUTHOR INFORMATION

Corresponding Author

Philippe Poizot − *Université de Nantes, CNRS, Institut des Matériaux Jean Rouxel, IMN, F-44000 Nantes, France;* orcid.org/0000-0003-1865-4902; Email: philippe.poizot@cnrs-imn.fr

Authors

Joël Gaubicher − *Université de Nantes, CNRS, Institut des Matériaux Jean Rouxel, IMN, F-44000 Nantes, France;* orcid.org/0000-0001-6229-740X

Stéven Renault − *Université de Nantes, CNRS, Institut des Matériaux Jean Rouxel, IMN, F-44000 Nantes, France*

Lionel Dubois − *Université Grenoble Alpes, CEA, 38000 Grenoble, France*

Yanliang Liang − *Department of Electrical and Computer Engineering and Texas Center for Superconductivity, University of Houston, Houston, Texas 77204, United States;* orcid.org/0000-0001-6771-5172

Yan Yao − *Department of Electrical and Computer Engineering and Texas Center for Superconductivity, University of Houston, Houston, Texas 77204, United States;* orcid.org/0000-0002-8785-5030

Complete contact information is available at: https://pubs.acs.org/10.1021/acs.chemrev.9b00482

Notes

The authors declare no competing financial interest.

Biographies

Philippe Poizot was born in Crépy en Valois (France) in 1975. After a Master of Science in analytical chemistry and electrochemistry (University of Paris VI, 1998), he obtained his Ph.D. degree in Materials Science (2001) focused on "conversion reactions" under the guidance of J.-M. Tarascon at the University of Picardy Jules Verne (UPJV-LRCS) in Amiens, France. After a postdoctoral training with J. A. Switzer at the University of Missouri—Rolla (USA) to develop the electrodeposition of nanostructured materials, he came back to UPJV-LRCS as Associate Professor in 2002. In 2007, he proposed the concept of "renewable" batteries by promoting novel electrode materials based on redox-active organic compounds deriving from biomass. In 2012, he was appointed as full Professor at University of Nantes (Institut des Matériaux Jean Rouxel, IMN-CNRS, Nantes, France). His current research topics are mainly focused on rechargeable batteries, molecular electrochemistry, and the development of organic batteries in both aqueous and nonaqueous electrolytes. He is a recipient of the Bronze Medal of the French

https://dx.doi.org/10.1021/acs.chemrev.9b00482
Chem. Rev. 2020, 120, 6490−6557

Society for Encouragement and Progress (2002) and was a Junior Fellow of the Institut Universitaire de France (2012−2017).

Joël Gaubicher was born in Saint-Germain-en-Laye (France) in 1972. He studied chemistry and materials engineering in Paris. After obtaining a Ph.D. from the P&M Curie University of Paris, he joined the University of Waterloo, Canada, as a postdoctoral fellow with Prof. L. F. Nazar where he worked on phosphates and borates for Li ion battery. In 2001, he obtained a full CNRS researcher position at the Institut des Matériaux Jean Rouxel in Nantes and developed research programs dealing with Li metal polymer, Li-ion, Na-ion, and Li/S batteries and supercapacitors. His main interests deal with solid state electrochemistry of inorganic and organic materials as well as synthesis and electrochemical mechanisms mainly through operando characterizations. He was the recipient of a CNRS award for his research in 2013. More recently, he has been developing aqueous battery and supercapacitor chemistries based on organic electroactive materials.

Stéven Renault was born in Longjumeau (France) in 1980. He studied biochemistry and chemistry and obtained his Ph.D. in chemistry from Université de Rennes 1 in 2007 focused on drug design and medicinal chemistry. After working as a postdoctoral fellow in Amiens, he joined the group of Kristina Edström and Daniel Brandell in the Ångström Advanced Battery Center (Uppsala University, Sweden) as a researcher in 2011. Since 2018, he joined Université de Nantes as an Associate Professor at the Institut des Matériaux Jean Rouxel. His research interests focus on Li/Na/Mg organic batteries and Li−air batteries.

Lionel Dubois was born in Strasbourg (France) in 1973. He studied chemistry at "Ecole Nationale Superieure de Chimie de Paris". After obtaining a Ph.D in molecular chemistry from Grenoble Alps University he joined the University of Groningen (NL) as a postdoctoral fellow with Prof. B. L. Feringa where he worked on new iron based catalyst for alkane oxidation by molecular oxygen. Then he moved to the NMR laboratory of the French Atomic Energy Commission in Saclay under the direction of Dr. H. Desvaux on the development of laser polarized xenon NMR. In 2004, he obtained an assistant professor position at the University Institute of Technology of Castres (France), before being recruited as researcher at the French Atomic Energy Commission (CEA) in Grenoble in 2005. He developed a program related to the use of molecular chemistry for communication and information technologies and since 2011 has been working on the use of molecular compounds for energy storage. In 2017 he took the head of the "Molecular Architecture Conception and Electronic Process" laboratory of the CEA—Grenoble. His main interest deals with coordination chemistry, synthesis of new ligands, graphene chemistry, solution electrochemistry, and diverse spectroscopies (NMR, EPR) or operando experiments for energy applications, mainly organic batteries and supercapacitors.

Yanliang Liang was born in Guangzhou (China) and studied materials physics and chemistry at Nankai University (China). He conducted his Ph.D. research on organic batteries and photovoltaics under the supervision of Prof. Jun Chen at Nankai University. After receiving his Ph.D. in 2012, he worked as a postdoctoral fellow with Prof. Yan Yao at University of Houston on low-cost safe battery technologies. He is now a Research Assistant Professor at University of Houston focusing on energy storage materials and next-generation battery developments.

Yan Yao was born in Nantong (China) and studied materials science in Fudan University (China). He conducted his Ph.D. research on organic photovoltaics under the supervision of Prof. Yang Yang at UCLA. He served as a senior scientist at Polyera Corporation from 2008 to 2010 and a postdoctoral fellow at Stanford University under the supervision of Prof. Yi Cui from 2010 to 2012. He joined the University of Houston as Assistant Professor of Electrical and Computer Engineering in 2012 and is now Associate Professor. His research interests focus on developing new materials for Li ion batteries and post-Li battery chemistries such as organic, Na, Mg, and solid-state batteries.

ACKNOWLEDGMENTS

The authors express their sincere gratitude to economist colleagues E. Hache (IFP Énergies Nouvelles, Rueil-Malmaison, France) and P. Menanteau (GAEL, Grenoble, France) for helpful comments and discussions on this manuscript. The authors are also grateful to J. Zhang and X. Wang (UH, Texas, USA) for the help on Table 2 as well as to F. Dolhem (LG2A, Amiens, France) for insightful comments. The authors are thankful to P. Berrezig and C. Doutriaux for helpful assistance in editing the manuscript and the graphical abstract, respectively.

REFERENCES

(1) Jain, A.; Ong, S. P.; Hautier, G.; Chen, W.; Richards, W. D.; Dacek, S.; Cholia, S.; Gunter, D.; Skinner, D.; Ceder, G.; et al. Commentary: The Materials Project: A materials genome approach to accelerating materials innovation. *APL Mater.* **2013**, *1*, 011002.
(2) *Linden's handbook of batteries*, 4th ed.; Reddy, T. B., Linden, D., Eds.; McGraw-Hill: New York, NY, 2011; ISBN 978-0-07-162421-3.
(3) Pavlov, D. D. *Lead-acid batteries: science and technology : a handbook of lead-acid battery technology and its influence on the product*; 2017; ISBN 978-0-444-59552-2.
(4) Young, K.-H. Research in Nickel/Metal Hydride Batteries 2016. *Batteries* **2016**, *2*, 31.
(5) Alotto, P.; Guarnieri, M.; Moro, F. Redox flow batteries for the storage of renewable energy: A review. *Renewable Sustainable Energy Rev.* **2014**, *29*, 325−335.
(6) Sum, E.; Skyllas-Kazacos, M. A study of the V(II)/V(III) redox couple for redox flow cell applications. *J. Power Sources* **1985**, *15*, 179−190.
(7) Sum, E.; Rychcik, M.; Skyllas-kazacos, M. Investigation of the V(V)/V(IV) system for use in the positive half-cell of a redox battery. *J. Power Sources* **1985**, *16*, 85−95.
(8) Rychcik, M.; Skyllas-Kazacos, M. Characteristics of a new all-vanadium redox flow battery. *J. Power Sources* **1988**, *22*, 59−67.
(9) Liang, Y.; Tao, Z.; Chen, J. Organic Electrode Materials for Rechargeable Lithium Batteries. *Adv. Energy Mater.* **2012**, *2*, 742−769.
(10) Janoschka, T.; Hager, M. D.; Schubert, U. S. Powering up the Future: Radical Polymers for Battery Applications. *Adv. Mater.* **2012**, *24*, 6397−6409.
(11) Song, Z.; Zhou, H. Towards sustainable and versatile energy storage devices: an overview of organic electrode materials. *Energy Environ. Sci.* **2013**, *6*, 2280.
(12) Gracia, R.; Mecerreyes, D. Polymers with redox properties: materials for batteries, biosensors and more. *Polym. Chem.* **2013**, *4*, 2206.
(13) Zhu, Z.; Chen, J. Review—Advanced Carbon-Supported Organic Electrode Materials for Lithium (Sodium)-Ion Batteries. *J. Electrochem. Soc.* **2015**, *162*, A2393−A2405.
(14) Häupler, B.; Wild, A.; Schubert, U. S. Carbonyls: Powerful Organic Materials for Secondary Batteries. *Adv. Energy Mater.* **2015**, *5*, 1402034.
(15) Gong, K.; Fang, Q.; Gu, S.; Li, S. F. Y.; Yan, Y. Nonaqueous redox-flow batteries: organic solvents, supporting electrolytes, and redox pairs. *Energy Environ. Sci.* **2015**, *8*, 3515−3530.
(16) Oltean, V.-A.; Renault, S.; Valvo, M.; Brandell, D. Sustainable Materials for Sustainable Energy Storage: Organic Na Electrodes. *Materials* **2016**, *9*, 142.

https://dx.doi.org/10.1021/acs.chemrev.9b00482
Chem. Rev. 2020, 120, 6490−6557

(17) Casado, N.; Hernández, G.; Sardon, H.; Mecerreyes, D. Current trends in redox polymers for energy and medicine. *Prog. Polym. Sci.* **2016**, *52*, 107−135.
(18) Muench, S.; Wild, A.; Friebe, C.; Häupler, B.; Janoschka, T.; Schubert, U. S. Polymer-Based Organic Batteries. *Chem. Rev.* **2016**, *116*, 9438−9484.
(19) Miroshnikov, M.; Divya, K. P.; Babu, G.; Meiyazhagan, A.; Reddy Arava, L. M.; Ajayan, P. M.; John, G. Power from nature: designing green battery materials from electroactive quinone derivatives and organic polymers. *J. Mater. Chem. A* **2016**, *4*, 12370−12386.
(20) Winsberg, J.; Hagemann, T.; Janoschka, T.; Hager, M. D.; Schubert, U. S. Redox-Flow Batteries: From Metals to Organic Redox-Active Materials. *Angew. Chem., Int. Ed.* **2017**, *56*, 686−711.
(21) Schon, T. B.; McAllister, B. T.; Li, P.-F.; Seferos, D. S. The rise of organic electrode materials for energy storage. *Chem. Soc. Rev.* **2016**, *45*, 6345−6404.
(22) Xie, J.; Zhang, Q. Recent progress in rechargeable lithium batteries with organic materials as promising electrodes. *J. Mater. Chem. A* **2016**, *4*, 7091−7106.
(23) Kowalski, J. A.; Su, L.; Milshtein, J. D.; Brushett, F. R. Recent advances in molecular engineering of redox active organic molecules for nonaqueous flow batteries. *Curr. Opin. Chem. Eng.* **2016**, *13*, 45−52.
(24) Son, E. J.; Kim, J. H.; Kim, K.; Park, C. B. Quinone and its derivatives for energy harvesting and storage materials. *J. Mater. Chem. A* **2016**, *4*, 11179−11202.
(25) Zhao, Q.; Guo, C.; Lu, Y.; Liu, L.; Liang, J.; Chen, J. Rechargeable Lithium Batteries with Electrodes of Small Organic Carbonyl Salts and Advanced Electrolytes. *Ind. Eng. Chem. Res.* **2016**, *55*, 5795−5804.
(26) Zhang, Y.; Wang, J.; Riduan, S. N. Strategies toward improving the performance of organic electrodes in rechargeable lithium (sodium) batteries. *J. Mater. Chem. A* **2016**, *4*, 14902−14914.
(27) Yang, G.; Zhang, Y.; Huang, Y.; Shakir, M. I.; Xu, Y. Incorporating conjugated carbonyl compounds into carbon nanomaterials as electrode materials for electrochemical energy storage. *Phys. Chem. Chem. Phys.* **2016**, *18*, 31361−31377.
(28) Zhao, Q.; Lu, Y.; Chen, J. Advanced Organic Electrode Materials for Rechargeable Sodium-Ion Batteries. *Adv. Energy Mater.* **2017**, *7*, 1601792.
(29) Kim, K. C. Design Strategies for Promising Organic Positive Electrodes in Lithium-Ion Batteries: Quinones and Carbon Materials. *Ind. Eng. Chem. Res.* **2017**, *56*, 12009−12023.
(30) Xie, J.; Gu, P.; Zhang, Q. Nanostructured Conjugated Polymers: Toward High-Performance Organic Electrodes for Rechargeable Batteries. *ACS Energy Lett.* **2017**, *2*, 1985−1996.
(31) Zhao, Q.; Zhu, Z.; Chen, J. Molecular Engineering with Organic Carbonyl Electrode Materials for Advanced Stationary and Redox Flow Rechargeable Batteries. *Adv. Mater.* **2017**, *29*, 1607007.
(32) Friebe, C.; Schubert, U. S. High-Power-Density Organic Radical Batteries. *Top. Curr. Chem.* **2017**, *375*, DOI: 10.1007/s41061-017-0103-1
(33) Wu, Y.; Zeng, R.; Nan, J.; Shu, D.; Qiu, Y.; Chou, S.-L. Quinone Electrode Materials for Rechargeable Lithium/Sodium Ion Batteries. *Adv. Energy Mater.* **2017**, *7*, 1700278.
(34) Leung, P.; Shah, A. A.; Sanz, L.; Flox, C.; Morante, J. R.; Xu, Q.; Mohamed, M. R.; Ponce de León, C.; Walsh, F. C. Recent developments in organic redox flow batteries: A critical review. *J. Power Sources* **2017**, *360*, 243−283.
(35) Wei, X.; Pan, W.; Duan, W.; Hollas, A.; Yang, Z.; Li, B.; Nie, Z.; Liu, J.; Reed, D.; Wang, W.; et al. Materials and Systems for Organic Redox Flow Batteries: Status and Challenges. *ACS Energy Lett.* **2017**, *2*, 2187−2204.
(36) Poizot, P.; Dolhem, F.; Gaubicher, J. Progress in all-organic rechargeable batteries using cationic and anionic configurations: Toward low-cost and greener storage solutions? *Curr. Opin. Electrochem.* **2018**, *9*, 70−80.
(37) Amin, K.; Mao, L.; Wei, Z. Recent Progress in Polymeric Carbonyl-Based Electrode Materials for Lithium and Sodium Ion Batteries. *Macromol. Rapid Commun.* **2019**, *40*, 1800565.
(38) Lu, Y.; Zhang, Q.; Li, L.; Niu, Z.; Chen, J. Design Strategies toward Enhancing the Performance of Organic Electrode Materials in Metal-Ion Batteries. *Chem.* **2018**, *4*, 2786−2813.
(39) Lee, S.; Kwon, G.; Ku, K.; Yoon, K.; Jung, S.-K.; Lim, H.-D.; Kang, K. Recent Progress in Organic Electrodes for Li and Na Rechargeable Batteries. *Adv. Mater.* **2018**, *30*, 1704682.
(40) Xu, Y.; Zhou, M.; Lei, Y. Organic materials for rechargeable sodium-ion batteries. *Mater. Today* **2018**, *21*, 60−78.
(41) Wang, H.; Zhang, X. Organic Carbonyl Compounds for Sodium-Ion Batteries: Recent Progress and Future Perspectives. *Chem. - Eur. J.* **2018**, *24*, 18235−18245.
(42) Liang, Y.; Yao, Y. Positioning Organic Electrode Materials in the Battery Landscape. *Joule* **2018**, *2*, 1690−1706.
(43) Bhosale, M. E.; Chae, S.; Kim, J. M.; Choi, J.-Y. Organic small molecules and polymers as an electrode material for rechargeable lithium ion batteries. *J. Mater. Chem. A* **2018**, *6*, 19885−19911.
(44) Armstrong, C. G.; Toghill, K. E. Stability of molecular radicals in organic non-aqueous redox flow batteries: A mini review. *Electrochem. Commun.* **2018**, *91*, 19−24.
(45) Ding, Y.; Zhang, C.; Zhang, L.; Zhou, Y.; Yu, G. Molecular engineering of organic electroactive materials for redox flow batteries. *Chem. Soc. Rev.* **2018**, *47*, 69−103.
(46) Zhao, Q.; Whittaker, A.; Zhao, X. Polymer Electrode Materials for Sodium-ion Batteries. *Materials* **2018**, *11*, 2567.
(47) Mauger, A.; Julien, C.; Paolella, A.; Armand, M.; Zaghib, K. Recent Progress on Organic Electrodes Materials for Rechargeable Batteries and Supercapacitors. *Materials* **2019**, *12*, 1770.
(48) Xie, J.; Zhang, Q. Recent Progress in Multivalent Metal (Mg, Zn, Ca, and Al) and Metal-Ion Rechargeable Batteries with Organic Materials as Promising Electrodes. *Small* **2019**, *15*, 1805061.
(49) Jia, X.; Ge, Y.; Shao, L.; Wang, C.; Wallace, G. G. Tunable Conducting Polymers: Toward Sustainable and Versatile Batteries. *ACS Sustainable Chem. Eng.* **2019**, *7*, 14321−14340.
(50) Heiska, J.; Nisula, M.; Karppinen, M. Organic electrode materials with solid-state battery technology. *J. Mater. Chem. A* **2019**, *7*, 18735−18758.
(51) Friebe, C.; Lex-Balducci, A.; Schubert, U. S. Sustainable Energy Storage: Recent Trends and Developments toward Fully Organic Batteries. *ChemSusChem* **2019**, *12*, 4093−4115.
(52) Wu, Z.; Xie, J.; Xu, Z. J.; Zhang, S.; Zhang, Q. Recent progress in metal−organic polymers as promising electrodes for lithium/sodium rechargeable batteries. *J. Mater. Chem. A* **2019**, *7*, 4259−4290.
(53) Oubaha, H.; Gohy, J.; Melinte, S. Carbonyl-Based π-Conjugated Materials: From Synthesis to Applications in Lithium-Ion Batteries. *ChemPlusChem* **2019**, *84*, 1179−1214.
(54) Han, C.; Li, H.; Shi, R.; Zhang, T.; Tong, J.; Li, J.; Li, B. Organic quinones towards advanced electrochemical energy storage: recent advances and challenges. *J. Mater. Chem. A* **2019**, *7*, 23378−23415.
(55) Peng, H.; Yu, Q.; Wang, S.; Kim, J.; Rowan, A. E.; Nanjundan, A. K.; Yamauchi, Y.; Yu, J. Molecular Design Strategies for Electrochemical Behavior of Aromatic Carbonyl Compounds in Organic and Aqueous Electrolytes. *Adv. Sci.* **2019**, *6*, 1900431.
(56) Luo, J.; Hu, B.; Hu, M.; Zhao, Y.; Liu, T. L. Status and Prospects of Organic Redox Flow Batteries toward Sustainable Energy Storage. *ACS Energy Lett.* **2019**, *4*, 2220−2240.
(57) Cao, X.; Liu, J.; Zhu, L.; Xie, L. Polymer Electrode Materials for High-Performance Lithium/Sodium-Ion Batteries: A Review. *Energy Technol.* **2019**, *7*, 1800759.
(58) Zhu, L.; Ding, G.; Xie, L.; Cao, X.; Liu, J.; Lei, X.; Ma, J. Conjugated Carbonyl Compounds as High-Performance Cathode Materials for Rechargeable Batteries. *Chem. Mater.* **2019**, *31*, 8582
(59) Novák, P.; Müller, K.; Santhanam, K. S. V.; Haas, O. Electrochemically Active Polymers for Rechargeable Batteries. *Chem. Rev.* **1997**, *97*, 207−282.

(60) Ito, T.; Shirakawa, H.; Ikeda, S. Simultaneous polymerization and formation of polyacetylene film on the surface of concentrated soluble Ziegler-type catalyst solution. *J. Polym. Sci., Polym. Chem. Ed.* **1974**, *12*, 11−20.
(61) Chiang, C. K.; Fincher, C. R.; Park, Y. W.; Heeger, A. J.; Shirakawa, H.; Louis, E. J.; Gau, S. C.; MacDiarmid, A. G. Electrical Conductivity in Doped Polyacetylene. *Phys. Rev. Lett.* **1977**, *39*, 1098−1101.
(62) Shirakawa, H.; Louis, E. J.; MacDiarmid, A. G.; Chiang, C. K.; Heeger, A. J. Synthesis of electrically conducting organic polymers: halogen derivatives of polyacetylene, $(CH)_x$. *J. Chem. Soc., Chem. Commun.* **1977**, 578
(63) Chiang, C. K.; Gau, S. C.; Fincher, C. R.; Park, Y. W.; MacDiarmid, A. G.; Heeger, A. J. Polyacetylene, $(CH)_x$: *n*-type and *p*-type doping and compensation. *Appl. Phys. Lett.* **1978**, *33*, 18−20.
(64) Shirakawa, H. Synthesis and characterization of highly conducting polyacetylene. *Synth. Met.* **1995**, *69*, 3−8.
(65) Nigrey, P. J.; MacInnes, D., Jr.; Nairns, D. P.; MacDiarmid, A. G.; Heeger, A. J. Lightweight Rechargeable Storage Batteries Using Polyacetylene, $(CH)_x$ as the Cathode-Active. *J. Electrochem. Soc.* **1981**, *128*, 1651.
(66) Ĉaja, J. A.; Kaner, R. B.; MacDiarmid, A. G. Rechargeable Battery Employing a Reduced Polyacetylene Anode and a Titanium Disulfide Cathode. *J. Electrochem. Soc.* **1984**, *131*, 2744.
(67) Naegele, D.; Bittihn, R. Electrically conductive polymers as rechargeable battery electrodes. *Solid State Ionics* **1988**, *28*−*30*, 983−989.
(68) Matsunaga, T.; Daifuku, H.; Nakajima, T.; Kawagoe, T. Development of polyaniline−lithium secondary battery. *Polym. Adv. Technol.* **1990**, *1*, 33−39.
(69) Miller, J. S. Conducting polymers−materials of commerce. *Adv. Mater.* **1993**, *5*, 671−676.
(70) Liu, M. Electrochemical Properties of Organic Disulfide/Thiolate Redox Couples. *J. Electrochem. Soc.* **1989**, *136*, 2570.
(71) Liu, M. Novel Solid Redox Polymerization Electrodes - All-Solid-State, Thin-Film, Rechargeable Lithium Batteries. *J. Electrochem. Soc.* **1991**, *138*, 1891.
(72) Liu, M. Novel Solid Redox Polymerization Electrodes - Electrochemical Properties. *J. Electrochem. Soc.* **1991**, *138*, 1896.
(73) Li, Y.; Zhan, H.; Kong, L.; Zhan, C.; Zhou, Y. Electrochemical properties of PABTH as cathode materials for rechargeable lithium battery. *Electrochem. Commun.* **2007**, *9*, 1217−1221.
(74) Preefer, M. B.; Oschmann, B.; Hawker, C. J.; Seshadri, R.; Wudl, F. High Sulfur Content Material with Stable Cycling in Lithium-Sulfur Batteries. *Angew. Chem., Int. Ed.* **2017**, *56*, 15118−15122.
(75) Nakahara, K.; Iwasa, S.; Satoh, M.; Morioka, Y.; Iriyama, J.; Suguro, M.; Hasegawa, E. Rechargeable batteries with organic radical cathodes. *Chem. Phys. Lett.* **2002**, *359*, 351−354.
(76) Anastas, P. T.; Zimmerman, J. B. *Innovations in Green Chemistry and Green Engineering Selected Entries from the Encyclopedia of Sustainability Science and Technology*; Springer: New York, NY, 2013; ISBN 978-1-4614-5817-3.
(77) Nakahara, K.; Oyaizu, K.; Nishide, H. Organic Radical Battery Approaching Practical Use. *Chem. Lett.* **2011**, *40*, 222−227.
(78) Iwasa, S.; Yasui, M.; Nishi, T.; Nakano, K. Development of Organic Radical Battery. *NEC Technol. J.* **2012**, *7*, 102−106.
(79) Ravet, N.; Michot, C.; Armand, M. Novel cathode materials based on organic couples for lithium batteries. *Mater. Res. Soc. Symp. Proc.* **1997**, *496*, 263−273.
(80) Han, X.; Chang, C.; Yuan, L.; Sun, T.; Sun, J. Aromatic Carbonyl Derivative Polymers as High-Performance Li-Ion Storage Materials. *Adv. Mater.* **2007**, *19*, 1616−1621.
(81) Xiang, J.; Chang, C.; Li, M.; Wu, S.; Yuan, L.; Sun, J. A Novel Coordination Polymer as Positive Electrode Material for Lithium Ion Battery. *Cryst. Growth Des.* **2008**, *8*, 280−282.
(82) Chen, H.; Armand, M.; Demailly, G.; Dolhem, F.; Poizot, P.; Tarascon, J.-M. From Biomass to a Renewable $Li_xC_6O_6$ Organic Electrode for Sustainable Li-Ion Batteries. *ChemSusChem* **2008**, *1*, 348−355.
(83) Chen, H.; Armand, M.; Courty, M.; Jiang, M.; Grey, C. P.; Dolhem, F.; Tarascon, J.-M.; Poizot, P. Lithium Salt of Tetrahydroxybenzoquinone: Toward the Development of a Sustainable Li-Ion Battery. *J. Am. Chem. Soc.* **2009**, *131*, 8984−8988.
(84) Poizot, P.; Dolhem, F. Clean energy new deal for a sustainable world: from non-CO_2 generating energy sources to greener electrochemical storage devices. *Energy Environ. Sci.* **2011**, *4*, 2003.
(85) Xu, Y.; Wen, Y.; Cheng, J.; Cao, G.; Yang, Y. Study on a single flow acid Cd−chloranil battery. *Electrochem. Commun.* **2009**, *11*, 1422−1424.
(86) Li, Z.; Li, S.; Liu, S.; Huang, K.; Fang, D.; Wang, F.; Peng, S. Electrochemical Properties of an All-Organic Redox Flow Battery Using 2,2,6,6-Tetramethyl-1-Piperidinyloxy and N-Methylphthalimide. *Electrochem. Solid-State Lett.* **2011**, *14*, A171.
(87) Anjos, D. M.; McDonough, J. K.; Perre, E.; Brown, G. M.; Overbury, S. H.; Gogotsi, Y.; Presser, V. Pseudocapacitance and performance stability of quinone-coated carbon onions. *Nano Energy* **2013**, *2*, 702−712.
(88) Assresahegn, B. D.; Brousse, T.; Bélanger, D. Advances on the use of diazonium chemistry for functionalization of materials used in energy storage systems. *Carbon* **2015**, *92*, 362−381.
(89) Brousse, T.; Cougnon, C.; Bélanger, D. Grafting of Quinones on Carbons as Active Electrode Materials in Electrochemical Capacitors. *J. Braz. Chem. Soc.* **2018**, *29*, 989997.
(90) Zeiger, M.; Weingarth, D.; Presser, V. Quinone-Decorated Onion-Like Carbon/Carbon Fiber Hybrid Electrodes for High-Rate Supercapacitor Applications. *ChemElectroChem* **2015**, *2*, 1117−1127.
(91) Madec, L.; Humbert, B.; Lestriez, B.; Brousse, T.; Cougnon, C.; Guyomard, D.; Gaubicher, J. Covalent vs. non-covalent redox functionalization of C−$LiFePO_4$ based electrodes. *J. Power Sources* **2013**, *232*, 246−253.
(92) Anothumakkool, B.; Taberna, P.-L.; Daffos, B.; Simon, P.; Sayed-Ahmad-Baraza, Y.; Ewels, C.; Brousse, T.; Gaubicher, J. Improved electro-grafting of nitropyrene onto onion-like carbon via in situ electrochemical reduction and polymerization: tailoring redox energy density of the supercapacitor positive electrode. *J. Mater. Chem. A* **2017**, *5*, 1488−1494.
(93) Madec, L.; Bouvrée, A.; Blanchard, P.; Cougnon, C.; Brousse, T.; Lestriez, B.; Guyomard, D.; Gaubicher, J. In situ redox functionalization of composite electrodes for high power−high energy electrochemical storage systems via a non-covalent approach. *Energy Environ. Sci.* **2012**, *5*, 5379−5386.
(94) Madec, L.; Robert, D.; Moreau, P.; Bayle-Guillemaud, P.; Guyomard, D.; Gaubicher, J. Synergistic Effect in Carbon Coated $LiFePO_4$ for High Yield Spontaneous Grafting of Diazonium Salt. Structural Examination at the Grain Agglomerate Scale. *J. Am. Chem. Soc.* **2013**, *135*, 11614−11622.
(95) Roldán, S.; Blanco, C.; Granda, M.; Menéndez, R.; Santamaría, R. Towards a Further Generation of High-Energy Carbon-Based Capacitors by Using Redox-Active Electrolytes. *Angew. Chem., Int. Ed.* **2011**, *50*, 1699−1701.
(96) Gorska, B.; Frackowiak, E.; Beguin, F. Redox active electrolytes in carbon/carbon electrochemical capacitors. *Curr. Opin. Electrochem.* **2018**, *9*, 95−105.
(97) Lebègue, E.; Brousse, T.; Gaubicher, J.; Retoux, R.; Cougnon, C. Toward fully organic rechargeable charge storage devices based on carbon electrodes grafted with redox molecules. *J. Mater. Chem. A* **2014**, *2*, 8599−8602.
(98) Naoi, K.; Morita, M. Advanced Polymers as Active Materials and Electrolytes for Electrochemical Capacitors and Hybrid Capacitor Systems. *Electrochem. Soc. Interface* **2008**, *17*, 44−48.
(99) Lang, A. W.; Ponder, J. F.; Österholm, A. M.; Kennard, N. J.; Bulloch, R. H.; Reynolds, J. R. Flexible, aqueous-electrolyte supercapacitors based on water-processable dioxythiophene polymer/carbon nanotube textile electrodes. *J. Mater. Chem. A* **2017**, *5*, 23887−23897.

https://dx.doi.org/10.1021/acs.chemrev.9b00482
Chem. Rev. 2020, 120, 6490−6557

(100) Kurra, N.; Hota, M. K.; Alshareef, H. N. Conducting polymer micro-supercapacitors for flexible energy storage and Ac line-filtering. *Nano Energy* **2015**, *13*, 500−508.
(101) Jeżowski, P.; Crosnier, O.; Deunf, E.; Poizot, P.; Béguin, F.; Brousse, T. Safe and recyclable lithium-ion capacitors using sacrificial organic lithium salt. *Nat. Mater.* **2018**, *17*, 167−173.
(102) Anothumakkool, B.; Wiemers-Meyer, S.; Guyomard, D.; Winter, M.; Brousse, T.; Gaubicher, J. Cascade-Type Prelithiation Approach for Li-Ion Capacitors. *Adv. Energy Mater.* **2019**, *9*, 1900078.
(103) Chen, X.; Wang, H.; Yi, H.; Wang, X.; Yan, X.; Guo, Z. Anthraquinone on Porous Carbon Nanotubes with Improved Supercapacitor Performance. *J. Phys. Chem. C* **2014**, *118*, 8262−8270.
(104) Lee, M.; Hong, J.; Kim, H.; Lim, H.-D.; Cho, S. B.; Kang, K.; Park, C. B. Organic Nanohybrids for Fast and Sustainable Energy Storage. *Adv. Mater.* **2014**, *26*, 2558−2565.
(105) Liu, T.; Kim, K. C.; Lee, B.; Chen, Z.; Noda, S.; Jang, S. S.; Lee, S. W. Self-polymerized dopamine as an organic cathode for Li- and Na-ion batteries. *Energy Environ. Sci.* **2017**, *10*, 205−215.
(106) Schwab, K. *The fourth industrial revolution*, First U.S. ed.; Crown Business: New York, 2017; ISBN 978-1-944835-00-2.
(107) Yli-Huumo, J.; Ko, D.; Choi, S.; Park, S.; Smolander, K. Where Is Current Research on Blockchain Technology?—A Systematic Review. *PLoS One* **2016**, *11*, e0163477.
(108) Alam, M. S.; Roychowdhury, A.; Islam, K. K.; Huq, A. M. Z. A revisited model for the physical quality of life (PQL) as a function of electrical energy consumption. *Energy* **1998**, *23*, 791−801.
(109) Antal, M.; Van Den Bergh, J. C. J. M. Green growth and climate change: conceptual and empirical considerations. *Clim. Policy* **2016**, *16*, 165−177.
(110) Global Warming 1.5°C - IPCC special report 2019, Available http://www.ipcc.ch/report/sr15/, last accessed June 2019.
(111) World Population Prospects 2019, Available https://population.un.org/wpp/, last accessed June 2019.
(112) Larcher, D.; Tarascon, J.-M. Towards greener and more sustainable batteries for electrical energy storage. *Nat. Chem.* **2015**, *7*, 19−29.
(113) Pichert, D.; Katsikopoulos, K. V. Green defaults: Information presentation and pro-environmental behaviour. *J. Environ. Psychol.* **2008**, *28*, 63−73.
(114) d'Adda, G.; Capraro, V.; Tavoni, M. Push, don't nudge: Behavioral spillovers and policy instruments. *Econ. Lett.* **2017**, *154*, 92−95.
(115) Dong, K.; Hochman, G.; Zhang, Y.; Sun, R.; Li, H.; Liao, H. CO_2 emissions, economic and population growth, and renewable energy: Empirical evidence across regions. *Energy Econ* **2018**, *75*, 180−192.
(116) Coumou, D.; Rahmstorf, S. A decade of weather extremes. *Nat. Clim. Change* **2012**, *2*, 491−496.
(117) Geissdoerfer, M.; Savaget, P.; Bocken, N. M. P.; Hultink, E. J. The Circular Economy − A new sustainability paradigm? *J. Cleaner Prod.* **2017**, *143*, 757−768.
(118) Carayannis, E. G.; Barth, T. D.; Campbell, D. F. The Quintuple Helix innovation model: global warming as a challenge and driver for innovation. *J. Innov. Entrep.* **2012**, *1*, 2.
(119) Ghisellini, P.; Cialani, C.; Ulgiati, S. A review on circular economy: the expected transition to a balanced interplay of environmental and economic systems. *J. Cleaner Prod.* **2016**, *114*, 11−32.
(120) Norhasyima, R. S.; Mahlia, T. M. I. Advances in CO_2 utilization technology: A patent landscape review. *J. CO2 Util.* **2018**, *26*, 323−335.
(121) Chu, S.; Majumdar, A. Opportunities and challenges for a sustainable energy future. *Nature* **2012**, *488*, 294−303.
(122) Liserre, M.; Sauter, T.; Hung, J. Future Energy Systems: Integrating Renewable Energy Sources into the Smart Power Grid Through Industrial Electronics. *IEEE Ind. Electron. Mag.* **2010**, *4*, 18−37.
(123) European Directive 2009/28/EC - https://eur-lex.europa.eu/legal-content/EN/ALL/?uri=celex%3A32009L0028, last accessed June 2019.
(124) Decarbonization Wedges - ANCRE report 2015, Available https://www.allianceenergie.fr/wp-content/uploads/2017/06/Decarbonization_Wedges_report_0.pdf, last accessed June 2019.
(125) Deep Decarbonization Pathways Project (DDPP). Available http://deepdecarbonization.org/, last accessed June 2019.
(126) Mathy, S.; Menanteau, P.; Criqui, P. After the Paris Agreement: Measuring the Global Decarbonization Wedges From National Energy Scenarios. *Ecol. Econ.* **2018**, *150*, 273−289.
(127) Aghaei, J.; Alizadeh, M.-I. Demand response in smart electricity grids equipped with renewable energy sources: A review. *Renewable Sustainable Energy Rev.* **2013**, *18*, 64−72.
(128) Gelazanskas, L.; Gamage, K. A. A. Demand side management in smart grid: A review and proposals for future direction. *Sustain. Cities Soc.* **2014**, *11*, 22−30.
(129) Bedi, G.; Venayagamoorthy, G. K.; Singh, R.; Brooks, R. R.; Wang, K.-C. Review of Internet of Things (IoT) in Electric Power and Energy Systems. *IEEE Internet Things J.* **2018**, *5*, 847−870.
(130) Dunn, B.; Kamath, H.; Tarascon, J.-M. Electrical Energy Storage for the Grid: A Battery of Choices. *Science* **2011**, *334*, 928−935.
(131) Zhang, C.; Wei, Y.-L.; Cao, P.-F.; Lin, M.-C. Energy storage system: Current studies on batteries and power condition system. *Renewable Sustainable Energy Rev.* **2018**, *82*, 3091−3106.
(132) Ceci, B. R.; Pinheiro Bernardon, D.; Canha, L. N.; Santana, T. Technology Roadmap Storage: Energy Storage Perspectives. In *Proceedings of the 2018 53rd International Universities Power Engineering Conference (UPEC)*; IEEE: Glasgow, 2018; pp 1−6.
(133) Lithium-Ion Battery Costs and Market - Claire Curry for Bloomberg New Energy Finance, Available https://data.bloomberglp.com/bnef/sites/14/2017/07/BNEF-Lithium-ion-battery-costs-and-market.pdf, last accessed June 2019.
(134) Fialka, J. *World's Largest Storage Battery Will Power Los Angeles*; 2016.
(135) Dubarry, M.; Devie, A.; Stein, K.; Tun, M.; Matsuura, M.; Rocheleau, R. Battery Energy Storage System battery durability and reliability under electric utility grid operations: Analysis of 3 years of real usage. *J. Power Sources* **2017**, *338*, 65−73.
(136) Darling, R. M.; Gallagher, K. G.; Kowalski, J. A.; Ha, S.; Brushett, F. R. Pathways to low-cost electrochemical energy storage: a comparison of aqueous and nonaqueous flow batteries. *Energy Environ. Sci.* **2014**, *7*, 3459−3477.
(137) Pawel, I. The Cost of Storage − How to Calculate the Levelized Cost of Stored Energy (LCOE) and Applications to Renewable Energy Generation. *Energy Procedia* **2014**, *46*, 68−77.
(138) Liang, F.-Y.; Ryvak, M.; Sayeed, S.; Zhao, N. The role of natural gas as a primary fuel in the near future, including comparisons of acquisition, transmission and waste handling costs of as with competitive alternatives. *Chem. Cent. J.* **2012**, *6*, S4.
(139) Sims, R.; Schaeffer, R.; Creutzig, F.; Cruz-Núñez, X.; D'Agosto, M.; Dimitriu, D.; Figueroa Meza, M. J.; Fulton, L.; Kobayashi, S.; Lah, O.; McKinnon, A.; Newman, P.; Ouyang, M.; Schauer, J. J.; Sperling, D.; Tiwari, G. Transport. In *Climate Change 2014: Mitigation of Climate Change. Contribution of Working Group III to the Fifth Assessment Report of the Intergovernmental Panel on Climate Change*; Edenhofer, O., Pichs-Madruga, R., Sokona, Y., Farahani, E., Kadner, S., Seyboth, K., Adler, A., Baum, I., Brunner, S., Eickemeier, P., Kriemann, B., Savolainen, J., Schlömer, S., von Stechow, C., Zwickel, T., Minx, J. C., Eds.; Cambridge University Press: Cambridge, United Kingdom and New York, NY, USA, 2014.
(140) International Organization of Motor Vehicle Manufacturers. All Vehicles in Use (2005−2015). Available http://www.oica.net/wp-content/uploads//Total_in-use-All-Vehicles.pdf, last accessed June 2019.
(141) Lo, P. L.; Martini, G.; Porta, F.; Scotti, D. The determinants of CO_2 emissions of air transport passenger traffic: An analysis of

https://dx.doi.org/10.1021/acs.chemrev.9b00482
Chem. Rev. 2020, 120, 6490−6557

Lombardy (Italy). *Transp. Policy* **2018**, DOI: 10.1016/j.tranpol.2018.11.010
(142) Parker, D. The ascendency of electric motive power as a gradual replacement for the internal combustion engine (ICE), 'Ockham's Electric Razor. *Int. J. Environ. Stud.* **2018**, *75*, 532−536.
(143) IEA (2018), Global EV Outlook, Available https://www.iea.org/gevo2018. All rights reserved. Last accessed June 2019.
(144) IEA (2010), Electric and Plug-in Hybrid Vehicle Roadmap, Available https://www.iea.org/reports/technology-roadmap-electric-and-plug-in-hybrid-electric-vehicles. All rights reserved. Last accessed June 2019.
(145) Saritas, O.; Meissner, D.; Sokolov, A. A Transition Management Roadmap for Fuel Cell Electric Vehicles (FCEVs). *J. Knowl. Econ.* **2019**.*10*1183
(146) Hache, E.; Seck, G. S.; Simoen, M.; Bonnet, C.; Carcanague, S. Critical raw materials and transportation sector electrification: A detailed bottom-up analysis in world transport. *Appl. Energy* **2019**, *240*, 6−25.
(147) Zawieska, J.; Pieriegud, J. Smart city as a tool for sustainable mobility and transport decarbonisation. *Transp. Policy* **2018**, *63*, 39−50.
(148) Galetovic, A.; Haber, S.; Zaretzki, L. An estimate of the average cumulative royalty yield in the world mobile phone industry: Theory, measurement and results. *Telecommun. Policy* **2018**, *42*, 263−276.
(149) Madakam, S.; Ramaswamy, R.; Tripathi, S. Internet of Things (IoT): A Literature Review. *J. Comput. Commun.* **2015**, *03*, 164−173.
(150) Xu, L. D.; He, W.; Li, S. Internet of Things in Industries: A Survey. *IEEE Trans. Ind. Inform.* **2014**, *10*, 2233−2243.
(151) https://theshiftproject.org/en/article/lean-ict-our-new-report/, last accessed June 2019.
(152) Yang, G.-Z.; Bellingham, J.; Dupont, P. E.; Fischer, P.; Floridi, L.; Full, R.; Jacobstein, N.; Kumar, V.; McNutt, M.; Merrifield, R.; et al. The grand challenges of Science Robotics. *Sci. Robot.* **2018**, *3*, eaar7650.
(153) Executive Summary World Robotics 2018 Service Robots - https://ifr.org/downloads/press2018/Executive%20Summary%20WR%202019%20Industrial%20Robots.pdf, last accessed June 2019.
(154) Vaalma, C.; Buchholz, D.; Weil, M.; Passerini, S. A cost and resource analysis of sodium-ion batteries. *Nat. Rev. Mater.* **2018**, *3*, DOI: 10.1038/natrevmats.2018.13
(155) Mayyas, A.; Steward, D.; Mann, M. The case for recycling: Overview and challenges in the material supply chain for automotive Li-ion batteries. *Sustain. Mater. Technol.* **2019**, *19*, e00087.
(156) https://www.bloomberg.com/news/articles/2018-11-19/evs-set-to-become-the-biggest-battery-users, last accessed June 2019.
(157) Some Geopolitical Issues of the Energy Transition, Available https://www.iris-france.org/notes/some-geopolitical-issues-of-the-energy-transition-2/, last accessed June 2019.
(158) Missemer, A. William Stanley Jevons' The Coal Question (1865), beyond the rebound effect. *Ecol. Econ.* **2012**, *82*, 97−103.
(159) Font Vivanco, D.; Kemp, R.; van der Voet, E. How to deal with the rebound effect? A policy-oriented approach. *Energy Policy* **2016**, *94*, 114−125.
(160) Graedel, T. E. On the Future Availability of the Energy Metals. *Annu. Rev. Mater. Res.* **2011**, *41*, 323−335.
(161) Zhang, S.; Ding, Y.; Liu, B.; Chang, C. Supply and demand of some critical metals and present status of their recycling in WEEE. *Waste Manage.* **2017**, *65*, 113−127.
(162) Vesborg, P. C. K.; Jaramillo, T. F. Addressing the terawatt challenge: scalability in the supply of chemical elements for renewable energy. *RSC Adv.* **2012**, *2*, 7933.
(163) Chancerel, P.; Marwede, M.; Nissen, N. F.; Lang, K.-D. Estimating the quantities of critical metals embedded in ICT and consumer equipment. *Resour. Conserv. Recycl.* **2015**, *98*, 9−18.
(164) Graedel, T. E.; Harper, E. M.; Nassar, N. T.; Nuss, P.; Reck, B. K. Criticality of metals and metalloids. *Proc. Natl. Acad. Sci. U. S. A.* **2015**, *112*, 4257−4262.
(165) Løvik, A. N.; Hagelüken, C.; Wäger, P. Improving supply security of critical metals: Current developments and research in the EU. *Sustain. Mater. Technol.* **2018**, *15*, 9−18.
(166) European Commission, Study on the Review of the List of Critical Raw Materials - https://publications.europa.eu/en/publication-detail/-/publication/08fdab5f-9766-11e7-b92d-01aa75ed71a1/language-en, (2017), last accessed June 2019.
(167) Department Of The Interior of the USA, Federal Register /Vol. *83*, No. 97/Friday, May 18, 2018, https://www.govinfo.gov/app/details/FR-2018-05-18/2018-10667, last accessed November 2019.
(168) Choi, J. W.; Aurbach, D. Promise and reality of post-lithium-ion batteries with high energy densities. *Nat. Rev. Mater.* **2016**, *1*, DOI: 10.1038/natrevmats.2016.13
(169) Kamaya, N.; Homma, K.; Yamakawa, Y.; Hirayama, M.; Kanno, R.; Yonemura, M.; Kamiyama, T.; Kato, Y.; Hama, S.; Kawamoto, K.; et al. A lithium superionic conductor. *Nat. Mater.* **2011**, *10*, 682−686.
(170) Kato, Y.; Hori, S.; Saito, T.; Suzuki, K.; Hirayama, M.; Mitsui, A.; Yonemura, M.; Iba, H.; Kanno, R. High-power all-solid-state batteries using sulfide superionic conductors. *Nat. Energy* **2016**, *1*, DOI: 10.1038/nenergy.2016.30
(171) Lei, D.; Shi, K.; Ye, H.; Wan, Z.; Wang, Y.; Shen, L.; Li, B.; Yang, Q.-H.; Kang, F.; He, Y.-B. Progress and Perspective of Solid-State Lithium-Sulfur Batteries. *Adv. Funct. Mater.* **2018**, *28*, 1707570.
(172) Richards, W. D.; Miara, L. J.; Wang, Y.; Kim, J. C.; Ceder, G. Interface Stability in Solid-State Batteries. *Chem. Mater.* **2016**, *28*, 266−273.
(173) Muñoz-Márquez, M.Á.; Saurel, D.; Gómez-Cámer, J. L.; Casas-Cabanas, M.; Castillo-Martínez, E.; Rojo, T. Na-Ion Batteries for Large Scale Applications: A Review on Anode Materials and Solid Electrolyte Interphase Formation. *Adv. Energy Mater.* **2017**, *7*, 1700463.
(174) Deng, J.; Luo, W.-B.; Chou, S.-L.; Liu, H.-K.; Dou, S.-X. Sodium-Ion Batteries: From Academic Research to Practical Commercialization. *Adv. Energy Mater.* **2018**, *8*, 1701428.
(175) Helbig, C.; Bradshaw, A. M.; Wietschel, L.; Thorenz, A.; Tuma, A. Supply risks associated with lithium-ion battery materials. *J. Cleaner Prod.* **2018**, *172*, 274−286.
(176) Tarascon, J.-M. Is lithium the new gold? *Nat. Chem.* **2010**, *2*, 510−511.
(177) Olivetti, E. A.; Ceder, G.; Gaustad, G. G.; Fu, X. Lithium-Ion Battery Supply Chain Considerations: Analysis of Potential Bottlenecks in Critical Metals. *Joule* **2017**, *1*, 229−243.
(178) Andersson, B. A.; Råde, I. Metal resource constraints for electric-vehicle batteries. *Transp. Res. Part Transp. Environ.* **2001**, *6*, 297−324.
(179) Nassar, N. T.; Graedel, T. E.; Harper, E. M. By-product metals are technologically essential but have problematic supply. *Sci. Adv.* **2015**, *1*, e1400180.
(180) Butsic, V.; Baumann, M.; Shortland, A.; Walker, S.; Kuemmerle, T. Conservation and conflict in the Democratic Republic of Congo: The impacts of warfare, mining, and protected areas on deforestation. *Biol. Conserv.* **2015**, *191*, 266−273.
(181) https://www.bloomberg.com/news/articles/2018-02-21/apple-is-said-to-negotiate-buying-cobalt-direct-from-miners, last accessed June 2019.
(182) Heelan, J.; Gratz, E.; Zheng, Z.; Wang, Q.; Chen, M.; Apelian, D.; Wang, Y. Current and Prospective Li-Ion Battery Recycling and Recovery Processes. *JOM* **2016**, *68*, 2632−2638.
(183) European Directive 2006/66/EC - https://eur-lex.europa.eu/legal-content/FR/ALL/?uri=CELEX%3A32006L0066, last accessed June 2019.
(184) *Lithium process chemistry: resources, extraction, batteries, and recycling*; Chagnes, A., Swiatowska, J., Eds.; Elsevier: Amsterdam, Boston, Heidelberg, 2015; ISBN 978-0-12-801417-2.
(185) Zhang, X.; Li, L.; Fan, E.; Xue, Q.; Bian, Y.; Wu, F.; Chen, R. Toward sustainable and systematic recycling of spent rechargeable batteries. *Chem. Soc. Rev.* **2018**, *47*, 7239−7302.

(186) Chagnes, A.; Pospiech, B. A brief review on hydrometallurgical technologies for recycling spent lithium-ion batteries: Technologies for recycling spent lithium-ion batteries. *J. Chem. Technol. Biotechnol.* **2013**, *88*, 1191−1199.
(187) Zeng, X.; Li, J.; Singh, N. Recycling of Spent Lithium-Ion Battery: A Critical Review. *Crit. Rev. Environ. Sci. Technol.* **2014**, *44*, 1129−1165.
(188) Simonin, L.; Simone, V.; Martinet, S.; Monconduit, L. Accumulateurs Na-ion : doit-on/peut-on remplacer le lithium? In *Batteries Li-ion Du présent au futur*; EDP Sciences, 2019; pp 113−134, ISBN 978-2-7598-2392-5.
(189) Haynes, W. M. Abundance of elements in the Earth's crust and in the sea. In *CRC Handbook of Chemistry and Physics*; 2026; Vol. *14*, p 18.
(190) https://nssdc.gsfc.nasa.gov/planetary/factsheet/earthfact.html, last accessed June 2019.
(191) Vassilev, S. V.; Baxter, D.; Andersen, L. K.; Vassileva, C. G. An overview of the chemical composition of biomass. *Fuel* **2010**, *89*, 913−933.
(192) Peters, J. F.; Baumann, M.; Zimmermann, B.; Braun, J.; Weil, M. The environmental impact of Li-Ion batteries and the role of key parameters − A review. *Renewable Sustainable Energy Rev.* **2017**, *67*, 491−506.
(193) Majeau-Bettez, G.; Hawkins, T. R.; Strømman, A. H. Life Cycle Environmental Assessment of Lithium-Ion and Nickel Metal Hydride Batteries for Plug-In Hybrid and Battery Electric Vehicles. *Environ. Sci. Technol.* **2011**, *45*, 4548−4554.
(194) Hiremath, M.; Derendorf, K.; Vogt, T. Comparative Life Cycle Assessment of Battery Storage Systems for Stationary Applications. *Environ. Sci. Technol.* **2015**, *49*, 4825−4833.
(195) Nordelöf, A.; Messagie, M.; Tillman, A.-M.; Ljunggren Söderman, M.; Van Mierlo, J. Environmental impacts of hybrid, plug-in hybrid, and battery electric vehicles—what can we learn from life cycle assessment? *Int. J. Life Cycle Assess.* **2014**, *19*, 1866−1890.
(196) Ellis, B. L.; Nazar, L. F. Sodium and sodium-ion energy storage batteries. *Curr. Opin. Solid State Mater. Sci.* **2012**, *16*, 168−177.
(197) Muñoz-Márquez, M.Á.; Saurel, D.; Gómez-Cámer, J. L.; Casas-Cabanas, M.; Castillo-Martínez, E.; Rojo, T. Na-Ion Batteries for Large Scale Applications: A Review on Anode Materials and Solid Electrolyte Interphase Formation. *Adv. Energy Mater.* **2017**, *7*, 1700463.
(198) Zhang, L.; Liu, Z.; Cui, G.; Chen, L. Biomass-derived materials for electrochemical energy storages. *Prog. Polym. Sci.* **2015**, *43*, 136−164.
(199) Corma, A.; Iborra, S.; Velty, A. Chemical Routes for the Transformation of Biomass into Chemicals. *Chem. Rev.* **2007**, *107*, 2411−2502.
(200) Bozell, J. J.; Petersen, G. R. Technology development for the production of biobased products from biorefinery carbohydrates—the US Department of Energy's "Top 10" revisited. *Green Chem.* **2010**, *12*, 539.
(201) Gandini, A.; Lacerda, T. M.; Carvalho, A. J. F.; Trovatti, E. Progress of Polymers from Renewable Resources: Furans, Vegetable Oils, and Polysaccharides. *Chem. Rev.* **2016**, *116*, 1637−1669.
(202) Gnedenkov, S. V.; Opra, D. P.; Sinebryukhov, S. L.; Tsvetnikov, A. K.; Ustinov, A. Y.; Sergienko, V. I. Hydrolysis lignin-based organic electrode material for primary lithium batteries. *J. Solid State Electrochem.* **2013**, *17*, 2611−2621.
(203) Milczarek, G.; Inganas, O. Renewable Cathode Materials from Biopolymer/Conjugated Polymer Interpenetrating Networks. *Science* **2012**, *335*, 1468−1471.
(204) Goriparti, S.; Harish, M. N. K.; Sampath, S. Ellagic acid − a novel organic electrode material for high capacity lithium ion batteries. *Chem. Commun.* **2013**, *49*, 7234.
(205) Reddy, A. L. M.; Nagarajan, S.; Chumyim, P.; Gowda, S. R.; Pradhan, P.; Jadhav, S. R.; Dubey, M.; John, G.; Ajayan, P. M. Lithium storage mechanisms in purpurin based organic lithium ion battery electrodes. *Sci. Rep.* **2012**, *2*, DOI: 10.1038/srep00960
(206) Miroshnikov, M.; Kato, K.; Babu, G.; Divya, K. P.; Reddy Arava, L. M.; Ajayan, P. M.; John, G. A common tattoo chemical for energy storage: henna plant-derived naphthoquinone dimer as a green and sustainable cathode material for Li-ion batteries. *RSC Adv.* **2018**, *8*, 1576−1582.
(207) Esquivel, J. P.; Alday, P.; Ibrahim, O. A.; Fernández, B.; Kjeang, E.; Sabaté, N. A Metal-Free and Biotically Degradable Battery for Portable Single-Use Applications. *Adv. Energy Mater.* **2017**, *7*, 1700275.
(208) Renault, S.; Gottis, S.; Barrès, A.-L.; Courty, M.; Chauvet, O.; Dolhem, F.; Poizot, P. A green Li−organic battery working as a fuel cell in case of emergency. *Energy Environ. Sci.* **2013**, *6*, 2124.
(209) Godet-Bar, T.; Leprêtre, J.-C.; Poizot, P.; Massuyeau, F.; Faulques, E.; Christen, A.; Minassian, F.; Poisson, J.-F.; Loiseau, F.; Lafolet, F. Light assisted rechargeable batteries: a proof of concept with BODIPY derivatives acting as a combined photosensitizer and electrical storage unit. *J. Mater. Chem. A* **2017**, *5*, 1902−1905.
(210) Li, W.; Kerr, E.; Goulet, M.; Fu, H.; Zhao, Y.; Yang, Y.; Veyssal, A.; He, J.; Gordon, R. G.; Aziz, M. J.; et al. A Long Lifetime Aqueous Organic Solar Flow Battery. *Adv. Energy Mater.* **2019**, *9*, 1900918.
(211) Zhu, X.-Q.; Wang, C.-H. Accurate Estimation of the One-Electron Reduction Potentials of Various Substituted Quinones in DMSO and CH_3CN. *J. Org. Chem.* **2010**, *75*, 5037−5047.
(212) Suga, T.; Sugita, S.; Ohshiro, H.; Oyaizu, K.; Nishide, H. p- and n-Type Bipolar Redox-Active Radical Polymer: Toward Totally Organic Polymer-Based Rechargeable Devices with Variable Configuration. *Adv. Mater.* **2011**, *23*, 751−754.
(213) Yao, M.; Sano, H.; Ando, H.; Kiyobayashi, T. Molecular ion battery: a rechargeable system without using any elemental ions as a charge carrier. *Sci. Rep.* **2015**, *5*, DOI: 10.1038/srep10962
(214) Tong, L.; Jing, Y.; Gordon, R. G.; Aziz, M. J. Symmetric All-Quinone Aqueous Battery. *ACS Appl. Energy Mater.* **2019**, *2*, 4016−4021.
(215) Jensen, W. B. The Origin of the Oxidation-State Concept. *J. Chem. Educ.* **2007**, *84*, 1418.
(216) Karen, P.; McArdle, P.; Takats, J. Toward a comprehensive definition of oxidation state (IUPAC Technical Report). *Pure Appl. Chem.* **2014**, *86*, 1017−1081.
(217) Walsh, A.; Sokol, A. A.; Buckeridge, J.; Scanlon, D. O.; Catlow, C. R. A. Oxidation states and ionicity. *Nat. Mater.* **2018**, *17*, 958−964.
(218) Klemm, L. H. A classification of organic redox reactions and writing balanced equations for them, with special attention to heteroatoms and heterocyclic compounds. *J. Heterocycl. Chem.* **1996**, *33*, 569−574.
(219) Deuchert, K.; Hünig, S. Multistage Organic Redox Systems—A General Structural Principle. *Angew. Chem., Int. Ed. Engl.* **1978**, *17*, 875−886.
(220) Nishinaga, T.; Komatsu, K. Persistent ? radical cations: self-association and its steric control in the condensed phase. *Org. Biomol. Chem.* **2005**, *3*, 561.
(221) *Stable radicals: fundamentals and applied aspects of odd-electron compounds*; Hicks, R. G., Ed.; Wiley: Chichester, 2010; ISBN 978-0-470-77083-2.
(222) Brenner, A. Note on an Organic-Electrolyte Cell with a High Voltage. *J. Electrochem. Soc.* **1971**, *118*, 461.
(223) Besenhard, J. O.; Fritz, H. P. The Electrochemistry of Black Carbons. *Angew. Chem., Int. Ed. Engl.* **1983**, *22*, 950−975.
(224) Guérard, D.; Fuzellier, H. The Graphite Intercalation Compounds and their Applications. In *Condensed Systems of Low Dimensionality*; Beeby, J. L., Bhattacharya, P. K., Gravelle, P.Ch., Koch, F., Lockwood, D. J., Eds.; Springer US: Boston, MA, 1991; Vol. *253*, pp 695−707, ISBN 978-1-4684-1350-2.
(225) Rothermel, S.; Meister, P.; Schmuelling, G.; Fromm, O.; Meyer, H.-W.; Nowak, S.; Winter, M.; Placke, T. Dual-graphite cells based on the reversible intercalation of bis(trifluoromethanesulfonyl)-imide anions from an ionic liquid electrolyte. *Energy Environ. Sci.* **2014**, *7*, 3412−3423.

(226) Mohammad, I.; Witter, R.; Fichtner, M.; Anji Reddy, M. Room-Temperature, Rechargeable Solid-State Fluoride-Ion Batteries. *ACS Appl. Energy Mater.* **2018**, *1*, 4766−4775.
(227) Yao, M.; Sano, H.; Ando, H.; Kiyobayashi, T. Molecular ion battery: a rechargeable system without using any elemental ions as a charge carrier. *Sci. Rep.* **2015**, *5*, 10962.
(228) Jouhara, A.; Quarez, E.; Dolhem, F.; Armand, M.; Dupré, N.; Poizot, P. Tuning the Chemistry of Organonitrogen Compounds for Promoting All-Organic Anionic Rechargeable Batteries. *Angew. Chem., Int. Ed.* **2019**, *58*, 15680−15684.
(229) Zhou, X.; Liu, Q.; Jiang, C.; Ji, B.; Ji, X.; Tang, Y.; Cheng, H.-M. Beyond Conventional Batteries: Strategies towards Low-Cost Dual-Ion Batteries with High Performance. *Angew. Chem., Int. Ed.* **2019**.
(230) Perticarari, S.; Sayed-Ahmad-Baraza, Y.; Ewels, C.; Moreau, P.; Guyomard, D.; Poizot, P.; Odobel, F.; Gaubicher, J. Dual Anion−Cation Reversible Insertion in a Bipyridinium−Diamide Triad as the Negative Electrode for Aqueous Batteries. *Adv. Energy Mater.* **2018**, *8*, 1701988.
(231) Perticarari, S.; Doizy, T.; Soudan, P.; Ewels, C.; Latouche, C.; Guyomard, D.; Odobel, F.; Poizot, P.; Gaubicher, J. Intermixed Cation−Anion Aqueous Battery Based on an Extremely Fast and Long-Cycling Di-Block Bipyridinium−Naphthalene Diimide Oligomer. *Adv. Energy Mater.* **2019**, *9*, 1803688.
(232) Perticarari, S.; Grange, E.; Doizy, T.; Pellegrin, Y.; Quarez, E.; Oyaizu, K.; Fernandez-Ropero, A. J.; Guyomard, D.; Poizot, P.; Odobel, F.; et al. Full Organic Aqueous Battery Based on TEMPO Small Molecule with Millimeter-Thick Electrodes. *Chem. Mater.* **2019**, *31*, 1869−1880.
(233) Chae, I. S.; Koyano, M.; Oyaizu, K.; Nishide, H. Self-doping inspired zwitterionic pendant design of radical polymers toward a rocking-chair-type organic cathode-active material. *J. Mater. Chem. A* **2013**, *1*, 1326−1333.
(234) Gottis, S.; Barrès, A.-L.; Dolhem, F.; Poizot, P. Voltage Gain in Lithiated Enolate-Based Organic Cathode Materials by Isomeric Effect. *ACS Appl. Mater. Interfaces* **2014**, *6*, 10870−10876.
(235) Rodríguez-Pérez, I. A.; Jian, Z.; Waldenmaier, P. K.; Palmisano, J. W.; Chandrabose, R. S.; Wang, X.; Lerner, M. M.; Carter, R. G.; Ji, X. A Hydrocarbon Cathode for Dual-Ion Batteries. *ACS Energy Lett.* **2016**, *1*, 719−723.
(236) Kim, J.-K.; Thébault, F.; Heo, M.-Y.; Kim, D.-S.; Hansson, Ö.; Ahn, J.-H.; Johansson, P.; Öhrström, L.; Matic, A.; Jacobsson, P. 2,3,6,7,10,11-Hexamethoxytriphenylene (HMTP): A new organic cathode material for lithium batteries. *Electrochem. Commun.* **2012**, *21*, 50−53.
(237) Inatomi, Y.; Hojo, N.; Yamamoto, T.; Watanabe, S.; Misaki, Y. Construction of Rechargeable Batteries Using Multifused Tetrathiafulvalene Systems as Cathode Materials. *ChemPlusChem* **2012**, *77*, 973−976.
(238) Kato, M.; Senoo, K.; Yao, M.; Misaki, Y. A pentakis-fused tetrathiafulvalene system extended by cyclohexene-1,4-diylidenes: a new positive electrode material for rechargeable batteries utilizing ten electron redox. *J. Mater. Chem. A* **2014**, *2*, 6747.
(239) Bugnon, L.; Morton, C. J. H.; Novak, P.; Vetter, J.; Nesvadba, P. Synthesis of Poly(4-methacryloyloxy-TEMPO) via Group-Transfer Polymerization and Its Evaluation in Organic Radical Battery. *Chem. Mater.* **2007**, *19*, 2910−2914.
(240) Oyaizu, K.; Kawamoto, T.; Suga, T.; Nishide, H. Synthesis and Charge Transport Properties of Redox-Active Nitroxide Polyethers with Large Site Density. *Macromolecules* **2010**, *43*, 10382−10389.
(241) Lee, S.; Hong, J.; Jung, S.-K.; Ku, K.; Kwon, G.; Seong, W. M.; Kim, H.; Yoon, G.; Kang, I.; Hong, K.; et al. Charge-transfer complexes for high-power organic rechargeable batteries. *Energy Storage Mater.* **2019**, *20*, 462−469.
(242) Zhang, C.; Yang, X.; Ren, W.; Wang, Y.; Su, F.; Jiang, J.-X. Microporous organic polymer-based lithium ion batteries with improved rate performance and energy density. *J. Power Sources* **2016**, *317*, 49−56.
(243) Deunf, É.; Jiménez, P.; Guyomard, D.; Dolhem, F.; Poizot, P. A dual−ion battery using diamino−rubicene as anion−inserting positive electrode material. *Electrochem. Commun.* **2016**, *72*, 64−68.
(244) Lee, M.; Hong, J.; Lee, B.; Ku, K.; Lee, S.; Park, C. B.; Kang, K. Multi-electron redox phenazine for ready-to-charge organic batteries. *Green Chem.* **2017**, *19*, 2980−2985.
(245) Deunf, É.; Moreau, P.; Quarez, É.; Guyomard, D.; Dolhem, F.; Poizot, P. Reversible anion intercalation in a layered aromatic amine: a high-voltage host structure for organic batteries. *J. Mater. Chem. A* **2016**, *4*, 6131−6139.
(246) Song, Z.; Qian, Y.; Zhang, T.; Otani, M.; Zhou, H. Poly(benzoquinonyl sulfide) as a High-Energy Organic Cathode for Rechargeable Li and Na Batteries. *Adv. Sci.* **2015**, *2*, 1500124.
(247) Yokoji, T.; Kameyama, Y.; Maruyama, N.; Matsubara, H. High-capacity organic cathode active materials of 2,2′-bis-p-benzoquinone derivatives for rechargeable batteries. *J. Mater. Chem. A* **2016**, *4*, 5457−5466.
(248) Wu, D.; Xie, Z.; Zhou, Z.; Shen, P.; Chen, Z. Designing high-voltage carbonyl-containing polycyclic aromatic hydrocarbon cathode materials for Li-ion batteries guided by Clar's theory. *J. Mater. Chem. A* **2015**, *3*, 19137−19143.
(249) Song, Z.; Qian, Y.; Liu, X.; Zhang, T.; Zhu, Y.; Yu, H.; Otani, M.; Zhou, H. A quinone-based oligomeric lithium salt for superior Li−organic batteries. *Energy Environ. Sci.* **2014**, *7*, 4077−4086.
(250) Yokoji, T.; Matsubara, H.; Satoh, M. Rechargeable organic lithium-ion batteries using electron-deficient benzoquinones as positive-electrode materials with high discharge voltages. *J. Mater. Chem. A* **2014**, *2*, 19347−19354.
(251) Wang, S.; Wang, L.; Zhang, K.; Zhu, Z.; Tao, Z.; Chen, J. Organic $Li_4C_8H_2O_6$ Nanosheets for Lithium-Ion Batteries. *Nano Lett.* **2013**, *13*, 4404−4409.
(252) Jouhara, A.; Dupré, N.; Gaillot, A.-C.; Guyomard, D.; Dolhem, F.; Poizot, P. Raising the redox potential in carboxyphenolate-based positive organic materials via cation substitution. *Nat. Commun.* **2018**, *9*, DOI: 10.1038/s41467-018-06708-x
(253) Lakraychi, A. E.; Deunf, E.; Fahsi, K.; Jimenez, P.; Bonnet, J.-P.; Djedaini-Pilard, F.; Bécuwe, M.; Poizot, P.; Dolhem, F. An air-stable lithiated cathode material based on a 1,4-benzenedisulfonate backbone for organic Li-ion batteries. *J. Mater. Chem. A* **2018**, *6*, 19182−19189.
(254) Hanyu, Y.; Honma, I. Rechargeable quasi-solid state lithium battery with organic crystalline cathode. *Sci. Rep.* **2012**, *2*, DOI: 10.1038/srep00453
(255) Nishida, S.; Yamamoto, Y.; Takui, T.; Morita, Y. Organic Rechargeable Batteries with Tailored Voltage and Cycle Performance. *ChemSusChem* **2013**, *6*, 794−797.
(256) Shimizu, A.; Tsujii, Y.; Kuramoto, H.; Nokami, T.; Inatomi, Y.; Hojo, N.; Yoshida, J. Nitrogen-Containing Polycyclic Quinones as Cathode Materials for Lithium-ion Batteries with Increased Voltage. *Energy Technol.* **2014**, *2*, 155−158.
(257) Liang, Y.; Zhang, P.; Chen, J. Function-oriented design of conjugated carbonyl compound electrodes for high energy lithium batteries. *Chem. Sci.* **2013**, *4*, 1330.
(258) Liang, Y.; Zhang, P.; Yang, S.; Tao, Z.; Chen, J. Fused Heteroaromatic Organic Compounds for High-Power Electrodes of Rechargeable Lithium Batteries. *Adv. Energy Mater.* **2013**, *3*, 600−605.
(259) Levi, M. D.; Aurbach, D. A short review on the strategy towards development of π-conjugated polymers with highly reversible p- and n-doping. *J. Power Sources* **2008**, *180*, 902−908.
(260) Renault, S.; Oltean, V. A.; Araujo, C. M.; Grigoriev, A.; Edström, K.; Brandell, D. Superlithiation of Organic Electrode Materials: The Case of Dilithium Benzenedipropiolate. *Chem. Mater.* **2016**, *28*, 1920−1926.
(261) Armand, M.; Grugeon, S.; Vezin, H.; Laruelle, S.; Ribière, P.; Poizot, P.; Tarascon, J.-M. Conjugated dicarboxylate anodes for Li-ion batteries. *Nat. Mater.* **2009**, *8*, 120−125.
(262) Lakraychi, A. E.; Dolhem, F.; Djedaïni-Pilard, F.; Thiam, A.; Frayret, C.; Becuwe, M. Decreasing redox voltage of terephthalate-

based electrode material for Li-ion battery using substituent effect. *J. Power Sources* **2017**, *359*, 198−204.
(263) Lakraychi, A. E.; Dolhem, F.; Djedaïni-Pilard, F.; Becuwe, M. Substituent effect on redox potential of terephthalate-based electrode materials for lithium batteries. *Electrochem. Commun.* **2018**, *93*, 71−75.
(264) Fédèle, L.; Sauvage, F.; Gottis, S.; Davoisne, C.; Salager, E.; Chotard, J.-N.; Becuwe, M. 2D-Layered Lithium Carboxylate Based on Biphenyl Core as Negative Electrode for Organic Lithium-Ion Batteries. *Chem. Mater.* **2017**, *29*, 546−554.
(265) Walker, W.; Grugeon, S.; Vezin, H.; Laruelle, S.; Armand, M.; Wudl, F.; Tarascon, J.-M. Electrochemical characterization of lithium 4,4′-tolane-dicarboxylate for use as a negative electrode in Li-ion batteries. *J. Mater. Chem.* **2011**, *21*, 1615−1620.
(266) Chung, W. J.; Griebel, J. J.; Kim, E. T.; Yoon, H.; Simmonds, A. G.; Ji, H. J.; Dirlam, P. T.; Glass, R. S.; Wie, J. J.; Nguyen, N. A.; et al. The use of elemental sulfur as an alternative feedstock for polymeric materials. *Nat. Chem.* **2013**, *5*, 518−524.
(267) Wang, J.; Yang, J.; Xie, J.; Xu, N. A Novel Conductive Polymer-Sulfur Composite Cathode Material for Rechargeable Lithium Batteries. *Adv. Mater.* **2002**, *14*, 963−965.
(268) Wei, S.; Ma, L.; Hendrickson, K. E.; Tu, Z.; Archer, L. A. Metal−Sulfur Battery Cathodes Based on PAN−Sulfur Composites. *J. Am. Chem. Soc.* **2015**, *137*, 12143−12152.
(269) Lu, Y.; Hou, X.; Miao, L.; Li, L.; Shi, R.; Liu, L.; Chen, J. Cyclohexanehexone with Ultrahigh Capacity as Cathode Materials for Lithium-Ion Batteries. *Angew. Chem., Int. Ed.* **2019**, *58*, 7020−7024.
(270) Yao, M.; Senoh, H.; Yamazaki, S.; Siroma, Z.; Sakai, T.; Yasuda, K. High-capacity organic positive-electrode material based on a benzoquinone derivative for use in rechargeable lithium batteries. *J. Power Sources* **2010**, *195*, 8336−8340.
(271) Lee, J.; Park, M. J. Tattooing Dye as a Green Electrode Material for Lithium Batteries. *Adv. Energy Mater.* **2017**, *7*, 1602279.
(272) Huang, W.; Zhu, Z.; Wang, L.; Wang, S.; Li, H.; Tao, Z.; Shi, J.; Guan, L.; Chen, J. Quasi-Solid-State Rechargeable Lithium-Ion Batteries with a Calix[4]quinone Cathode and Gel Polymer Electrolyte. *Angew. Chem., Int. Ed.* **2013**, *52*, 9162−9166.
(273) Zhu, Z.; Hong, M.; Guo, D.; Shi, J.; Tao, Z.; Chen, J. All-Solid-State Lithium Organic Battery with Composite Polymer Electrolyte and Pillar[5]quinone Cathode. *J. Am. Chem. Soc.* **2014**, *136*, 16461−16464.
(274) Liu, K.; Zheng, J.; Zhong, G.; Yang, Y. Poly(2,5-dihydroxy-1,4-benzoquinonyl sulfide) (PDBS) as a cathode material for lithium ion batteries. *J. Mater. Chem.* **2011**, *21*, 4125.
(275) Song, Z.; Qian, Y.; Gordin, M. L.; Tang, D.; Xu, T.; Otani, M.; Zhan, H.; Zhou, H.; Wang, D. Polyanthraquinone as a Reliable Organic Electrode for Stable and Fast Lithium Storage. *Angew. Chem., Int. Ed.* **2015**, *54*, 13947−13951.
(276) Petronico, A.; Bassett, K. L.; Nicolau, B. G.; Gewirth, A. A.; Nuzzo, R. G. Toward a Four-Electron Redox Quinone Polymer for High Capacity Lithium Ion Storage. *Adv. Energy Mater.* **2018**, *8*, 1700960.
(277) Peng, C.; Ning, G.-H.; Su, J.; Zhong, G.; Tang, W.; Tian, B.; Su, C.; Yu, D.; Zu, L.; Yang, J.; et al. Reversible multi-electron redox chemistry of π-conjugated N-containing heteroaromatic molecule-based organic cathodes. *Nat. Energy* **2017**, *2*, DOI: 10.1038/nenergy.2017.74
(278) Hanyu, Y.; Sugimoto, T.; Ganbe, Y.; Masuda, A.; Honma, I. Multielectron Redox Compounds for Organic Cathode Quasi-Solid State Lithium Battery. *J. Electrochem. Soc.* **2014**, *161*, A6−A9.
(279) Guo, W.; Yin, Y.-X.; Xin, S.; Guo, Y.-G.; Wan, L.-J. Superior radical polymer cathode material with a two-electron process redox reaction promoted by graphene. *Energy Environ. Sci.* **2012**, *5*, 5221−5225.
(280) Kolek, M.; Otteny, F.; Schmidt, P.; Mück-Lichtenfeld, C.; Einholz, C.; Becking, J.; Schleicher, E.; Winter, M.; Bieker, P.; Esser, B. Ultra-high cycling stability of poly(vinylphenothiazine) as a battery cathode material resulting from π−π interactions. *Energy Environ. Sci.* **2017**, *10*, 2334−2341.
(281) Liang, Y.; Chen, Z.; Jing, Y.; Rong, Y.; Facchetti, A.; Yao, Y. Heavily n-Dopable π-Conjugated Redox Polymers with Ultrafast Energy Storage Capability. *J. Am. Chem. Soc.* **2015**, *137*, 4956−4959.
(282) Fan, X.; Wang, F.; Ji, X.; Wang, R.; Gao, T.; Hou, S.; Chen, J.; Deng, T.; Li, X.; Chen, L.; et al. A Universal Organic Cathode for Ultrafast Lithium and Multivalent Metal Batteries. *Angew. Chem., Int. Ed.* **2018**, *57*, 7146−7150.
(283) Wang, S.; Wang, Q.; Shao, P.; Han, Y.; Gao, X.; Ma, L.; Yuan, S.; Ma, X.; Zhou, J.; Feng, X.; et al. Exfoliation of Covalent Organic Frameworks into Few-Layer Redox-Active Nanosheets as Cathode Materials for Lithium-Ion Batteries. *J. Am. Chem. Soc.* **2017**, *139*, 4258−4261.
(284) Schon, T. B.; Tilley, A. J.; Kynaston, E. L.; Seferos, D. S. Three-Dimensional Arylene Diimide Frameworks for Highly Stable Lithium Ion Batteries. *ACS Appl. Mater. Interfaces* **2017**, *9*, 15631−15637.
(285) Chen, D.; Avestro, A.-J.; Chen, Z.; Sun, J.; Wang, S.; Xiao, M.; Erno, Z.; Algaradah, M. M.; Nassar, M. S.; Amine, K.; et al. A Rigid Naphthalenediimide Triangle for Organic Rechargeable Lithium-Ion Batteries. *Adv. Mater.* **2015**, *27*, 2907−2912.
(286) Bhosale, M. E.; Krishnamoorthy, K. Chemically Reduced Organic Small-Molecule-Based Lithium Battery with Improved Efficiency. *Chem. Mater.* **2015**, *27*, 2121−2126.
(287) Luo, Z.; Liu, L.; Zhao, Q.; Li, F.; Chen, J. An Insoluble Benzoquinone-Based Organic Cathode for Use in Rechargeable Lithium-Ion Batteries. *Angew. Chem., Int. Ed.* **2017**, *56*, 12561−12565.
(288) Jing, Y.; Liang, Y.; Gheytani, S.; Yao, Y. Cross-conjugated oligomeric quinones for high performance organic batteries. *Nano Energy* **2017**, *37*, 46−52.
(289) Luo, C.; Ji, X.; Hou, S.; Eidson, N.; Fan, X.; Liang, Y.; Deng, T.; Jiang, J.; Wang, C. Azo Compounds Derived from Electrochemical Reduction of Nitro Compounds for High Performance Li-Ion Batteries. *Adv. Mater.* **2018**, *30*, 1706498.
(290) Lee, J.; Kim, H.; Park, M. J. Long-Life, High-Rate Lithium-Organic Batteries Based on Naphthoquinone Derivatives. *Chem. Mater.* **2016**, *28*, 2408−2416.
(291) Bachman, J. C.; Kavian, R.; Graham, D. J.; Kim, D. Y.; Noda, S.; Nocera, D. G.; Shao-Horn, Y.; Lee, S. W. Electrochemical polymerization of pyrene derivatives on functionalized carbon nanotubes for pseudocapacitive electrodes. *Nat. Commun.* **2015**, *6*, DOI: 10.1038/ncomms8040
(292) Shinozaki, K.; Tomizuka, Y.; Nojiri, A. Performance of Lithium/Polyacetylene Cell. *Jpn. J. Appl. Phys.* **1984**, *23*, L892−L894.
(293) Dai, Y.; Zhang, Y.; Gao, L.; Xu, G.; Xie, J. A Sodium Ion Based Organic Radical Battery. *Electrochem. Solid-State Lett.* **2010**, *13*, A22−A24.
(294) Zhao, L.; Zhao, J.; Hu, Y.-S.; Li, H.; Zhou, Z.; Armand, M.; Chen, L. Disodium Terephthalate ($Na_2C_8H_4O_4$) as High Performance Anode Material for Low-Cost Room-Temperature Sodium-Ion Battery. *Adv. Energy Mater.* **2012**, *2*, 962−965.
(295) Park, Y.; Shin, D.-S.; Woo, S. H.; Choi, N. S.; Shin, K. H.; Oh, S. M.; Lee, K. T.; Hong, S. Y. Sodium Terephthalate as an Organic Anode Material for Sodium Ion Batteries. *Adv. Mater.* **2012**, *24*, 3562−3567.
(296) Abouimrane, A.; Weng, W.; Eltayeb, H.; Cui, Y.; Niklas, J.; Poluektov, O.; Amine, K. Sodium insertion in carboxylate based materials and their application in 3.6 V full sodium cells. *Energy Environ. Sci.* **2012**, *5*, 9632−9638.
(297) Wan, F.; Wu, X.-L.; Guo, J.-Z.; Li, J.-Y.; Zhang, J.-P.; Niu, L.; Wang, R.-S. Nanoeffects promote the electrochemical properties of organic $Na_2C_8H_4O_4$ as anode material for sodium-ion batteries. *Nano Energy* **2015**, *13*, 450−457.
(298) Wang, Y.; Kretschmer, K.; Zhang, J.; Mondal, A. K.; Guo, X.; Wang, G. Organic sodium terephthalate@graphene hybrid anode materials for sodium-ion batteries. *RSC Adv.* **2016**, *6*, 57098−57102.
(299) Han, S.; Kim, Y.; Pyo, M. Reduced Graphene Oxide/Disodium Terephthalate Composites via Ultrasonic-assisted Co-Precipitation for Sodium Ion Battery Anodes. *Bull. Korean Chem. Soc.* **2016**, *37*, 1838−1845.

(300) Deng, Q.; Wang, Y.; Zhao, Y.; Li, J. Disodium terephthalate/multiwall-carbon nanotube nanocomposite as advanced anode material for Li-ion batteries. *Ionics* **2017**, *23*, 2613−2619.
(301) Cao, T.; Lv, W.; Zhang, S.-W.; Zhang, J.; Lin, Q.; Chen, X.; He, Y.; Kang, F.-Y.; Yang, Q.-H. A Reduced Graphene Oxide/Disodium Terephthalate Hybrid as a High-Performance Anode for Sodium-Ion Batteries. *Chem. - Eur. J.* **2017**, *23*, 16586−16592.
(302) Zhao, Q.; Lu, Y.; Chen, J. Advanced Organic Electrode Materials for Rechargeable Sodium-Ion Batteries. *Adv. Energy Mater.* **2017**, *7*, 1601792.
(303) Zhao, R.; Zhu, L.; Cao, Y.; Ai, X.; Yang, H. X. An aniline-nitroaniline copolymer as a high capacity cathode for Na-ion batteries. *Electrochem. Commun.* **2012**, *21*, 36−38.
(304) Zhou, M.; Zhu, L.; Cao, Y.; Zhao, R.; Qian, J.; Ai, X.; Yang, H. $Fe(CN)_6^{-4}$-doped polypyrrole: a high-capacity and high-rate cathode material for sodium-ion batteries. *RSC Adv.* **2012**, *2*, 5495−5498.
(305) Zhou, M.; Xiong, Y.; Cao, Y.; Ai, X.; Yang, H. Electroactive organic anion-doped polypyrrole as a low cost and renewable cathode for sodium-ion batteries. *J. Polym. Sci., Part B: Polym. Phys.* **2013**, *51*, 114−118.
(306) Zhu, L.; Niu, Y.; Cao, Y.; Lei, A.; Ai, X.; Yang, H. n-Type redox behaviors of polybithiophene and its implications for anodic Li and Na storage materials. *Electrochim. Acta* **2012**, *78*, 27−31.
(307) Deng, W.; Liang, X.; Wu, X.; Qian, J.; Cao, Y.; Ai, X.; Feng, J.; Yang, H. A low cost, all-organic Na-ion Battery Based on Polymeric Cathode and Anode. *Sci. Rep.* **2013**, *3*, 2671.
(308) Obrezkov, F. A.; Shestakov, A. F.; Traven, V. F.; Stevenson, K. J.; Troshin, P. A. An ultrafast charging polyphenylamine-based cathode material for high rate lithium, sodium and potassium batteries. *J. Mater. Chem. A* **2019**, *7*, 11430−11437.
(309) Huang, Y.; Fang, C.; Zeng, R.; Liu, Y.; Zhang, W.; Wang, Y.; Liu, Q.; Huang, Y. In Situ-Formed Hierarchical Metal−Organic Flexible Cathode for High-Energy Sodium-Ion Batteries. *ChemSusChem* **2017**, *10*, 4704−4708.
(310) Fang, C.; Huang, Y.; Yuan, L.; Liu, Y.; Chen, W.; Huang, Y.; Chen, K.; Han, J.; Liu, Q.; Huang, Y. A Metal-Organic Compound as Cathode Material with Superhigh Capacity Achieved by Reversible Cationic and Anionic Redox Chemistry for High-Energy Sodium-Ion Batteries. *Angew. Chem., Int. Ed.* **2017**, *56*, 6793−6797.
(311) Deng, W.; Qian, J.; Cao, Y.; Ai, X.; Yang, H. Graphene-Wrapped $Na_2C_{12}H_6O_4$ Nanoflowers as High Performance Anodes for Sodium-Ion Batteries. *Small* **2016**, *12*, 583−587.
(312) Padhy, H.; Chen, Y.; Lüder, J.; Gajella, S. R.; Manzhos, S.; Balaya, P. Charge and Discharge Processes and Sodium Storage in Disodium Pyridine-2,5-Dicarboxylate Anode-Insights from Experiments and Theory. *Adv. Energy Mater.* **2018**, *8*, 1701572.
(313) Choi, A.; Kim, Y. K.; Kim, T. K.; Kwon, M.-S.; Lee, K. T.; Moon, H. R. 4,4′-Biphenyldicarboxylate sodium coordination compounds as anodes for Na-ion batteries. *J. Mater. Chem. A* **2014**, *2*, 14986−14993.
(314) López-Herraiz, M.; Castillo-Martínez, E.; Carretero-González, J.; Carrasco, J.; Rojo, T.; Armand, M. Oligomeric-Schiff bases as negative electrodes for sodium ion batteries: unveiling the nature of their active redox centers. *Energy Environ. Sci.* **2015**, *8*, 3233−3241.
(315) Fernández, N.; Sánchez-Fontecoba, P.; Castillo-Martínez, E.; Carretero-González, J.; Rojo, T.; Armand, M. Polymeric Redox-Active Electrodes for Sodium-Ion Batteries. *ChemSusChem* **2018**, *11*, 311−319.
(316) Castillo-Martínez, E.; Carretero-González, J.; Armand, M. Polymeric Schiff Bases as Low-Voltage Redox Centers for Sodium-Ion Batteries. *Angew. Chem.* **2014**, *126*, 5445−5449.
(317) Zhang, Y.; Yang, S.; Chang, X.; Guo, H.; Li, Y.; Wang, M.; Li, W.; Jiao, L.; Wang, Y. MOF based on a longer linear ligand: electrochemical performance, reaction kinetics, and use as a novel anode material for sodium-ion batteries. *Chem. Commun.* **2018**, *54*, 11793−11796.
(318) Yabuuchi, N.; Kubota, K.; Dahbi, M.; Komaba, S. Research Development on Sodium-Ion Batteries. *Chem. Rev.* **2014**, *114*, 11636−11682.
(319) Cui, J.; Yao, S.; Kim, J.-K. Recent progress in rational design of anode materials for high-performance Na-ion batteries. *Energy Storage Mater.* **2017**, *7*, 64−114.
(320) Zhao, C.; Lu, Y.; Li, Y.; Jiang, L.; Rong, X.; Hu, Y.-S.; Li, H.; Chen, L. Novel Methods for Sodium-Ion Battery Materials. *Small Methods* **2017**, *1*, 1600063.
(321) Sun, Y.; Guo, S.; Zhou, H. Exploration of Advanced Electrode Materials for Rechargeable Sodium-Ion Batteries. *Adv. Energy Mater.* **2019**, *9*, 1800212.
(322) Li, F.; Wei, Z.; Manthiram, A.; Feng, Y.; Ma, J.; Mai, L. Sodium-based batteries: from critical materials to battery systems. *J. Mater. Chem. A* **2019**, *7*, 9406−9431.
(323) Wu, X.; Jin, S.; Zhang, Z.; Jiang, L.; Mu, L.; Hu, Y.-S.; Li, H.; Chen, X.; Armand, M.; Chen, L.; et al. Unraveling the storage mechanism in organic carbonyl electrodes for sodium-ion batteries. *Sci. Adv.* **2015**, *1*, e1500330.
(324) Medabalmi, V.; Kuanr, N.; Ramanujam, K. Sodium Naphthalene Dicarboxylate Anode Material for Inorganic-Organic Hybrid Rechargeable Sodium-Ion Batteries. *J. Electrochem. Soc.* **2018**, *165*, A175−A180.
(325) Chen, L.; Li, W.; Wang, Y.; Wang, C.; Xia, Y. Polyimide as anode electrode material for rechargeable sodium batteries. *RSC Adv.* **2014**, *4*, 25369−25373.
(326) Chihara, K.; Chujo, N.; Kitajou, A.; Okada, S. Cathode properties of $Na_2C_6O_6$ for sodium-ion batteries. *Electrochim. Acta* **2013**, *110*, 240−246.
(327) Lee, M.; Hong, J.; Lopez, J.; Sun, Y.; Feng, D.; Lim, K.; Chueh, W. C.; Toney, M. F.; Cui, Y.; Bao, Z. High-performance sodium−organic battery by realizing four-sodium storage in disodium rhodizonate. *Nat. Energy* **2017**, *2*, 861−868.
(328) Banda, H.; Damien, D.; Nagarajan, K.; Hariharan, M.; Shaijumon, M. M. A polyimide based all-organic sodium ion battery. *J. Mater. Chem. A* **2015**, *3*, 10453−10458.
(329) Wang, S.; Wang, L.; Zhu, Z.; Hu, Z.; Zhao, Q.; Chen, J. All Organic Sodium-Ion Batteries with $Na_4C_8H_2O_6$. *Angew. Chem., Int. Ed.* **2014**, *53*, 5892−5896.
(330) Sun, T.; Li, Z.; Wang, H.; Bao, D.; Meng, F.; Zhang, X. A Biodegradable Polydopamine-Derived Electrode Material for High-Capacity and Long-Life Lithium-Ion and Sodium-Ion Batteries. *Angew. Chem., Int. Ed.* **2016**, *55*, 10662−10666.
(331) Wu, S.; Wang, W.; Li, M.; Cao, L.; Lyu, F.; Yang, M.; Wang, Z.; Shi, Y.; Nan, B.; Yu, S.; et al. Highly durable organic electrode for sodium-ion batteries via a stabilized α-C radical intermediate. *Nat. Commun.* **2016**, *7*, 13318.
(332) Gu, S.; Wu, S.; Cao, L.; Li, M.; Qin, N.; Zhu, J.; Wang, Z.; Li, Y.; Li, Z.; Chen, J.; et al. Tunable Redox Chemistry and Stability of Radical Intermediates in 2D Covalent Organic Frameworks for High Performance Sodium Ion Batteries. *J. Am. Chem. Soc.* **2019**, *141*, 9623−9628.
(333) Zhao, H.; Wang, J.; Zheng, Y.; Li, J.; Han, X.; He, G.; Du, Y. Organic Thiocarboxylate Electrodes for a Room-Temperature Sodium-Ion Battery Delivering an Ultrahigh Capacity. *Angew. Chem., Int. Ed.* **2017**, *56*, 15334−15338.
(334) Tang, M.; Zhu, S.; Liu, Z.; Jiang, C.; Wu, Y.; Li, H.; Wang, B.; Wang, E.; Ma, J.; Wang, C. Tailoring π-Conjugated Systems: From π-π Stacking to High-Rate-Performance Organic Cathodes. *Chem.* **2018**, *4*, 2600−2614.
(335) Luo, C.; Xu, G.-L.; Ji, X.; Hou, S.; Chen, L.; Wang, F.; Jiang, J.; Chen, Z.; Ren, Y.; Amine, K.; et al. Reversible Redox Chemistry of Azo Compounds for Sodium-Ion Batteries. *Angew. Chem., Int. Ed.* **2018**, *57*, 2879−2883.
(336) Tripathi, A.; Chen, Y.; Padhy, H.; Manzhos, S.; Balaya, P. Experimental and Theoretical Studies of Trisodium-1,3,5-Benzene Tricarboxylate as a Low-Voltage Anode Material for Sodium-Ion Batteries. *Energy Technol.* **2019**, *7*, 1801030.
(337) Sakaushi, K.; Hosono, E.; Nickerl, G.; Gemming, T.; Zhou, H.; Kaskel, S.; Eckert, J. Aromatic porous-honeycomb electrodes for a sodium-organic energy storage device. *Nat. Commun.* **2013**, *4*, 1485.

https://dx.doi.org/10.1021/acs.chemrev.9b00482
Chem. Rev. 2020, 120, 6490−6557

(338) Zhang, Y.; An, Y.; Dong, S.; Jiang, J.; Dou, H.; Zhang, X. Enhanced Cycle Performance of Polyimide Cathode Using a Quasi-Solid-State Electrolyte. *J. Phys. Chem. C* **2018**, *122*, 22294−22300.
(339) Wang, H.; Yuan, S.; Ma, D.; Huang, X.; Meng, F.; Zhang, X. Tailored Aromatic Carbonyl Derivative Polyimides for High-Power and Long-Cycle Sodium-Organic Batteries. *Adv. Energy Mater.* **2014**, *4*, 1301651.
(340) Wu, D.; Zhang, G.; Lu, D.; Ma, L.; Xu, Z.; Xi, X.; Liu, R.; Liu, P.; Su, Y. Perylene diimide-diamine/carbon black composites as high performance lithium/sodium ion battery cathodes. *J. Mater. Chem. A* **2018**, *6*, 13613−13618.
(341) Zhang, Y.; Huang, Y.; Yang, G.; Bu, F.; Li, K.; Shakir, I.; Xu, Y. Dispersion−Assembly Approach to Synthesize Three-Dimensional Graphene/Polymer Composite Aerogel as a Powerful Organic Cathode for Rechargeable Li and Na Batteries. *ACS Appl. Mater. Interfaces* **2017**, *9*, 15549−15556.
(342) Tang, W.; Liang, R.; Li, D.; Yu, Q.; Hu, J.; Cao, B.; Fan, C. Highly Stable and High Rate-Performance Na-Ion Batteries Using Polyanionic Anthraquinone as the Organic Cathode. *ChemSusChem* **2019**, *12*, 2181−2185.
(343) Li, Z.; Zhou, J.; Xu, R.; Liu, S.; Wang, Y.; Li, P.; Wu, W.; Wu, M. Synthesis of three dimensional extended conjugated polyimide and application as sodium-ion battery anode. *Chem. Eng. J.* **2016**, *287*, 516−522.
(344) Li, H.; Tang, M.; Wu, Y.; Chen, Y.; Zhu, S.; Wang, B.; Jiang, C.; Wang, E.; Wang, C. Large π-Conjugated Porous Frameworks as Cathodes for Sodium-Ion Batteries. *J. Phys. Chem. Lett.* **2018**, *9*, 3205−3211.
(345) Xu, Y.-S.; Duan, S.-Y.; Sun, Y.-G.; Bin, D.-S.; Tao, X.-S.; Zhang, D.; Liu, Y.; Cao, A.-M.; Wan, L.-J. Recent developments in electrode materials for potassium-ion batteries. *J. Mater. Chem. A* **2019**, *7*, 4334−4352.
(346) Lei, K.; Li, F.; Mu, C.; Wang, J.; Zhao, Q.; Chen, C.; Chen, J. High K-storage performance based on the synergy of dipotassium terephthalate and ether-based electrolytes. *Energy Environ. Sci.* **2017**, *10*, 552−557.
(347) Tang, M.; Wu, Y.; Chen, Y.; Jiang, C.; Zhu, S.; Zhuo, S.; Wang, C. An organic cathode with high capacities for fast-charge potassium-ion batteries. *J. Mater. Chem. A* **2019**, *7*, 486−492.
(348) Zhao, Q.; Wang, J.; Lu, Y.; Li, Y.; Liang, G.; Chen, J. Oxocarbon Salts for Fast Rechargeable Batteries. *Angew. Chem., Int. Ed.* **2016**, *55*, 12528−12532.
(349) Li, C.; Xue, J.; Huang, A.; Ma, J.; Qing, F.; Zhou, A.; Wang, Z.; Wang, Y.; Li, J. Poly(N-vinylcarbazole) as an advanced organic cathode for potassium-ion-based dual-ion battery. *Electrochim. Acta* **2019**, *297*, 850−855.
(350) Gao, H.; Xue, L.; Xin, S.; Goodenough, J. B. A High-Energy-Density Potassium Battery with a Polymer-Gel Electrolyte and a Polyaniline Cathode. *Angew. Chem., Int. Ed.* **2018**, *57*, 5449−5453.
(351) Wang, C.; Tang, W.; Yao, Z.; Cao, B.; Fan, C. Potassium perylene-tetracarboxylate with two-electron redox behaviors as a highly stable organic anode for K-ion batteries. *Chem. Commun.* **2019**, *55*, 1801−1804.
(352) Li, C.; Deng, Q.; Tan, H.; Wang, C.; Fan, C.; Pei, J.; Cao, B.; Wang, Z.; Li, J. *Para*-Conjugated Dicarboxylates with Extended Aromatic Skeletons as the Highly Advanced Organic Anodes for K-Ion Battery. *ACS Appl. Mater. Interfaces* **2017**, *9*, 27414−27420.
(353) Liang, Y.; Luo, C.; Wang, F.; Hou, S.; Liou, S.-C.; Qing, T.; Li, Q.; Zheng, J.; Cui, C.; Wang, C. An Organic Anode for High Temperature Potassium-Ion Batteries. *Adv. Energy Mater.* **2019**, *9*, 1802986.
(354) Fan, L.; Ma, R.; Wang, J.; Yang, H.; Lu, B. An Ultrafast and Highly Stable Potassium-Organic Battery. *Adv. Mater.* **2018**, *30*, 1805486.
(355) Chen, L.; Liu, S.; Wang, Y.; Liu, W.; Dong, Y.; Kuang, Q.; Zhao, Y. Ortho-di-sodium salts of tetrahydroxyquinone as a novel electrode for lithium-ion and potassium-ion batteries. *Electrochim. Acta* **2019**, *294*, 46−52.
(356) Tian, B.; Zheng, J.; Zhao, C.; Liu, C.; Su, C.; Tang, W.; Li, X.; Ning, G.-H. Carbonyl-based polyimide and polyquinoneimide for potassium-ion batteries. *J. Mater. Chem. A* **2019**, *7*, 9997−10003.
(357) Canepa, P.; Sai Gautam, G.; Hannah, D. C.; Malik, R.; Liu, M.; Gallagher, K. G.; Persson, K. A.; Ceder, G. Odyssey of Multivalent Cathode Materials: Open Questions and Future Challenges. *Chem. Rev.* **2017**, *117*, 4287−4341.
(358) Ponrouch, A.; Bitenc, J.; Dominko, R.; Lindahl, N.; Johansson, P.; Palacin, M. R. Multivalent rechargeable batteries. *Energy Storage Mater.* **2019**, *20*, 253−262.
(359) Aurbach, D.; Lu, Z.; Schechter, A.; Gofer, Y.; Gizbar, H.; Turgeman, R.; Cohen, Y.; Moshkovich, M.; Levi, E. Prototype systems for rechargeable magnesium batteries. *Nature* **2000**, *407*, 724−727.
(360) Liao, C.; Guo, B.; Jiang, D.; Custelcean, R.; Mahurin, S. M.; Sun, X.-G.; Dai, S. Highly soluble alkoxide magnesium salts for rechargeable magnesium batteries. *J. Mater. Chem. A* **2014**, *2*, 581−584.
(361) Sun, X.; Bonnick, P.; Duffort, V.; Liu, M.; Rong, Z.; Persson, K. A.; Ceder, G.; Nazar, L. F. A high capacity thiospinel cathode for Mg batteries. *Energy Environ. Sci.* **2016**, *9*, 2273−2277.
(362) Du, A.; Zhang, Z.; Qu, H.; Cui, Z.; Qiao, L.; Wang, L.; Chai, J.; Lu, T.; Dong, S.; Dong, T.; et al. An efficient organic magnesium borate-based electrolyte with non-nucleophilic characteristics for magnesium−sulfur battery. *Energy Environ. Sci.* **2017**, *10*, 2616−2625.
(363) McAllister, B. T.; Kyne, L. T.; Schon, T. B.; Seferos, D. S. Potential for Disruption with Organic Magnesium-Ion Batteries. *Joule* **2019**, *3*, 620−624.
(364) Attias, R.; Salama, M.; Hirsch, B.; Gofer, Y.; Aurbach, D. Solvent Effects on the Reversible Intercalation of Magnesium-Ions into V_2O_5 Electrodes. *ChemElectroChem* **2018**, *5*, 3514−3524.
(365) Salama, M.; Shterenberg, I.; Gizbar, H.; Eliaz, N. N.; Kosa, M.; Keinan-Adamsky, K.; Afri, M.; Shimon, L. J. W.; Gottlieb, H. E.; Major, D. T.; et al. Unique Behavior of Dimethoxyethane (DME)/$Mg(N(SO_2CF_3)_2)_2$ Solutions. *J. Phys. Chem. C* **2016**, *120*, 19586−19594.
(366) Dong, H.; Liang, Y.; Tutusaus, O.; Mohtadi, R.; Zhang, Y.; Hao, F.; Yao, Y. Directing Mg-Storage Chemistry in Organic Polymers toward High-Energy Mg Batteries. *Joule* **2019**, *3*, 782−793.
(367) Ju, Q.; Shi, Y.; Kan, J. Performance study of magnesium-polyaniline rechargeable battery in 1-ethyl-3-methylimidazolium ethyl sulfate electrolyte. *Synth. Met.* **2013**, *178*, 27−33.
(368) Lu, D.; Liu, H.; Huang, T.; Xu, Z.; Ma, L.; Yang, P.; Qiang, P.; Zhang, F.; Wu, D. Magnesium ion based organic secondary batteries. *J. Mater. Chem. A* **2018**, *6*, 17297−17302.
(369) Ha, S.-Y.; Lee, Y.-W.; Woo, S. W.; Koo, B.; Kim, J.-S.; Cho, J.; Lee, K. T.; Choi, N.-S. Magnesium(II) Bis(trifluoromethane sulfonyl) Imide-Based Electrolytes with Wide Electrochemical Windows for Rechargeable Magnesium Batteries. *ACS Appl. Mater. Interfaces* **2014**, *6*, 4063−4073.
(370) Pan, B.; Zhou, D.; Huang, J.; Zhang, L.; Burrell, A. K.; Vaughey, J. T.; Zhang, Z.; Liao, C. 2,5-Dimethoxy-1,4-Benzoquinone (DMBQ) as Organic Cathode for Rechargeable Magnesium-Ion Batteries. *J. Electrochem. Soc.* **2016**, *163*, A580−A583.
(371) Bitenc, J.; Pirnat, K.; Mali, G.; Novosel, B.; Randon Vitanova, A.; Dominko, R. Poly(hydroquinoyl-benzoquinonyl sulfide) as an active material in Mg and Li organic batteries. *Electrochem. Commun.* **2016**, *69*, 1−5.
(372) Bitenc, J.; Pirnat, K.; Bančič, T.; Gaberšček, M.; Genorio, B.; Randon-Vitanova, A.; Dominko, R. Anthraquinone-Based Polymer as Cathode in Rechargeable Magnesium Batteries. *ChemSusChem* **2015**, *8*, 4128−4132.
(373) NuLi, Y.; Chen, Q.; Wang, W.; Wang, Y.; Yang, J.; Wang, J. Carbyne Polysulfide as a Novel Cathode Material for Rechargeable Magnesium Batteries. *Sci. World J.* **2014**, *2014*, 1−7.
(374) Sano, H.; Senoh, H.; Yao, M.; Sakaebe, H.; Kiyobayashi, T. Mg 2+ Storage in Organic Positive-electrode Active Material Based on 2,5-Dimethoxy-1,4-benzoquinone. *Chem. Lett.* **2012**, *41*, 1594−1596.

https://dx.doi.org/10.1021/acs.chemrev.9b00482
Chem. Rev. 2020, 120, 6490−6557

(375) Hudak, N. S. Chloroaluminate-Doped Conducting Polymers as Positive Electrodes in Rechargeable Aluminum Batteries. *J. Phys. Chem. C* **2014**, *118*, 5203−5215.
(376) Guerfi, A.; Trottier, J.; Boyano, I.; De Meatza, I.; Blazquez, J. A.; Brewer, S.; Ryder, K. S.; Vijh, A.; Zaghib, K. High cycling stability of zinc-anode/conducting polymer rechargeable battery with non-aqueous electrolyte. *J. Power Sources* **2014**, *248*, 1099−1104.
(377) Walter, M.; Kravchyk, K. V.; Böfer, C.; Widmer, R.; Kovalenko, M. V. Polypyrenes as High-Performance Cathode Materials for Aluminum Batteries. *Adv. Mater.* **2018**, *30*, 1705644.
(378) Lin, M.-C.; Gong, M.; Lu, B.; Wu, Y.; Wang, D.-Y.; Guan, M.; Angell, M.; Chen, C.; Yang, J.; Hwang, B.-J.; et al. An ultrafast rechargeable aluminium-ion battery. *Nature* **2015**, *520*, 324−328.
(379) Yang, H.; Li, H.; Li, J.; Sun, Z.; He, K.; Cheng, H.-M.; Li, F. The Rechargeable Aluminum Battery: Opportunities and Challenges. *Angew. Chem., Int. Ed.* **2019**, *58*, 11978
(380) Kim, D. J.; Yoo, D.-J.; Otley, M. T.; Prokofjevs, A.; Pezzato, C.; Owczarek, M.; Lee, S. J.; Choi, J. W.; Stoddart, J. F. Rechargeable aluminium organic batteries. *Nat. Energy* **2019**, *4*, 51−59.
(381) Han, X.; Qing, G.; Sun, J.; Sun, T. How Many Lithium Ions Can Be Inserted onto Fused C6 Aromatic Ring Systems? *Angew. Chem., Int. Ed.* **2012**, *51*, 5147−5151.
(382) Luo, W.; Allen, M.; Raju, V.; Ji, X. An Organic Pigment as a High-Performance Cathode for Sodium-Ion Batteries. *Adv. Energy Mater.* **2014**, *4*, 1400554.
(383) Chen, Y.; Luo, W.; Carter, M.; Zhou, L.; Dai, J.; Fu, K.; Lacey, S.; Li, T.; Wan, J.; Han, X.; et al. Organic electrode for non-aqueous potassium-ion batteries. *Nano Energy* **2015**, *18*, 205−211.
(384) Wang, Y.; Deng, Y.; Qu, Q.; Zheng, X.; Zhang, J.; Liu, G.; Battaglia, V. S.; Zheng, H. Ultrahigh-Capacity Organic Anode with High-Rate Capability and Long Cycle Life for Lithium-Ion Batteries. *ACS Energy Lett.* **2017**, *2*, 2140−2148.
(385) Tian, N.; Gao, Y.; Li, Y.; Wang, Z.; Song, X.; Chen, L. Li_2C_2, a High-Capacity Cathode Material for Lithium Ion Batteries. *Angew. Chem., Int. Ed.* **2016**, *55*, 644−648.
(386) Li, Y.; Song, X.; Tang, F.; Hou, C.; He, J.; Wang, H.; Liu, X. In situ study on the charge/discharge of nanocrystalline Li_2C_2 as a new cathode material. *RSC Adv.* **2016**, *6*, 54256−54262.
(387) Kang, H.; Liu, H.; Li, C.; Sun, L.; Zhang, C.; Gao, H.; Yin, J.; Yang, B.; You, Y.; Jiang, K.-C.; et al. Polyanthraquinone-Triazine—A Promising Anode Material for High-Energy Lithium-Ion Batteries. *ACS Appl. Mater. Interfaces* **2018**, *10*, 37023−37030.
(388) Schon, T. B.; An, S. Y.; Tilley, A. J.; Seferos, D. S. Unusual Capacity Increases with Cycling for Ladder-Type Microporous Polymers. *ACS Appl. Mater. Interfaces* **2019**, *11*, 1739−1747.
(389) Wu, J.; Rui, X.; Wang, C.; Pei, W.-B.; Lau, R.; Yan, Q.; Zhang, Q. Nanostructured Conjugated Ladder Polymers for Stable and Fast Lithium Storage Anodes with High-Capacity. *Adv. Energy Mater.* **2015**, *5*, 1402189.
(390) Wu, J.; Rui, X.; Long, G.; Chen, W.; Yan, Q.; Zhang, Q. Pushing Up Lithium Storage through Nanostructured Polyazaacene Analogues as Anode. *Angew. Chem., Int. Ed.* **2015**, *54*, 7354−7358.
(391) Li, W.; Dahn, J. R.; Wainwright, D. S. Rechargeable Lithium Batteries with Aqueous Electrolytes. *Science* **1994**, *264*, 1115−1118.
(392) Alt, H.; Binder, H.; Klempert, G.; Köhling, A.; Sandstede, G. Evaluation of organic battery electrodes: Voltammetric study of the redox behaviour of solid quinones. *J. Appl. Electrochem.* **1972**, *2*, 193−200.
(393) Sun, D.; Tang, Y.; He, K.; Ren, Y.; Liu, S.; Wang, H. Long-lived Aqueous Rechargeable Lithium Batteries Using Mesoporous $LiTi_2(PO_4)_3$@C Anode. *Sci. Rep.* **2015**, *5*, 17452.
(394) Zhao, B.; Lin, B.; Zhang, S.; Deng, C. A frogspawn-inspired hierarchical porous $NaTi_2(PO_4)_3$ -C array for high-rate and long-life aqueous rechargeable sodium batteries. *Nanoscale* **2015**, *7*, 18552−18560.
(395) Liang, Y.; Jing, Y.; Gheytani, S.; Lee, K.-Y.; Liu, P.; Facchetti, A.; Yao, Y. Universal quinone electrodes for long cycle life aqueous rechargeable batteries. *Nat. Mater.* **2017**, *16*, 841−848.
(396) Li, Z.; Young, D.; Xiang, K.; Carter, W. C.; Chiang, Y.-M. Towards High Power High Energy Aqueous Sodium-Ion Batteries: The $NaTi_2(PO_4)_3/Na_{0.44}MnO_2$ System. *Adv. Energy Mater.* **2013**, *3*, 290−294.
(397) Whitacre, J. F.; Shanbhag, S.; Mohamed, A.; Polonsky, A.; Carlisle, K.; Gulakowski, J.; Wu, W.; Smith, C.; Cooney, L.; Blackwood, D.; et al. A Polyionic, Large-Format Energy Storage Device Using an Aqueous Electrolyte and Thick-Format Composite $NaTi_2(PO_4)_3$/Activated Carbon Negative Electrodes. *Energy Technol.* **2015**, *3*, 20−31.
(398) Hatakeyama-Sato, K.; Wakamatsu, H.; Katagiri, R.; Oyaizu, K.; Nishide, H. An Ultrahigh Output Rechargeable Electrode of a Hydrophilic Radical Polymer/Nanocarbon Hybrid with an Exceptionally Large Current Density beyond 1 A cm^{-2}. *Adv. Mater.* **2018**, *30*, 1800900.
(399) Suo, L.; Borodin, O.; Gao, T.; Olguin, M.; Ho, J.; Fan, X.; Luo, C.; Wang, C.; Xu, K. Water-in-salt" electrolyte enables high-voltage aqueous lithium-ion chemistries. *Science* **2015**, *350*, 938−943.
(400) Yamada, Y.; Usui, K.; Sodeyama, K.; Ko, S.; Tateyama, Y.; Yamada, A. Hydrate-melt electrolytes for high-energy-density aqueous batteries. *Nat. Energy* **2016**, *1*, 16129.
(401) Yamada, Y.; Wang, J.; Ko, S.; Watanabe, E.; Yamada, A. Advances and issues in developing salt-concentrated battery electrolytes. *Nat. Energy* **2019**, DOI: 10.1038/s41560-019-0336-z
(402) Yang, C.; Chen, J.; Qing, T.; Fan, X.; Sun, W.; von Cresce, A.; Ding, M. S.; Borodin, O.; Vatamanu, J.; Schroeder, M. A.; et al. 4.0 V Aqueous Li-Ion Batteries. *Joule* **2017**, *1*, 122−132.
(403) Ko, S.; Yamada, Y.; Miyazaki, K.; Shimada, T.; Watanabe, E.; Tateyama, Y.; Kamiya, T.; Honda, T.; Akikusa, J.; Yamada, A. Lithium-salt monohydrate melt: A stable electrolyte for aqueous lithium-ion batteries. *Electrochem. Commun.* **2019**, *104*, 106488.
(404) Qin, H.; Song, Z. P.; Zhan, H.; Zhou, Y. H. Aqueous rechargeable alkali-ion batteries with polyimide anode. *J. Power Sources* **2014**, *249*, 367−372.
(405) Viehbeck, A. Electrochemical Properties of Polyimides and Related Imide Compounds. *J. Electrochem. Soc.* **1990**, *137*, 1460.
(406) Dong, X.; Chen, L.; Liu, J.; Haller, S.; Wang, Y.; Xia, Y. Environmentally-friendly aqueous Li (or Na)-ion battery with fast electrode kinetics and super-long life. *Sci. Adv.* **2016**, *2*, e1501038.
(407) Fernández-Ropero, A. J.; Saurel, D.; Acebedo, B.; Rojo, T.; Casas-Cabanas, M. Electrochemical characterization of $NaFePO_4$ as positive electrode in aqueous sodium-ion batteries. *J. Power Sources* **2015**, *291*, 40−45.
(408) Pasta, M.; Wessells, C. D.; Liu, N.; Nelson, J.; McDowell, M. T.; Huggins, R. A.; Toney, M. F.; Cui, Y. Full open-framework batteries for stationary energy storage. *Nat. Commun.* **2014**, *5*, 3007.
(409) Gao, H.; Goodenough, J. B. An Aqueous Symmetric Sodium-Ion Battery with NASICON-Structured $Na_3MnTi(PO_4)_3$. *Angew. Chem., Int. Ed.* **2016**, *55*, 12768−12772.
(410) Wang, Y.; Liu, J.; Lee, B.; Qiao, R.; Yang, Z.; Xu, S.; Yu, X.; Gu, L.; Hu, Y.-S.; Yang, W.; et al. Ti-substituted tunnel-type Na0.44MnO2 oxide as a negative electrode for aqueous sodium-ion batteries. *Nat. Commun.* **2015**, *6*, 6401.
(411) Jiang, L.; Lu, Y.; Zhao, C.; Liu, L.; Zhang, J.; Zhang, Q.; Shen, X.; Zhao, J.; Yu, X.; Li, H.; et al. Building aqueous K-ion batteries for energy storage. *Nat. Energy* **2019**, *4*, 495.
(412) Zhao, Q.; Huang, W.; Luo, Z.; Liu, L.; Lu, Y.; Li, Y.; Li, L.; Hu, J.; Ma, H.; Chen, J. High-capacity aqueous zinc batteries using sustainable quinone electrodes. *Sci. Adv.* **2018**, *4*, eaao1761.
(413) Chen, L.; Bao, J. L.; Dong, X.; Truhlar, D. G.; Wang, Y.; Wang, C.; Xia, Y. Aqueous Mg-Ion Battery Based on Polyimide Anode and Prussian Blue Cathode. *ACS Energy Lett.* **2017**, *2*, 1115−1121.
(414) Wang, F.; Fan, X.; Gao, T.; Sun, W.; Ma, Z.; Yang, C.; Han, F.; Xu, K.; Wang, C. High-Voltage Aqueous Magnesium Ion Batteries. *ACS Cent. Sci.* **2017**, *3*, 1121−1128.
(415) Gheytani, S.; Liang, Y.; Wu, F.; Jing, Y.; Dong, H.; Rao, K. K.; Chi, X.; Fang, F.; Yao, Y. An Aqueous Ca-Ion Battery. *Adv. Sci.* **2017**, *4*, 1700465.

https://dx.doi.org/10.1021/acs.chemrev.9b00482
Chem. Rev. 2020, 120, 6490−6557

(416) Wu, X.; Qi, Y.; Hong, J. J.; Li, Z.; Hernandez, A. S.; Ji, X. Rocking-Chair Ammonium-Ion Battery: A Highly Reversible Aqueous Energy Storage System. *Angew. Chem., Int. Ed.* **2017**, *56*, 13026−13030.
(417) Poizot, P.; Dolhem, F.; Gaubicher, J. Progress in all-organic rechargeable batteries using cationic and anionic configurations: Toward low-cost and greener storage solutions? *Curr. Opin. Electrochem.* **2018**, *9*, 70−80.
(418) Sano, N.; Tomita, W.; Hara, S.; Min, C.-M.; Lee, J.-S.; Oyaizu, K.; Nishide, H. Polyviologen Hydrogel with High-Rate Capability for Anodes toward an Aqueous Electrolyte-Type and Organic-Based Rechargeable Device. *ACS Appl. Mater. Interfaces* **2013**, *5*, 1355−1361.
(419) Chikushi, N.; Yamada, H.; Oyaizu, K.; Nishide, H. TEMPO-substituted polyacrylamide for an aqueous electrolyte-typed and organic-based rechargeable device. *Sci. China: Chem.* **2012**, *55*, 822−829.
(420) Dong, X.; Yu, H.; Ma, Y.; Bao, J. L.; Truhlar, D. G.; Wang, Y.; Xia, Y. All-Organic Rechargeable Battery with Reversibility Supported by "Water-in-Salt" Electrolyte. *Chem. - Eur. J.* **2017**, *23*, 2560−2565.
(421) https://blue-storage.com/bollore-assets/uploads/2019/05/presentation-bluesolutions.pdf and https://blue-storage.com/bollore-assets/uploads/2019/05/flyer-bluestorage.pdf, last accessed June 2019.
(422) Liu, W.; Lu, W.; Zhang, H.; Li, X. Aqueous Flow Batteries: Research and Development. *Chem. - Eur. J.* **2019**, *25*, 1649−1664.
(423) Ye, R.; Henkensmeier, D.; Yoon, S. J.; Huang, Z.; Kim, D. K.; Chang, Z.; Kim, S.; Chen, R. Redox Flow Batteries for Energy Storage: A Technology Review. *J. Electrochem. Energy Convers. Storage* **2018**, *15*, 010801.
(424) Xu, Q.; Ji, Y. N.; Qin, L. Y.; Leung, P. K.; Qiao, F.; Li, Y. S.; Su, H. N. Evaluation of redox flow batteries goes beyond round-trip efficiency: A technical review. *J. Energy Storage* **2018**, *16*, 108−115.
(425) Khor, A.; Leung, P.; Mohamed, M. R.; Flox, C.; Xu, Q.; An, L.; Wills, R. G. A.; Morante, J. R.; Shah, A. A. Review of zinc-based hybrid flow batteries: From fundamentals to applications. *Mater. Today Energy* **2018**, *8*, 80−108.
(426) Duduta, M.; Ho, B.; Wood, V. C.; Limthongkul, P.; Brunini, V. E.; Carter, W. C.; Chiang, Y.-M. Semi-Solid Lithium Rechargeable Flow Battery. *Adv. Energy Mater.* **2011**, *1*, 511−516.
(427) Wang, X.; Xing, X.; Huo, Y.; Zhao, Y.; Li, Y. A systematic study of the co-solvent effect for an all-organic redox flow battery. *RSC Adv.* **2018**, *8*, 24422−24427.
(428) Ding, Y.; Zhang, C.; Zhang, L.; Wei, H.; Li, Y.; Yu, G. Insights into Hydrotropic Solubilization for Hybrid Ion Redox Flow Batteries. *ACS Energy Lett.* **2018**, *3*, 2641−2648.
(429) Zhang, C.; Zhang, L.; Ding, Y.; Guo, X.; Yu, G. Eutectic Electrolytes for High-Energy-Density Redox Flow Batteries. *ACS Energy Lett.* **2018**, *3*, 2875−2883.
(430) Gerhardt, M. R.; Tong, L.; Gómez-Bombarelli, R.; Chen, Q.; Marshak, M. P.; Galvin, C. J.; Aspuru-Guzik, A.; Gordon, R. G.; Aziz, M. J. Anthraquinone Derivatives in Aqueous Flow Batteries. *Adv. Energy Mater.* **2017**, *7*, 1601488.
(431) Ji, Y.; Goulet, M.; Pollack, D. A.; Kwabi, D. G.; Jin, S.; Porcellinis, D.; Kerr, E. F.; Gordon, R. G.; Aziz, M. J. A Phosphonate-Functionalized Quinone Redox Flow Battery at Near-Neutral pH with Record Capacity Retention Rate. *Adv. Energy Mater.* **2019**, *9*, 1900039.
(432) Wang, C.; Yang, Z.; Wang, Y.; Zhao, P.; Yan, W.; Zhu, G.; Ma, L.; Yu, B.; Wang, L.; Li, G.; et al. High-Performance Alkaline Organic Redox Flow Batteries Based on 2-Hydroxy-3-carboxy-1,4-naphthoquinone. *ACS Energy Lett.* **2018**, *3*, 2404−2409.
(433) Beh, E. S.; De Porcellinis, D.; Gracia, R. L.; Xia, K. T.; Gordon, R. G.; Aziz, M. J. A Neutral pH Aqueous Organic−Organometallic Redox Flow Battery with Extremely High Capacity Retention. *ACS Energy Lett.* **2017**, *2*, 639−644.
(434) Lin, K.; Chen, Q.; Gerhardt, M. R.; Tong, L.; Kim, S. B.; Eisenach, L.; Valle, A. W.; Hardee, D.; Gordon, R. G.; Aziz, M. J.; et al. Alkaline quinone flow battery. *Science* **2015**, *349*, 1529−1532.
(435) Hoober-Burkhardt, L.; Krishnamoorthy, S.; Yang, B.; Murali, A.; Nirmalchandar, A.; Prakash, G. K. S.; Narayanan, S. R. A New Michael-Reaction-Resistant Benzoquinone for Aqueous Organic Redox Flow Batteries. *J. Electrochem. Soc.* **2017**, *164*, A600−A607.
(436) Carney, T. J.; Collins, S. J.; Moore, J. S.; Brushett, F. R. Concentration-Dependent Dimerization of Anthraquinone Disulfonic Acid and Its Impact on Charge Storage. *Chem. Mater.* **2017**, *29*, 4801−4810.
(437) DeBruler, C.; Hu, B.; Moss, J.; Liu, X.; Luo, J.; Sun, Y.; Liu, T. L. Designer Two-Electron Storage Viologen Anolyte Materials for Neutral Aqueous Organic Redox Flow Batteries. *Chem.* **2017**, *3*, 961−978.
(438) Orita, A.; Verde, M. G.; Sakai, M.; Meng, Y. S. The impact of pH on side reactions for aqueous redox flow batteries based on nitroxyl radical compounds. *J. Power Sources* **2016**, *321*, 126−134.
(439) Wedege, K.; Dražević, E.; Konya, D.; Bentien, A. Organic Redox Species in Aqueous Flow Batteries: Redox Potentials, Chemical Stability and Solubility. *Sci. Rep.* **2016**, *6*, DOI: 10.1038/srep39101
(440) Chen, Q.; Gerhardt, M. R.; Hartle, L.; Aziz, M. J. A Quinone-Bromide Flow Battery with 1 W/cm 2 Power Density. *J. Electrochem. Soc.* **2016**, *163*, A5010−A5013.
(441) Janoschka, T.; Martin, N.; Hager, M. D.; Schubert, U. S. An Aqueous Redox-Flow Battery with High Capacity and Power: The TEMPTMA/MV System. *Angew. Chem., Int. Ed.* **2016**, *55*, 14427−14430.
(442) Janoschka, T.; Martin, N.; Martin, U.; Friebe, C.; Morgenstern, S.; Hiller, H.; Hager, M. D.; Schubert, U. S. An aqueous, polymer-based redox-flow battery using non-corrosive, safe, and low-cost materials. *Nature* **2015**, *527*, 78−81.
(443) Luo, J.; Wu, W.; Debruler, C.; Hu, B.; Hu, M.; Liu, T. L. A 1.51 V pH neutral redox flow battery towards scalable energy storage. *J. Mater. Chem. A* **2019**, *7*, 9130−9136.
(444) Hu, B.; DeBruler, C.; Rhodes, Z.; Liu, T. L. Long-Cycling Aqueous Organic Redox Flow Battery (AORFB) toward Sustainable and Safe Energy Storage. *J. Am. Chem. Soc.* **2017**, *139*, 1207−1214.
(445) Yang, B.; Hoober-Burkhardt, L.; Krishnamoorthy, S.; Murali, A.; Prakash, G. K. S.; Narayanan, S. R. High-Performance Aqueous Organic Flow Battery with Quinone-Based Redox Couples at Both Electrodes. *J. Electrochem. Soc.* **2016**, *163*, A1442−A1449.
(446) Yang, B.; Hoober-Burkhardt, L.; Wang, F.; Surya Prakash, G. K.; Narayanan, S. R. An Inexpensive Aqueous Flow Battery for Large-Scale Electrical Energy Storage Based on Water-Soluble Organic Redox Couples. *J. Electrochem. Soc.* **2014**, *161*, A1371−A1380.
(447) Wang, W.; Xu, W.; Cosimbescu, L.; Choi, D.; Li, L.; Yang, Z. Anthraquinone with tailored structure for a nonaqueous metal−organic redox flow battery. *Chem. Commun.* **2012**, *48*, 6669.
(448) Wei, X.; Xu, W.; Vijayakumar, M.; Cosimbescu, L.; Liu, T.; Sprenkle, V.; Wang, W. TEMPO-Based Catholyte for High-Energy Density Nonaqueous Redox Flow Batteries. *Adv. Mater.* **2014**, *26*, 7649−7653.
(449) Wei, X.; Cosimbescu, L.; Xu, W.; Hu, J. Z.; Vijayakumar, M.; Feng, J.; Hu, M. Y.; Deng, X.; Xiao, J.; Liu, J.; et al. Towards High-Performance Nonaqueous Redox Flow Electrolyte Via Ionic Modification of Active Species. *Adv. Energy Mater.* **2015**, *5*, 1400678.
(450) Chen, H.; Zhou, Y.; Lu, Y.-C. Lithium−Organic Nanocomposite Suspension for High-Energy-Density Redox Flow Batteries. *ACS Energy Lett.* **2018**, *3*, 1991−1997.
(451) Huang, J.; Cheng, L.; Assary, R. S.; Wang, P.; Xue, Z.; Burrell, A. K.; Curtiss, L. A.; Zhang, L. Liquid Catholyte Molecules for Nonaqueous Redox Flow Batteries. *Adv. Energy Mater.* **2015**, *5*, 1401782.
(452) Wei, X.; Duan, W.; Huang, J.; Zhang, L.; Li, B.; Reed, D.; Xu, W.; Sprenkle, V.; Wang, W. A High-Current, Stable Nonaqueous Organic Redox Flow Battery. *ACS Energy Lett.* **2016**, *1*, 705−711.
(453) Duan, W.; Huang, J.; Kowalski, J. A.; Shkrob, I. A.; Vijayakumar, M.; Walter, E.; Pan, B.; Yang, Z.; Milshtein, J. D.; Li, B.; et al. Wine-Dark Sea" in an Organic Flow Battery: Storing Negative Charge in 2,1,3-Benzothiadiazole Radicals Leads to Improved Cyclability. *ACS Energy Lett.* **2017**, *2*, 1156−1161.

(454) Milshtein, J. D.; Kaur, A. P.; Casselman, M. D.; Kowalski, J. A.; Modekrutti, S.; Zhang, P. L.; Harsha Attanayake, N.; Elliott, C. F.; Parkin, S. R.; Risko, C.; et al. High current density, long duration cycling of soluble organic active species for non-aqueous redox flow batteries. *Energy Environ. Sci.* **2016**, *9*, 3531−3543.
(455) Milton, M.; Cheng, Q.; Yang, Y.; Nuckolls, C.; Hernández Sánchez, R.; Sisto, T. J. Molecular Materials for Nonaqueous Flow Batteries with a High Coulombic Efficiency and Stable Cycling. *Nano Lett.* **2017**, *17*, 7859−7863.
(456) Zhang, J.; Huang, J.; Robertson, L. A.; Shkrob, I. A.; Zhang, L. Comparing calendar and cycle life stability of redox active organic molecules for nonaqueous redox flow batteries. *J. Power Sources* **2018**, *397*, 214−222.
(457) Goulet, M.-A.; Tong, L.; Pollack, D. A.; Tabor, D. P.; Odom, S. A.; Aspuru-Guzik, A.; Kwan, E. E.; Gordon, R. G.; Aziz, M. J. Extending the Lifetime of Organic Flow Batteries via Redox State Management. *J. Am. Chem. Soc.* **2019**, DOI: 10.1021/jacs.8b13295
(458) Fongy, C.; Gaillot, A.-C.; Jouanneau, S.; Guyomard, D.; Lestriez, B. Ionic vs Electronic Power Limitations and Analysis of the Fraction of Wired Grains in $LiFePO_4$ Composite Electrodes. *J. Electrochem. Soc.* **2010**, *157*, A885.
(459) Lestriez, B.; Bahri, S.; Sandu, I.; Roue, L.; Guyomard, D. On the binding mechanism of CMC in Si negative electrodes for Li-ion batteries. *Electrochem. Commun.* **2007**, *9*, 2801−2806.
(460) Guy, D.; Lestriez, B.; Bouchet, R.; Guyomard, D. Critical Role of Polymeric Binders on the Electronic Transport Properties of Composites Electrode. *J. Electrochem. Soc.* **2006**, *153*, A679.
(461) Wang, Y.; Xia, Y. Hybrid Aqueous Energy Storage Cells Using Activated Carbon and Lithium-Intercalated Compounds. *J. Electrochem. Soc.* **2006**, *153*, A450.
(462) Park, K.-S.; Schougaard, S. B.; Goodenough, J. B. Conducting-Polymer/Iron-Redox- Couple Composite Cathodes for Lithium Secondary Batteries. *Adv. Mater.* **2007**, *19*, 848−851.
(463) Huang, Y.-H.; Goodenough, J. B. High-Rate $LiFePO_4$ Lithium Rechargeable Battery Promoted by Electrochemically Active Polymers. *Chem. Mater.* **2008**, *20*, 7237−7241.
(464) Wang, Q.; Evans, N.; Zakeeruddin, S. M.; Exnar, I.; Grätzel, M. Molecular Wiring of Insulators: Charging and Discharging Electrode Materials for High-Energy Lithium-Ion Batteries by Molecular Charge Transport Layers. *J. Am. Chem. Soc.* **2007**, *129*, 3163−3167.
(465) Hatakeyama-Sato, K.; Masui, T.; Serikawa, T.; Sasaki, Y.; Choi, W.; Doo, S.-G.; Nishide, H.; Oyaizu, K. Nonconjugated Redox-Active Polymer Mediators for Rapid Electrocatalytic Charging of Lithium Metal Oxides. *ACS Appl. Energy Mater.* **2019**, *2*, 6375−6382.
(466) Lepage, D.; Michot, C.; Liang, G.; Gauthier, M.; Schougaard, S. A Soft Chemistry Approach to Coating of $LiFePO_4$ with a Conducting Polymer. *Angew. Chem. Int. Ed.* **2011**, *123*, 70167019.
(467) Yassin, Y.; Jiménez, P.; Lestriez, B.; Moreau, P.; Leriche, P.; Roncali, J.; Blanchard, P.; Terrisse, H.; Guyomard, D.; Gaubicher, J. Engineered Electronic Contacts for Composite Electrodes in Li Batteries Using Thiophene-based Molecular Junctions. *Chem. Mater.* **2015**, *27*, 40574065.

https://dx.doi.org/10.1021/acs.chemrev.9b00482
Chem. Rev. 2020, 120, 6490−6557